

ASMS 2020 Posters



Poster Reprint

ASMS 2020

MP 176

Using ICP-MS/MS with M-Lens for the analysis of high silicon matrix samples

Yu Ying¹; Xiangcheng Zeng¹

¹Agilent Technologies, China, Shanghai,
China

Introduction

The expansion of the connected devices and the Internet of Things (IoT) has resulted in semiconductor processing facilities (known as an Integrated Circuit Foundry) to increase production to meet the requirements of this rapidly expanding market. As IC Foundries turn silicon wafers into integrated circuits, the determination and control of trace metal impurities in a high silicon matrix has become crucial in the manufacturing process.

Single quadrupole ICP-MS is the most widely used atomic spectrometry technique for the measurement of trace elements but with advanced semiconductor processes requiring elemental impurities on the silicon wafer to be 1.0^{E+7} atom/cm² level, it can be difficult to meet these specifications.

The development of triple quadrupole ICP-MS with MS/MS capabilities that can selectively remove interferences caused by silicon, as well as many other interferences, has greatly enhanced the obtainable detection limits (DLs) to less than 1ppt.

Another critical issue encountered in this analysis is the high silicon matrix can cause severe suppression of analytes and silicon deposition, which impacts the stability of the measurement. To address the sensitivity suppression caused by the silicon matrix as well as the need for improved stability in this matrix, a new lens (M-lens) was developed. The new M-lens was designed with the high purity chemical market in mind, allowing sub-ppt BEC of Na, K, and Ca in hot plasma conditions ($CeO^+/Ce^+ < 1.5\%$) as well as improved stability in difficult matrixes.

In this study, using an ICP-MS/MS with the M-lens, we investigated two kinds of common silicon matrix samples used in the semiconductor industry.

Experimental

Instrumentation

An Agilent 8900 ICP-MS/MS was used for this study. The configuration of the instrument included helium, hydrogen, oxygen and ammonium as collision/reaction gases used to remove the polyatomic interferences. The M-lens was also used for its high silicon matrix tolerance and ability to achieve excellent measurement stability in difficult samples.

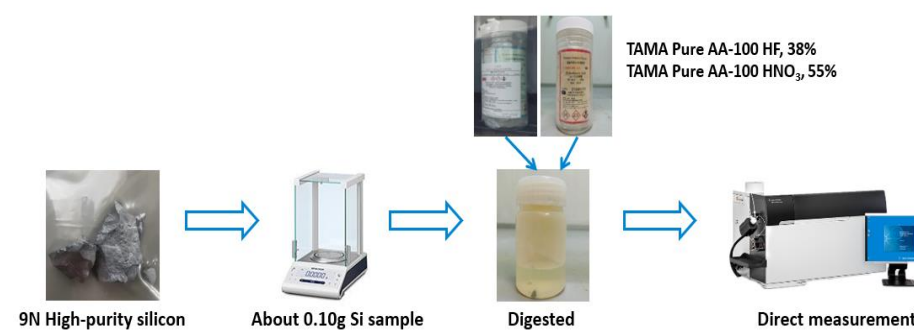
Experimental



Sample preparation

Electrotonic grade silicon of 9N purity was used as the base material. Trace-level of nitric acid (TAMAPure AA-100, Kanagawa, Japan) and hydrofluoric acid (TAMAPure AA-100, Kanagawa, Japan) were used as the reagents to produce high silicon matrix samples.

The sample preparation followed was to weigh the electrotonic grade silicon to the nearest 0.05g, clean the surface with HNO₃ and ultrapure water, then digest the silicon with 38% HF and 55% HNO₃ 1:1 (w/w) mix acid to the nearest 50.0g. Dilute this 1000ppm Si matrix solution to get two typical high silicon matrix samples: 10ppm Si for the concentration of typical bare wafer; 100ppm Si for poly-Si after sample preparation.



ICP-MS/MS Operating Parameters

The operating parameters of the Agilent 8900 Triple Quadrupole ICP-MS/MS for advanced applications was used along with a 200 μ L/min PFA MicroFlow nebulizer and 2.5mm sapphire injector and inert torch. Three modes (all hot plasma) were used in this study.

Table 1. Operating parameters of ICP-MS/MS

Parameter	Value	Parameter	Value
RF (W)	1550	Spray chamber temp. (°C)	2
Sampling depth (mm)	8.0	He flow rate (mL/min)	4.5
Carrier gas (L/min)	0.8	H ₂ flow rate (mL/min)	10.0
Makeup gas (L/min)	0.4	NH ₃ flow rate (mL/min)	2.0
Integration time (s)	0.6		

Spectral interferences

Possible spectral interferences caused by high level silicon in samples, are listed in Table 2.

Table 2. Spectral interferences caused by silicon matrix

Analyte ion	Interferences	Analyte ion	Interferences
$^{46}\text{Ti}^+$	$^{30}\text{Si}^{16}\text{O}^+$	$^{58}\text{Ni}^+$	$^{28}\text{Si}^{30}\text{Si}^+$ $^{29}\text{Si}^{29}\text{Si}^+$
$^{47}\text{Ti}^+$	$^{28}\text{Si}^{19}\text{F}^+$ $^{30}\text{Si}^{16}\text{OH}^+$	$^{60}\text{Ni}^+$	$^{28}\text{Si}^{16}\text{O}_2^+$ $^{30}\text{Si}^{30}\text{Si}^+$
$^{48}\text{Ti}^+$	$^{28}\text{Si}^{19}\text{F}^+$ $^{30}\text{Si}^{18}\text{O}^+$	$^{63}\text{Cu}^+$	$^{28}\text{Si}^{16}\text{O}^{19}\text{F}^+$
$^{49}\text{Ti}^+$	$^{30}\text{Si}^{19}\text{F}^+$	$^{65}\text{Cu}^+$	$^{30}\text{Si}^{16}\text{O}^{19}\text{F}^+$ $^{28}\text{Si}^{18}\text{O}^{19}\text{F}^+$
$^{56}\text{Fe}^+$	$^{28}\text{Si}^{28}\text{Si}^+$		

To obtain ppt level DLs, spectral interferences are removed by the use of ammonium as a reaction gas. In the example below, we take ^{48}Ti and share how ICP-MS/MS removes the interferences in mass-shift mode, as shown in Fig.1.

Figure 1. Mechanism of MS/MS mass-shift mode, using NH_3 for the measurement of ^{48}Ti

The SiF^+ and SiO^+ interferences on ^{48}Ti were removed by NH_3 mass-shift mode. This is possible as in the reaction cell, the analyte ion $^{48}\text{Ti}^+$ combines with the reaction gas NH_3 to form the "new" analyte ion $\text{TiNH}(\text{NH}_3)_3^+$, while the interference ions (SiF^+ and SiO^+) do not react with NH_3 . In Q2, only ions of mass $m/z=114$ $\text{TiNH}(\text{NH}_3)_3^+$ are transmitted to the detector, while interference ions (SiF^+ and SiO^+) are removed and do not contribute to the signal at the "new" analyte ion.

In order to ensure the spectral interferences were being properly removed by the MS/MS reaction mechanism, results of different masses of the same element (^{58}Ni & ^{60}Ni , ^{63}Cu & ^{65}Cu) were evaluated to determine the effectiveness of MS/MS. The results of a 100ppm Si matrix sample measurement is shown in Fig. 2.

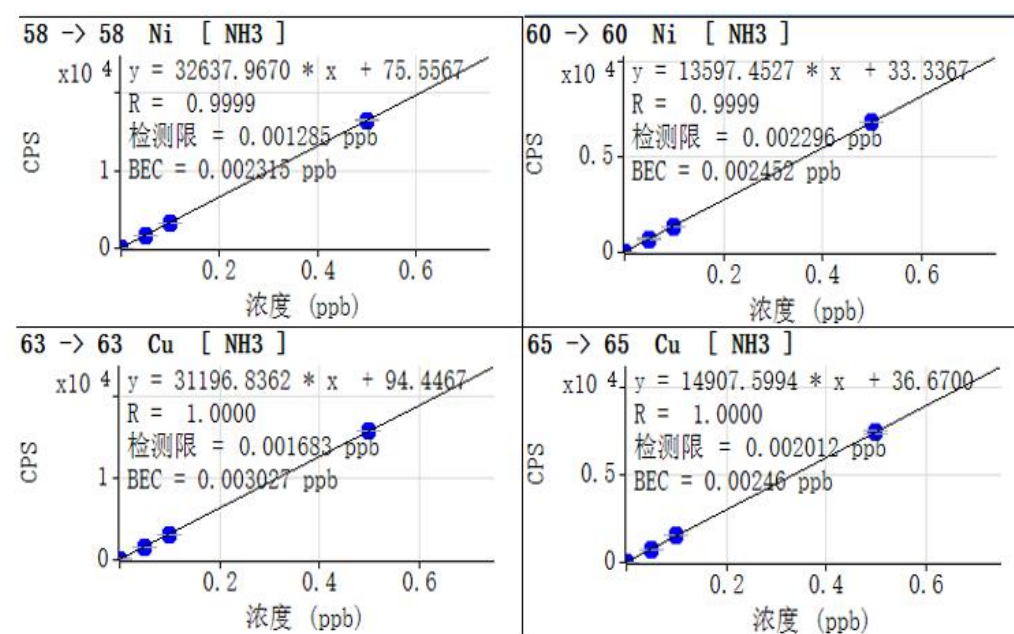


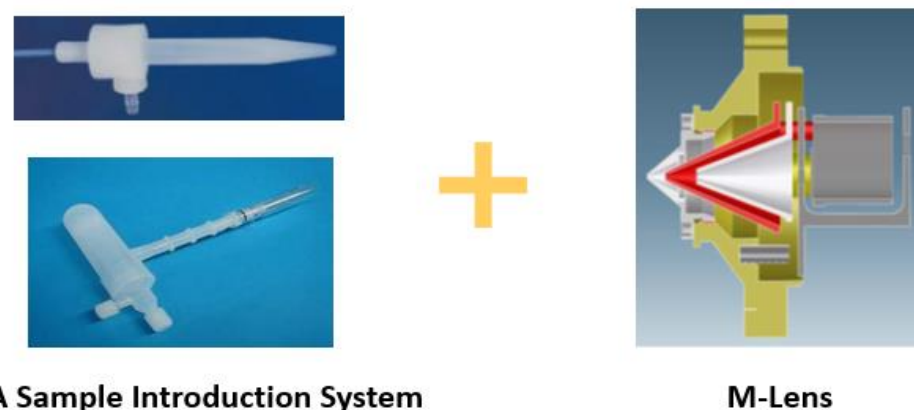
Figure 2. Measurement result of ^{58}Ni & ^{60}Ni , ^{63}Cu & ^{65}Cu

From the results shown in Fig. 2, the BEC (Background Equivalent Concentration) of different mass are in very good agreement which indicates that MS/MS mass-shift mode is effective at removing the spectral interferences.

The robust performance of ICP-QQQ with MS/MS mode is effective at removing the Si interferences, allowing ppt level analysis in the high silicon matrix. The BECs of all 38 analyte ions are lower than 50ng/L in both 10ppm & 100ppm Si matrix samples. Also, the achieved DLs of all elements are at the ppt level.

Stability of measurement

To test both the stability of the specially designed M-Lens and the robustness of the MS/MS reaction mechanism with the high silicon matrix, a standard solution of 50ng/L was spiked in the prepared 10ppm & 100ppm Si matrix samples. Each sample had 11 replicate measurements performed and the analysis was carried out over a 1h time period. The results are shown in Table 3.



PFA Sample Introduction System

M-Lens

Results and Discussion

Table 3. Analysis stability result of 10ppm & 100ppm silicon matrix samples

Analyte ion	10ppm Si			100ppm Si		
	Spike Average (ug/L)	RSD	Recovery	Spike Average (ug/L)	RSD	Recovery
Li	0.051	3.7%	101.40%	0.053	3.4%	107.27%
Be	0.050	3.6%	99.36%	0.053	4.7%	105.66%
B	0.053	4.0%	105.94%	0.055	3.2%	109.68%
Na	0.051	5.6%	101.84%	0.049	2.9%	96.71%
Mg	0.047	3.0%	93.92%	0.054	4.4%	108.20%
Al	0.051	3.8%	103.12%	0.048	2.2%	97.67%
K	0.047	2.3%	93.56%	0.053	2.6%	105.11%
Ca	0.048	2.1%	95.77%	0.054	3.3%	108.88%
Ti	0.051	5.6%	101.28%	0.050	5.1%	101.68%
V	0.045	2.5%	90.80%	0.051	4.6%	102.28%
Cr	0.048	2.5%	95.86%	0.050	2.8%	101.42%
Mn	0.052	3.8%	103.76%	0.048	1.5%	96.20%
Fe	0.056	6.0%	112.01%	0.053	3.9%	106.90%
Co	0.045	2.4%	90.02%	0.049	3.2%	99.11%
Ni	0.046	4.0%	92.23%	0.048	2.3%	96.74%
Cu	0.050	5.6%	99.39%	0.047	5.9%	94.48%
Zn	0.051	5.1%	101.08%	0.047	5.7%	95.69%
Ga	0.048	2.4%	94.84%	0.055	2.8%	109.81%
Ge	0.046	2.0%	90.68%	0.049	1.7%	98.05%
As	0.045	4.7%	90.27%	0.050	5.9%	100.41%
Nb	0.045	5.0%	90.38%	0.048	4.5%	97.19%
Mo	0.048	2.0%	96.48%	0.051	4.5%	100.58%
Ag	0.048	2.0%	95.30%	0.051	2.5%	101.23%
Se	0.048	1.9%	94.93%	0.051	2.3%	102.23%
Rb	0.046	2.6%	91.48%	0.049	2.7%	98.20%
Sr	0.047	2.9%	93.81%	0.049	4.3%	98.03%
Zr	0.049	1.9%	98.17%	0.051	1.6%	100.77%
Cd	0.048	1.7%	95.85%	0.049	2.5%	98.07%
Sn	0.048	2.5%	96.68%	0.049	2.1%	97.55%
Sb	0.047	2.3%	93.93%	0.048	2.6%	95.25%
Cs	0.047	2.7%	94.61%	0.049	1.8%	97.01%
Ba	0.049	2.3%	97.55%	0.050	1.9%	98.43%
Ta	0.050	2.2%	98.84%	0.048	1.6%	96.40%
W	0.050	4.2%	99.19%	0.048	2.2%	96.13%
Re	0.048	2.9%	95.82%	0.048	1.9%	95.91%
Tl	0.052	3.0%	104.21%	0.052	1.3%	103.17%
Pb	0.049	2.2%	98.01%	0.048	1.9%	96.07%
U	0.052	3.3%	103.15%	0.051	1.0%	101.20%

The data shows good RSD's (<6%) across all 38 elements for both the 10ppm silicon and the 100ppm silicon matrixes.

This confirms that the M-lens greatly reduces signal suppression and offers excellent robustness and sensitivity as spike recoveries in both silicon matrixes ranged from 90% to 110%, except iron (Fe) in 10ppm silicon sample. The slightly high Fe result was likely the result of environmental contamination during the 1h analysis time.

Conclusions

8900 ICP-MS/MS with M-lens: effective analysis solution of high silicon matrix samples

- ICP-MS/MS operated in tandem MS/MS mode using NH₃ as a reaction gas is effective at controlling the reaction process and preventing unwanted ions from contributing to elevated BEC's and DL's.
- M-Lens can reduce the impact on signal suppression caused by high silicon deposition and improve measurement stability
- 8900 ICP-MS\MS can completely remove the spectral interferences caused by high sample matrixes while offering ultra-trace analysis to meet the specifications of the most advanced IC manufacturing process.

References

- ¹Ed McCurdy, Glenn Woods, Naoki Sugiyama. Method Development with ICP-MS/MS: Tools and Techniques to Ensure Accurate Results in Reaction Mode[J].Spectroscopy, 2019(9):20-27.
- ²Eduardo Bolea-Fernandez, Lieve Balcaen, Martin Resano, Frank Vanhaecke. Overcoming spectral overlap via inductively coupled plasma-tandem mass spectrometry (ICP-MS/MS)[J].Journal of Analytical Atomic Spectrometry, 2017(9):1660-1679.

Poster Reprint

ASMS 2020

MP 194

Targeted Peptide Quantitation of Seven Food Allergens in Dark Chocolate Using Triple Quadrupole LC/MS

Lee Sun New¹, Jerry Zweigenbaum² and Chee Sian Gan¹

¹ Agilent Technologies Singapore (Sales) Pte Ltd. Singapore

² Agilent Technologies, Inc., Wilmington, DE, USA

Introduction

Food allergy presents a significant public health issue. Hence, mandatory allergen labelling laws have been enacted to protect the allergic consumers, but allergens may be unintentionally present in food products due to cross-contact. To address this uncertainty, food manufacturers use precautionary allergen labelling (PAL). However, the lack of global consistency in PAL confuses many consumers. Thus, scientific-based allergen risk assessment has been increasingly used by the food authorities and industry to improve management of food allergens via PAL.

Allergen analysis plays an important role in the application of action levels for either voluntary or legislative labeling. A quick sample preparation procedure together with a sensitive and reliable analysis method was developed for the simultaneous targeted quantitation of egg, milk, soy, peanut, almond, hazelnut and walnut in dark chocolate.

Experimental

Materials and sample preparation

Reference materials for milk, egg, soy and peanut were obtained from NIST (Gaithersburg, MD, USA). Baked almond, hazelnut and walnut were purchased from a local supermarket and homogenized into fine pastes. For each allergen, 50 mg/mL stock solution was prepared following the second and third steps in Figure 1. They were combined and serially diluted into allergen working solutions used for spiking dark chocolate to prepare calibration standard and QC samples (Figure 1).

Targeted peptide analysis

Peptides (10 μ L) were separated by a Poroshell 120 EC-C18 column using an Agilent 1290 Infinity II UHPLC system coupled to a 6495 triple quadrupole mass LC/MS (LC/TQ) system. The detailed LC and MS parameters are shown in Table 1 and 2, respectively.

Table 1. Agilent 1290 Infinity II UHPLC parameters.

LC Parameter	Value
Column	Agilent Poroshell 120 EC-C18, 2.1 \times 100 mm, 2.7 μ m (P/N 695775-902)
Mobile phase A	0.1% formic acid in water
Mobile phase B	0.1% formic acid in acetonitrile
Flow rate	0.4 mL/min
Column temp	40°C
Gradient	0.0 min \rightarrow 2%B; 1.0 min \rightarrow 2%B; 11.0 min \rightarrow 40%B; 12.5 min \rightarrow 98%B; 14.5 min \rightarrow 98%B; 14.6 min \rightarrow 98%B
Post time	2.4 min

Experimental

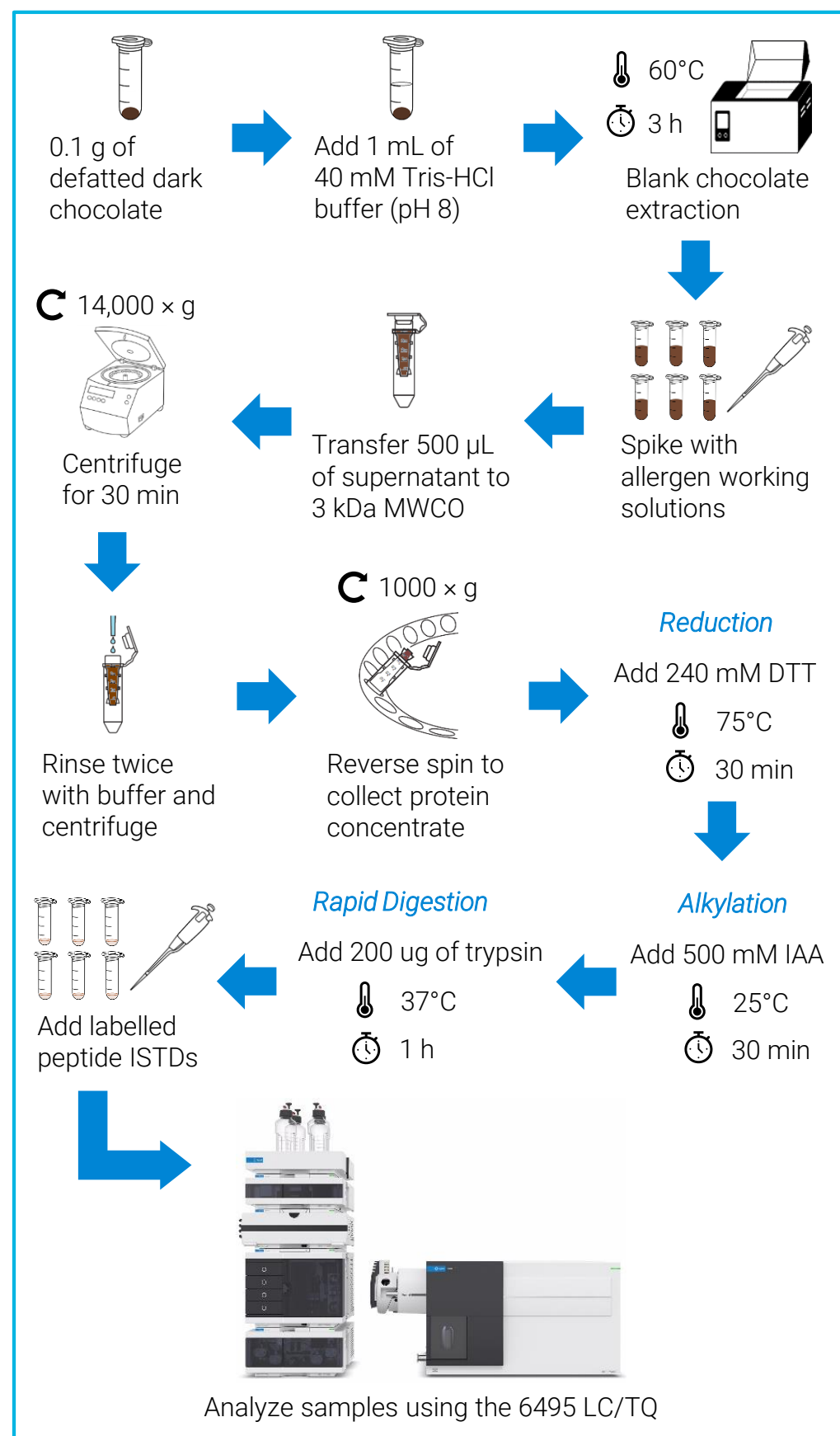


Figure 1. Sample preparation workflow.

Table 2. Agilent 6495 LC/TQ MS parameters.

MS Parameter	Value
Ionization mode	Positive AJS ESI
Gas temperature	150°C
Drying gas flow	16 L/min
Nebulizer gas	30 psi
Sheath gas temperature	350°C
Sheath gas flow	11 L/min
Capillary voltage	3500 V
Nozzle voltage	300 V
High/Low RF pressure voltage	145/65 V
Delta EMV	200 V
Scan type	Dynamic MRM
Cycle time	500 ms

Selection of peptide markers

The peptide markers were selected from peptide mapping experiments and rigorously checked to make sure that they are unique to each food allergen and have no interference with the food matrix, other food allergens or commonly used ingredients of plant or mammal origins. To ensure optimal MS sensitivity, two peptides and two MRM transitions per peptide, were used as positive identification for each allergen (Table 3). Optimal separation of the peptides was achieved using a short 10 min LC gradient (Figure 2).

Table 3. MRM transitions of the peptide markers.

Allergen	Peptide ID	Precursor m/z	Product m/z	CE (V)	Function
Milk casein	MC1	692.9	920.5	17	Quantitation
		692.9	991.5	23	
	MC2	390.8	568.3	7	Confirmation
		390.8	372.2	16	
Milk whey	MW1	533.3	853.4	15	Quantitation
		533.3	754.4	15	
	MW2	858.4	1254.6	31	Confirmation
		858.4	627.8	31	
Egg white	EW1	844.4	666.3	27	Quantitation
		844.4	1331.7	30	
	EW2	298.5	397.7	3	Confirmation
		298.5	326.7	6	
Soy	SY1	347.5	407.2	5	Quantitation
		347.5	464.3	5	
	SY2	478.3	643.4	19	Confirmation
		478.3	434.8	16	
Peanut	PN1	543.3	429.7	15	Quantitation
		543.3	858.4	18	
	PN2	628.4	741.5	21	Confirmation
		628.4	1083.7	21	
Almond	AM1	571.8	369.2	16	Quantitation
		571.8	858.4	19	
	AM2	686.9	594.8	19	Confirmation
		686.9	748.4	31	
Hazelnut	HN1	514.3	616.3	17	Quantitation
		514.3	729.4	17	
	HN2	576.3	689.4	22	Confirmation
		576.3	852.4	22	
Walnut	WN1	636.4	875.4	18	Quantitation
		636.4	397.3	15	
	WN2	479.6	662.4	13	Confirmation
		479.6	618.9	13	

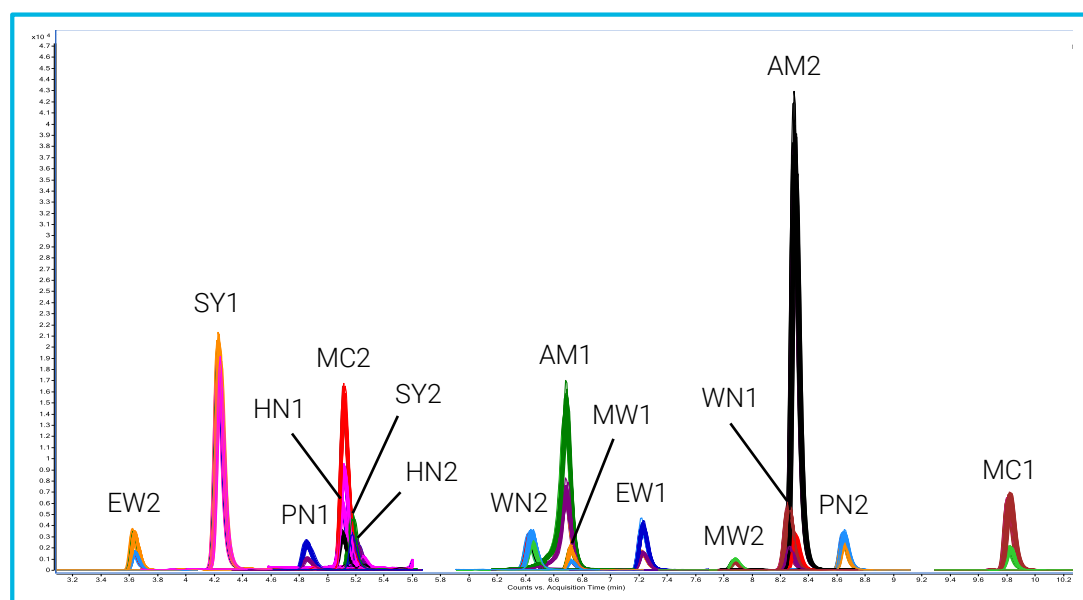


Figure 2. MRM chromatograms of the 14 peptides representing the 7 food allergens in 100 mg/kg spiked dark chocolate (overlay of 104 replicate injections).

Method sensitivity

The method limit of quantitation (LOQ) was defined as the concentration where S/N is greater than 10 and benchmarked against the recommended sensitivity levels from VITAL 3.0 and AOAC SMPR 2016.002. All peptide markers in this method demonstrated excellent sensitivity and were able to meet the minimum sensitivity levels described in VITAL 3.0 and AOAC SMPR (Table 4). The method also demonstrated good specificity and was able to accurately detect the peptides at LOQ in the dark chocolate matrix (Figure 3).

Table 4. Comparison of the method LOQ to the recommended sensitivity levels from VITAL 3.0 (reference amount of 40 g) and AOAC SMPR 2016.002.

Allergen	mg allergen per kg food		
	Method LOQ	VITAL 3.0 Action Level ¹	AOAC SMPR MQL ²
Milk casein	10	20	10
Milk whey	10	20	10
Egg white	5	10	5
Soy	5	23	Not defined
Peanut	10	23	10
Almond	2.5	12	Not defined
Hazelnut	5	17	10
Walnut	5	5	Not defined

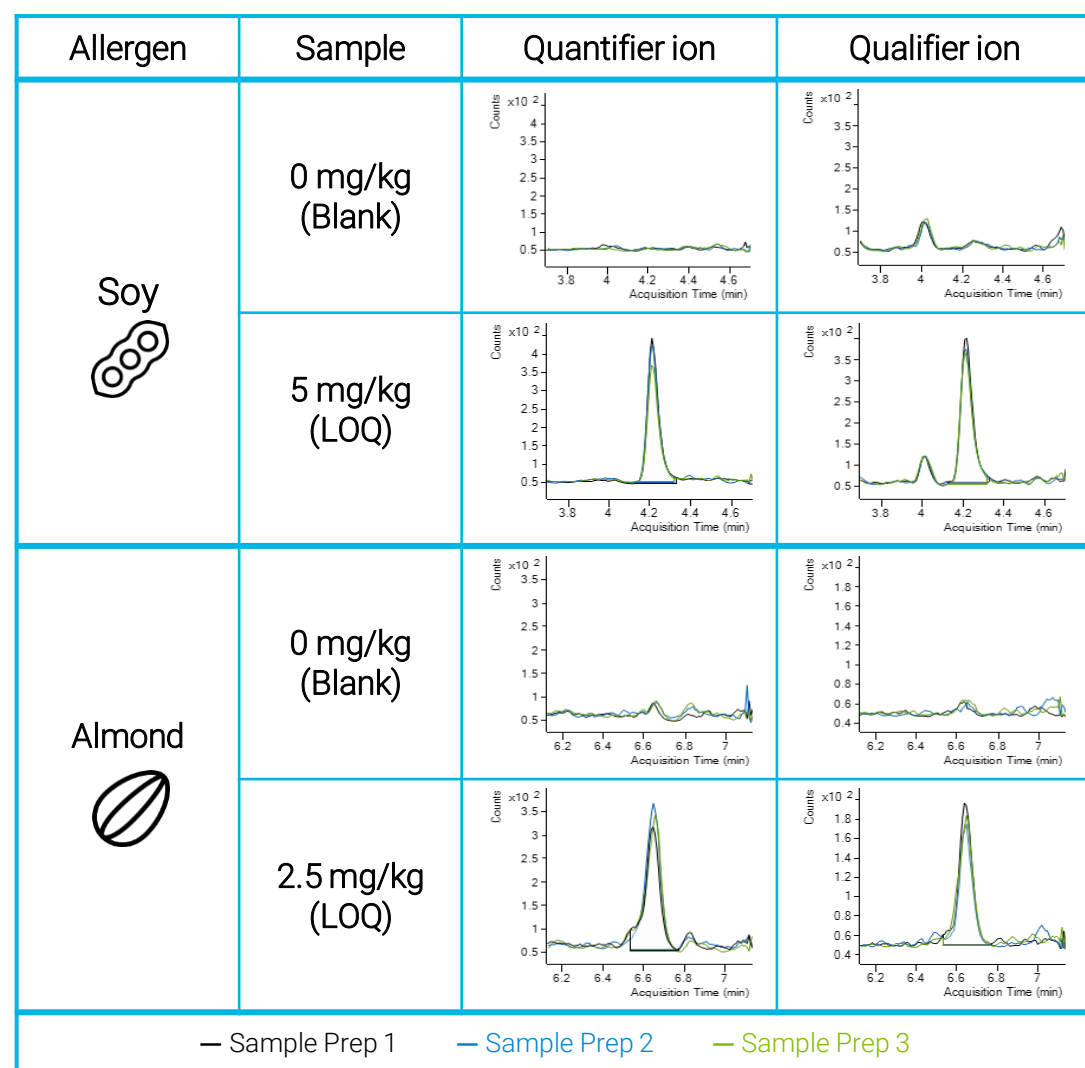


Figure 3. Overlay of MRM chromatograms for soy and almond in blank (0 mg/kg) and LOQ chocolate samples.

Analytical range and accuracy

As shown in Figure 4, all peptides demonstrated a wide analytical range of 3 to 4 orders of magnitude across 2.5 – 1000 mg/kg for almond; 5 – 1000 mg/kg for egg white, soy and walnut; 10 – 1000 mg/kg for milk and peanut; and 5 – 500 mg/kg for hazelnut. All calibration curves demonstrated good linearity with R^2 values greater than 0.99.

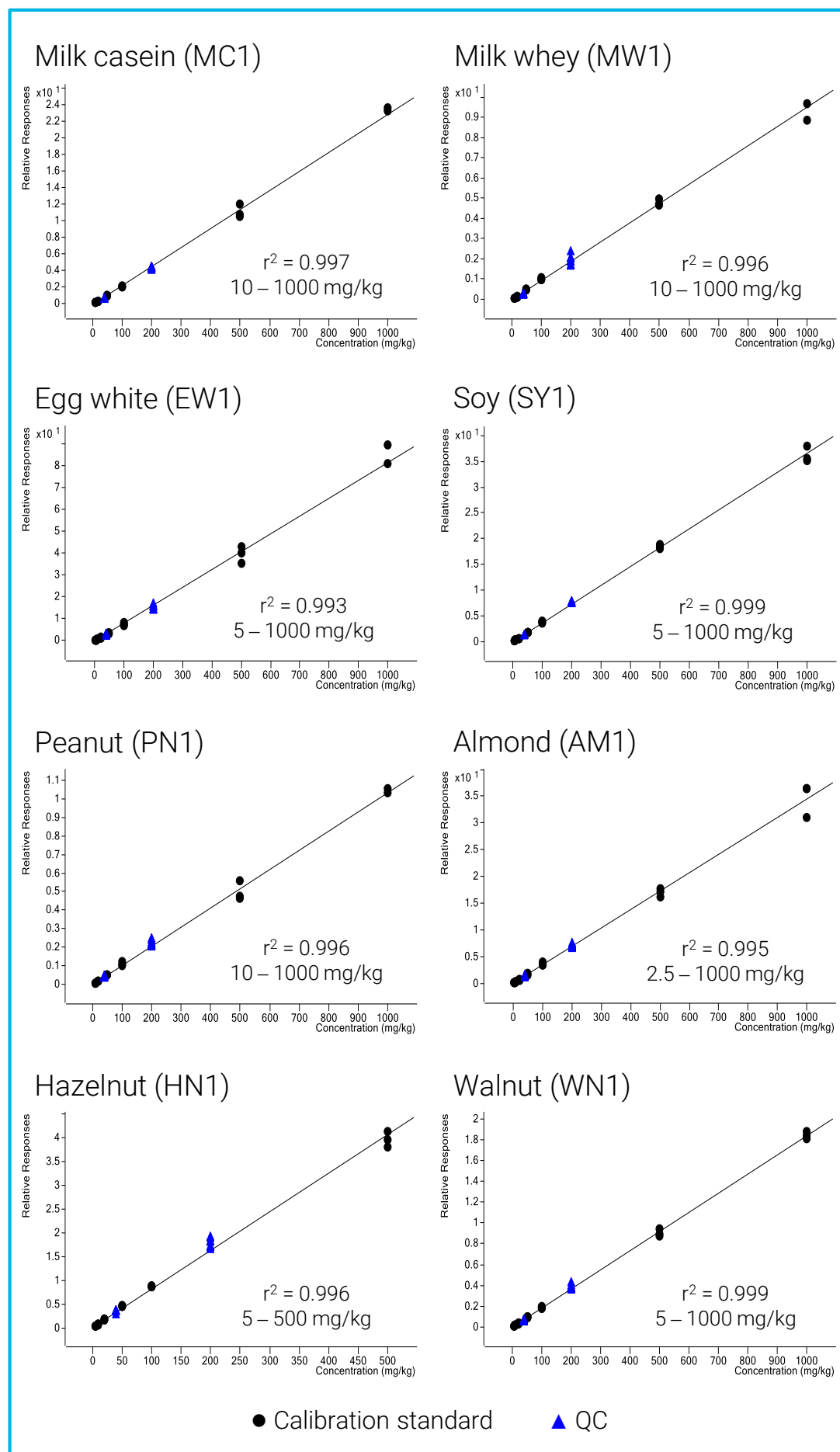


Figure 4. Calibration curves of the quantitation peptides in dark chocolate spiked with the 7 allergens (n = 3 per calibration concentration).

Method recovery and precision

The recovery and precision of the peptide markers were evaluated at two QC levels at 40 and 200 mg/kg. Nine replicate analyses of each QC level were evaluated. As shown in Figure 5, method recoveries were 75 – 102% at both QC levels for most quantitation peptides and are well within the AOAC recommended recovery of 60 – 120%. The method also demonstrated excellent precision (RSD) of 1.5 – 8.6% and 1.7 – 10.4% for 40 and 200 mg/kg, respectively.

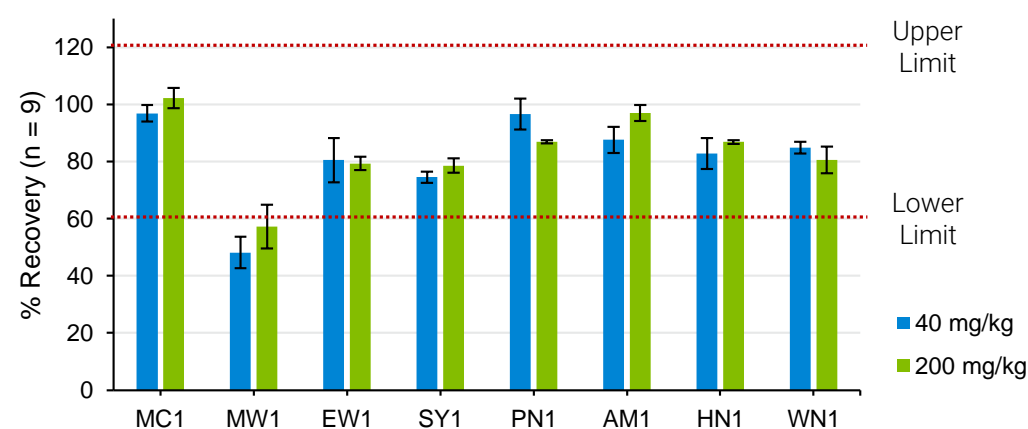


Figure 5. Recovery of allergens in QC samples at 40 and 200 mg/kg spiking levels.

Conclusions

- A rapid and simple sample preparation method was successfully developed for extracting milk (casein and whey), egg white, soy, peanut, almond, hazelnut and walnut from dark chocolate and analyzed using the Agilent 6495 Triple Quadrupole LC/MS system.
- The method was sensitive enough to meet the minimum sensitivity level recommendations in VITAL 3.0 and AOAC SMPR 2016.002, and demonstrated good analytical range, recovery and precision.
- Preliminary data showed that this method is applicable for cookies and further studies will be performed.

References

- 1 The Allergen Bureau Limited. Food Industry Guide to the Voluntary Incidental Trace Allergen Labelling (VITAL) Program Version 3.0, 2019
- 2 Paez V, et al. AOAC SMPR 2016.002 Standard Method Performance Requirements (SMPRs) for Detection and Quantitation of Selected Food Allergens. J AOAC Int. 2016, 99(4), 1122–1124

Poster Reprint

ASMS 2020

MP 201

Workflow for food classification and authenticity using yerba mate and high-resolution GC/Q-TOF

Sofia Nieto, Melissa Churley

Agilent Technologies, Santa Clara, CA

Introduction

Food fraud is a highly profitable business and includes activities such as misbranding, mislabeling, dilution, counterfeiting and adulteration. Among foods and food ingredients most frequently found adulterated, there are olive oil, seafood, milk, honey, fruit juices, spices, coffee and tea. In order to streamline the characterization of foods, a novel workflow using high-resolution GC/Q-TOF and Classifier software has been developed. The workflow was evaluated using yerba mate, a traditional South American caffeinated tea. The model was able to easily distinguish between different brands of commercially available yerba mate. In addition, compounds that are characteristic to yerba mate and contribute to its unique flavor are discussed, as well as the presence of contaminating polycyclic aromatic hydrocarbons (PAHs).

Experimental

Yerba mate samples, purchased at a supermarket in Buenos Aires, Argentina, were extracted using a standard QuEChERS protocol. The samples were analyzed using a 7890 GC with and the 7250 high-resolution Q-TOF MS in full acquisition mode. The retention indices were calculated based on the alkane ladder to ensure compound identification. The GC/Q-TOF data were processed using the Unknowns Analysis tool of MassHunter Quantitative Analysis Software 10.1, Mass Profiler Professional (MPP) 15.1 and Classifier 1.1. The parameters are described in detail in Table 1.

GC and MS Conditions:	Q-TOF (7250)
GC	7890
Column	30-5MS UI, 15 m, 0.25 mm, 0.25 μ m
Inlet	MMI, 4-mm UI liner single taper w wool
Injection volume	1 μ L
Injection mode	Splitless
Inlet temperature	280°C
Oven temperature program	50°C for 2 min; 10°C/min to 300°C, 10 min hold
Carrier gas	Helium
Column flow	1.2 mL/min
Transfer line temperature	300°C
Quadrupole temperature	150°C
Source temperature	200°C
Electron energy	70 eV
Emission current	5 μ A
Spectral acquisition rate	5 Hz
Mass range	45 to 650 m/z

Table 1. GC/Q-TOF acquisition parameters.

Results and Discussion

Classification Workflow

To build the classification model, six replicates of each type of yerba mate from three different brands were extracted and analyzed using a high-resolution GC/Q-TOF (Figure 1).

The general workflow is outlined in Figure 2. First, a classification model is built and validated in MPP and Classifier following the feature finding step in Unknowns Analysis tool (Figure 2a). After the classification model is created and exported, unknown samples can be characterized directly using Unknowns Analysis and Classifier, bypassing MPP (Figure 2b).

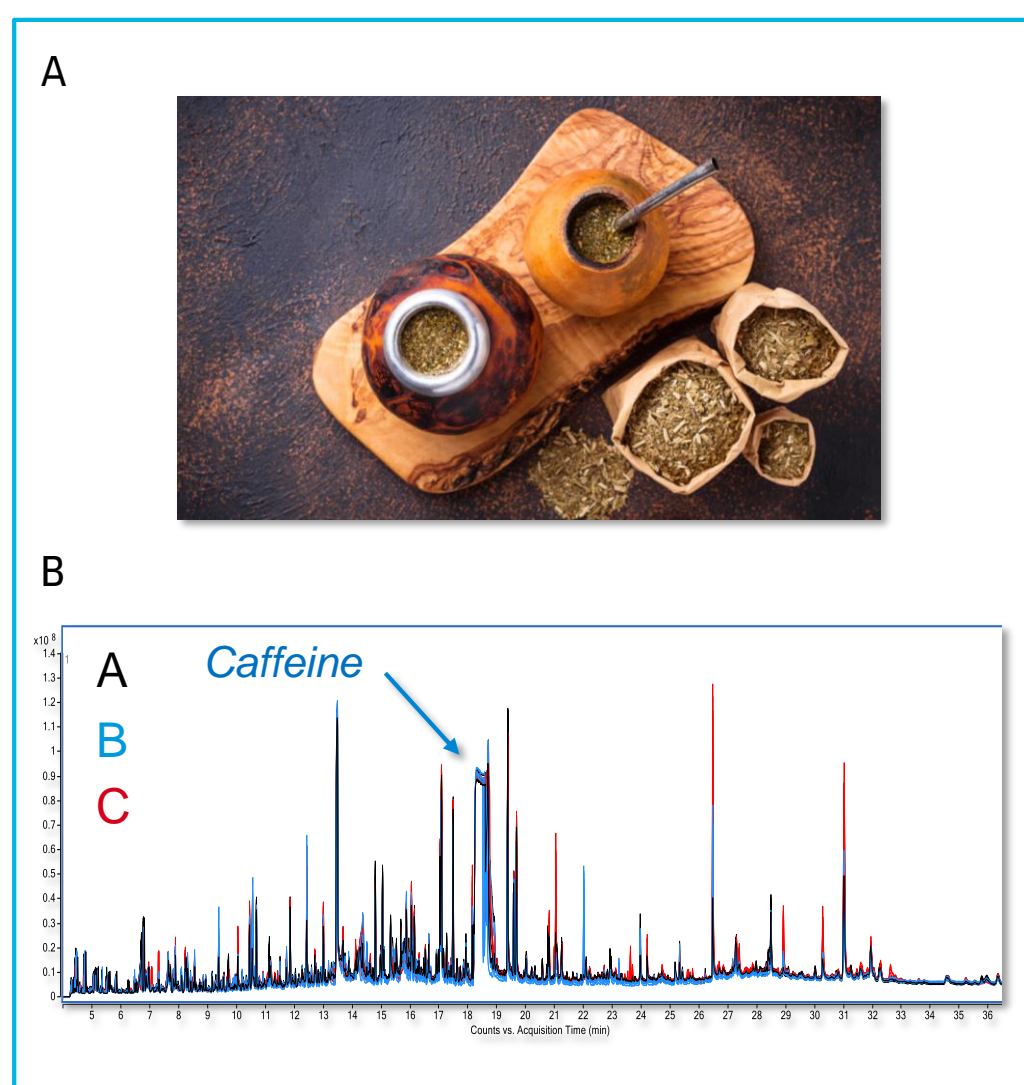


Figure 1. A) Yerba mate and mate gourds B) Overlaid chromatograms from the extracts of the three brands of yerba mate labeled A, B and C. Arrow points to caffeine.

Feature finding was performed in Unknowns Analysis using SureMass deconvolution followed by NIST17.L library search (Figure 3). Identity of the compounds was confirmed with Retention Indices (RI) as well as accurate mass (facilitated by ExactMass feature of Unknowns Analysis).

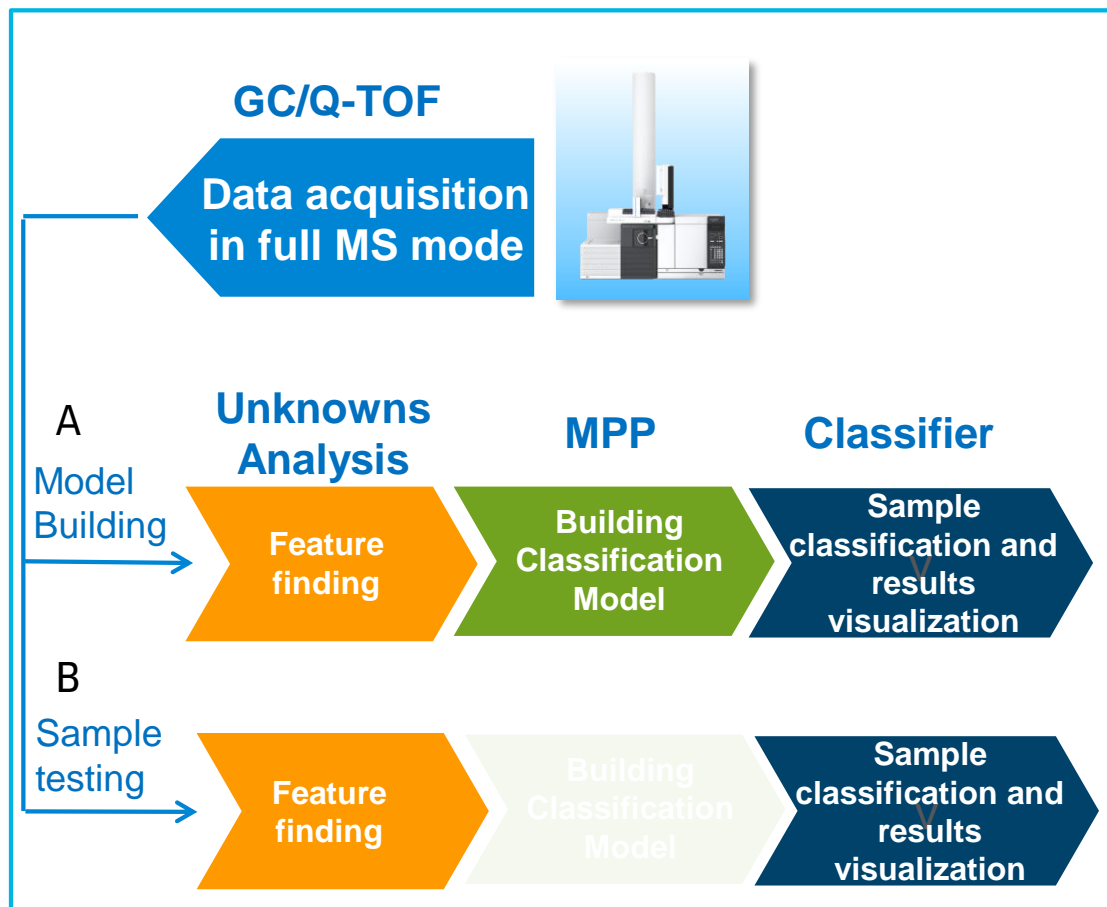


Figure 2. Workflow for sample classification. A) Model building and validation. B) Unknown samples classification.

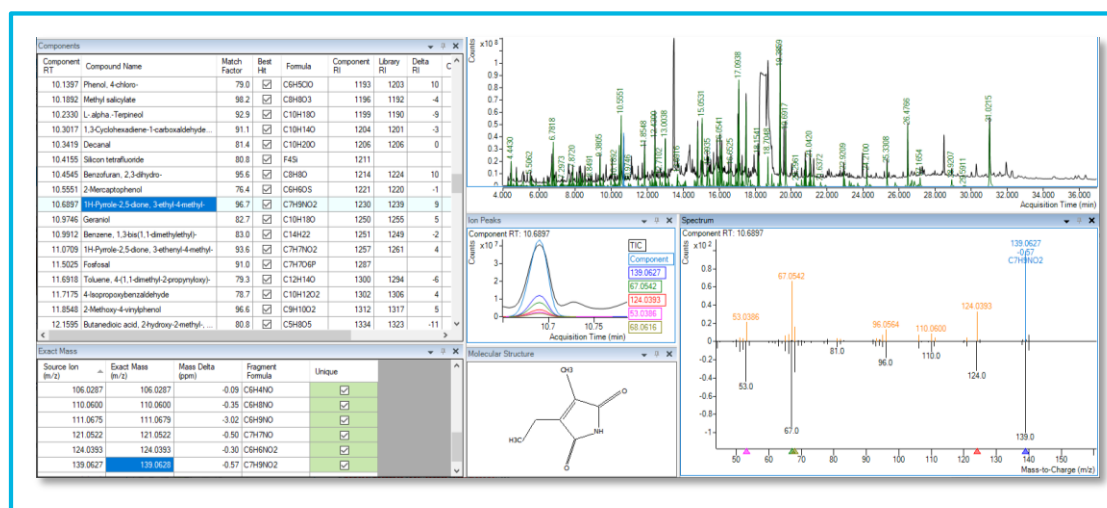


Figure 3. Feature finding in Unknowns Analysis. Yerba mate sample A. RI calibration supports compound ID. ExactMass feature provides additional ID confirmation using accurate mass.

Then, classification models using two different algorithms, PLSDA (Partial Least Square Discrimination) and SIMCA (Soft Independent Modeling of Class Analogy), were built in Mass Profiler Professional (MPP) using CEF files imported from Unknowns Analysis.

Once the data are imported into MPP, sample grouping, alignment, normalization, filtering, QC using Principle Component Analysis (PCA, Figure 4), statistical analysis and Fold Change analysis were performed.

The models were exported from MPP directly to the Classifier software.

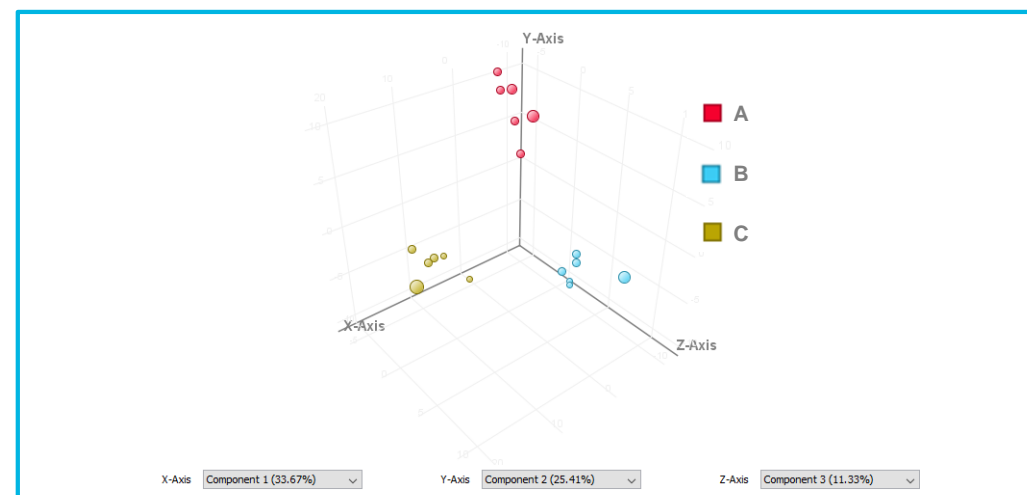


Figure 4. All the three samples groups can be easily separated on PCA plot.

To validate the classification model, both positive and negative controls were prepared using pure and mixed with various proportions of yerba samples.

Results of Differential Analysis, Flavors and Contaminants Screening

Characteristic volatile compounds that predominantly occur in one of the yerba mate brands tested, including those associated with flavor and aroma, have been identified.

Selected results from the Fold Change Analysis performed in MPP are shown on the Volcano plot (Figure 5) comparing extracts from brands A vs C. Compounds highlighted in red are those that are present in significantly higher levels in A as compared to C, and those labeled in blue accumulated in sample C vs A.

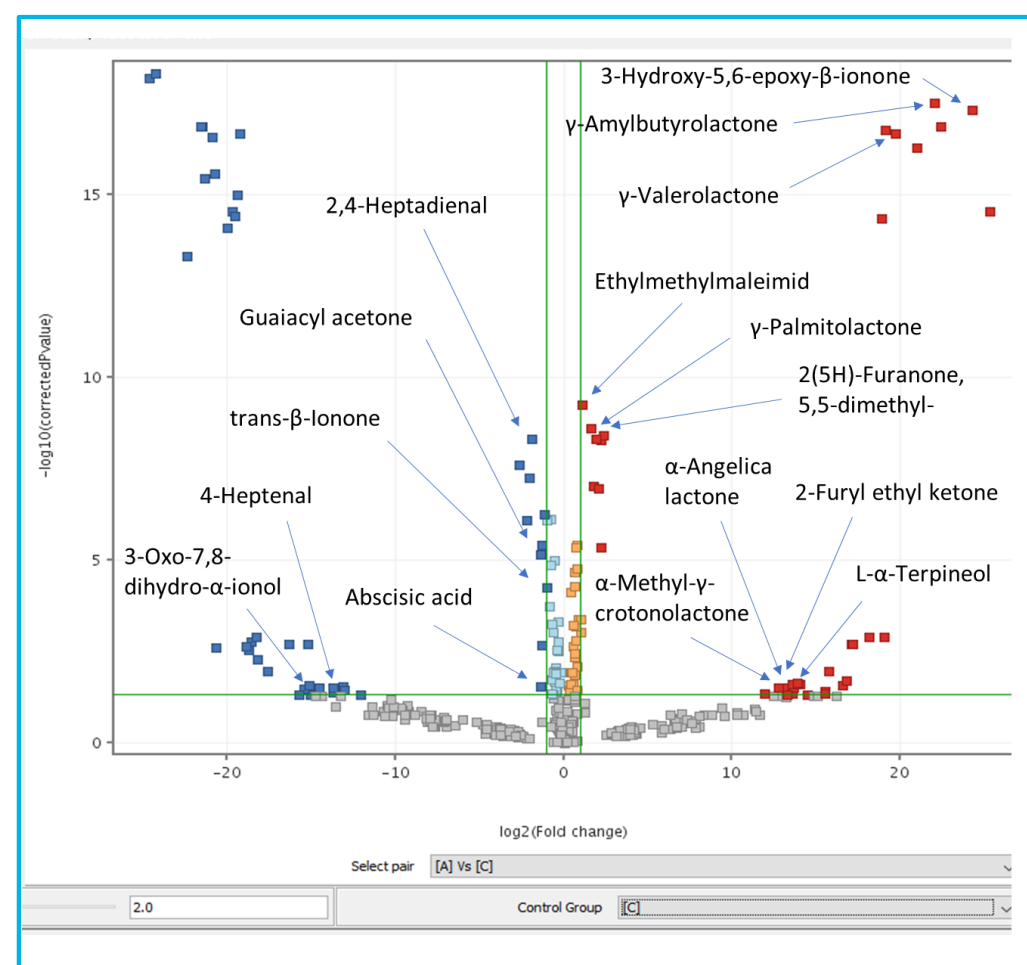


Figure 5. Volcano plot and Fold Change analysis.

Volatile compounds are labeled. Further details for these potential compounds of interest are shown in Table 2. 3-Hydroxy-5,6-epoxy-β-ionone showed one of the most significant Fold Change among identified flavor compounds (with high p-Value) between the two groups, thus potentially contributing to a significant difference in flavor between these brands of yerba mate.

RT	Compound	Mass Error*	p	Regulation	Log FC	Alias	Flavor
4.96	2(3H)-Furanone, 5-methyl-	0.8	0.006450	up	14.0	α-Angelica lactone	Sweet, solvent-like, oily, coconut, nutty with coumarin, tobacco nuances ¹
5.51	4-Heptenal, (Z)-	1.0	0.013103	down	-13.7		oily, dairy, creamy ²
6.25	2(5H)-Furanone, 5,5-dimethyl-	0.5	2.557E-10	up	2.4	4,4-Dimethyl-2-buten-4-olide	Aroma component of hop extract, and of lavender, sagebrush, narcissus and salmon oils ²
6.29	2(3H)-Furanone, dihydro-5-methyl-	0.4	5.834E-19	up	19.7	γ-Valerolactone	milky, fatty ¹
6.64	2(5H)-Furanone, 3-methyl-	0.4	0.009483	up	13.1	α-Methyl-γ-crotonolactone	sweet, tobacco-like odor ³
7.22	1-Propanone, 1-(2-furanyl)-	0.5	0.006653	up	13.5	2-Furyl ethyl ketone	Fuity taste, sweet and caramelic odor ⁴
7.3	2,4-Heptadienal, (E,E)-	0.3	3.468E-10	down	-1.9		fatty, oily, cinnamon ¹
10.23	L-α-Terpineol	0.6	0.017277	up	14.4		citrus, tropical fruits, apple, tomato and coffee flavors ¹
10.69	1H-Pyrrole-2,5-dione, 3-ethyl-4-methyl-	0.3	3.401E-11	up	1.1	Ethylmethylmaleimide	sweet, adds body, flue-cured note ⁵
14.12	trans-β-ionone	1.1	0.000007	down	-1.0		Cedar woods, violets ²
14.63	2-Propanone, 1-(4-hydroxy-3-methoxyphenyl)-	0.4	3.949E-07	down	-1.3	Guaiacylacetone	vanilla, wood origin ⁶
16.48	3-Buten-2-one, 4-(4-hydroxy-2,2,6-trimethyl-7-oxabicyclo[4.1.0]hept-1-yl)-	0.6	5.053E-20	up	24.3	3-Hydroxy-5,6-epoxy-β-ionone	fruity, sweet, berry, woody, violet, orris, powdery ¹
16.72	2-Cyclohexen-1-one, 4-(3-hydroxybutyl)-3,5,5-trimethyl-	0.9	0.000446	down	-18.9	3-Oxo-7,8-dihydro-α-ionone	unknown
21.23	Abscisic acid	0.6	0.008350	down	-1.4		plant hormone

*Mass error shown for quant ion

¹The Good Scents Company

²PubChem

³Perfume and Flavor Chemicals (Aroma Chemicals) Vol.1, By Steffen Arctander, Lulu.com, May 10, 2019

⁴Coffee Flavor Chemistry. Ivon Flament. 2002

⁵Tobacco Flavoring for Smoking Products. John C. Leffingwell, Harvey J. Young & Edward Bernasek. 1972

⁶Red Wine Technology. Antonio Morata. 2019

Table 2. Results of Fold Change analysis for selected volatile compounds. Note, some of these compounds were not necessarily included in the final classification model.

Several PAHs and other environmental contaminants have also been identified, and typically predominated in one brand versus another (Figure 6).

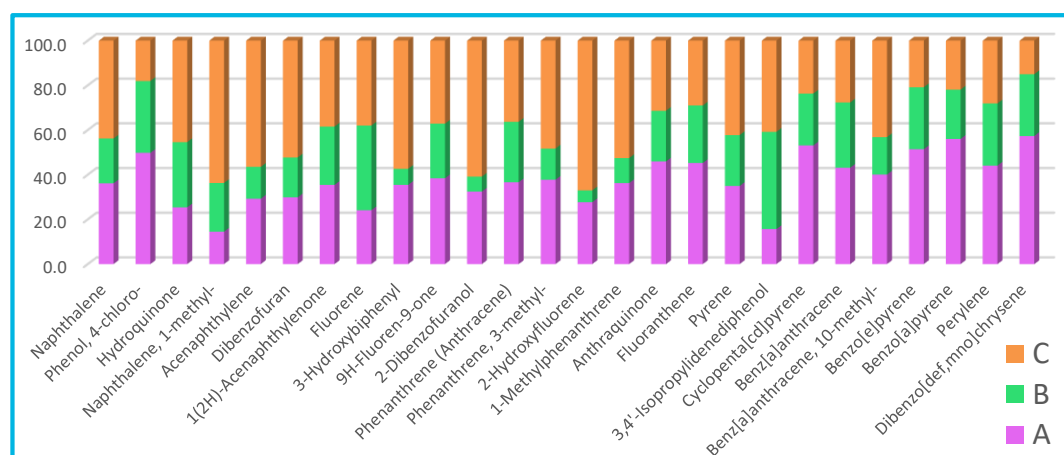


Figure 6. PAH and other environmental contaminants identified in yerba mate extracts

Classification results

The classification models were evaluated using the “adulterated” yerba mate samples created by mixing 5-80% of one of the brands (C) into the other one (A). Both PLSDA and SIMCA models were tested. SIMCA model showed a better distinction between the sample groups. The visualization examples for SIMCA are shown in Figure 7. Note that for a positive control for the extract A most of the model compounds are in the model range (highlighted in green, Figure 7a). For a sample A adulterated with 5% C, a few compounds are out of the model range (Figure 7b).

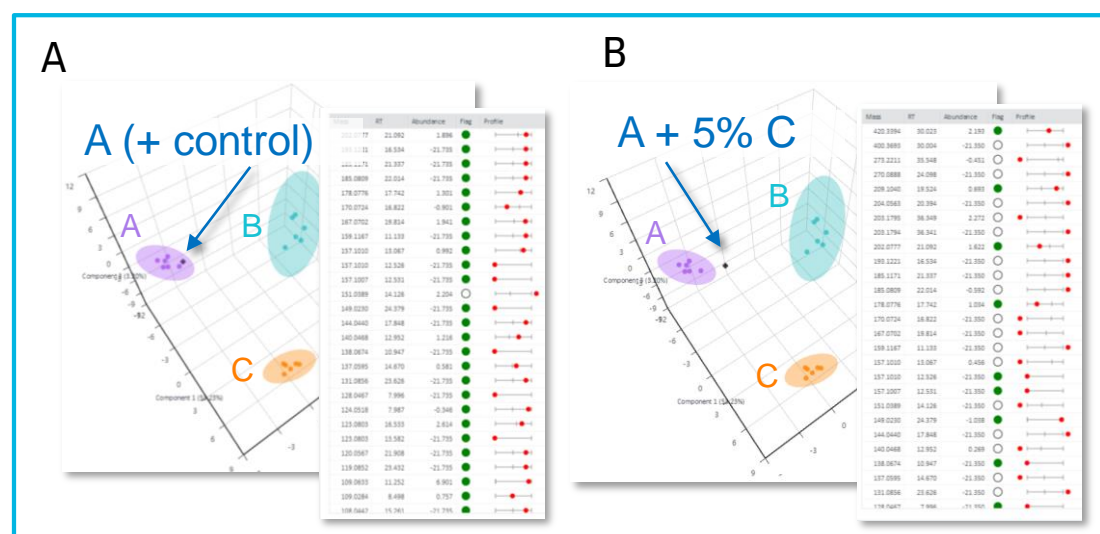


Figure 7. Results visualization in Classifier

SIMCA model was able to successfully distinguish pure samples A from other brands, including one not considered in the model (D), as well as yerba A adulterated with various levels of yerba C (Figure 8).

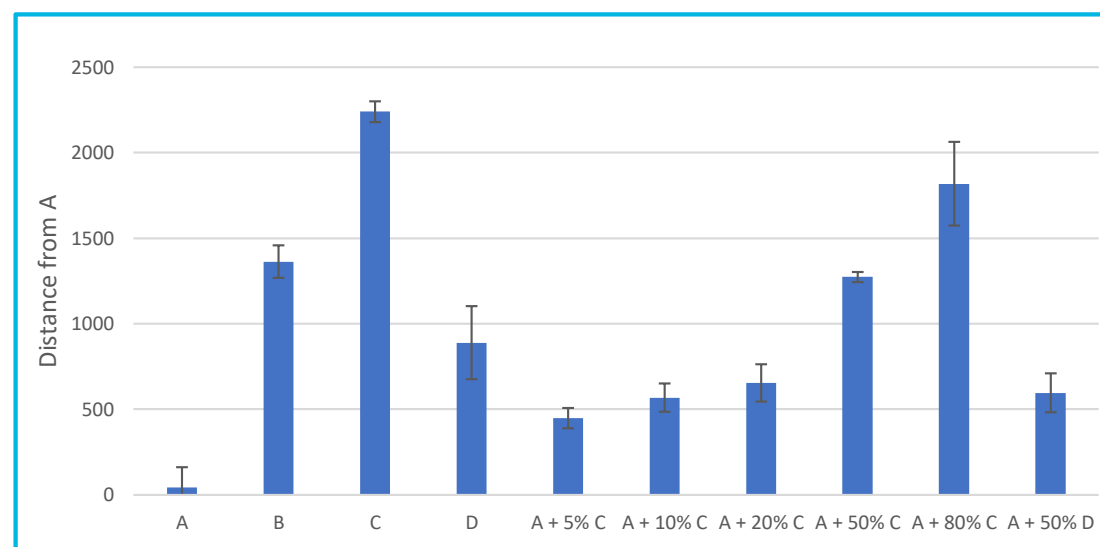


Figure 8. Classification results using SIMCA model. The distance from sample A is displayed

Conclusions

- Novel classification workflow for yerba mate authenticity using high-resolution GC/Q-TOF and Classifier software has been demonstrated.
- A classification model was able to distinguish between different brands of yerba mate as well as “adulterated” yerba mate samples
- Several PAHs have been identified in yerba mate extracts.
- A variety of flavor compounds were identified predominantly in brand A

Poster Reprint

ASMS 2020

MP 399

Assessment of a Metabolomics Automated Sample Prep Platform for Low Volume Plasma Samples

Mark Sartain¹, Manuel Gomez¹, Genevieve
Van de Bittner¹, Henry Shu¹

¹Agilent Technologies, Inc., Santa Clara, CA,
USA

Introduction

In basic and translational research settings, sample preparation prior to LC/MS based analysis of plasma metabolites is challenging for several reasons including the presence of compounds with different physical properties, variability between operators and inter-day reproducibility. Additionally, in some research settings limited amounts of plasma can be obtained from infants/children or from animal models. Here we evaluate a modification to an existing automated metabolomics sample prep method to accommodate low volume plasma samples (25 μL). This method precipitates plasma proteins to quench enzymatic activity, depletes lipids, and extracts metabolites, providing a clean metabolite sample for LC/MS analysis. With this modified protocol we evaluated metabolite recovery and reproducibility compared to a manual preparation processed by multiple laboratory staff.

Experimental

Samples and Reagents

A single healthy pooled human plasma sample (BioIVT) was used for all experiments. Chemical standards from the MSMLS library (IROA Technologies) were individually acquired with the LC/MS method to obtain retention times and MS/MS spectra. Unlabeled and ^{13}C -labeled yeast metabolite extracts ("ISO1-UNL" and "ISO1", Cambridge Isotopes) were used to aid in metabolite identification. ISO1 was additionally used as a spike-in for recovery estimation and normalization purposes.

Software

Compounds confidently identified in plasma and yeast samples were used to create a subset Personal Compound Database and Library (PCDL) from the Agilent METLIN PCDL. The custom PCDL with curated retention times was imported by Agilent MassHunter Quantitative Analysis software (Ver 10.1) to easily create a quantitative method.

Method and Workflow Overview

Beginning with the Agilent Bravo Metabolomics Sample Prep Platform¹, modifications were made to the protocol that include reducing the starting plasma volume from 100 μL to 25 μL :

Experimental

Low Volume Plasma Protocol On-site version

Plasma, 25 μL per well is placed in Bravo 96-well plate

Transfer 112.5 μL 1:1 ethanol/methanol to plasma, pipet mix and shake, wait 10 min

Transfer 87.5 μL water to quenched plasma, pipet mix and shake, wait 10 min

Transfer sample to Captiva EMR-lipid plate

Remove proteins and lipids. Collect metabolites in filtrate.

Wash Captiva EMR-lipid plate twice with 250 μL 2:1:1 water/ethanol/methanol. Collect metabolites in filtrate

Dry samples (optionally store).

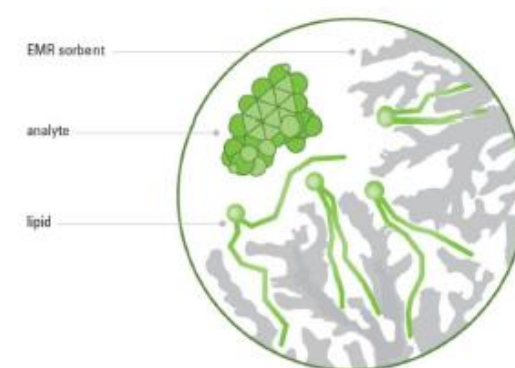
Reconstitute samples in 100 μL suitable LC/MS solvent

LC/MS Analysis

Bravo automation steps shown in green



Captiva EMR-Lipid 96-well plate traps lipids efficiently



InfinityLab Poroshell 120 HILIC-Z column



6546 LC/Q-TOF System

A 1260 Infinity II Prime LC system was coupled to a 6546 LC/Q-TOF with a Jet Stream ionization source. Negative-ion mode LC conditions and MS parameters were very similar to those previously described².

Tiered Selection of Targets Provide Confident Metabolite IDs

An approach was taken to select only the most confident metabolite identifications for the following studies (Fig 1).



Figure 1. Metabolite selection strategy

Method Provides Overall Excellent Metabolite Recoveries

The ISO1¹³C-labeled yeast extract was spiked into plasma before and after low volume Bravo metabolite extraction. The ¹³C-compound peak area ratios from six pairs of pre- and post-spiked samples were used to calculate recovery.

Fig 2 shows example chromatograms for two metabolites. Fig 3 shows a histogram summarizing the recoveries, and Table 1 lists individual results. Excellent recoveries (>80%) were observed for 28 of the 32 compounds covering diverse chemical classes. One compound showed poor recovery (D-fructose 1,6-bisphosphate, 38.7%). However, this compound was considered nonendogenous as it was not found at detectable levels in plasma.

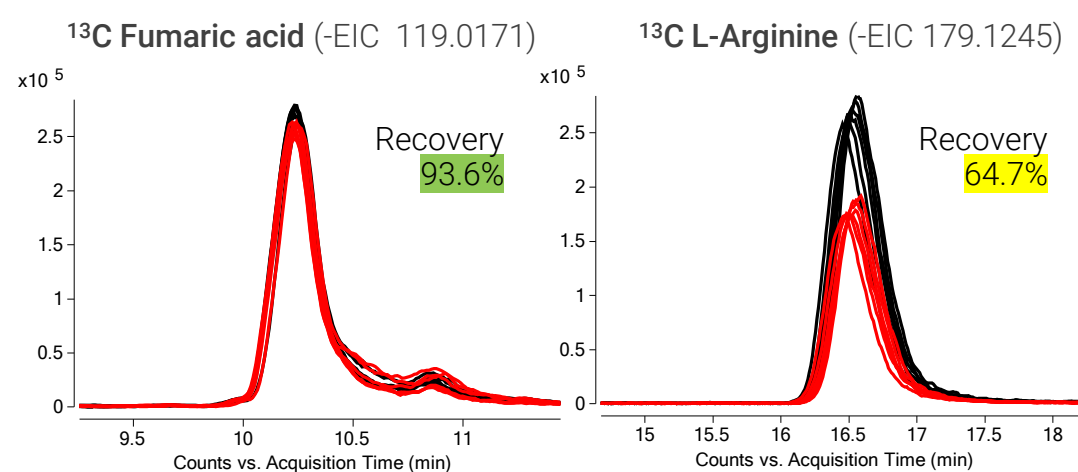


Figure 2. Example EICs for two selected metabolites across 6 pre-spike samples (red) and 6 post-spike samples (black)

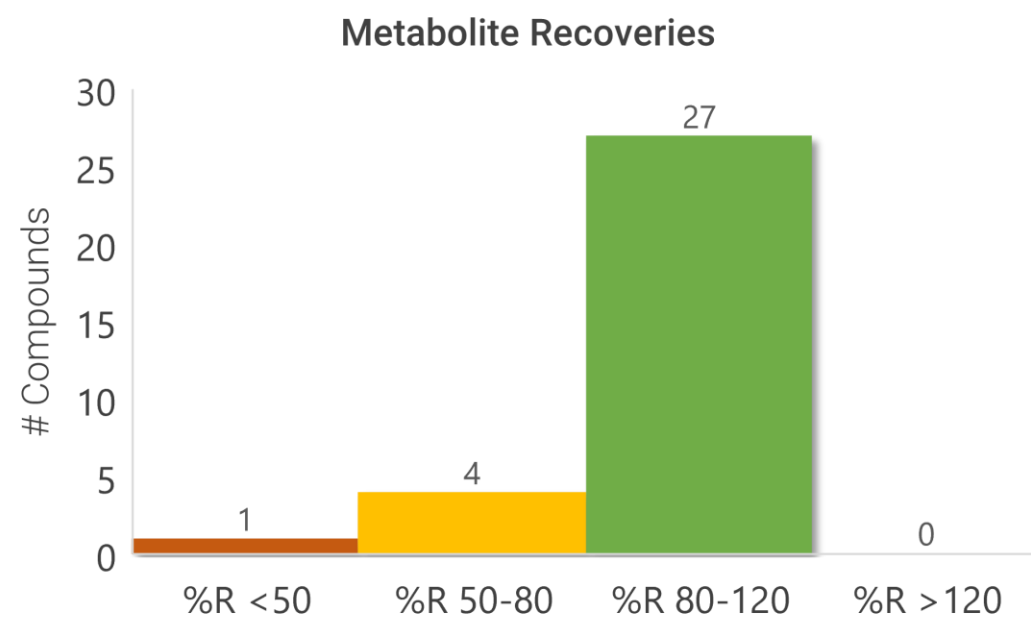


Figure 3. Summary of recoveries

Spiked ¹³ C Metabolite	Endogenous to Plasma	% Recovery	% RSD
Amino Acids and Derivatives			
Glycine	✓	91.6%	4.6%
L-Alanine	✓	89.2%	1.6%
L-Arginine	✓	64.7%	2.4%
L-Asparagine	✓	87.2%	8.4%
L-Aspartic Acid	✓	91.6%	5.6%
L-Citrulline	✓	88.1%	3.0%
L-Glutamic acid	✓	92.5%	5.1%
L-Glutamine	✓	91.0%	3.3%
L-Histidine	✓	90.0%	6.3%
L-Isoleucine	✓	84.4%	9.2%
L-Leucine	✓	84.8%	6.2%
L-Proline	✓	90.1%	4.8%
L-Serine	✓	96.1%	7.8%
L-Threonine	✓	91.1%	1.8%
L-Tryptophan	✓	94.6%	8.1%
L-Tyrosine	✓	84.5%	6.1%
L-Valine	✓	78.6%	8.9%
SAH / S-Adenosyl-L-homocysteine	✓	90.3%	8.6%
Nucleobases, Nucleosides, and Nucleotides			
Adenine	✓	77.1%	13.2%
5'-AMP / Adenosine 5'-monophosphate	✓	89.9%	18.1%
IMP / Inosine 5'-monophosphate	✓	84.3%	16.4%
Uridine	✓	101.2%	10.3%
Organic Acids			
alpha-Ketoglutaric acid	✓	95.5%	10.2%
Fumaric acid	✓	93.6%	6.9%
D-Gluconic acid	✓	92.7%	6.8%
Malic acid	✓	84.7%	9.1%
Sugars, Sugar Alcohols, and Sugar Phosphates			
D-Arabitol	✓	92.3%	2.5%
D-Fructose 1,6-bisphosphate	✓	38.7%	11.9%
D-Mannose 6-phosphate	✓	72.8%	12.7%
Trehalose	✓	84.1%	9.4%
Vitamins and Coenzymes			
Nicotinamide adenine dinucleotide (NAD)	✓	81.3%	7.3%
Average		86.2%	8.2%

Table 1. Metabolite Recoveries

Automation Improves Reproducibility



versus



**Manual
Preparation
3 Users**

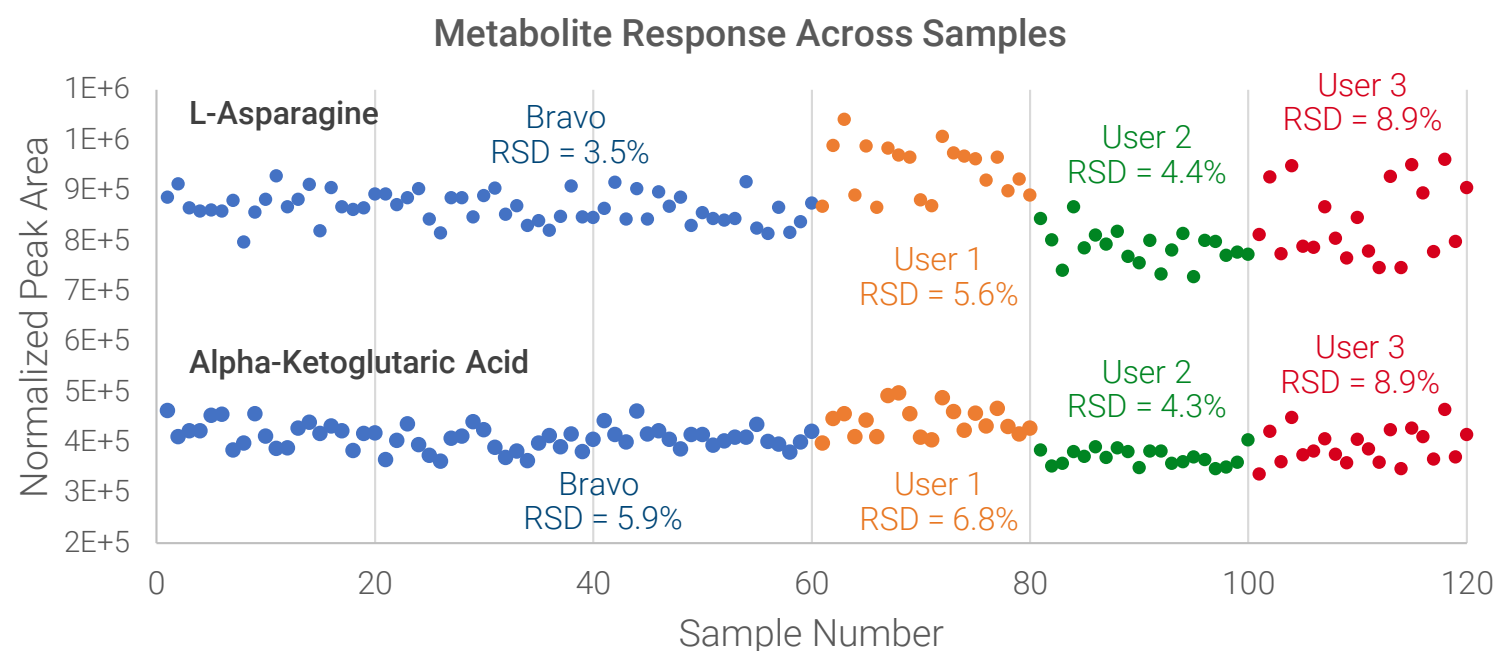


Figure 4. Normalized peak area % RSDs for L-asparagine and alpha-ketoglutaric acid (the actual injection order was randomized)

The performance of the automated method was compared against manual preparation. Sixty 25- μ L plasma samples were processed with the low volume plasma protocol using the Bravo instrument. A manual version of the protocol, with the same key steps, was provided to three experienced technicians and each processed twenty samples. Prior to drying and reconstitution, a ^{13}C metabolite extract was added for normalization purposes to remove effects from LC/MS instrument variation. The sample injection order was randomized. Fig 4 shows results for two representative metabolites, and Table 2 summarizes the results for all metabolites. Bravo metabolite extraction reproducibility was comparable to User 2, and outperformed User 1 and 3. For all metabolites, the Bravo % RSDs were significantly lower than the combined % RSDs for the 60 manually-prepared samples across the three users.

	Bravo n=60	User 1 n=20	User 2 n=20	User 3 n=20	Users Combined n=60
α -Ketoglutaric acid	5.9%	6.8%	4.3%	8.9%	10.2%
Fumaric acid	7.5%	5.2%	7.0%	9.8%	10.3%
Glycine	4.1%	6.2%	5.2%	7.3%	9.1%
L-Alanine	5.5%	8.0%	4.9%	9.8%	11.4%
L-Arginine	6.0%	7.6%	5.7%	13.8%	12.6%
L-Asparagine	3.5%	5.6%	4.4%	8.9%	9.9%
L-Aspartic Acid	3.9%	6.2%	4.7%	9.4%	9.7%
L-Citrulline	3.1%	5.5%	2.6%	8.5%	9.4%
L-Glutamic acid	3.3%	6.4%	2.8%	9.4%	10.3%
L-Glutamine	3.6%	5.1%	2.8%	9.4%	10.1%
L-Histidine	3.2%	4.6%	2.7%	8.3%	8.5%
L-Isoleucine	7.0%	8.5%	5.2%	10.6%	11.1%
L-Methionine	5.1%	6.6%	3.4%	8.3%	10.6%
L-Ornithine	4.9%	6.8%	6.2%	13.2%	12.3%
L-Proline	6.6%	8.9%	5.3%	11.6%	12.4%
L-Serine	3.6%	5.3%	5.2%	8.5%	9.4%
L-Threonine	4.7%	5.0%	4.2%	10.5%	10.5%
Malic acid	5.0%	4.9%	4.4%	6.8%	7.5%
Average	4.8%	6.3%	4.5%	9.6%	10.3%

Table 2. Normalized peak area % RSDs across metabolites

Conclusions

We describe modifications to the Agilent Bravo Metabolomics Sample Prep Platform that reduce the required starting plasma volume from 100 μ L to 25 μ L. Excellent metabolite recovery with the method was demonstrated across representative chemical classes of compounds. We also showed that the automated method offers improved reproducibility when compared to a laboratory environment where multiple users manually processed samples.

References

¹Automated Metabolite Extraction for Plasma using the Agilent Bravo Platform. *Agilent Technologies Technical Overview*, publication number [5994-0685](#), 2019.

²Discovery Metabolomics LC/MS Methods Optimized for Polar Metabolites. *Agilent Technologies Application Note*, publication number [5994-1492](#), 2019

For Research Use Only. Not for use in diagnostic procedures.

Poster Reprint

ASMS 2020

MP 417

Screening and Quantitation of Amino Acids and Other Nutrients In Spent Media

Swarnendu Kaviraj¹, Sunil Raut¹, Vikrant
Goel², Ashish Pargaonkar², Saikat Banerjee²

1. Genova Biopharmaceuticals Ltd., India

2. Agilent Technologies India Pvt Ltd.

Abstract

This poster demonstrates the usage of Agilent 1290 Infinity II LC system coupled with Ultivo LC/TQ Mass Spectrometry system to screen major nutrients as present in Spent Media. The method provide fast separation with low ppb level quantitation solution for researchers from fermentation industry.

Introduction

The spent medium is useful for some industries as a nutrient and for others it is a discarded liquor. Recent years has seen interest in knowing the components of such viscous liquids to understand nutritional uptakes from cultures at various stages of growth including amino acids, vitamins, sugars etc.

This poster describes a solution to the challenging task of screening constituents of spent medium by making usage of Agilent AdvanceBio MS Spent Media columns for normal phase separation of amino acids and small, polar metabolites in media samples⁽¹⁾. The zwitterionic phase bonded onto superficially porous silica particles supported efficient and reproducible separations of small, charged molecules⁽²⁾. The Ultivo LC/TQ system supported quantitation of 24 analytes of interest focus in MRM scan mode.



Figure 1: Ultivo LC/TQ and Advance Bio columns

Sample Preparation

Amino Acid Supplement Kit (Agilent P No 5062-2478), Amino Acids Standard (Agilent P No 5061-3330) and Vitamin B compounds were diluted with 1% FA in 50/50 ACN/H₂O for stock and working concentration. The spent media samples were diluted upto 100X.

Reagents and Chemicals

All LCMS grade chemical were purchased from Honeywell.

Ultivo LC/TQ Conditions

Ionization Source = Agilent Jet Stream
 Nebulizer Gas = 20psi
 Drying Gas = 12L/min at 150° C
 Sheath Gas = 12L/min at 390° C
 Capillary Voltage = +/- 2000 V
 Nozzle Voltage = +/- 0 V

UHPLC Conditions

Mobile Phase A = 20mM Amm Acetate with 0.1%FA
 Mobile Phase B = 20mM Amm Acetate in 90% ACN

Parameter	Value
Column	Agilent AdvanceBio MS Spent Media, 2.1x100 mm (Agilent P No - 675775-901)
Flow Rate	300 µl/min
Injection Vol	10 µL
Column Temp.	25° C

Time (min)	% B
0.0	100
11.5	70
12.0	40
13.0	40
13.5	100
20.0	100

Table 1: HPLC parameters and gradient program

Results and Discussion

In this study 21 amino acids and 3 compounds from Vit B (table 2) showed good chromatographic separation in a total runtime of 20 min, as seen in fig 2. A calibration plot with minimum 5 level was generated from 1ppb to 1ppm with variable LOQs of 1ppb to 20ppb and R2 values between 0.993 to 0.999 with representative plots shown in Fig 3.

#	Analyte	#	Analyte	#	Analyte
1	Alanine	9	Glutamine	17	Phenylalanine
2	Arginine	10	Histidine	18	Proline
3	Asparagine	11	Hydroxyproline	19	Sarcosine
4	Aspartic Acid	12	Leucine	20	Serine
5	Cyanocobalamin	13	Lysine	21	Threonine
6	Cystine	14	Methionine	22	Tryptophan
7	Folic Acid	15	Nicotinic Acid	23	Tyrosine
8	Glutamic Acid	16	Norvaline	24	Valine

Table 2: 24 Compounds as quantified in methodology

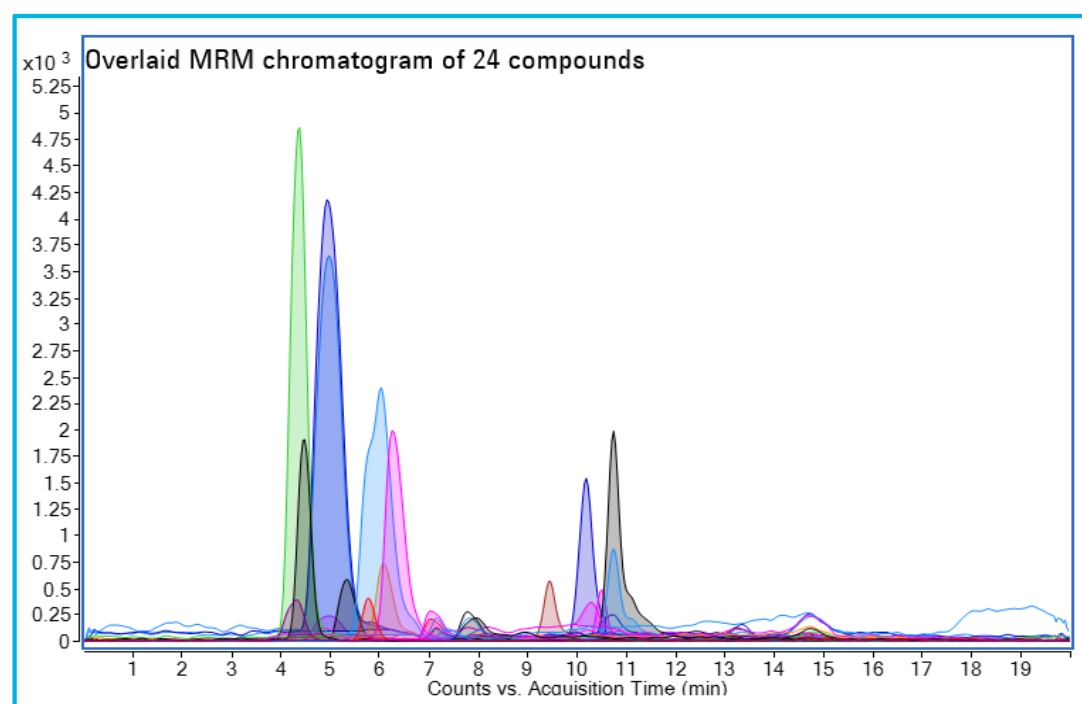


Figure 2: Chromatographic separation of 24 analytes

Spent media samples were taken at every 24 hour across 10 days, labelled as S1 to S10. The 24 nutrients were quantified in 10x, 100x diluted spent media samples. TIC profiles as seen in fig 4 confirm that there are differences in abundance of nutrients on Zero time (100x_Med) vs 8 day (S8_100).

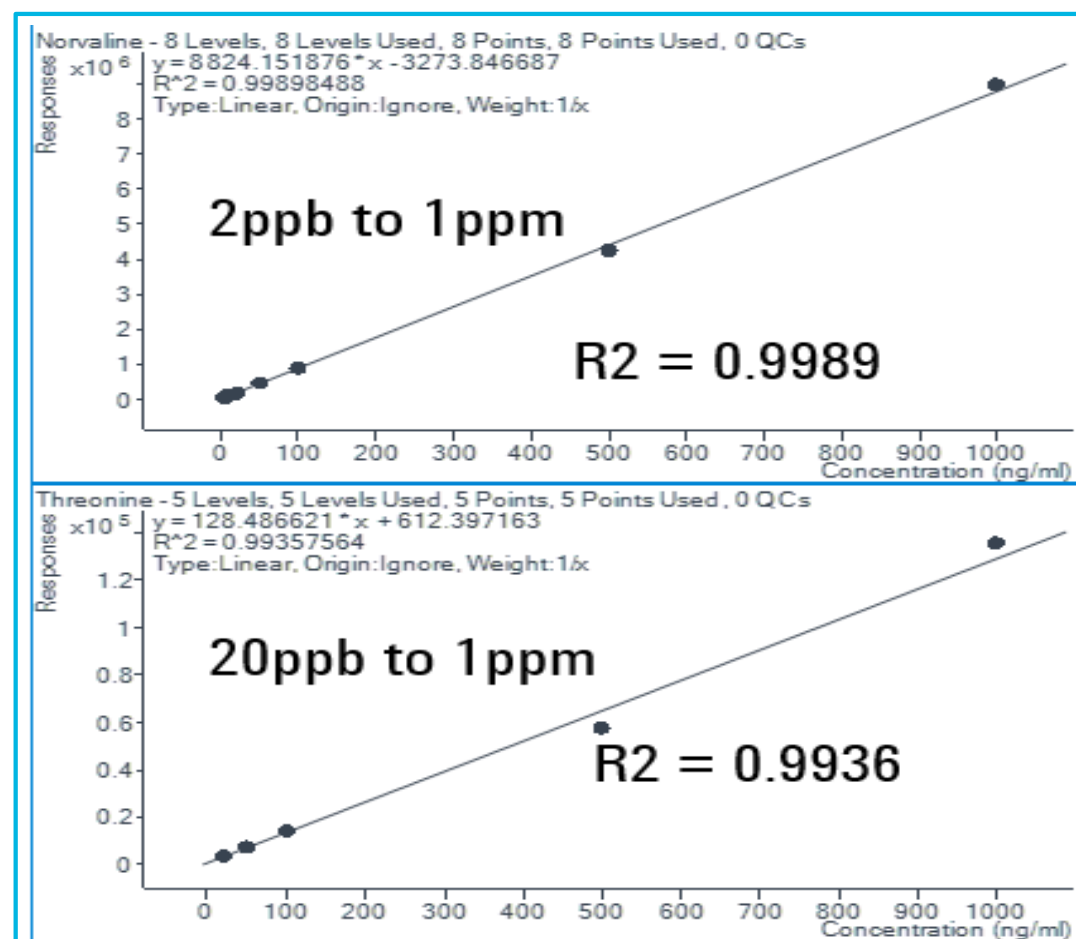


Figure 3: Calibration plots with R2 from 0.993 to 0.999

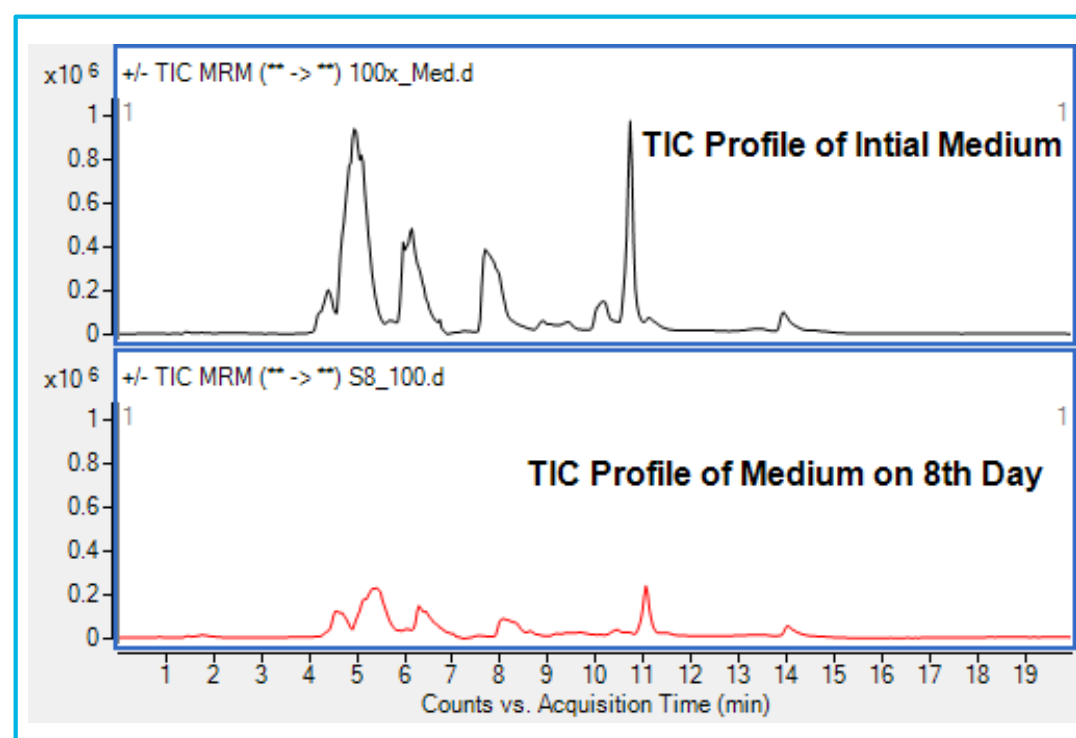


Figure 4: TIC profile comparison of Spent Media sample at Initial Medium *s 8th day.

The 24 analytes had variable responses for 100X dilution as seen for 8th day sample in Fig 5. All analytes, present in Initial sample to 10 days samples, were quantified using Mass Hunter Quant-My-Way s/w with $\pm 20\%$ accuracy and Qualifier/Quantifier Ion response ratio. Bar chart of analyte vs media sample, as plotted for Aspartic Acid, Methionine, Proline and Sarcosine as representative plots confirms the behavior, as seen in fig 6.

Results and Discussion

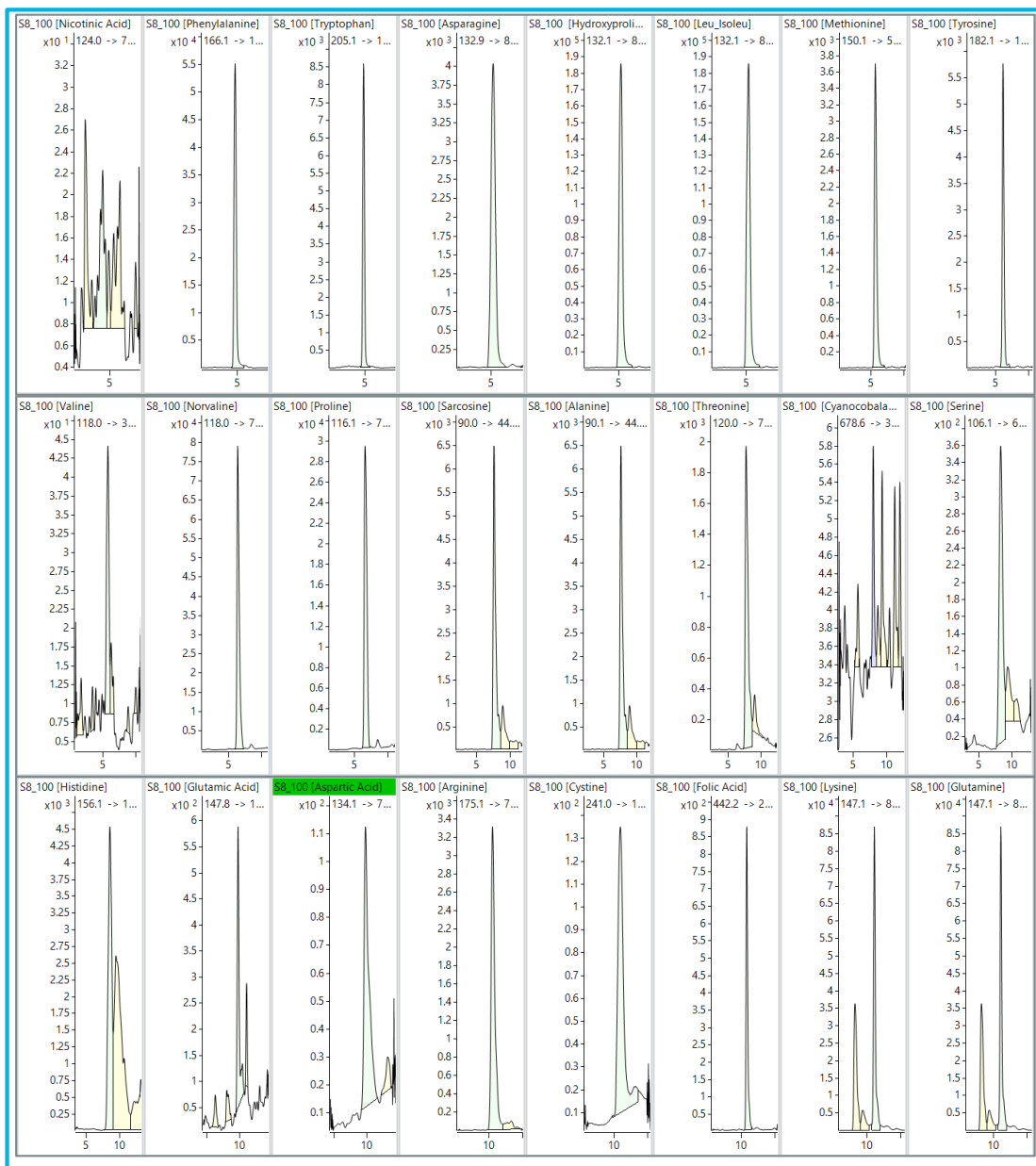


Figure 5: MRM Chromatogram from 100x diluted Spent Media sample on day 8, having good response of 22 metabolites.

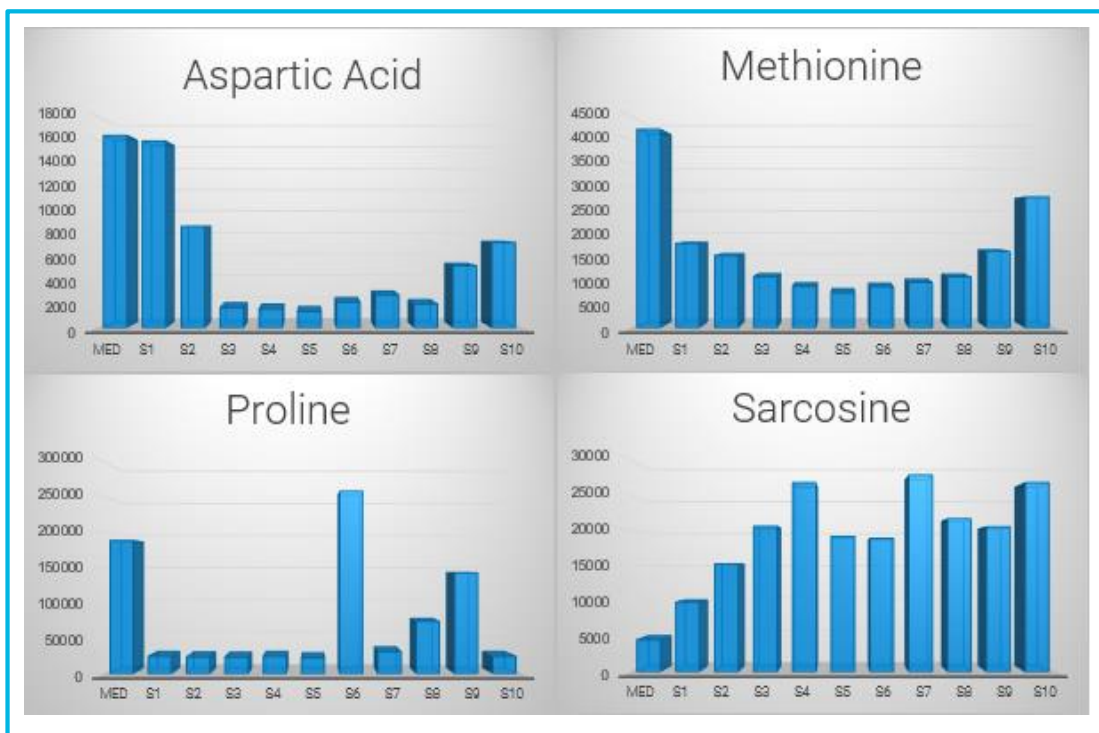


Figure 6: Variable amount of 4 representative nutrients in ng/ml (ppb) from initial stage (Med) to day 10 (S1, S2...S10) of spent media.

Conclusions

- Low ppb (picogram quantity) level analytical sensitivity of nutrients attained using Triple Quadrupole LC/TQ.
- Fast chromatographic separation is achieved for amino acids and vitamin B compounds.
- A cost effective and quick method requiring minimal sample preparation is proposed, since derivatization steps are not used.
- Expected variations in concentration level from ppb to ppm are well estimated.
- Spent Media samples must be 100 times diluted.
- Single dual polarity LC/TQ method for analytes.
- Method can be utilized by academia, research and other fermentation-based laboratories.

References

1. Agilent AdvancedBio workflows for spent media analysis; Agilent Publication No 5991-8817EN
2. Agilent AdvanceBio MS Spent Media Column, User Guide; Agilent Publication No 820120-015

For Research Use Only. Not for use in diagnostic procedures.

Poster Reprint

ASMS 2020
MP 477

Analysis of Vitamin E and Vitamin E Acetate in Hemp Vaping Oil Products

Sue Dantonio¹; Robert A. Dantonio²; Nikolas Lau³

¹Agilent Technologies, Cedar Creek, TX;
²Texas A & M University, Corpus Christi, Texas; ³Agilent Technologies, Chicago, IL

Introduction

Vitamin E and vitamin E acetate are sometimes used in the production of eCigarettes and cannabinoid vaping oils. By December 2019, more than 2400 hospitalizations occurred in the U.S. for Electronic-cigarette, or Vaping, product use-Associated Lung Injury (EVALI) with an interstate study indicating 94% of the EVALI cases were positive for vitamin E acetate compared to 0/99 “healthy comparator” controls [1]. To support these studies, manufacturers and regulatory agencies need a quick, simple and accurate method for additionally testing relevant vaping products for vitamin E and vitamin E acetate. Herein, we adapted a published cannabinoid method for hemp analysis [2] to simultaneously identify and quantify vitamin E acetate and vitamin E.

Experimental

Five samples of commercially-available vaping oil were diluted 1000-fold and analyzed using an Agilent LC/MSD iQ system with an ESI source and OpenLab CDS 2.4 Software. Chromatographic conditions were optimized by adapting a published methodology [3] of a 16 cannabinoid mixture to improve analysis speed while maintaining separation (Figure 1). For identification and quantification of the vitamin E compounds, m/z 431.1 and 473.2, were monitored in addition to the cannabinoid compounds.

16 cannabinoid UV method

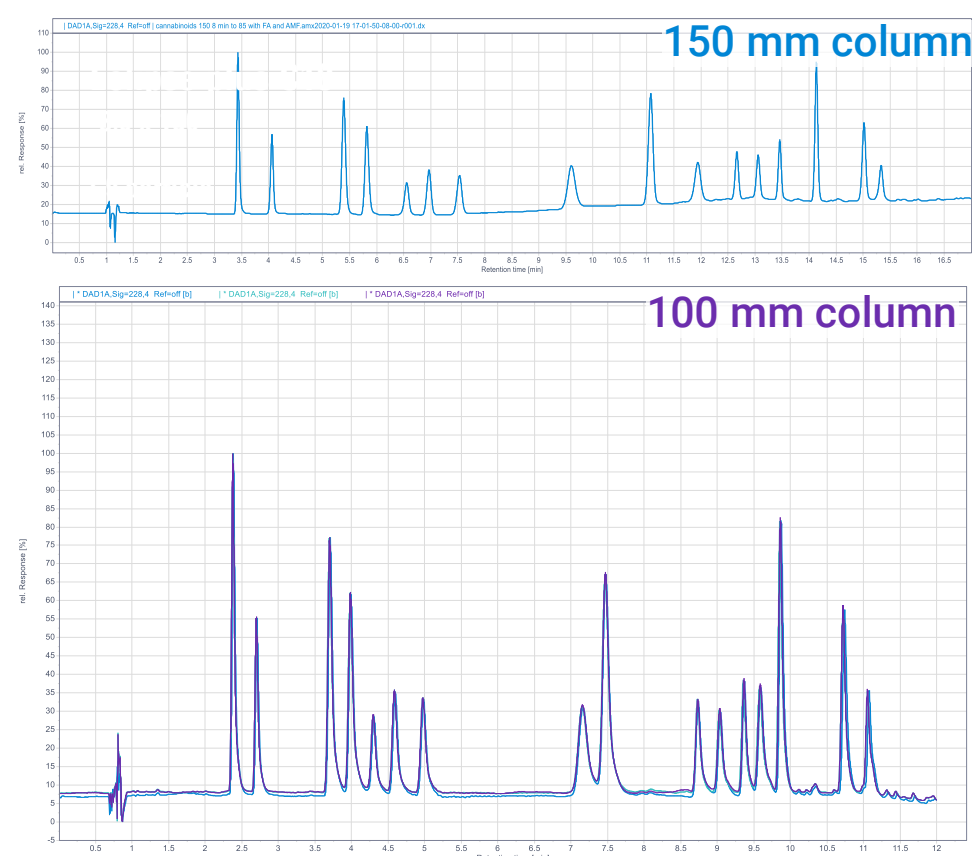


Figure 1: The upper UV chromatogram utilized the published [3] 150 mm column for an elution period of 15.5 minutes; the lower UV chromatogram utilized a 100 mm column for an 11 minute elution period.

Experimental

Analytical Method

Parameter	Value			
Column	Agilent Poroshell 120 EC-C18, 3.0 × 100 mm, 1.9 μm @ 30.0 °C			
Flow rate	0.500 mL/min			
Solvent A	0.1% Formic Acid in H ₂ O			
Solvent B	100% ACN			
Solvent C	100% MeOH			
Solvent D	10 mM NH ₄ HCO ₂ in H ₂ O			
Gradient	%A	%B	%C	%D
Time: 0.0	29	70	0	1
3.20	29	70	0	1
7.20	12	0	87	1
10.00	0	0	95	5
Post Time	5 minutes			
UV Signal	228 nm			

MS Parameter	Value
Mode	Positive Ion
Gas Temp.	325 °C
Gas Flow	13 L/min
Nebulizer Pressure	55 psi
Capillary Voltage	3500 V
Acquisition	SIM/Scan

MS Signals	Value	
Scan	200-700 m/z, 89 ms, Frag=110V 300-700 m/z, 71 ms, Frag=110V	
SIM (m/z)	Vit. E. Acetate: 495.4	CBG: 317.2
Time = 15 ms	Vitamin E: 473.4	CBD, THC (ISO): 316.5
Frag = 135V	CBGA: 361.2	THC CBD CBL CBC: 315.2
	CBCA THCA CBDA: 359.2	CBN: 311.2
	CBNA: 355.1	CBDV, THCV: 287.2
	CBDVA THCVA: 331.2	

Analytical Configuration



Figure 2: Analytical Configuration: Agilent 1260 HPLC with mass detection using the LC/MSD iQ

Calibration Curve - Vitamin E Acetate.

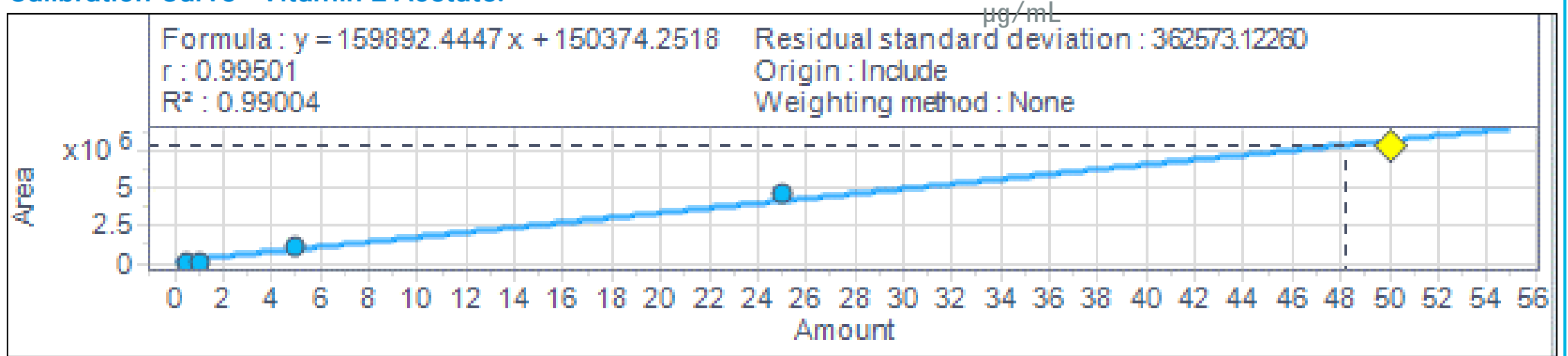
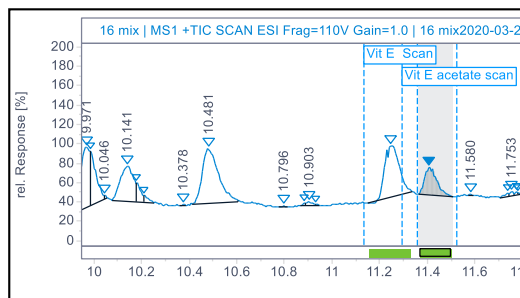


Figure 3: Calibration Curve – Vitamin E Acetate

Spectral library confirmation: Spectral matching and purity results

Peaks #	Summary Name	Signal description	RT (min)	MS Conf. Matcl	MS Purity
74	Vit E acetate scan	MS1 +TIC SCAN ESI Frag=110V Gain...	11.409	1000	100.00
73	Vit E Scan	MS1 +TIC SCAN ESI Frag=110V Gain...	11.248	1000	100.00



Spectral matching is compared to a known reference spectra. Scan data was used for the library search. 1000 == 100% match compared to the library. Unknown spectra can be exported and searched against the library.

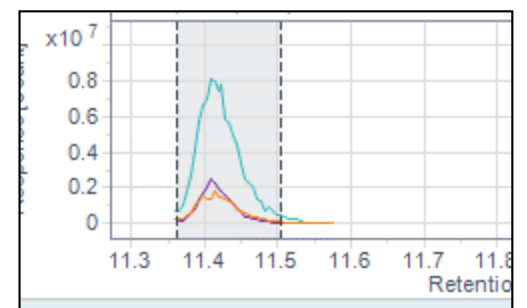


Figure 4: Spectral Library Matching of Vitamin E and Vitamin E Acetate

LOD and LOQ based on SIM data.

Analyte	LOD	LOQ
Vitamin E	0.010 µg/mL	0.025 µg/mL
Vit. E acetate	0.010 µg/mL	0.025 µg/mL

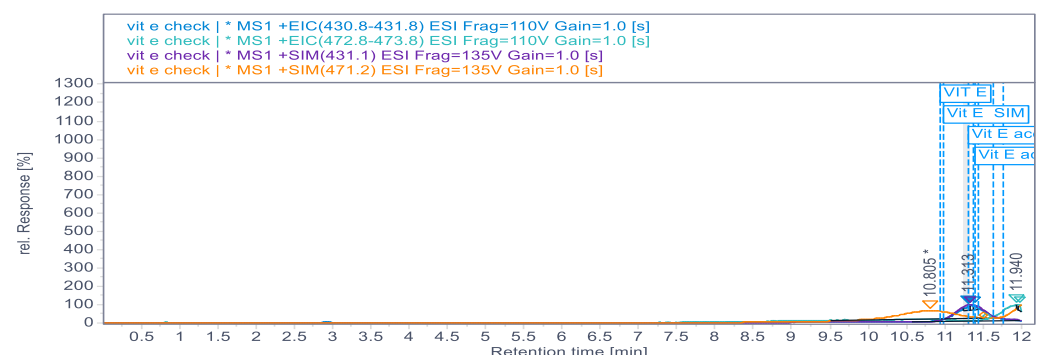


Figure 5: Limits of Detection and Limits of Quantitation for Vitamin E and Vitamin E Acetate by LC/MSD iQ

SIM ions of spiked chromatogram

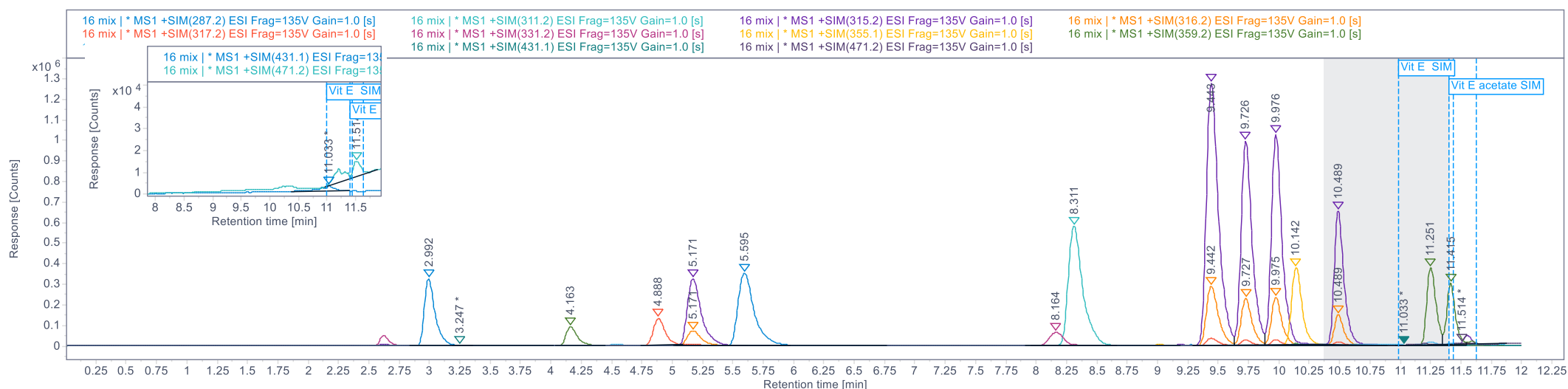


Figure 6: Overlay of all SIM ions in spike of vitamin E and vitamin E acetate into 16 cannabinoid mix in hemp seed oil

Analytical Results (n.d. = not detected)

Sample #	Vitamin E	Vitamin E acetate
1	n.d	0.06 ug/ml
2	n.d.	0.04 ug/ml
3	n.d.	n.d.
4	n.d	n.d
5	0.09 ug/ml	0.02 ug/ml
6	n.d.	0.09 ug/ml
7	n.d.	0.05 ug/ml
8	0.04 ug/ml	0.07 ug/ml
9	n.d	0.05 ug/ml
10	n.d	0.02 ug/ml
11	n.d	0.03 ug/ml
12	n.d	1125 ug/ml

Larger calibration curve was created for a commercial sample of vitamin E acetate oil.

Conclusions

In this study, vitamin E acetate and vitamin E was appended to a previously published method for the quantitation of cannabinoids in hemp seed oil. Low PPM LOD and LOQ values were established in this matrix.

The results determined that, without changes to the published method, vitamin E and vitamin E acetate can be appended for identification and quantification in vaping oil samples. Further, the full scan data of the unknown samples were successfully used with a known library to identify vitamin E and vitamin E acetate in the samples.

References

- [1] Blount BC, et al. (2020) Vitamin E Acetate in Bronchoalveolar-Lavage Fluid Associated with EVALI. N Engl J Med. 382(8):697-705.
- [2] D'Antonio S, et al. (2020) Quantitation of Phytocannabinoid Oils Using the Agilent Infinity II 1260 Prime/InfinityLab LC/MSD iQ LC/MS System. Agilent Application Note 5994-1706EN, Agilent Technologies, Inc.
- [3] Kowalski, D. Laine, Improved Routine Cannabinoids Analysis with Liquid Chromatography-Diode Array Ultraviolet Detection for the Current Cannabis Market, Oral presentation, AOAC International Conference, August 26- August 29, Toronto, Ontario, Canada, 2018.

Agilent products and solutions are intended to be used for cannabis quality control and safety testing in laboratories where such use is permitted under state/country law.

Poster Reprint

ASMS 2020

MP 499

High Throughput Native MS With Robust Ion Source Operation For The Analysis Of Proteins And Protein Complexes

Caroline S. Chu, Patrick D. Perkins, Christian
Klein

Agilent Technologies, Santa Clara, CA USA

Introduction

Native mode proteins and protein complexes are typically analyzed using nanospray techniques or at capillary LC flow rates with gentle ionization conditions to achieve best responses and preserve the native conformations. However, a few recent publications suggest that higher flow LC/MS techniques perform acceptably well for native mode protein and protein complexes¹. The current work was undertaken to examine this feasibility in detail.

Experimental

Samples

Protein standards were obtained from MilliporeSigma and used as received. Typical protein concentration was 20 μ M based on the molecular weight of the protein or protein complex, dissolved in 200 mM ammonium acetate.

Software

MassHunter versions 10 and 9.1 software were used for 6545XT AdvanceBio LC/Q-TOF and IM-QTOF acquisition control, respectively. MassHunter data processing software version 10 was used throughout (Qualitative Analysis, Quantitative Analysis, BioConfirm, IM-QTOF). For some processing, UniDec deconvolution software was also used^{2,3}.

LC: 1260 Infinity II Biolnert LC or 1290 Infinity II UHPLC, with 6-port valve and isocratic pump

Column flow was diverted to waste after the protein eluted to minimize fouling of the ion source by salts and low MW species. The isocratic pump was used to maintain flow to the Q-TOF during this time¹.



Figure 1. 10-port valve installed in column compartment, emulating a 6-port valve for diverting the salts and low MW species to waste.

Experimental

LC:

Parameter	Value
Column	AdvanceBio SEC guard column, 4.6 x 30 mm, 1.9 μ m, 200 \AA (PL1580-1201)
Mobile phase (both pumps)	200 mM ammonium acetate
Flow rate	0.1 mL/min
Column to waste at:	3.8 minutes
Column temp:	30 $^{\circ}$ C
Stop time	6.0 minutes
Injection volume	1.0 μ L

Parameter	Value
Nebulizer pressure	60 psig
Nozzle voltage	2000 V
Capillary voltage	5500 V
Sheath gas temperature	400 $^{\circ}$ C
Sheath gas flow	12 L/min
Drying gas temperature	350 $^{\circ}$ C
Drying gas flow	12 L/min

MS: 6545XT AdvanceBio LC/Q-TOF or 6560 IM-QTOF

Parameter	Value
Fragmentor	250 V
Skimmer (6545XT Q-TOF only)	90 V
Quad AMU setting	400 or 700
Trap RF (IM-QTOF only)	200 V
Collision energy	0 V
Mass range	m/z 90-10,000 or m/z 790-14,100
Acquisition rate	0.5 spectra/sec

Source parameter optimization using yeast alcohol dehydrogenase (ADH) tetramer

Repetitive injections of ADH tetramer were made, varying source parameters to locate the optimum response. The highest signals were obtained with high gas temperatures and flows.

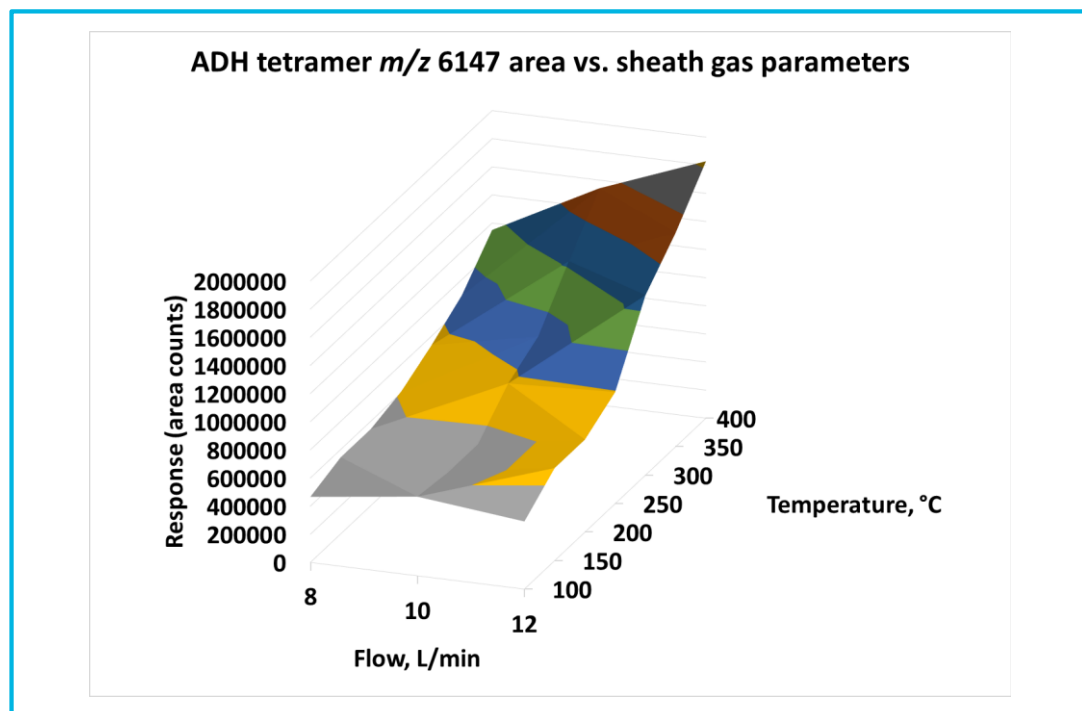


Figure 2. Example of the response of ADH tetramer (m/z 6147 area, 24+ charge state) to sheath gas parameters temperature and flow.

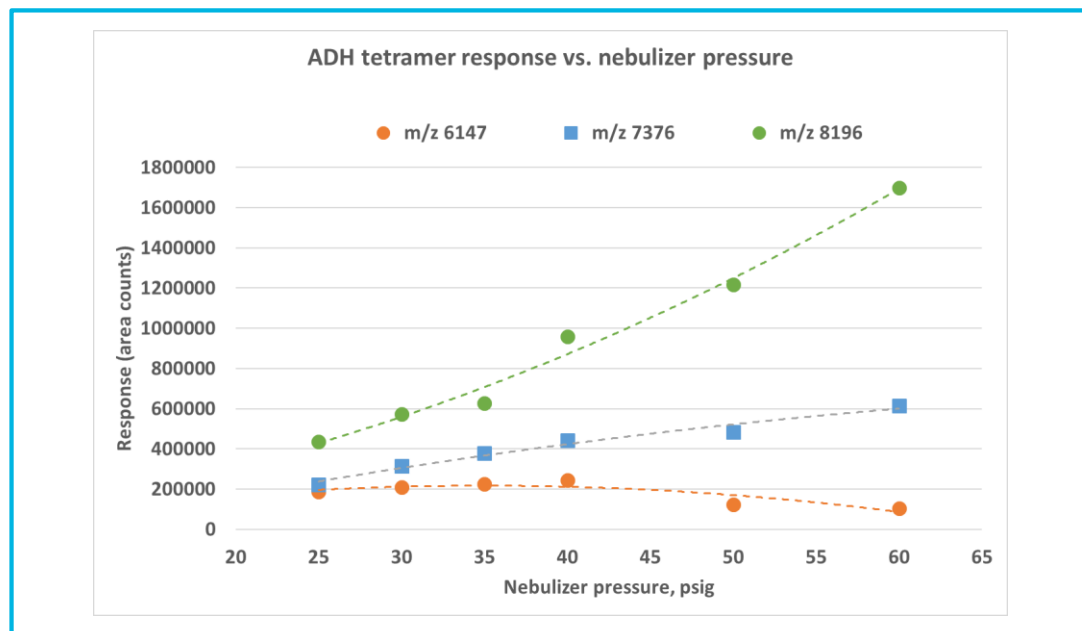


Figure 3. Response of ADH tetramer m/z 6147 (24+), m/z 7376 (20+), m/z 8196 (18+) to nebulizer pressure. Overall response increased with increasing nebulizer pressure.

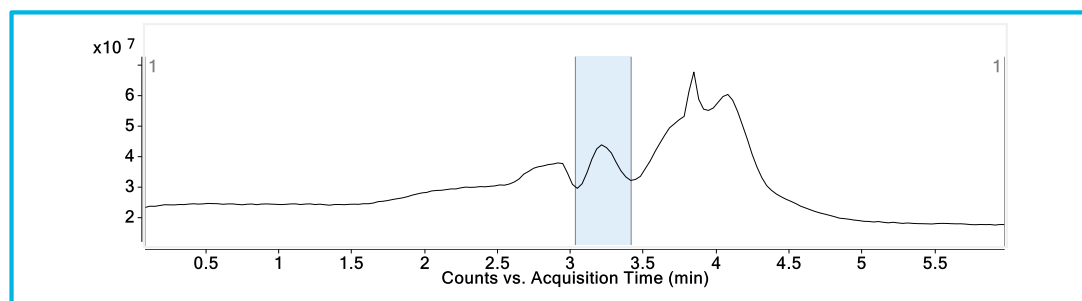


Figure 4. TIC of ADH tetramer (elution region highlighted). The large response at the end of the analysis was due to small MW singly-charged species.

ADH tetramer (6545XT AdvanceBio LC/Q-TOF)

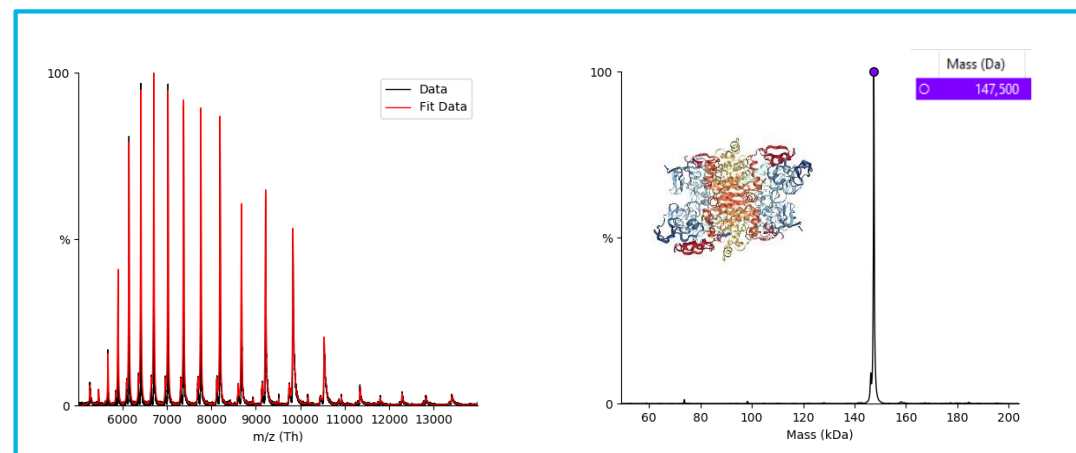


Figure 5. ADH tetramer (3 μ g on-column) spectrum and deconvoluted results (expected MW 147.5 kDa). An extended charge state envelope (\sim 26+ to 14+) was detected, more extensive than when using nanospray⁴. The cause is currently under investigation.

β -Galactosidase tetramer

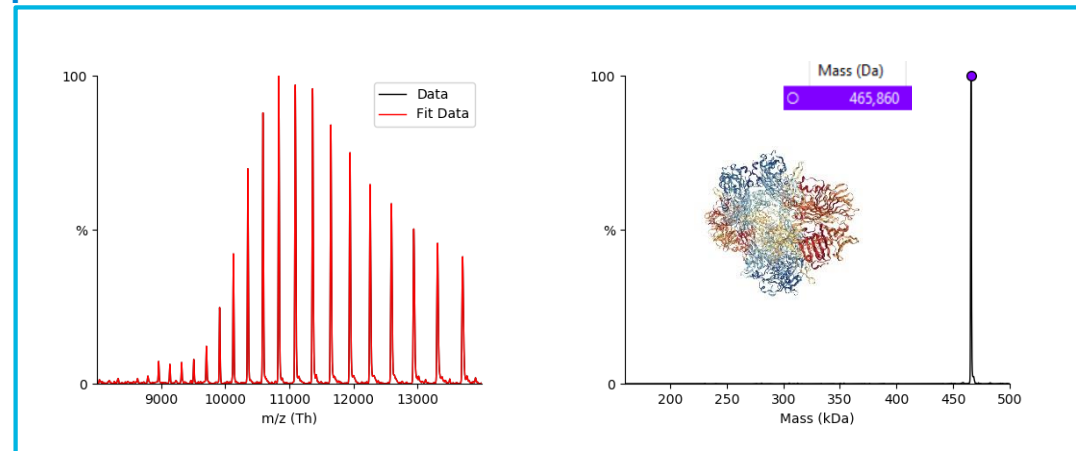


Figure 6. β -galactosidase tetramer (9 μ g) spectrum and deconvoluted results (expected MW 465 kDa).

NIST mAb

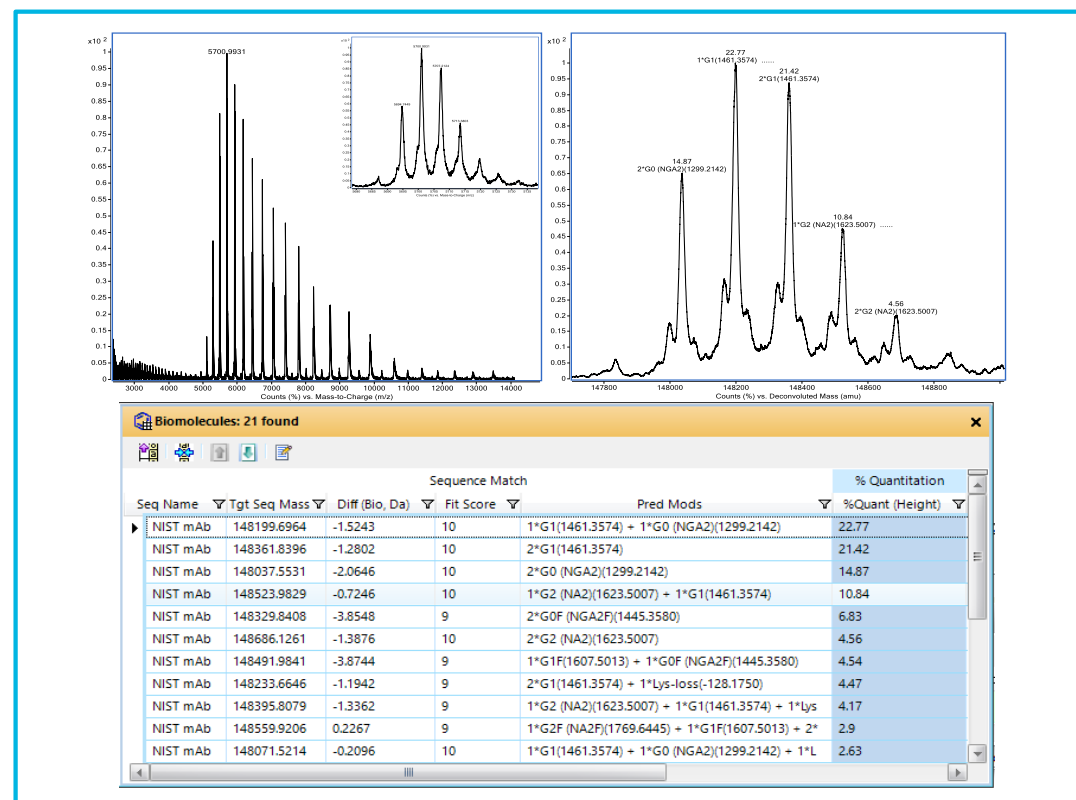


Figure 7. NIST mAb (3 μ g on-column) spectrum and deconvoluted results. Denaturation appeared to be minimal (peaks m/z 2500-4500). Several known modifications were identified (zoom view and table).

Results and Discussion

ADH tetramer (6560 IM-QTOF)

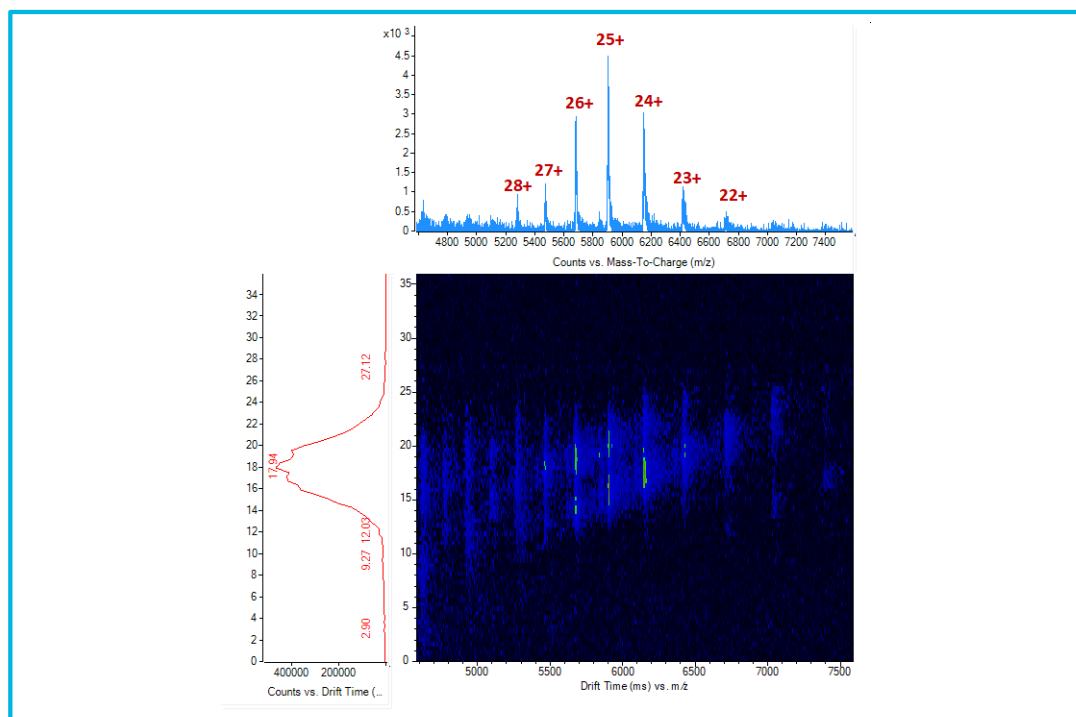


Figure 8. ADH tetramer by ion mobility Q-TOF, showing a spectrum with charge state assignments (top) and a full drift spectrum (left). Two species with overlapping charge states were apparent.

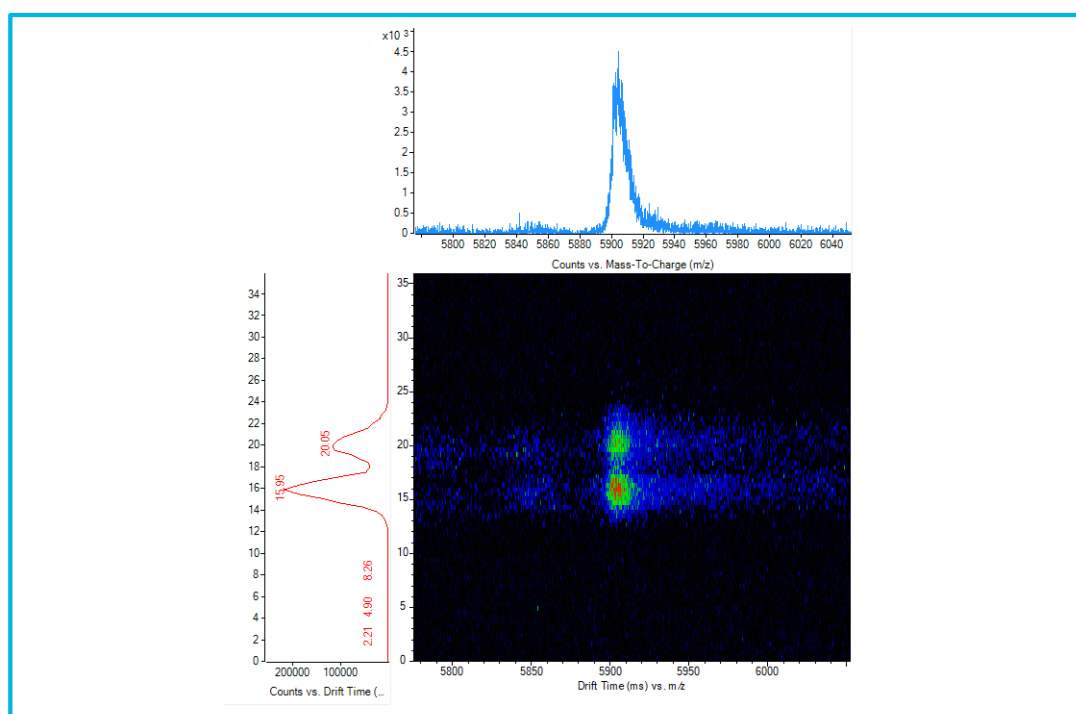


Figure 9. ADH tetramer showing charge state 25+ with two conformers.

The same ion source parameters were used on both instruments to obtain the ADH tetramer spectra shown in Figures 5 and 8. It is conjectured that the differences in charge state distribution may be due to different internal instrument/method parameters, different conformations or structures⁵ resulting from different sample preparations,... The cause of the differences is currently under investigation.

Conclusions

- Robust, routine analysis of protein and protein complexes in the native mode
- One set of ion source parameters was used throughout (though further optimization likely will improve the response for some species)
- Unattended operation, 6 minutes per sample
- An extended charge state envelope was present for many proteins/protein complexes

References

- ¹VanAernum, Z., Busch, F., Jones, B. J., Jia, M., Chen, Z., Boyken, S. E., Sahasrabudde, A., Baker, D., Wysocki, V.: Rapid Online Buffer Exchange: A Method for Screening of Proteins, Protein Complexes, and Cell Lysates by Native Mass Spectrometry. *ChemRxiv* (2019) doi.org/10.26434/chemrxiv.8792177.v1
- ²Marty, M. T., Baldwin, A. J., Marklund, E. G., Hochberg, G. K. A., Benesch, J. L. P., Robinson, C. V.: Bayesian Deconvolution of Mass and Ion Mobility Spectra: From Binary Interactions to Polydisperse Ensembles. *Anal. Chem.* **87**, 4370-4376 (2015) DOI:10.1021/acs.analchem.5b00140.
- ³Marty, M. T.: Eliminating Artifacts in Electrospray Deconvolution with a SoftMax Function. *J. Am. Soc. Mass Spectrom.* **30**, 2174-2177 (2019) DOI: 10.1007/s13361-019-02286-4.
- ⁴Schachner, L. F., Ives, A. N., McGee, J. P., Melani, R. D., Kafader, J. O., Compton, P. D., Patrie, S. M., Kelleher, N. L.: Standard Proteoforms and Their Complexes for Native Mass Spectrometry *J. Am. Soc. Mass Spectrom.* **30**, 1190-1198 (2019) DOI: 10.1007/s13361-019-02191-w.
- ⁵Raj, S. B., Ramaswamy, S., Plapp, B. V.: Yeast Alcohol Dehydrogenase Structure and Catalysis. *Biochem.* **53**, 5791-5803 (2014) DOI:10.1021/bi5006442.

For Research Use Only. Not for use in diagnostic procedures.

Poster Reprint

ASMS 2020

MP 574

An SLE-Based Workflow for the Analysis of the SAMHSA Oral Fluid Drug List by LC/TQ

Jennifer Hitchcock, Tina Chambers, Andre
Szczesniewski

Agilent Technologies, Santa Clara, CA, USA

Overview

This research study outlines a simple cleanup workflow for oral fluid samples that enables analytical sensitivity on par with the guidelines set forth by SAMHSA for workplace drug testing while minimizing the amount of instrument maintenance that would be required with dirtier samples. Herein, this study aims to outline the typical analytical performance of a panel of drugs in oral fluid via an SLE cleanup and detection with an Ultivo LC/TQ system. Lower limits of quantitation, precision and linearity, range, and accuracy will be discussed.

Introduction

The introduction and implementation of guidelines from SAMHSA for oral fluid testing offers a newer and easier option for workplace drug testing. While use of oral fluid is less invasive and more tamper-resistant, samples can suffer from suppression due to the matrix when analyzed via mass spectrometry. Historically, sample preparation involved compound class-based cleanups using solid phase extraction (SPE), which can increase cost and decrease throughput in the analysis process. In an effort to minimize cost and to increase throughput while using a cleaner matrix than would be achieved through simple dilute and shoot, samples were prepared using Agilent's Chem Elut S supported liquid extraction (SLE) cartridges and analyzed on the Ultivo LC/TQ. The 16 compounds included in this study were 6-acetylmorphine, amphetamine, benzoylecgonine, cocaine, codeine, hydrocodone, hydromorphone, MDA, MDEA, MDMA, methamphetamine, morphine, oxycodone, oxymorphone, phencyclidine (PCP), and THC. Calibration concentrations ranged from 0.1 ng/mL to 125 ng/mL in vial, corresponding to an in-mouth concentration range of 0.4 ng/mL to 500 ng/mL. The injection to injection cycle time was about 8 minutes, and multiple transitions were monitored for each of the analytes of interest.

Calibration curve accuracies were within 20% of the expected concentration at the lowest calibration level, and reproducibility across all levels was acceptable with CVs less than 15%. R^2 values were all greater than 0.992, and all but one of the compounds displayed linear responses throughout the concentration range, while the remaining one required a quadratic fit.

Experimental

Reagent and Chemicals

All reagents used in this application were HPLC or LCMS grade. Acetonitrile and methanol were purchased from Honeywell (Morristown, NJ, USA) and ultrapure water was sourced from a Milli-Q Integral system with an LC-Pak Polisher and a 0.22 μm point-of-use membrane filter cartridge (EMD Millipore, Billerica, MA, USA). Formic acid and ammonium formate were purchased from Fluka (Sigma-Aldrich Corp., St. Louis, MO, USA). Chemical standards were purchased from Cerilliant (Sigma-Aldrich Corp., Round Rock, TX, USA).

Sample Preparation

Negative synthetic oral fluid prediluted with extraction buffer was spiked with drug standards of the 16 compounds to achieve the top concentration, while the rest of the calibration standards were created by serial dilution. Each sample was combined with an internal standard solution and pretreated with ammonium hydroxide as per collection device instructions. Samples were applied to the extraction cartridges and allowed to equilibrate on the sorbent bed for at least 5 minutes before elution with a DCM:MTBE mixture under gravity. The eluate was dried under nitrogen and reconstituted in chromatographic starting conditions prior to introduction into the LCMS system.

Analytical Method and Data Analysis

The LC/MS/MS system consisted of a 1290 binary pump, a thermostatted autosampler, a temperature-controlled column compartment, and a triple quad mass spectrometer. Separation conditions are given in Tables 1 and 2. System control and data acquisition were performed by Agilent MassHunter Acquisition Software (Version 1.1 for Ultivo LC/TQ). Data were analyzed using Agilent MassHunter Quantitative Analysis Software (Version 10.0) and Qualitative Analysis Software (Version 10.0).

Table 1. The 1290 Infinity II HPLC conditions.

Column	Poroshell 120 EC-C18 2.1 x 100 mm, 2.7 μm	
Mobile phase	A: 10 mM ammonium formate + 0.01% formic acid in water B: Methanol + 0.01% formic acid	
Flow rate	0.500 mL/min	
Gradient	Time	B%
	0	10
	0.5	10
	1.0	15
	4.0	50
	5.0	95
	7.0	95
	7.01	10

Experimental

Capillary voltage on the Agilent Jet Stream ESI source was set at 2500 V with 0 V for the nozzle. The sheath gas temperature was 400°C coupled with a drying gas temperature at 300°C. The sheath gas and drying gas flows were 11 L/min and 12 L/min, respectively. The nebulizer pressure was set to 50 psi. Positive ionization was utilized.

Table 2. Transitions for amino acid detection in MRM mode

Compound Name	Precursor (m/z)	Product (m/z)	RT (min)	Frag (V)	CE (V)	Compound Name	Precursor (m/z)	Product (m/z)	RT (min)	Frag (V)	CE (V)
6MAM	328.2	211.1 165	2.22	130	24 48	MDEA	208.1	163 105	2.73	70	12 28
6MAM-D6	334.2	165.1 152.1	2.20	130	44 80	MDEA-D6	214.2	166.1 108	2.72	70	12 28
Amphetamine	136.1	119 90.9	2.27	55	4 16	MDMA	194.1	163 105	2.42	65	8 24
Amphetamine-D8	144.2	127 97	2.23	60	4 16	MDMA-D5	199.1	165.1 107	2.40	65	8 24
Benzoylcegonine	290.1	168.1 104.9	2.97	105	16 32	Methamphetamine	150.1	119 91	2.39	65	8 20
Benzoylcegonine-D8	298.2	171.1 81.9	2.93	95	20 76	Methamphetamine-D5	155.2	121 92	2.38	65	8 20
Cocaine	304.2	182.1 81.9	3.39	95	16 32	Morphine	286.2	165 128	0.78	120	52 72
Cocaine-D3	307.2	185.2 76.9	3.39	95	20 72	Morphine-D6	292.2	151.9 127.8	0.78	120	72 72
Codeine	300.2	165.1 114.9	1.82	120	52 80	Oxycodone	316.2	298.1 256.2	1.99	100	16 24
Codeine-D6	306.2	152.1 114.9	1.79	125	80 80	Oxycodone-D6	322.2	304.2 247.2	1.97	95	16 32
Hydrocodone	300.2	199.1 171.1	2.13	135	32 44	Oxymorphone	302.1	284.1 227.1	0.87	95	16 28
Hydrocodone-D3	303.2	199 127.9	2.12	135	32 72	Oxymorphone-D3	305.2	287.1 232.3	0.86	105	20 28
Hydromorphone	286.2	185.1 128	1.00	135	32 72	PCP	244.2	159.1 86	4.16	60	12 8
Hydromorphone-D3	289.2	185 156.9	0.99	130	32 48	PCP-D5	249.2	95.9 86	4.14	60	44 8
MDA	180.1	163 105	2.35	60	4 20	THC	315.2	193 123	6.03	110	24 36
MDA-D5	185.1	168.1 110.1	2.33	60	8 24	THC-D3	318.2	196.1 135	6.03	170	28 24

Results and Discussion

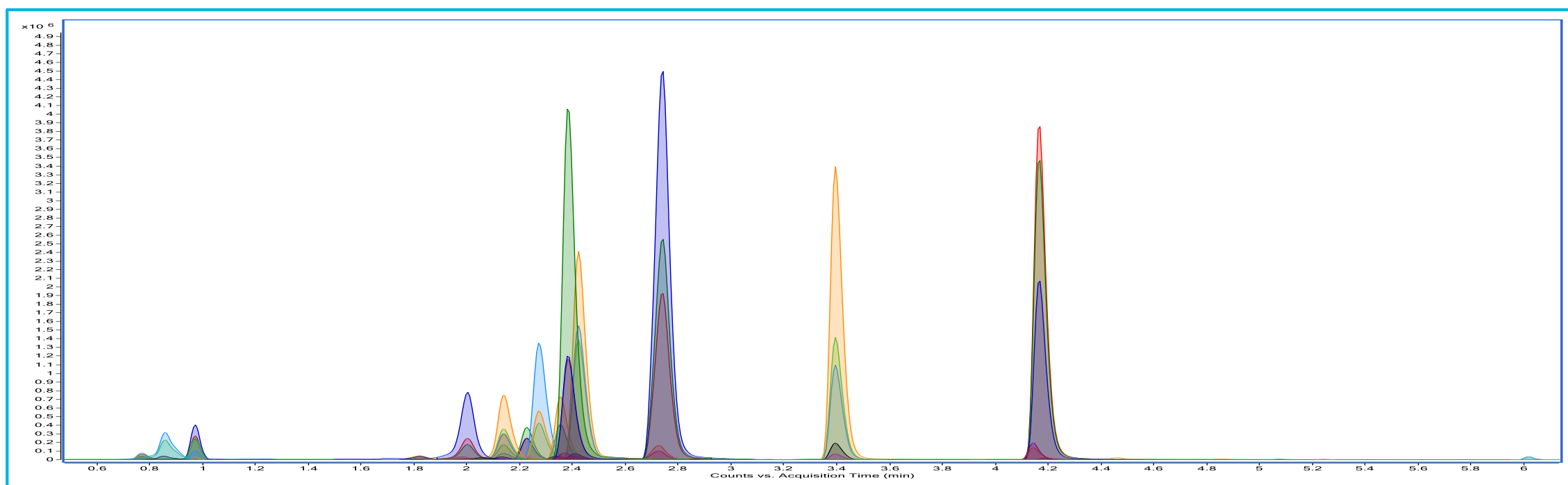


Figure 1. Composite MRM chromatogram showing 16 analytes.

Results and Discussion

Linearity, Accuracy, and Reproducibility

The calibration concentrations ranged from 0.1 ng/mL to 125 ng/mL for the various analytes, corresponding to an in-mouth concentration range of 0.4 ng/mL to 500 ng/mL. Limits of quantitation (LOQs), along with curve fit parameters, are given in Table 3. Each curve had an R^2 value greater than 0.992 and responses showed excellent reproducibility from run to run. Calibration curve accuracies were within 13.5% of the expected concentration at the lowest level, while RSDs were within 16% at the LOQs and within 5% at the higher levels.

Table 3. Calibration curve fit, LOQs (in-vial), and signal-to-noise (S/N).

Compound Name	Curve Fit	R^2	LOQ (ng/mL)	S/N at LOQ
6MAM	Linear	0.9987	0.25	300.92
Amphetamine	Linear	0.9989	0.25	38.06
Benzoyllecgonine	Linear	0.9927	0.5	145.95
Cocaine	Linear	0.9961	0.25	566.20
Codeine	Linear	0.9974	0.5	58.39
Hydrocodone	Linear	0.9994	0.25	759.83
Hydromorphone	Linear	0.9923	0.25	468.17
MDA	Linear	0.9948	0.25	22.68
MDEA	Linear	0.9966	0.25	464.67
MDMA	Linear	0.9984	0.25	323.41
Methamphetamine	Linear	0.9972	0.1	137.74
Morphine	Quadratic	0.9920	2.0	40.37
Oxycodone	Linear	0.9996	0.1	38.94
Oxymorphone	Linear	0.9955	0.25	46.97
PCP	Linear	0.9983	0.25	2132.89
THC	Linear	0.9938	0.5	44.95

Figure 2 shows examples of calibration curves for 6 selected compounds, while replicate injections of 4 selected compounds in matrix are shown in Figure 3, demonstrating excellent precision and chromatographic separation of the isomers.

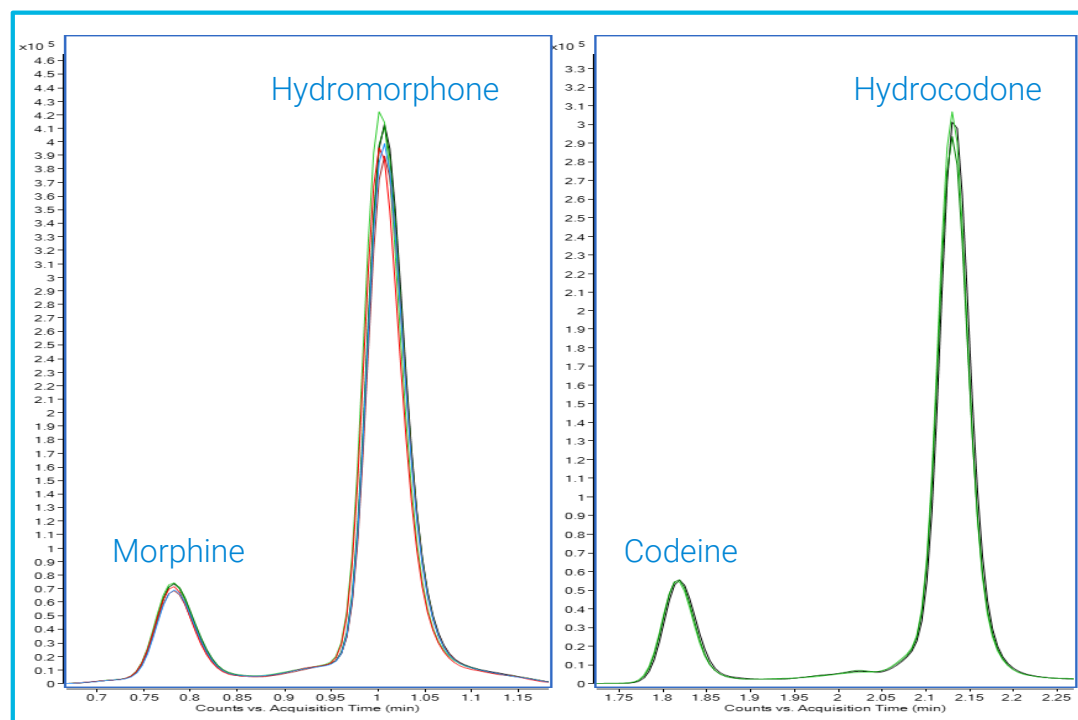


Figure 3. Excellent precision demonstrated for replicate injections of selected isomers in sample matrix.

Conclusions

A simple cleanup workflow for oral fluid samples can decrease matrix effects and downtime for maintenance without dramatically increasing cost. This study demonstrated an efficient and simple cleanup process and showed analytical sensitivity that met or exceeded the guidelines set forth by SAMHSA for workplace drug testing in oral fluid.

References

- Agilent Application Note 5991-1667EN—Comprehensive LC/MS Analysis of Opiates, Opioids, Benzodiazepines, Amphetamines, Illicits, and Metabolites in Urine
- Agilent Application Note 5994-0950EN—Drug of Abuse Analysis in Human Urine Using Agilent Chem Elut S Supported Liquid Extraction by LC/MS/MS

For Forensic Use

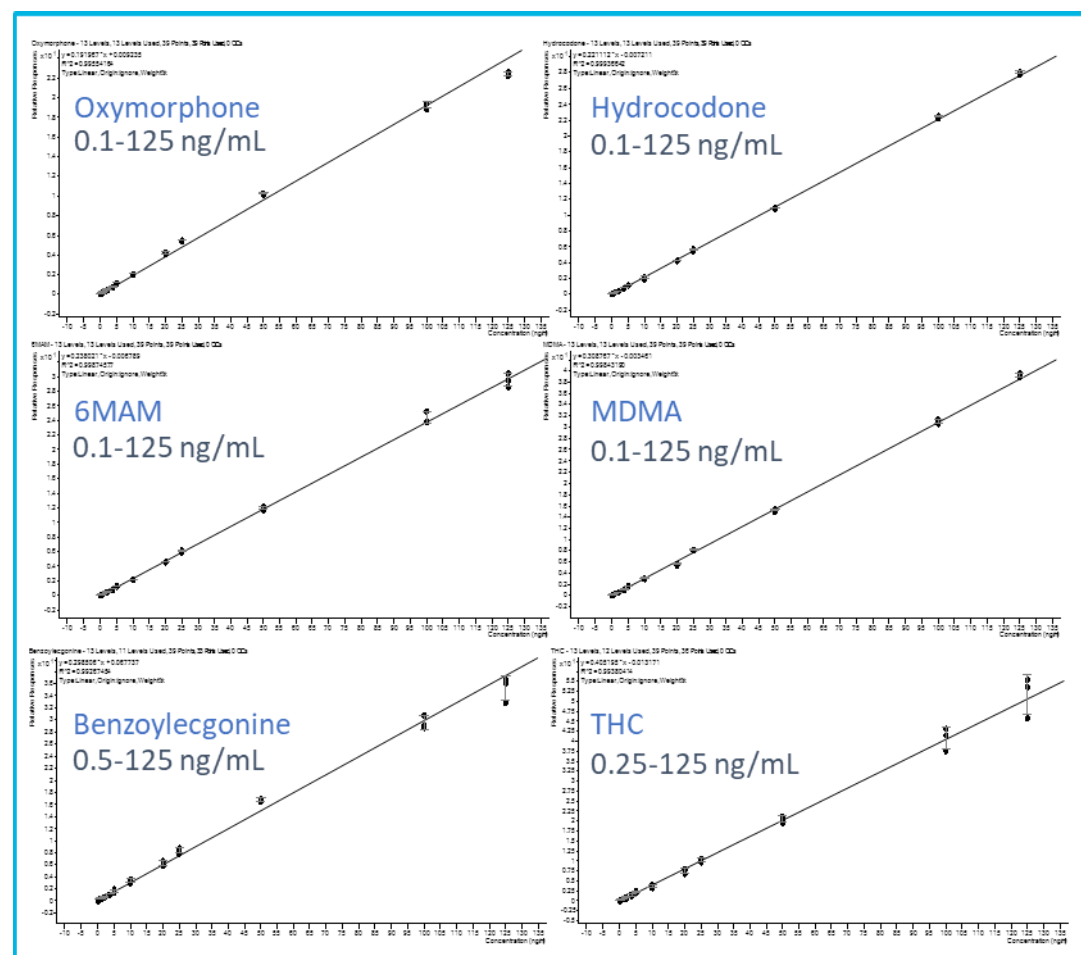


Figure 2. Calibration curves of selected compounds.

Poster Reprint

ASMS 2020

ThP 020

Rapid High-Throughput Profiling and Quantitation of Sialic Acids in Biotherapeutics

Anna Fong¹; Ace G. Galermo¹; John Yan¹;
Tom Rice¹; Aled Jones¹; Archana Datt¹;
Hamutal Bonen¹; Gregory Staples^{1, 2}; Ted
Haxo¹

¹Agilent Technologies, Hayward, CA; ²Agilent
Technologies, Santa Clara, CA

The composition of glycans present on biotherapeutic glycoproteins can affect immunogenicity, pharmacokinetics and pharmacodynamics.¹ Glycans are carbohydrates composed of monosaccharides arranged into many different possible oligosaccharide structures based on composition and linkage position. Sialic acid capping at the non-reducing terminal of N- or O-glycans can serve a key role in mediating the effectiveness of therapeutic glycoproteins.² Depending on the molecule and the application, terminal sialic acid may reduce the rate of clearance, reduce antibody-dependent cellular cytotoxicity (ADCC) activity, or can be anti-inflammatory.³⁻⁵ Two forms commonly found in biotherapeutics are N-acetylneuraminic acid (Neu5Ac) and N-glycoylneuraminic acid (Neu5Gc). Neu5Ac is usually the predominant species while Neu5Gc is not synthesized by humans and its presence on biotherapeutics can be immunogenic. Therefore, it is essential to monitor not only the absolute quantity of sialic acid, but also the levels of different sialic acid species present in therapeutic glycoproteins.

Here we present a new high-throughput workflow based on a 96-well plate format for the release, labeling, and analysis of sialic acids from therapeutic glycoproteins using rituximab, etanercept, and NISTmAb as examples. Sialic acid residues are released then labeled with 1,2-diamino-4,5-methylenedioxybenzene (DMB) in a two-step procedure. The DMB-labeled sialic acids are then separated and analyzed using a rapid 10-minute method based on reversed-phase ultra high-performance liquid chromatography (UHPLC) coupled with fluorescence and optional mass spectrometry detection. The workflow offers both qualitative characterization of Neu5Ac, Neu5Gc and other sialic acid species using a sialic acid reference panel (SARP), as well as absolute quantitation with picomol level sensitivity using included Neu5Ac and Neu5Gc quantitative standards. The workflow enables reliable and reproducible high-throughput profiling and quantitation of sialic acids, providing a broad detection range and improved sensitivity for molecules with low levels of sialylation.

Sample Preparation

Samples were prepared using a developmental protocol using a 96-well plate format. Sialic acids were released from rituximab (Rituxan, lot # M190170), etanercept (Enbrel, lot # M190088), NISTmAb (lot # 14HB-D-002) and erbitux (Cetuximab, lot # M160886) through an acid hydrolysis reaction. The method eliminates the need for a dry down step, thereby, decreases overall sample preparation time by 1-2 hours. The sample amount is typically 200 µg of glycoprotein with low level sialylation and 5 µg of highly sialylated glycoprotein. Serial dilutions of sialic acid reference standards were used to prepare a standard curve for Neu5Ac and Neu5Gc. Released sialic acids, SARP, and standards were then derivatized with DMB. Sialic acid release and labeling steps were performed in a thermocycler. The workflow is illustrated in Figure 1.

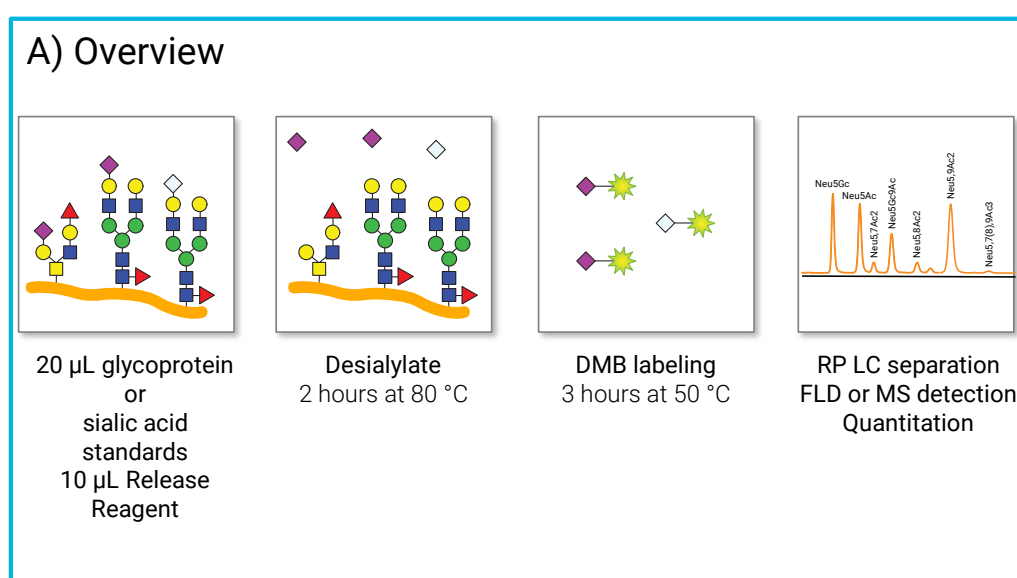


Figure 1A. Sialic acid release and DMB labeling workflow A) overview B) DMB labeling mechanism.

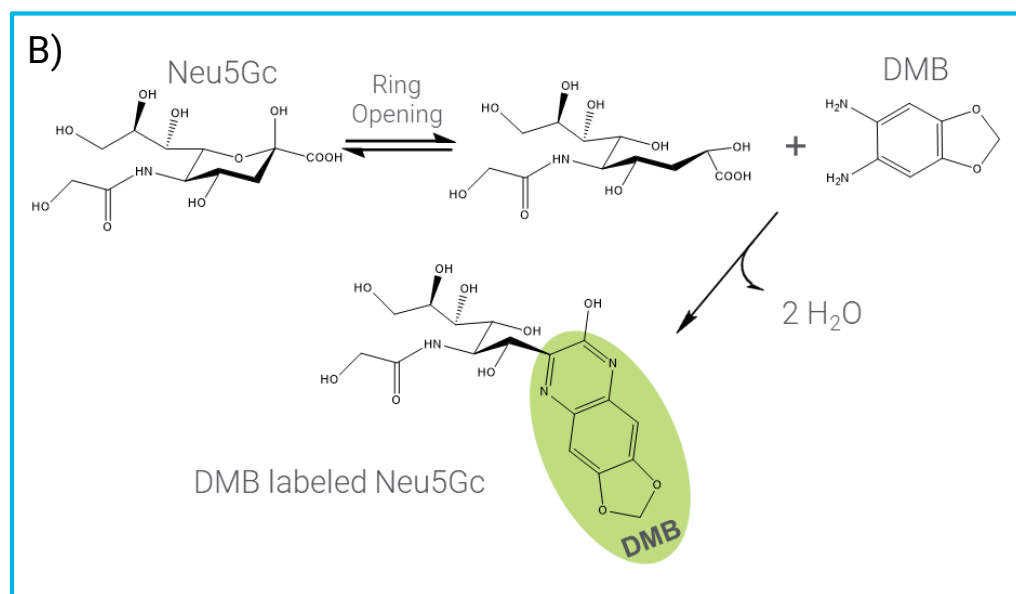


Figure 1B. Sialic acid release and DMB labeling workflow A) overview B) DMB labeling mechanism of sialic acid Neu5Ac

LC/FLD/MS Analysis of DMB Labeled Sialic Acids

DMB labeled sialic acids from Rituxan, Enbrel, NISTmAb and Cetuximab were analyzed using reversed-phase (RP) separation with an Agilent 1290 Infinity II UHPLC system in conjunction with fluorescence detection (FLD) for quantitation. All RP-UHPLC separations were conducted under the conditions described in Table 1. Additional in-line analysis using a 6545XT AdvanceBio LC/Q-TOF (Table 2) was performed to confirm elution order of the DMB-labeled sialic acids present in the SARP. A fixed flow splitter was utilized post-FLD, diverting approximately 50% of the flow to waste and 50% to the MS. The data was analyzed with Agilent OpenLab CDS and MassHunter Qualitative Analysis 10.0 software. Neu5Gc and Neu5Ac were quantified using the calibration curves.

Parameter	Value																																
Instrument	Agilent 1290 Infinity II LC System																																
Column	Agilent InfinityLab Poroshell 120 EC-C18, 2.1 x 75 mm, 2.7 µm (p/n 697775-902).																																
Column Temp	30 °C																																
Mobile Phase	A) Methanol:acetonitrile:water (4:8:88) B) Acetonitrile																																
Gradient Program	<table border="1"> <thead> <tr> <th>Time (min)</th> <th>%A</th> <th>%B</th> <th>Flow rate (mL/min)</th> <th></th> </tr> </thead> <tbody> <tr> <td>0.00</td> <td>100</td> <td>0</td> <td>0.4</td> <td rowspan="2">Isocratic elution</td> </tr> <tr> <td>6.00</td> <td>100</td> <td>0</td> <td>0.4</td> </tr> <tr> <td>6.25</td> <td>20</td> <td>80</td> <td>0.4</td> <td rowspan="2">Wash</td> </tr> <tr> <td>7.30</td> <td>20</td> <td>80</td> <td>0.4</td> </tr> <tr> <td>7.50</td> <td>100</td> <td>0</td> <td>0.4</td> <td rowspan="2">Re-equilibration</td> </tr> <tr> <td>10.00</td> <td>100</td> <td>0</td> <td>0.4</td> </tr> </tbody> </table>	Time (min)	%A	%B	Flow rate (mL/min)		0.00	100	0	0.4	Isocratic elution	6.00	100	0	0.4	6.25	20	80	0.4	Wash	7.30	20	80	0.4	7.50	100	0	0.4	Re-equilibration	10.00	100	0	0.4
Time (min)	%A	%B	Flow rate (mL/min)																														
0.00	100	0	0.4	Isocratic elution																													
6.00	100	0	0.4																														
6.25	20	80	0.4	Wash																													
7.30	20	80	0.4																														
7.50	100	0	0.4	Re-equilibration																													
10.00	100	0	0.4																														
Injection Volume	10 µL (Equivalent to 0.25 pmol of Enbrel-10pmol of Rituxan)																																
Detection	Agilent 1260 Infinity II FLD λ _{Ex} 373 nm, λ _{Em} 448 nm																																

Table 1. Reversed-phase UHPLC conditions

6545XT AdvanceBio LC/Q-TOF	
Source	Dual AJS ESI
Gas Temperature	350 °C
Drying Gas Flow	11 L/min
Nebulizer	15 psi
Sheath Gas Temperature	400 °C
Sheath Gas Flow	12 L/min
Vcap	1400 V
Nozzle Voltage	1800 V
Fragmentor	120 V
Skimmer	65 V
Oct 1 VF Vpp	600 V
Mass Range (MS)	m/z 400-1000
Mass Range (MS/MS)	m/z 100-550
Acquisition Mode	High resolution (4 GHz)

Table 2. 6545XT AdvanceBio LC/Q-TOF parameters

LC/FLD/MS analysis of DMB Labeled SARP

RP-UHPLC analysis of DMB labeled SARP results in the separation and detection of six sialic acid derivatives: Neu5Gc, Neu5Ac, Neu5,7Ac2, Neu5Gc,9Ac, Neu5,8Ac2, Neu5,9Ac2, and Neu5,7(8),9Ac3. While differences in retention times may be observed with different columns, flow rate, solvents or laboratory conditions, the elution order of DMB derivatized sialic acids remain consistent. The reference panel is used to evaluate the resolution and accuracy of the chromatographic system at the beginning of the sample sequence. A typical chromatogram of DMB-labeled SARP is shown in Figure 2. Identification of the DMB-sialic acid derivatives were confirmed by mass spectrometry (Figure 2b).

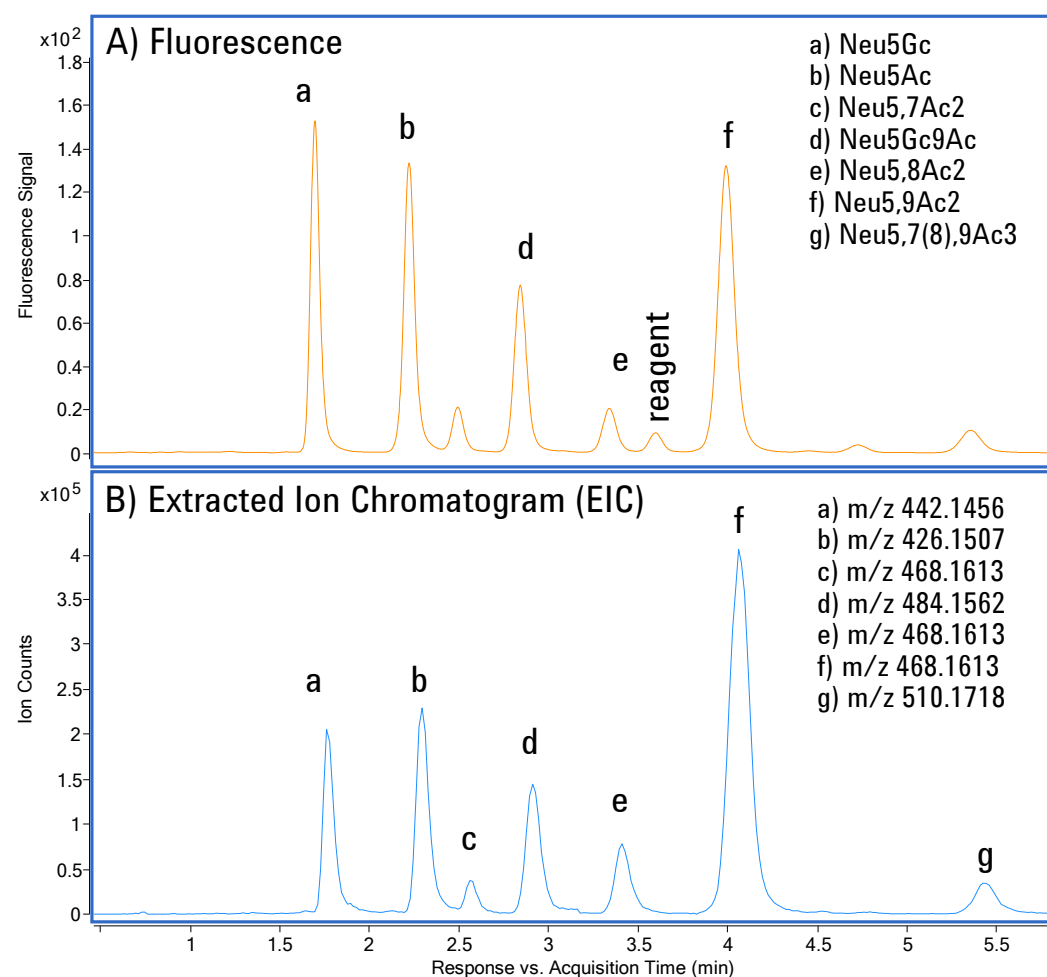


Figure 2. UHPLC chromatogram of DMB labeled SARP. A) fluorescence B) Extracted ion chromatogram of DMB labeled sialic acid species, $[M+H]^+$.

Analysis of Sialic Acid Content of Biotherapeutics and NISTmAb

DMB labeled sialic acids identified by applying the workflow to Rituxan, Enbrel, Cetuximab and the NISTmAb are shown in Figure 3. Both Rituxan (Figure 3A) and Enbrel (Figure 3B) contain primarily Neu5Ac while NISTmAb (Figure 3C) and Cetuximab (Figure 3D) contains primarily Neu5Gc. Mass spectra of major peaks in DMB labeled samples from Enbrel and Cetuximab confirm their identities as Neu5Ac and Neu5Gc respectively (Figure 4).

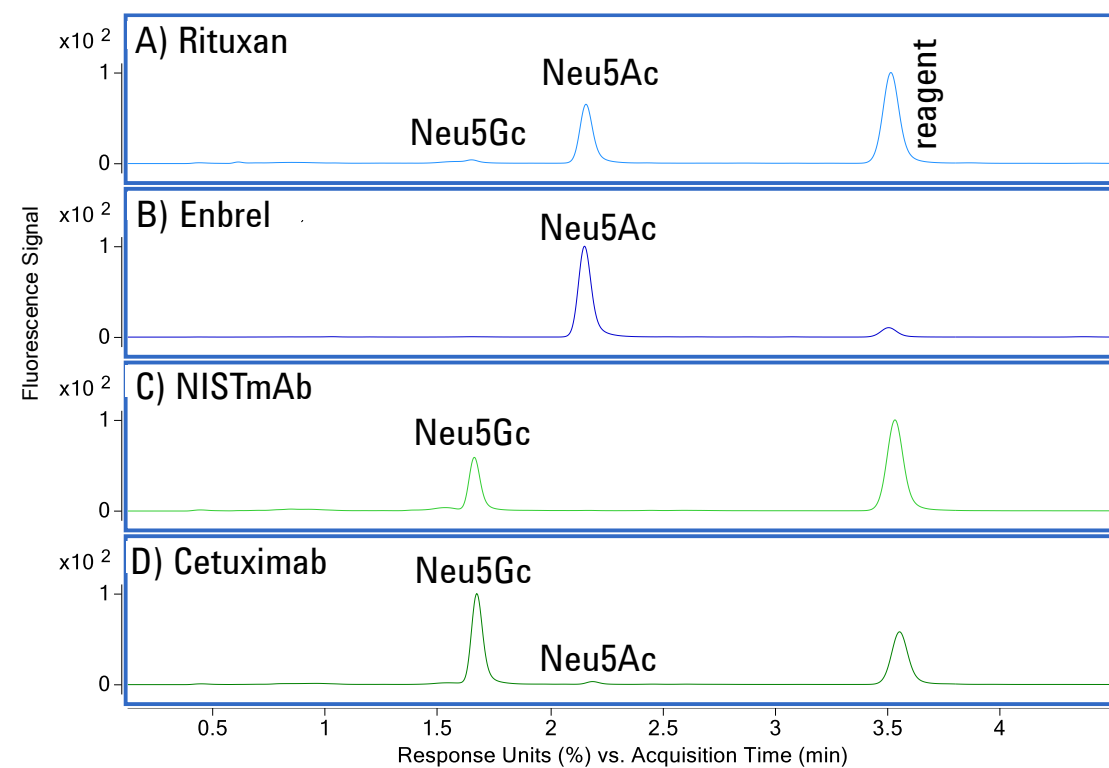


Figure 3. UHPLC fluorescence profiles of DMB labeled sialic acids from different glycoproteins. A) Rituxan, B) Enbrel, C) NISTmAb and D) Cetuximab.

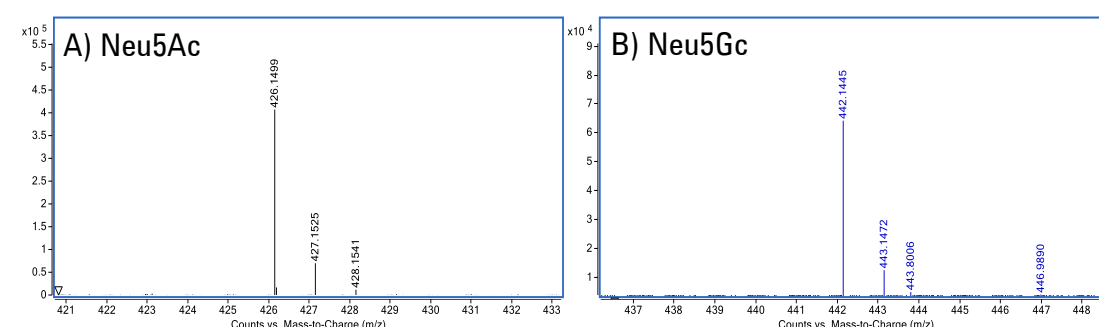


Figure 4. Mass spectra of DMB labeled sialic acid A) Neu5Ac from Enbrel and B) Neu5Gc from Cetuximab.

Quantitative Analysis of Sialic Acid Content

Based on the chromatographic separation and fluorescence response of Neu5Gc and Neu5Ac standards labeled with DMB, a quantitative calibration curve was generated (Figure 5). The LOD and LOQ was calculated using the noise determined by OpenLab CDS using P2P noise calculation (Table 3). The detected molar quantities of Neu5Gc and Neu5Ac from Rituxan, Enbrel, NISTmAb and Cetuximab was determined based on integrated peak areas and are listed in Table 4.

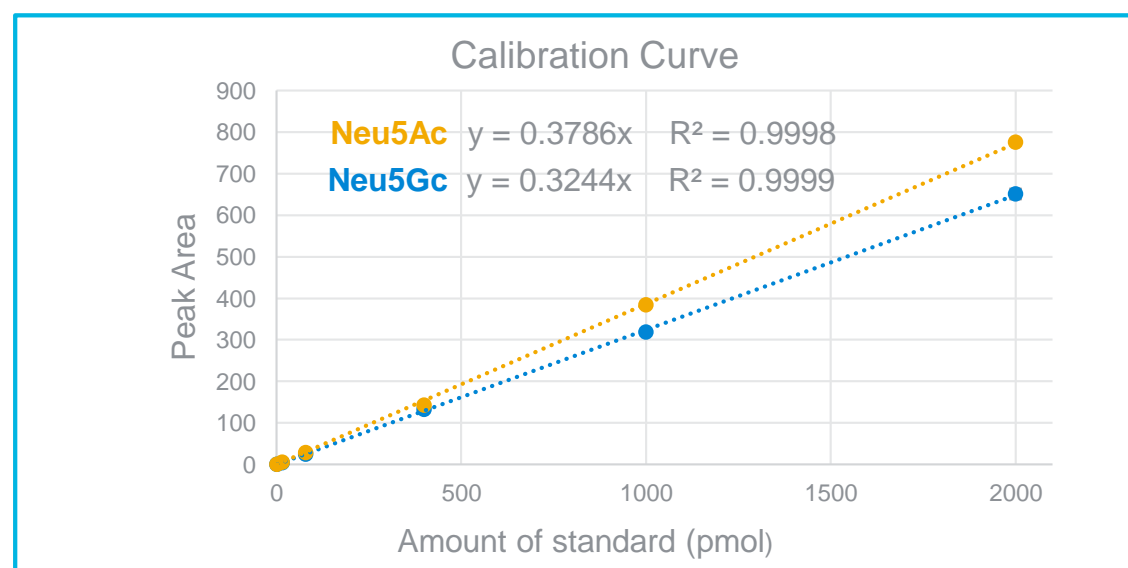


Figure 5. Neu5Gc and Neu5Ac calibration curves, n=2.

Results and Discussion

Sialic Acid	LOD (pmol)	LOQ (pmol)
Neu5Gc	0.012	0.040
Neu5Ac	0.016	0.053

Table 3. LOD and LOQ for Neu5G and Neu5Ac are shown in the table.

	Concentration (mg/ml)	Sample Mass (µg)	Neu5Gc (pmol/µg)	%CV	Neu5Ac (pmol/µg)	%CV
Rituxan	10	200	0.02	1.8%	0.60	4.2%
Enbrel	0.25	5	n.d.	-	228	6.9%
NIST mAb	10	200	0.36	1.8%	n.d.	-
Cetuximab	2	40	3.72	7.1%	0.12	10.9%

Table 4. Compiled table of Table of calculated mol/sialic acid for Rituxan, Enbrel, cetuximab, and NISTmAb. N=3, n.d.=not detectable

Conclusions

- DMB labeled sialic acids shows improved sensitivity for proteins with low levels of sialylation such as monoclonal antibodies with a single N-glycosylation site in the Fc region.
- The updated DMB labeling workflow eliminates the dry down step of samples, decreasing sample preparation time.
- This workflow provides a method to determine both absolute molar quantities and relative % area of Neu5Gc and Neu5Ac in biotherapeutics.
- Sample preparation uses a high throughput 96 well plate format, and is highly reproducible.
- Quantitative data is comparable to older DMB labeling workflows (GKK-407) and AdvanceBio total sialic acid quantitation kit (GS48-SAQ) results (data not shown).

References

- ¹Liu, L. Antibody Glycosylation and its Impact on the Pharmacokinetics and Pharmacodynamics of Monoclonal Antibodies and Fc-Fusion Proteins. *J. Pharm. Sci.* **2015**, *104*(6), 1866–1884.
- ²Varki, A. Sialic acids in human health and disease. *Trends Mol Med.* **2008**, *14*(8), 351-360.
- ³Li, Y. *et al.* Sialylation on O-glycans protects platelets from clearance by liver Kupffer cells. *Proc Natl Acad Sci USA.* **2017**, *114*(31), 8360-8365.
- ⁴Scallon, B. J. *et al.* Higher levels of sialylated Fc glycans in immunoglobulin G molecules can adversely impact functionality. *Mol Immunol.* **2007**, *44*(7), 1524-1534.
- ⁵Kaneko, Y. *et al.* Anti-inflammatory Activity of Immunoglobulin G Resulting from Fc Sialylation. *Science.* **2006**, *313*, 670-673.

For Research Use Only. Not for use in diagnostic procedures.

Poster Reprint

ASMS 2020

ThP 103

Multiresidue Pesticides Analysis in Food Matrices Using an Enhanced Triple Quadrupole LC/MS System

Kyle Covert¹, Linfeng Wu¹

¹ Agilent Technologies, Inc., Santa Clara, CA

Introduction

Pesticides are integral for protecting crops, but there is concern in the current market of organic and non-organic labeled products – where food authenticity or contamination can affect the quality of organic products. Typical Maximum Residue Limits (MRLs) are on the order of $\mu\text{g}/\text{kg}$ food (parts-per-billion) and thus require very sensitive instrumentation to detect compounds. This is especially true for food products that have many endogenous components that cause heavy matrix effects, such as black tea.

An LC-MS/MS screening method for the detection and quantification of 244 pesticides in heavy & diverse food matrixes was developed:

- Organic loose-leaf black tea and whole organic oranges were obtained from a local grocery store.
- Extracts were prepared following Agilent's QuEChERS extract and EN dispersive SPE protocols.
- Agilent's comprehensive pesticide mixture (p/n 5190-0551) was spiked into extracts of organic black tea and whole orange, respectively.
- Samples were analyzed with a dynamic Multiple Reaction Monitoring (dMRM) method using the 1290 Infinity II LC system coupled to the 6470B triple quadrupole LC/MS (LC/TQ).

The 6470B Triple Quadrupole LC/MS contains hardware improvements on several aspects:

- VacShield technology allowing vent-free ion source maintenance to increase instrument uptime
- Faster electronics with improved settling time parameterization providing chromatographic peak reproducibility at very low dwell times.



Figure 1. 6470B Triple Quadrupole LC/MS with 1290 Infinity II LC system

Experimental

Instrumentation

- 1290 Infinity II High Speed Pump (G7120A)
- 1290 Infinity II Multisampler with Sample Cooler (G7167B, #100)
- 1290 Infinity II Multicolumn Thermostat (G7116B)
- 6470B Triple Quadrupole LC/MS (G6470B) w/ Jet Steam electrospray ionization source (G1958-65638)

MassHunter Acquisition (ver. 10.1) and MassHunter Quantitative Analysis (ver. 10.1) software was used for data acquisition and analysis respectively.

1290 Infinity II UHPLC System

Column	ZORBAX RRHD Eclipse Plus C18, 3.0 x 100 mm, 1.8 μm at 40 °C (p/n 959758-302)	
Inj. Vol.	2 μL	
Sampler temperature	4 °C	
Needle wash	10 second wash in flush port (75:25 methanol/H ₂ O)	
Mobile phase	A) 5 mM ammonium formate + 0.1% formic acid in H ₂ O B) 5 mM ammonium formate + 0.1% formic acid in methanol	
Flow rate	0.400 mL/min	
Gradient program	Time	B (%)
	0.00	5
	0.50	5
	2.00	40
	13.00	98
	14.50	98
	14.60	5
Post time	2 minutes	

Table 1. 1290 Infinity II LC Method

6470B Triple Quadrupole Mass Spectrometer

Ion source	Agilent Jet Stream (AJS) source
Polarity	Positive and Negative
Gas temperature	225 °C
Drying gas	11 L/min
Nebulizer gas	30 psi
Sheath gas	350 °C
Sheath gas flow	12 L/min
Capillary voltage	3500 \pm V
Nozzle voltage	500 \pm V
Scan type	Dynamic MRM (dMRM)
Q1/Q2 Resolution	Unit (0.7 amu)
Delta EMV	\pm 200 V
Cell accel. voltage	3–7 V
Cycle time	500 ms

Table 2. 6470B Triple Quadrupole LC/MS Method

Dynamic MRM Method with Fast Separation

The multiresidue pesticide screening method developed for the previous Agilent LC/TQ instrument model (G6470A) was directly applied in the 6470B Triple Quadrupole LC/MS system (G6470B). The MassHunter Software Dynamic MRM Update Options was used to automatically adjust retention times that may have shifted due to LC or column changes.

Figure 2 shows the overlapped MRM chromatogram of 244 pesticides spiked in orange extract at a concentration of 1 ng/g. All compounds MRM transitions are baseline separated within a 14.5-minute LC gradient. Most pesticides were quantifiable at 10% of the default MRL (1/10 of MRL), which is the highest level of a pesticide residue that is legally tolerated in or on food or feed when pesticides are applied correctly (Good Agricultural Practice).

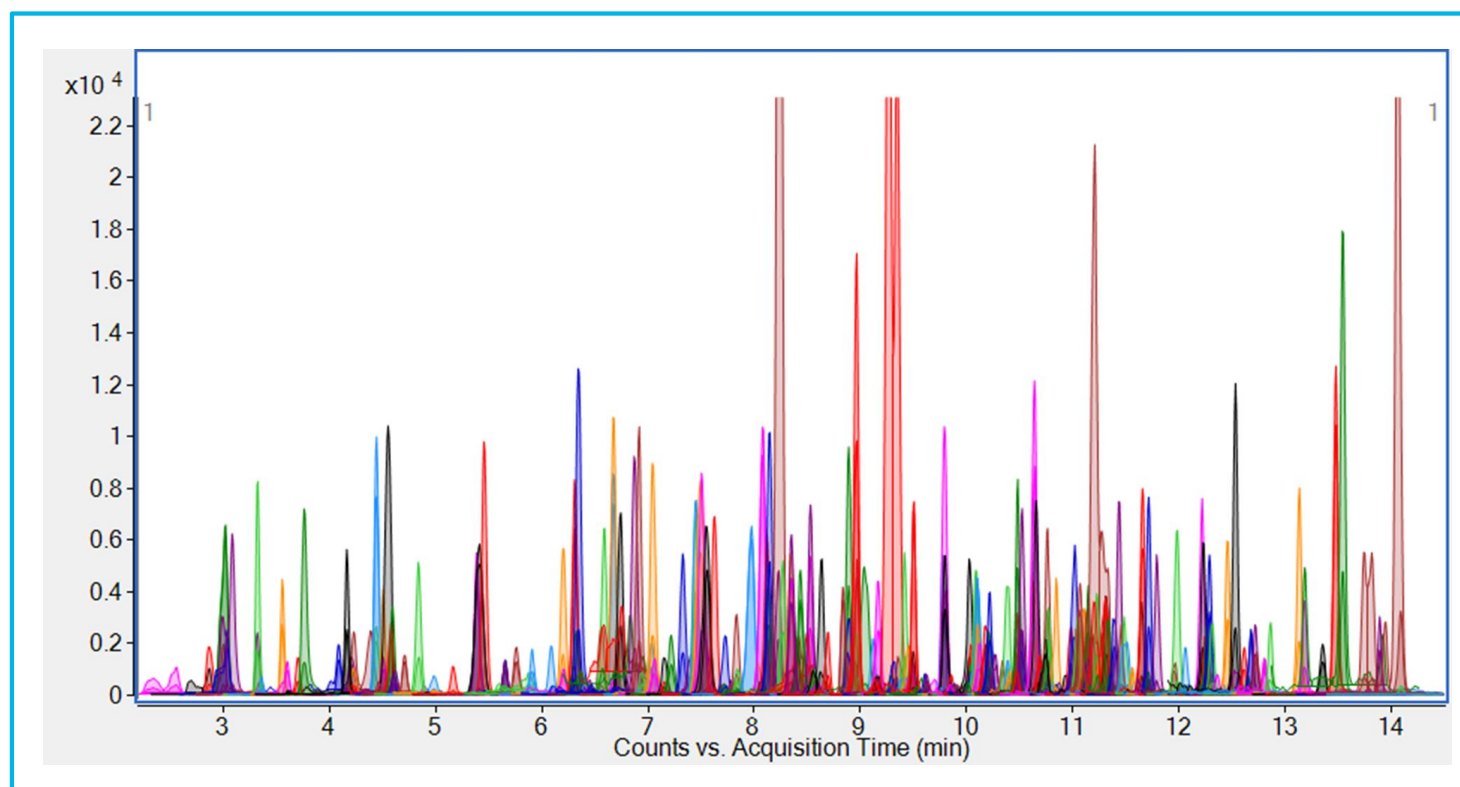


Figure 2. Overlapped MRM chromatograms of 244 pesticides spiked into orange at 1 ng/g

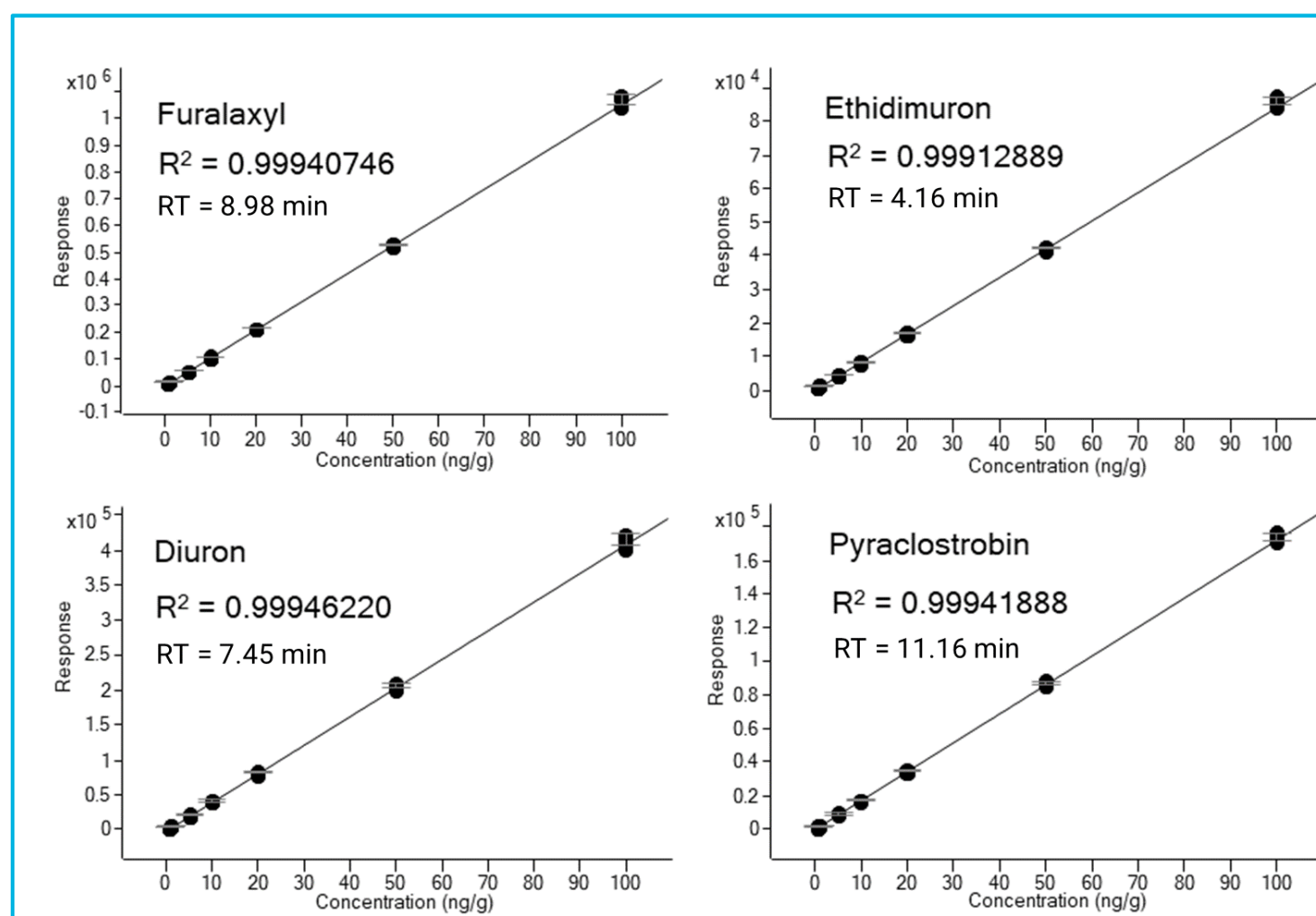


Figure 3. Calibration curves of Furalaxyl, Ethidimuron, Diuron, and Pyraclostrobin pesticide residues spiked into black tea

Standards Curve Analysis

The precision and accuracy of multi-residue pesticide measurements were evaluated in both black tea and orange matrix by injecting a matrix-matched calibration curve at 7 concentrations ranging from 0.5 to 100 ng/g with replicates (n=6).

The results show:

- Excellent precision with relative standard deviation (RSD) < 20% and average accuracy (calculated concentration/expected concentration) within 80-120% at and above LLOQ
- Correlation coefficients (R^2) for calibration curves were higher than 0.99 for all 244 pesticides in the orange extract
- 230 out 244 pesticides in the black tea extract show $R^2 > 0.99$
- Calibration curves for four selected representative pesticides in black tea matrix are shown in Figure 3

6470B Triple Quadrupole LC/MS Demonstrates Great Sensitivity even in Heavy Matrices

In this study, calibration curves were used to determine LLOQ of each pesticide in the matrix, defined as the lowest level with an accuracy within 80-120% and RSD < 20% for peak areas from all 6 replicates. Figure 4 shows the LLOQs distribution for pesticide compounds in both black tea and orange matrices.

The new 6470B Triple Quadrupole LC/MS system allows quantitation of most targeted pesticides in black tea and orange below the default MRL of 10 µg/kg specified by the European Commission¹:

- 239 out of 244 pesticides in the black tea and 243 out of 244 pesticides in the orange have an LLOQ equal to or below 10 ng/g, respectively
- For compounds with specific tolerances by the US-EPA², all of them were quantified below or at their MRL

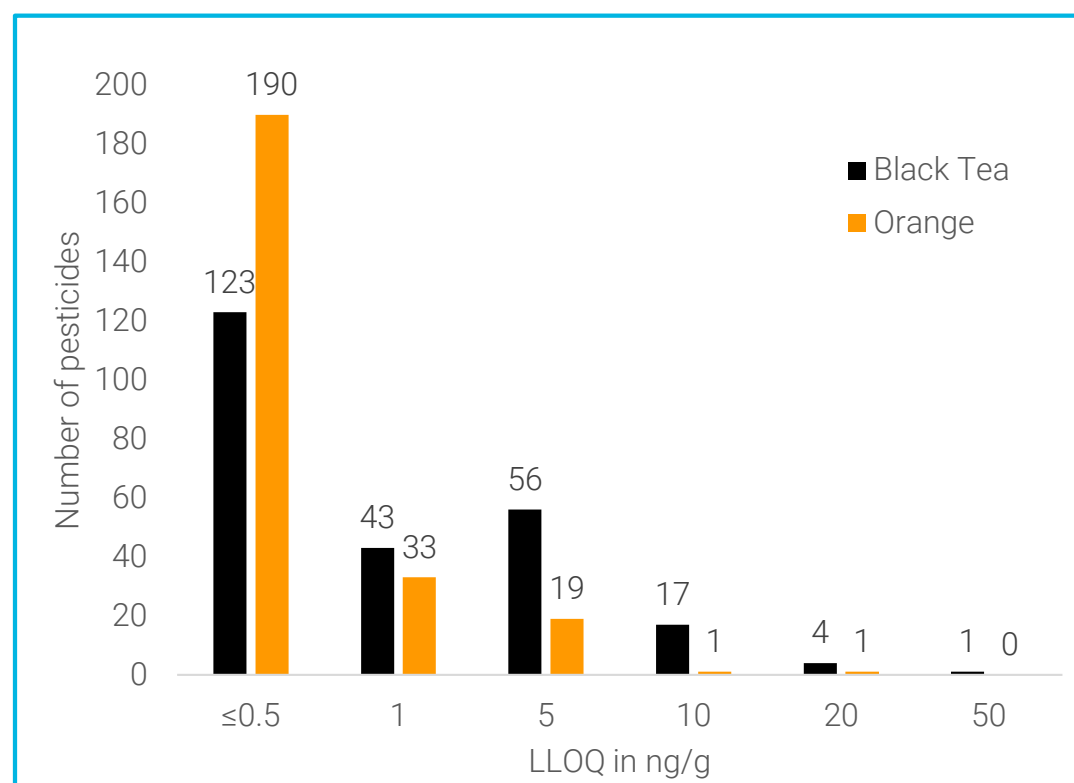


Figure 4. LLOQs for pesticides spiked into black tea and orange

Conclusions

The excellent quantification performance of 244 pesticide residues in black tea and orange has been demonstrated on an improved LC/MS platform, including the ultra-high-performance Agilent 1290 Infinity II LC system coupled to the 6470B Triple Quadrupole LC/MS with the high sensitivity Jet Stream Technology Ion Source (AJS).

Recoveries in Food Matrices

In order to evaluate matrix effects (ion suppression and enhancement), recoveries were calculated by comparing the response of pesticides in the matrix, against those in neat solvent at the default MRL of 10 µg/kg, as shown in Figure 5.

- In the orange matrix, about 50% of the compounds achieved a recovery within SANTE guidelines³ of 80–120%
- In the black tea matrix, about 40% of compounds were recovered within the guideline.³
- The black tea matrix showed more matrix effects than the orange matrix
- A matrix-matched calibration curve is generally recommended for samples with heavy matrix effects

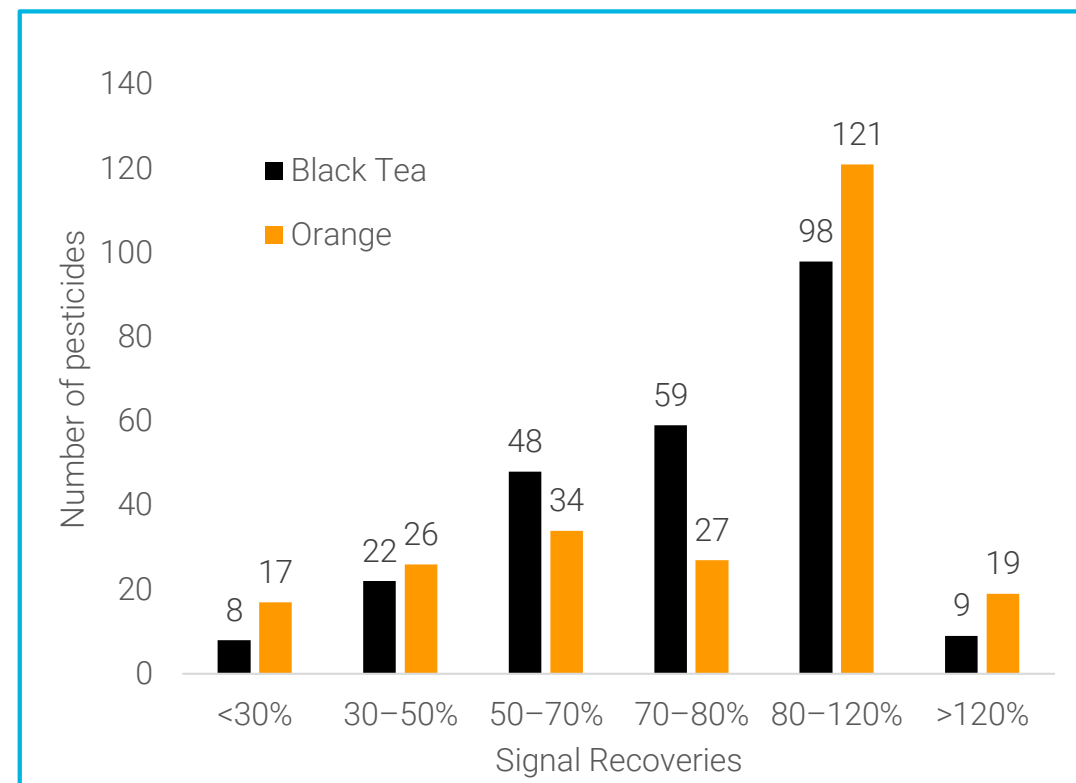


Figure 5. Histogram of recoveries for pesticides spiked into black tea and orange at the default MRL of 10 µg/kg

References

1. Regulation (EC) No 396/2005. European Commission. Retrieved 04/09/20
2. Title 40 U.S. Code of Federal Regulations – Part 180. US-EPA. Retrieved 04/09/20
3. SANTE/12682/2019 European Commission. Retrieved 04/20/20.

Poster Reprint

ASMS 2020

ThP 117

Improving reproducibility and recovery by reducing ionization suppression of LC-MS/MS for quantitation of pesticide residues in chickpea powder

Prasanth Joseph¹; Parul Thakur²; Saikat Banerjee¹; Samir Vyas²

¹Agilent Technologies, BENGALURU, India;

²Agilent Technologies, Mumbai, India

Introduction

Chickpea is one of the earliest cultivated legumes and is high in protein. It is an important cuisine in India, the Middle East, and Mediterranean countries. For food safety, pesticide testing needs to be sensitive and selective. Described here is a LC-MS/MS method is a LC-MS/MS method to quantitate pesticide residues in chickpea.

Even though tandem mass spectrometry is highly selective and sensitive, matrix co-extractives can change the ionization efficiency of pesticides and thereby cause signal suppression or enhancement. QuEChERS based extraction followed by dispersive solid-phase clean up reduces the concentration of matrix in the final extract. Dilution of this sample extract further reduces the matrix effect result in improved recovery and reproducible results. Matrix effect can be further compensated by either strategy like matrix-matched or matrix-based calibration.



Figure 1. 1290 Infinity II coupled to 6470 TQ.

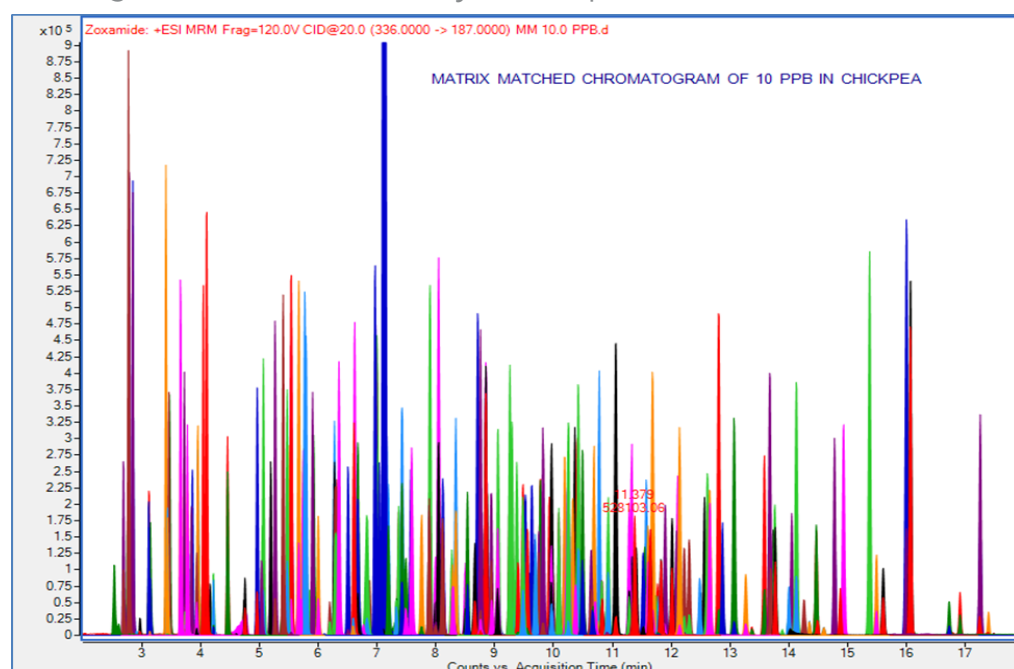


Figure 2. 253 pesticides in chickpea matrix at 10 ppb.

Experimental

Sample Preparation

Approximately two-gram chickpea powder is accurately weighed into a 50mL centrifuge tube. Sample soaked in water was extracted using the AOAC QuEChERS extraction kit and ten mL of acetonitrile. The mixture is then centrifuged, and the supernatant is taken for clean-up. MgSO₄, PSA, and C-18 were ingredients in the cleanup kit. Cleaned up extract is further diluted five times before instrumental analysis. Agilent 6470 TQ was used for the analysis. Multiple reaction monitoring (MRM)-based method with specified retention time is employed to analyze pesticides in chickpea powder. Extracted chickpea samples are spiked at different concentration levels of pesticides to prepare the matrix-matched calibration curves.

Chromatographic conditions

Mobile Phase A

0.5mM Ammonium Fluoride and 4.5mM ammonium formate + 0.1% Formic acid in water

Mobile phase B

0.5mM Ammonium Fluoride and 4.5mM ammonium formate + 0.1% Formic acid in water: Methanol (5:95, V/V)

Column

Agilent Zorbax Eclipse plus RP C18, (150 mm X 3.0 mm, 1.8 μm)

The data acquisition with specified retention time provided a greater number of data points across the chromatographic peak.

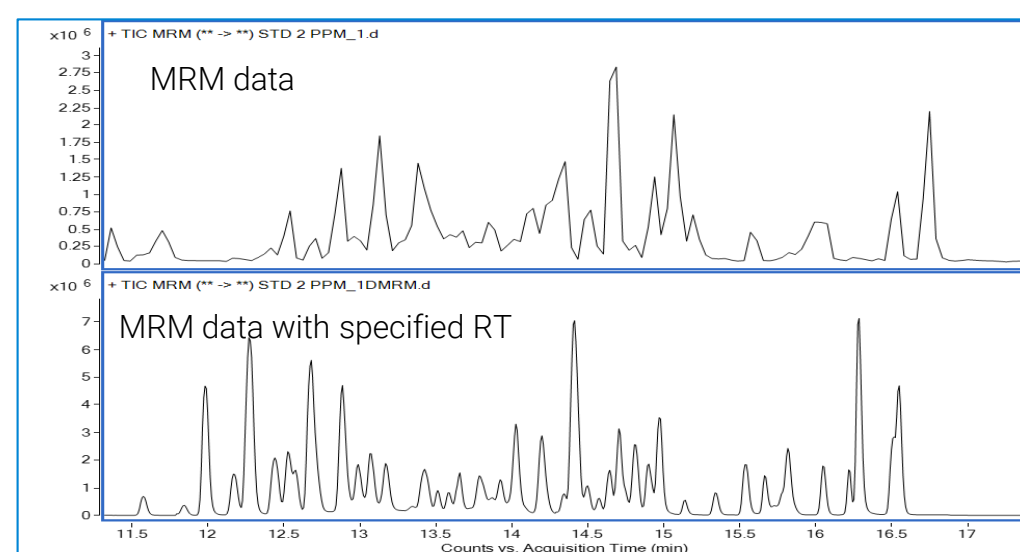


Figure 3: MRM acquisition data vs MRM acquisition with specified retention time (RT) data.

Data generated as a part of method development

Pesticide method is developed by using Agilent MassHunter Pesticide personal compound triggered MRM database. tMRM database and library for more than 700 pesticides that includes compound names, up to 10 MRM transitions, MRM method parameters such as Fragmentor voltages for parent m/z and collision energies for each of the fragments. This also enables pesticide screening with tMRM library verification and thereby avoid any false positive result.

Comprehensive pesticide mix used containing 253 LC-MS amenable pesticides is used for generating the calibration curves. Extracted chickpea samples are spiked at different concentration levels of pesticides to prepare the matrix matched calibration curves.

The developed method is partially validated as per SANTE/11813/2017. Matrix matched calibration curves were made between 0.1 to 50 ppb. The overall limit of detection (LOD) and limit of quantification (LOQ) for the method by considering all analytes were 2 ppb and 10 ppb, respectively. Regression coefficients for the majority of the analytes were found to be more than 0.9950. For each analyte, 2 MRM transitions are selected which satisfy the requirement of 4 identification points for the confirmation of analytes in the sample.

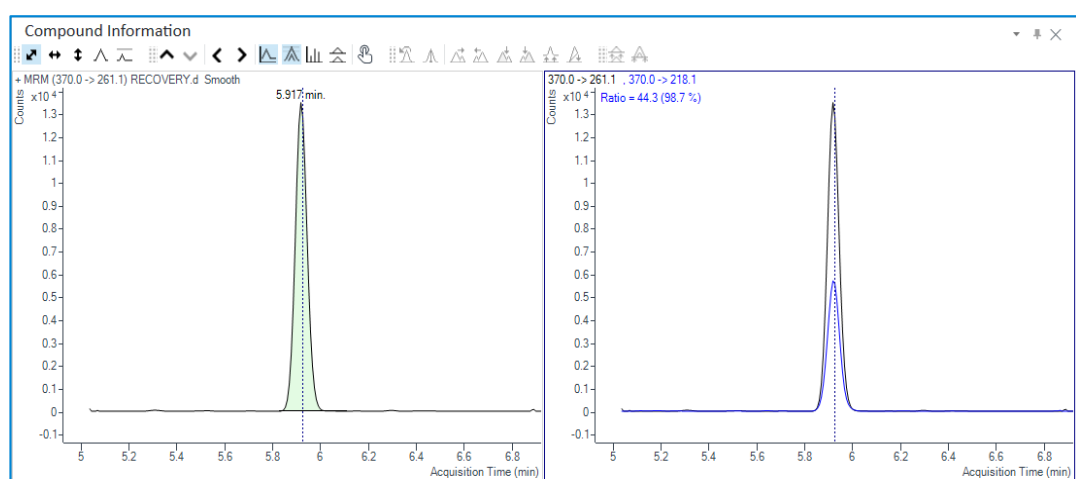


Figure 4: Ion transition ratio of Amidosulfuron calculated by MassHunter quant software

Identification of parent ion give 1 point and identification of each fragment ions in the sample provide 1.5 points.

MassHunter Quant software automatically identifies the quantifier and qualifier ions and calculates the ion transition ratio of standards and samples. It also shows how much the sample ratio is varying from the standard MRM ratio.

Representative matrix matched calibration curves

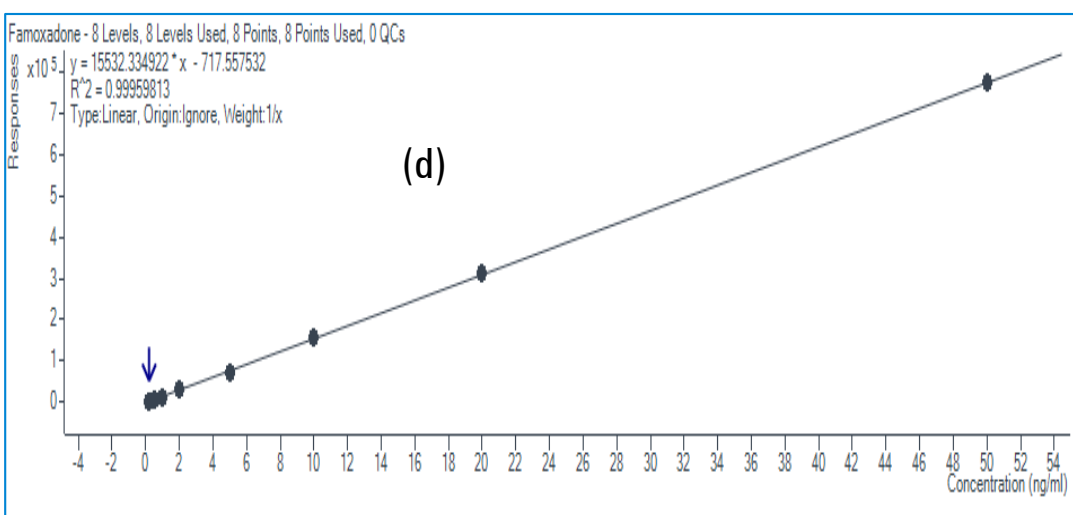
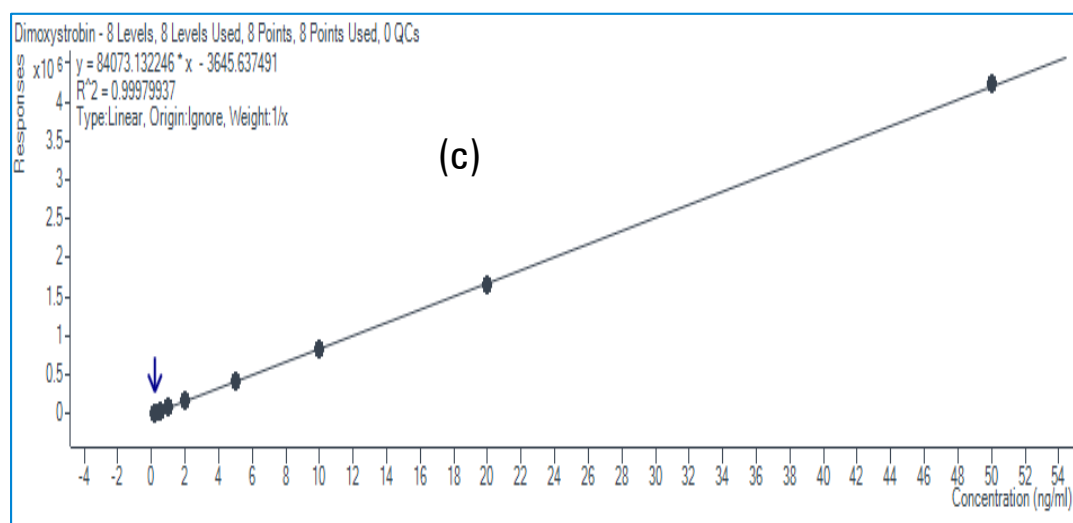
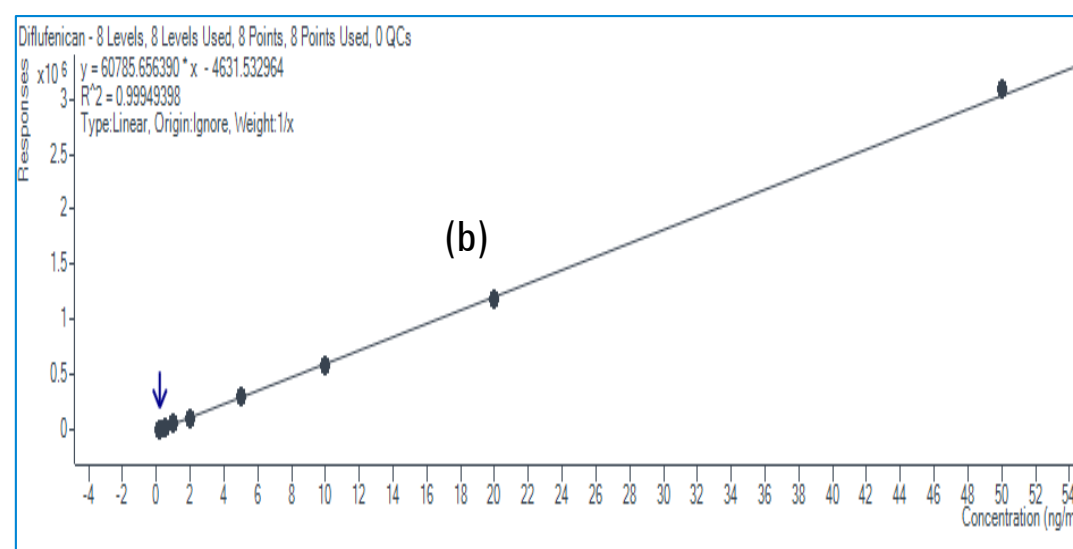
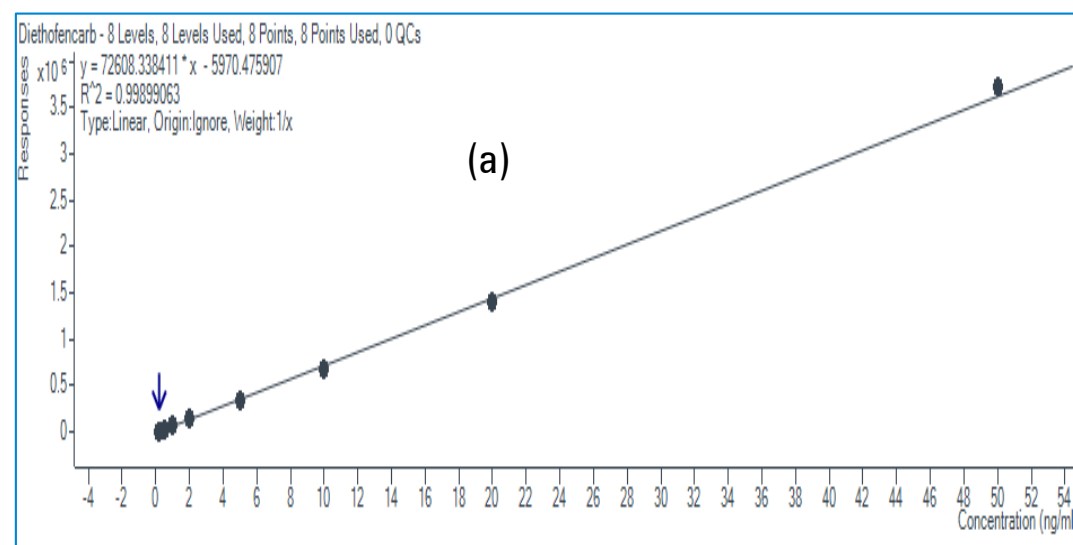


Figure 5. Matrix matched calibration curves (0.1 ng/ml to 50 ng/ml) of a) diethofencarb, b) Diflufenican, c) dimoxystrobin & d) Famoxadone.

Recovery study result

Recovery study was also performed at the LOQ level by spiking pesticide standards in blank extracted samples. 10 ppb spiking level in sample gives an absolute quantity of 0.4 ppb in the final extract after dilutions. 20 μ L of 1 ppm (ug/mL) pesticide standard mix is spiked to 2 g Chickpea Powder. Absolute quantity of pesticides presents in 20 μ L of 1 ppm pesticide mix = 20.0 ng. 20 ng is spiked to 2 g Chickpea powder. Concentration spiked is 20ng/2g = 10 ppb. After following the sample preparation protocol for the spiked samples, effective final concentration injected to the system would become 0.4 ppb for Spike level 1, 10 ppb.

More than 80% of the pesticides in this study showed a recovery above 75%. For most of the compounds, recovery improved after dilution of extract.

For example, Trimethacarb showed a recovery of 36% before dilution. Recovery improved to 79% after dilution. For low recovery analytes, matrix-based calibration curves are used, and recovery losses are compensated. Chickpea samples purchased from local grocery shops were analyzed and quantified against the prepared calibration curves. Results obtained from the calibration table was multiplied with a dilution factor of 25.

None of the analyzed samples were detected with pesticides above the LOQ level. Software used to provide the qualifier to quantifier ratio (ion ratio) for both standard and sample. Activation of the feature of simultaneous collection of additional fragment ions found to be very useful for spectral library matching and thereby confirmation in case of any positive result.

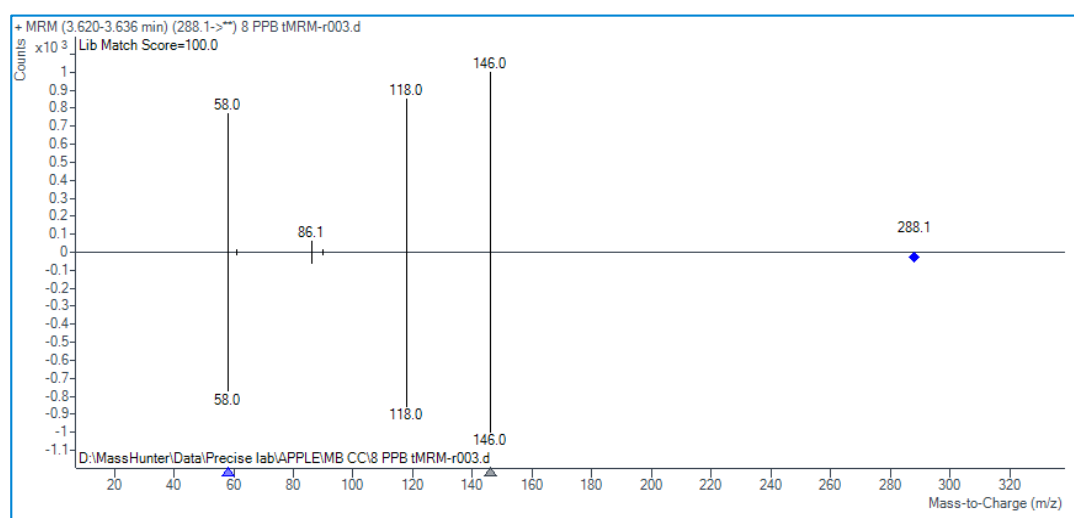


Figure 6: Simultaneous collection of additional fragment ions for Vamidation

The sensitivity of the LC-MS/MS system used in this study allowed the user to dilute the extract. Dilution reduces the matrix effect which results in, improved recovery, consistent performance of the instrument and thereby achieves reproducible results over long batches of sample analysis.

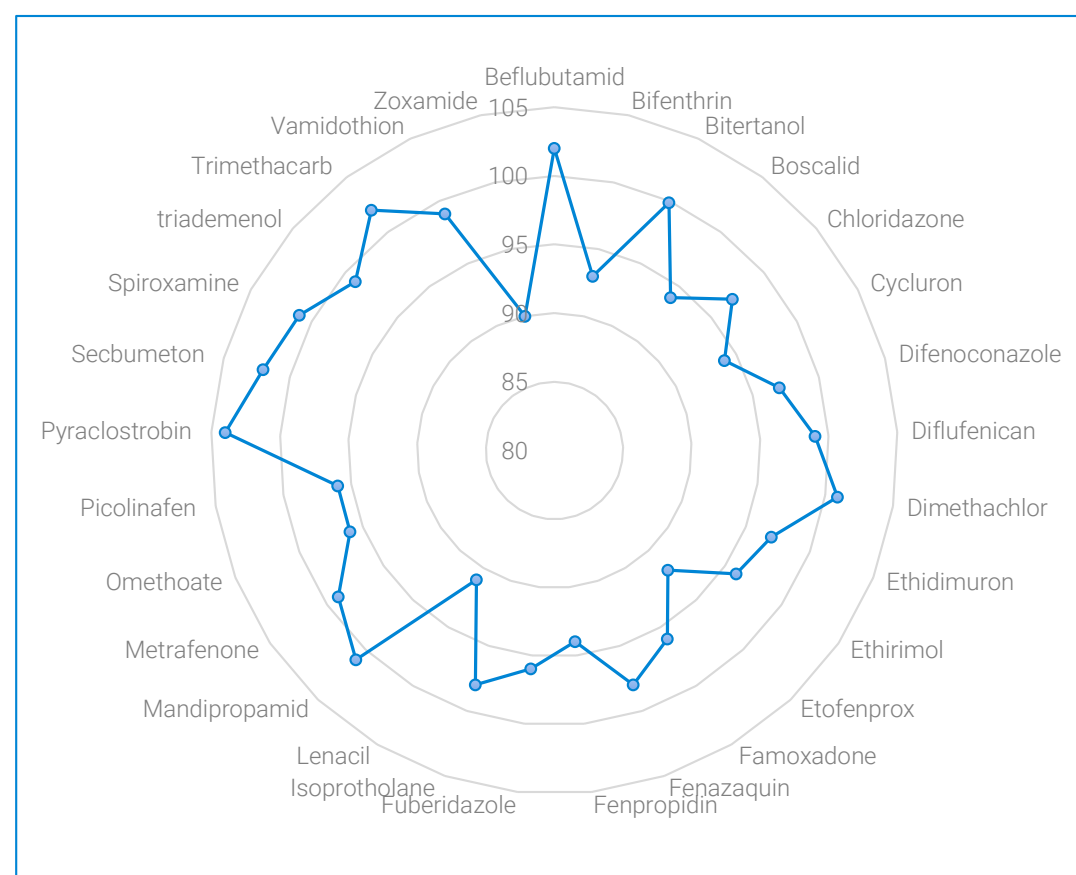


Figure 7: RADAR plot of recovery values of various pesticides in the study.

Conclusions

- LC-MS/MS method is developed for the analysis of pesticides in Chickpea powder samples.
- Retention time based acquisition provide more number of data points across the chromatographic peak compared to MRM in case of multi residue method.
- Recoveries of most of the analytes are above 80% with respect to matrix matched calibration curve. In case of low recovery analytes, matrix-based calibration curves are used, and recovery losses are compensated.
- Clean up followed by dilution of chickpea extract reduce ionization suppression, provide improved recovery and reproducible results for long batches.

References

1. Agilent Application note 5991-8154EN
2. Agilent Application note 5991-6357EN

For Research Use Only. Not for use in diagnostic procedures.

Poster Reprint

ASMS 2020

ThP 125

Drug Screening in Whole Blood Using a High-Resolution LC/Q- TOF and Novel Software Screener Tool

Karen E. Yannell, PhD and Manuel Gomez

Agilent Technologies, Santa Clara, CA

Drug Screening is Routine with LC/Q-TOF.

New drugs are continuously being introduced to the market. Whether it is a new illegal, prescription, or over-the-counter substance, laboratories need to test for these analytes. Targeted methodologies, like immunoassays or triple quadrupole mass spectrometer (MS) methods, do not allow the flexibility to quickly add these analytes to the method. Quadrupole Time-of-Flight (Q-TOF) MS methods allow for new analytes to be added without redeveloping the method because they can operate in a data independent acquisition (DIA) mode.

In this method, the 6546 LC/Q-TOF (Fig 1) was used for data acquisition. This instrument was chosen because it's high resolution ($>30,000$ at m/z 118), isotopic fidelity, and extended dynamic range produced confident identifications even when using fast chromatography with a whole blood sample. The extended dynamic range also made it possible to detect analytes at low levels even when there are often co-eluting analytes at higher abundances.



Figure 1. Bravo Automated Liquid Handling Platform (left) and the 6546 LC/Q-TOF (right) were the two instruments used in this method

In the past, Q-TOF data analysis has been complicated and challenging to implement in a high throughput way. This process is now routine and designed with the analyst in mind with a novel software tool. The LC Screener, in the MassHunter Quantitative Analysis 10.1 extracts the information for analytes of interest, applies identification criteria set in the method, and presents the data in an easy to understand manner. This software makes the analysis fast and simple.

Additionally, the Bravo Automated Liquid Handling Platform (Fig 1) was utilized with the Captiva EMR-Lipid 96 well plates to make extracting drugs from a whole blood sample routine. This instrument required minimal user intervention which lowers error and increases reproducibility.

Sample Preparation and Data Independent Acquisition Methodology.

A solid phase extraction was performed on blood samples spiked with 153 analytes and ten deidentified samples from a crime lab. The sample prep steps are outlined in Figure 2. The 10 minute liquid chromatography (LC) method is described in Table 1.

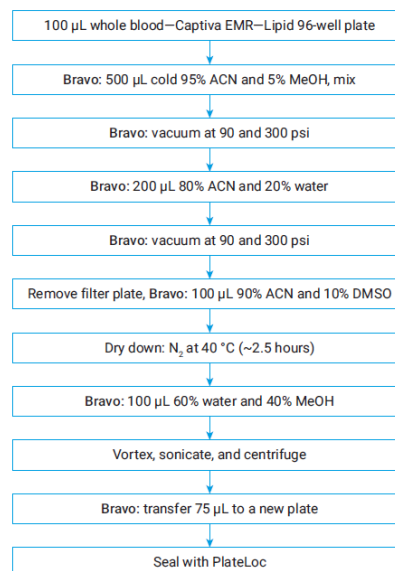


Figure 2. This workflow describes the steps for drug extraction and matrix removal for whole blood using the Captiva EMR-Lipid 96 well plates. Steps performed by the Bravo are labeled. Note, no sample concentration was performed for this method.

Table 1. LC method using an Agilent 1290 Infinity II.

Parameter	Value
Analytical column	Agilent Poroshell 120 EC-C18, 2.1 × 100 mm, 2.7 µm, narrow bore
Column temperature	55 °C
Injection volume	1 µL
Autosampler temperature	7 °C
Needle wash	Standard wash, 10 s, 80% methanol, 20% water
Mobile phase A	Water + 0.1% formic acid, 5 mM ammonium formate, 0.5 mM ammonium fluoride
Mobile phase B	Methanol + 0.1% formic acid, 5 mM ammonium formate, 0.5 mM ammonium fluoride
Flow rate	0.5 mL/min
Flow rate gradient	Time (min) % A % B
	0 95 5
	0.5 92 8
	1.2 89 11
	2 75 25
	6 55 45
	7.5 30 70
	8.5 2 98
	9.5 2 98
9.51 95 5	
Stop time	10 min
Post time	1 min

An Agilent 6546 LC/Q-TOF with an AJS ion source were used to acquire molecular ion and fragment data in positive mode. The instrument operated from m/z 40-1000 at 8 Hz and used collision energies (CE) 20 and 40 to fragment molecular ions. Two reference ions were used to ensure mass accuracy.

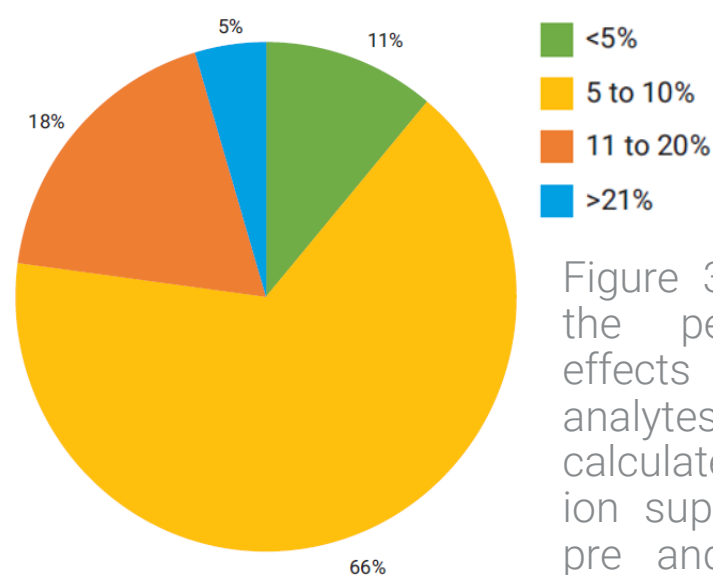


Figure 3. Pie chart of the percent matrix effects for the 153 analytes. This calculated the matrix ion suppression using pre and post spiked samples (n = 6).

Low Matrix Effects and High Recoveries were Achieved. The Fast Q-TOF Acquisition Speed Gave Robust Integration Without a Decrease to Mass Resolution.

The Captiva EMR-Lipid solid phase extraction procedure removed much of the matrix leaving a clean extract for injection. The matrix effects were very low with 77% of analytes have less than 10% matrix effects (Fig 3). Additionally recoveries were high with 91% of analytes falling between 70% and 130% recovery. Cannabinoids had lower recoveries with this solid phase chemistry.

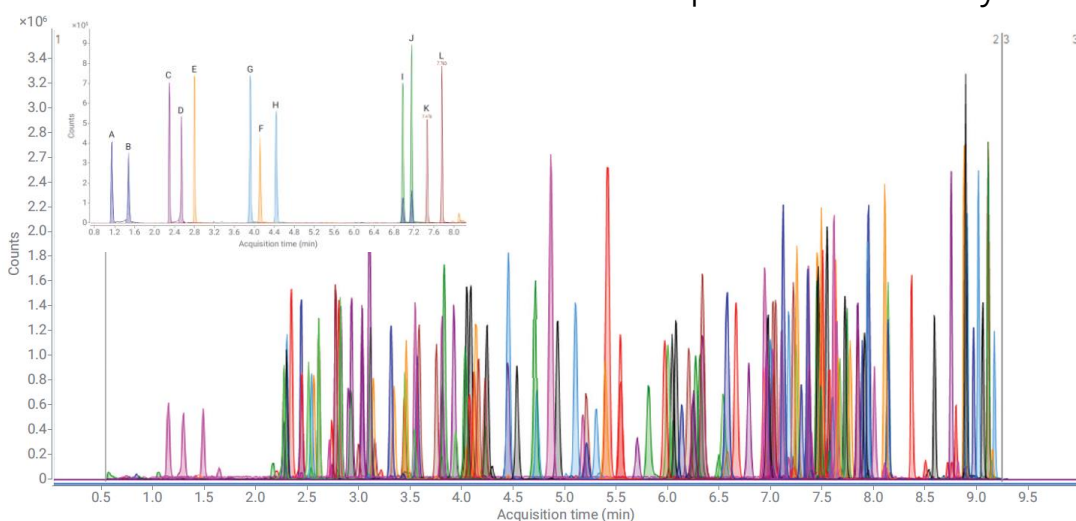


Figure 4. Separation of 153 analytes over 10 min. Inset chromatogram shows the baseline separation of isobaric analytes: morphine (A), hydromorphone (B), codeine (C), hydrocodone (D), O-desmethyl- tramadol (E), N-desmethyl-tramadol (F), methylphenidate (G), normeperidine (H), promethazine (I), promazine (J), temazepam (K), and clonazepam (L).

Chromatography was under 10 min and achieved good separation of all analytes tested. Baseline separation was achieved for six pairs of isobaric analytes in the method (Fig 4). Due to the Q-TOF's fast acquisition rate, plenty of data points were taken across the chromatographic peak allowing for robust integration of the molecular ion and fragment ions. With this instrument, the mass accuracy and resolution was maintained (Fig 5).

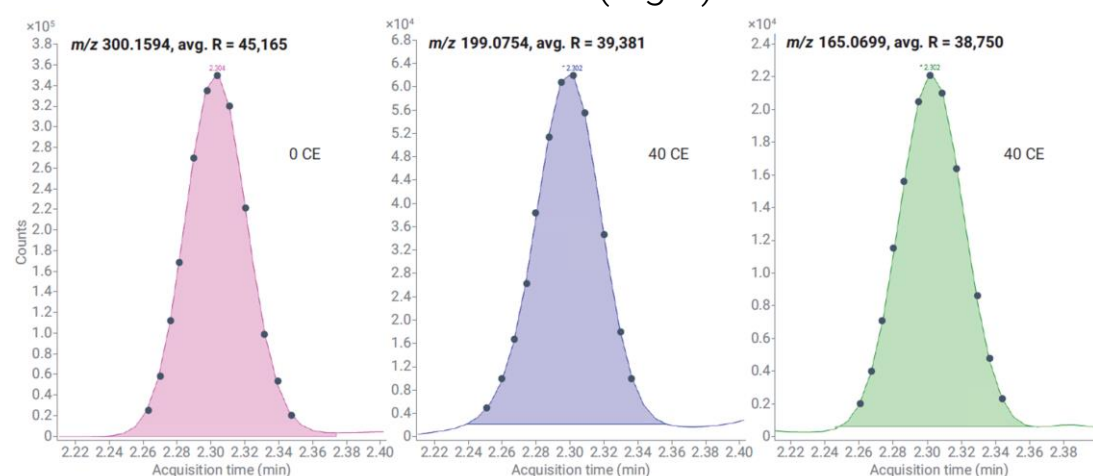


Figure 5. Chromatographic peaks for cocaine precursor (left) and two fragments (center and right). Using an acquisition speed of 8 Hz produced twelve data points (black dots) to be taken across the peaks which gave robust integration. With the Q-TOF, at these higher acquisition rates the resolution was not lowered.

MassHunter Quantitative Analysis and the LC Screener Make Q-TOF Analysis and Reporting Routine and Easy.

A screening method was built using a method creation wizard and a Personal Compound Database and Library containing MS/MS spectra for each analyte of interest. Criteria were set for identifying an analyte as positive namely, mass accuracy (5 ppm), signal to noise (3), retention time difference (10%), and at least two overlapping ions found (coelution > 80). The software filtered that data and labeled the analytes as positively identified (green) when all criteria were met, needs review (orange) if one criteria is out of bounds, or negatively identified (red) if more than one criteria are out of bounds.

The LC Screener displays all the analytes in the sample, filters the results based on identification category, and shows the isotope and chromatograms in a digestible manner (Fig 6). This allows for hundreds of analytes to be tested in a high throughput manner.

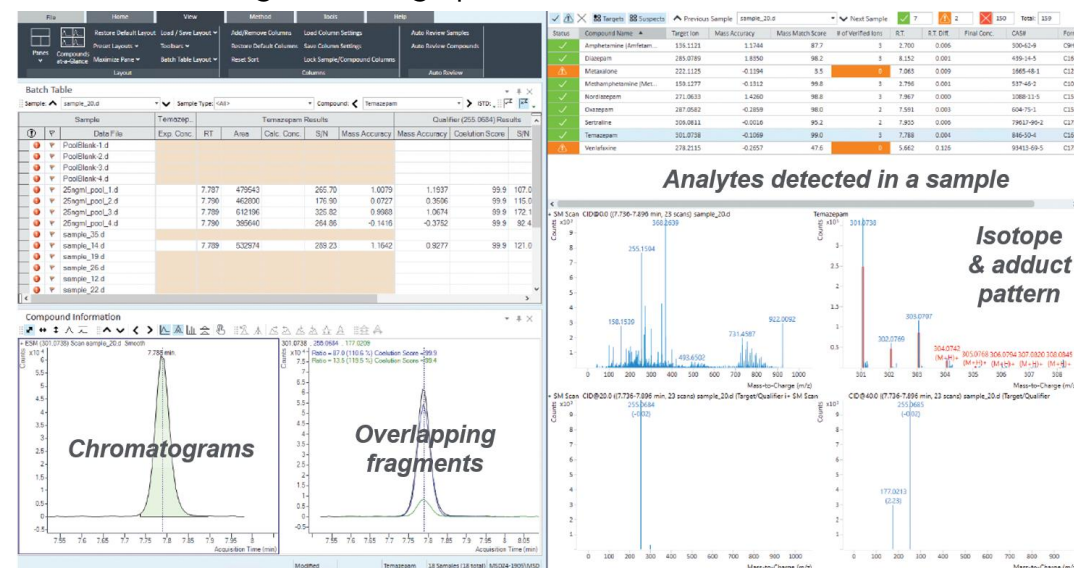


Figure 6. Analysis software display of the quant-my-way user interface and LC Screener Tool. Analytes in a sample, which are labeled as positively identified, needs review, or negatively identified, are displayed in the top right panel where they can be filtered. Each panel gives pertinent information for reviewing and confirming an identification.

Because the LC Screener Tool is located in the Quantitative Analysis software, simultaneous quantitation is possible for some or all analytes when you test calibration samples made from analytical standards (Fig 7). This means commonly found analytes may be quantified on the first injection while less common ones screened for only.

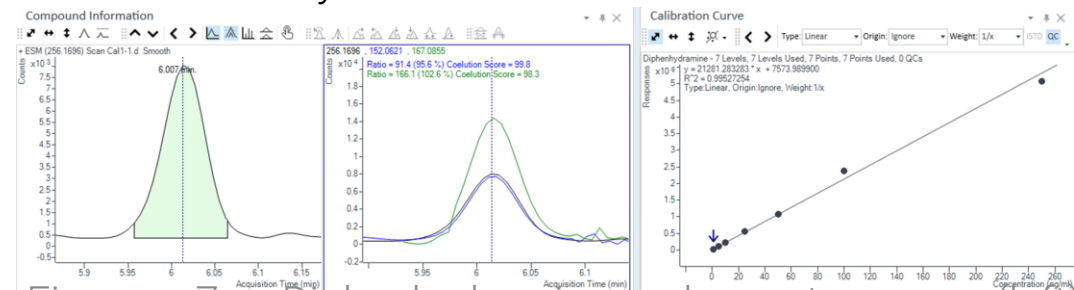


Figure 7. Diphenhydramine chromatogram (left), overlapping fragments (middle), and calibration curve (right) from 1 – 250 ng/mL where $R^2 = 0.995$ when weighting is $1/x$.

Analytes were Detected as Positively Identified at Low Concentrations and Found in Crime Lab Samples.

The concentration at which an analyte can be reproducibly detected as positive was evaluated. Even without concentrating the sample, 91% were detected at 5 ng/mL or less in six replicate samples (Fig 8).

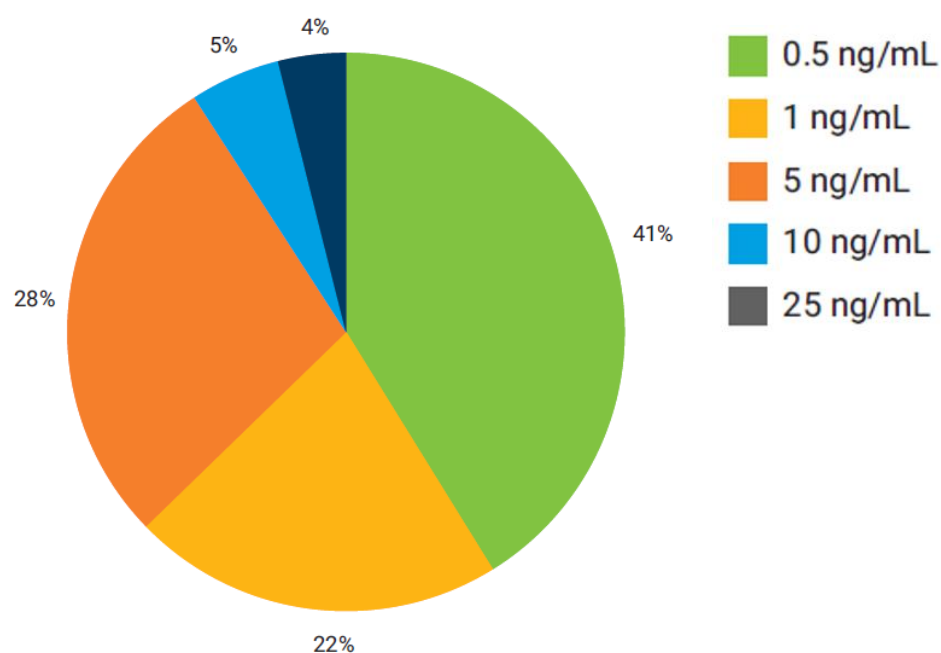


Figure 8. Pie chart of the concentration at which 153 analytes were detected as positively identified by the LC Screener Tool in six replicate samples. A positive identification was made when the molecular ion and one fragment had a mass accuracy = 5 ppm, RT difference <10%, S/N = 3, co-elution >80, and RSD of molecular ion <20%.

Ten deidentified samples from a crime lab were tested with the method. Many were found to be positive with the parent drug and, in some cases, a related metabolite (Table 2).

Table 2. Drugs detected in ten deidentified human samples.

Sample	Drugs Detected
1	Methamphetamine
2	Dihydrocodeine, oxycodone, hydrocodone, oxazepam, temazepam, nordiazepam, diazepam
3	Methamphetamine
4	Diphenhydramine, diazepam, nordiazepam
5	Amphetamine, methamphetamine, oxazepam, temazepam, sertraline, diazepam, nordiazepam
6	None
7	None
8	Amphetamine, methamphetamine, sertraline
9	Amphetamine, methamphetamine
10	Gabapentin, 7-aminoclonazepam, EDDP, clonazepam, methadone, lorazepam

To evaluate the robustness of the method and instrument, a 10 ng/mL sample extract was injected over 1400 times. During this time, minimal maintenance was performed- LC solvents refilled and calibration every few days. The data showed stable retention times, mass accuracy, and area counts for analytes. The data for morphine is showed in Fig 9. The study stopped after 1465 injections due to project timeline and not because of a decrease in the instrument's performance.

Data Quality Remained High for Over 1400+ Injections of Whole Blood Sample with Minimal Maintenance.

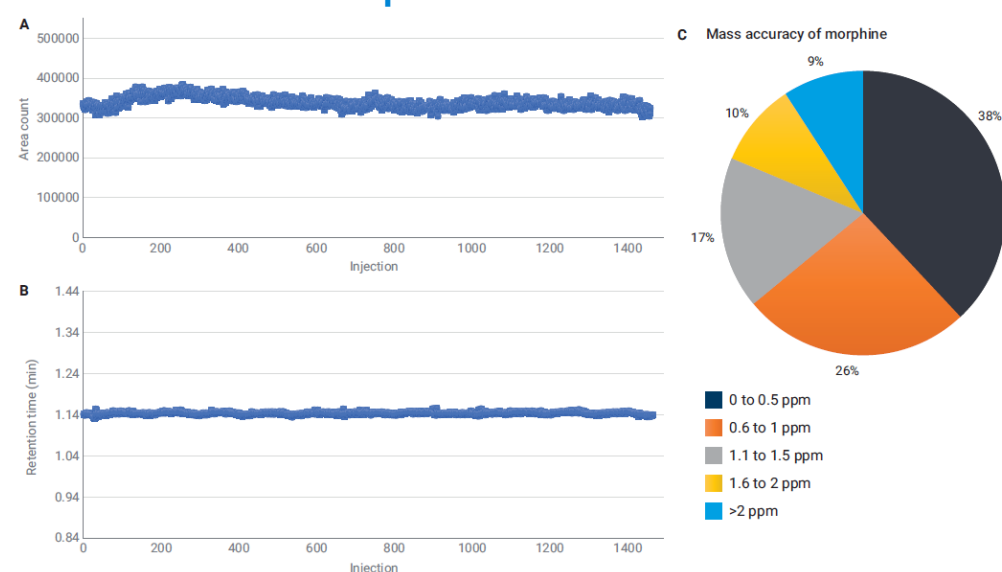


Figure 9. Morphine results for 1465 injections of a blood extract sample. The area counts (A), RTs (B), and mass accuracy (C) were all stable over this experiment.

Because this data is collected with a Q-TOF using DIA, at any point, if a new drug needs to be tested, it can be added to the analysis method with no effect on existing analytes and no redevelopment of the acquisition method needed.

Conclusions

Robust Routine Drug Screening with Automated Sample Prep is Achieved with the Bravo Liquid Handler, the 6546 LC/Q-TOF, and the LC Screener Tool.

- Sample prep with the Bravo Liquid Handler and Captiva EMR-Lipid plates was reproducible, removed matrix, and gave good analyte recoveries.
- 6546 LC/Q-TOF is a robust platform that consistently yielded high resolution results with excellent isotopic fidelity. In a complex sample, it could detect analytes at low concentration even over long periods of time with minimal maintenance.
- LC Screener tool made analyzing data fast and simple with the capability of quantitating some of the most commonly found drugs at the same time.

References

Yannell, K.E. and Gomes, M. Drug Screening in Whole Blood Using the Agilent 6546 LC/Q-TOF and the LC Screener Tool with Automated Sample Preparation. Agilent Technologies. March 20, 2020.

For Forensic Use

Poster Reprint

ASMS 2020

ThP 177

Optimum molecular descriptors based on 89 machine learning methods for predicting the recovery rate of pesticides in crops by GC-MS

Takeshi Serino^{1,2}, Sadao Nakamura¹,
Yoshizumi Takigawa¹, Tarun Anumol³, Md.
Altaf-UI-Amin², Shigehiko Kanaya²

¹ Agilent Technologies, Hachioji, Tokyo, Japan

² Nara Institute of Science and Technology,
Ikoma, Nara, Japan

³ Agilent Technologies, Wilmington, DE,
United States

Introduction

GC-MS is widely used for analysis of residual pesticides in fruits and vegetables (crops). Pesticide recovery ratio by GC-MS can vary by the residual matrix of the crops. We previously developed the prediction models with 89 machine learning methods (Table 1) for pesticide recovery rate using molecular descriptors (MDs)^[1]. With rcdk package of R program, 178 MDs were obtained by the canonical SMILES of each pesticide (Table 2). All MDs were used as the explanatory variables for predicting the pesticide recovery rate. Correlation coefficient of some MDs obtained by rcdk were over 0.7, i.e. highly correlated. Some combinations among these MDs are correlated strongly that can influence the performance of regression for pesticide recovery rate prediction such as the multicollinearity^[2]. The procedure to select the optimum MD for regression analysis using the correlation analysis and graph clustering tool^[3] is developed.

Experimental

There are two considerations below on selection of MDs for machine learning.

1. Reduction of highly correlated MDs

Select unique MDs utilizing the correlation analysis, i.e. select the MD with less correlations with any other MDs.

2. Minimize the loss of information

Select as many MDs as possible in order to minimize the loss of the information utilizing the graph clustering tool.

Correlation analysis among molecular descriptors

In order to select the optimum MDs for machine learning based on the two considerations, I propose the process of the flow chart for MD selection shown in the Figure 1. There are 5 steps for selection of MDs as below.

The 1st step is to list the correlations of all possible combinations among 178 MDs. MD-MD correlations were calculated by the Pearson's correlation coefficient r using "corr" package of R program and "strech" function for all 178 MDs. Based on the guidance of pearson correlation coefficient, the threshold at $r = 0.7$ is set for the "Highly correlated" of MD combination. The MDs in the combinations of $r > 0.7$ are classified as "Strongly correlated MD" and the other MDs are "Weakly correlated MD group".

The 2nd step is pick up the MDs of weak correlation (i.e. $r < 0.7$) with any other MDs. These MDs are grouped as "MD-r1a" which are used for regression analysis of machine learning later.

Experimental

Table 1. Machine Learning methods for regression analysis used in present study

Algorithm	Methods in caret
(a) Ordinary learning methods	
Kernel (17)	gaussprRadial, gaussprPoly, krlsPoly, gaussprLinear, krlsRadial, rvmLinear, rvmRadial, rvmPoly, svmRadial, svmRadialCost, svmRadialSigma, svmLinear, svmLinear2, svmPoly, svmLinear3, kernelpls (PLS), widekernelpls (PLS)
Simple Linear (16)	lm, leapSeq, leapForward, leapBackward, lmStepAIC, bridge, bayesglm (GLM), glmStepAIC (GLM), icr (ICA), pcr (PCA), superpc (PCA), superpc (PCA), nnls (PLS), simpls (PLS), pls (PLS), plsRglm (PLS, GLM), glm (GLM)
Sparse modeling (11)	penalized, blassoAveraged, foba, ridge, relaxo, lasso, Blasso, lars, lars2, glmnet, enet
Neural Network (9)	rbfDDA, dnn, neuralnet, brnn, mlpML, mlp, mlpWeightDecay, msaenet, monmlp
Decision Tree (8)	rpart, rpart1SE, ctree, ctree2, evtree, M5Rules, M5, WM
Centroid kNN (3)	knn, kkn, SBC
Spline (2)	gcvEarth, earth
Others (3)	ppr, spikeslab, xyf (LVQ)
(b) Ensemble learning methods	
Decision Tree (14)	cforest, ranger, qrf, rf, parRF, extraTrees, Rborist, RRFglobal, RRF, treebag, bstTree, gbm, xgbTree, nodeHarvest
Simple Linear (3)	BstLm, glmboost (GLM), xgbLinear
Spline (3)	bagEarthGCV, bagEarth, xgbDART

Table 2. 178 molecular descriptors in present study

Descriptor Class	Descriptor (Description)
ALOGP Descriptor (2)	ALOGP (Ghose-Crippen LogKow), ALOGP2 (Square of ALOGP)
APol Descriptor (1)	APol (Sum of the atomic polarizabilities (including implicit hydrogens))
Aromatic Atoms Count Descriptor (1)	naAromAtom (Number of aromatic atoms)
Aromatic Bonds Count Descriptor (1)	nAromBond (Number of aromatic bonds)
Atom Count Descriptor (2)	nAtom (Number of atoms), nB (Number of boron atoms)
Autocorrelation Descriptor Charge (5)	ATSc1, ATSc2, ATSc3, ATSc4, ATSc5 (ATS autocorrelation descriptor, weighted by charges)
Autocorrelation Descriptor Mass (5)	ATSm1, ATSm2, ATSm3, ATSm4, ATSm5 (ATS autocorrelation descriptor, weighted by scaled atomic mass)
Autocorrelation Descriptor Polarizability (5)	ATSp1, ATSp2, ATSp3, ATSp4, ATSp5 (ATS autocorrelation descriptor, weighted by polarizability)
BCUT Descriptor (6)	BCUTw.1l (nhigh lowest atom weighted BCUTs), BCUTw.1h (nlow highest atom), BCUTc.1l (nhigh lowest partial charge), BCUTc.1h (nlow highest partial charge) BCUTp.1l (nhigh lowest polarizability), BCUTp.1h (nlow highest polarizability)
BPolDescriptor (1)	bpol (Sum of the absolute value of the difference between atomic polarizabilities of all bonded atoms in the molecule (including implicit hydrogens))
Carbon Types Descriptor (9)	C1SP1 (Triply bound carbon bound to one other carbon), C2SP1 (Triply bound carbon bound to two other carbons), C1SP2 (Doubly bound carbon bound to one other carbon), C2SP2 (Doubly bound carbon bound to two other carbons), C3SP2 (Doubly bound carbon bound to three other carbons), C1SP3 (Singly bound carbon bound to one other carbon), C2SP3 (Singly bound carbon bound to two other carbons), C3SP3 (Singly bound carbon bound to three other carbons), C4SP3 (Singly bound carbon bound to four other carbons)
Chi Chain Descriptor (10)	SCH.3-7 (Simple chain, orders 3-7), VCH.3-7 (Valence chain, orders 3-7)
Chi Cluster Descriptor (8)	SC.3-6 (Simple cluster, orders 3-6), VC.3-6 (Valence cluster, orders 3-6)
Chi Path Cluster Descriptor (6)	SPC.4-6 (Simple path cluster, orders 4 to 6), VPC.4-6 (Valence path cluster, orders 4-6)
Chi Path Descriptor (16)	SP.0-7 (Simple path, orders 0-7), VP.0-7 (Valence path, orders 0-7)
Eccentric Connectivity Index Descriptor (38)	ECCEN (A topological descriptor combining distance and adjacency information), khs.sCH3 (Count of atom-type E-State: -CH3), khs.dCH2 (=CH2), khs.ssCH2 (-CH2-), khs.tCH (#CH), khs.dsCH (=CH-), khs.aaCH (CH-), khs.sssCH (-CH-), khs.tsC (#C), khs.dssC (=C-), khs.aasC (C-), khs.aaaC (C-), khs.ssssc (-C-), khs.ssnH (-NH2), khs.ssnH (-NH2-), khs.aanH (NH-), khs.tN (#N), khs.ssnH (-NH-), khs.dsn (=N-), khs.aan (N-), khs.ssn (-N-), khs.dsn (-N-), khs.aan (N-), khs.sOH (-OH), khs.dO (=O), khs.sO (-O-), khs.aaO (O-), khs.sF (-F), khs.sssSi (-Si-), khs.dssP (-P=), khs.ds (=S), khs.sS (-S-), khs.aas (aS), khs.dssS (-S=), khs.dssS (-S=), khs.sCl (-Cl), khs.sBr (-Br)
Fragment Complexity Descriptor (1)	fragC (Complexity of a system)
H Bond Acceptor Count Descriptor (1)	nHBAcc (Number of hydrogen bond acceptors)
H Bond Donor Count Descriptor (1)	nHBDon (Number of hydrogen bond donors)
KappaShape Indices Descriptor (3)	Kier1-3 (First, Second, Third kappa (k) shape indexes)
Largest Chain Descriptor (1)	nAtomLC (Number of atoms in the largest chain)
Longest Aliphatic Chain Descriptor (1)	nAtomLAC (Number of atoms in the longest aliphatic chain)
Mannhold LogP Descriptor (1)	MLogP (Mannhold LogP)
MDEDescriptor (19)	MDEC.11 (Molecular distance edge between all primary carbons), MDEC.12 (between all primary and secondary carbons), MDEC.13 (between all primary and tertiary carbons), MDEC.14 (between all primary and quaternary carbons), MDEC.22 (between all secondary carbons), MDEC.23 (between all secondary and tertiary carbons), MDEC.24 (between all secondary and quaternary carbons), MDEC.33 (between all tertiary carbons), MDEC.34 (between all tertiary and quaternary carbons), MDEC.44 (between all quaternary carbons), MDEO.11 (between all primary oxygens), MDEO.12 (between all primary and secondary oxygens), MDEO.22 (between all secondary oxygens), MDEN.11 (between all primary nitrogens), MDEN.12 (between all primary and secondary nitrogens), MDEN.13 (between all primary and tertiary nitrogens), MDEN.22 (between all secondary nitrogens), MDEN.23 (between all secondary and tertiary nitrogens), MDEN.33 (between all tertiary nitrogens)
PetitjeanNumberDescriptor (1)	PetitjeanNumber (Petitjean number)
RotatableBondsCountDescriptor (1)	nRotB (Number of rotatable bonds, excluding terminal bonds)
RuleOfFiveDescriptor (1)	LipinskiFailures (Number failures of the Lipinski's Rule Of 5)
TPSADescriptor (19)	TopoPSA (Topological polar surface area)
VAdjMaDescriptor (1)	VAdjMat (Vertex adjacency information (magnitude))
WeightDescriptor (1)	MW (Molecular weight)
WeightedPathDescriptor (5)	WTPT.1 (Molecular ID), WTPT.2 (Molecular ID / number of atoms), WTPT.3 (Sum of path lengths starting from heteroatoms), WTPT.4 (Sum of path lengths starting from oxygens), WTPT.5 (Sum of path lengths starting from nitrogens)
WienerNumbersDescriptor (2)	WPATH (Weiner path number), WPOL (Weiner polarity number)
XLogPDescriptor (1)	XLogP (XLogP)
ZagrebIndexDescriptor (1)	Zagreb (Sum of the squares of atom degree over all heavy atoms i)
Petitjean Shape Index Descriptor (1)	topoShape (Petitjean topological shape index)
Others (17)	nAcid (Acidic group count descriptor), nBase (Basic group count descriptor), nSmallRings (the number of small rings from size 3 to 9), nAromRings (the number of aromatic rings), nRingBlocks (total number of distinct ring blocks), nAromBlocks (total number of "aromatically connected components"), nRings3, 5, 6, 7 (individual breakdown of small rings), tpsaEfficiency (Polar surface area expressed as a ratio to molecular size), VABC (Atomic and Bond Contributions of van der Waals volume), HybRatio (the ratio of heavy atoms in the framework to the total number of heavy atoms in the molecule), tpsaEfficiency.1 (Polar surface area expressed as a ratio to molecular size), TopoPSA.1 (Topological polar surface area), topoShape.1 (A measure of the anisotropy in a molecule)

Table 3. DPPlus parameters

Parameter	Value
CP Value	0.5
Density Value	0.9
Minimum Cluster Value	2

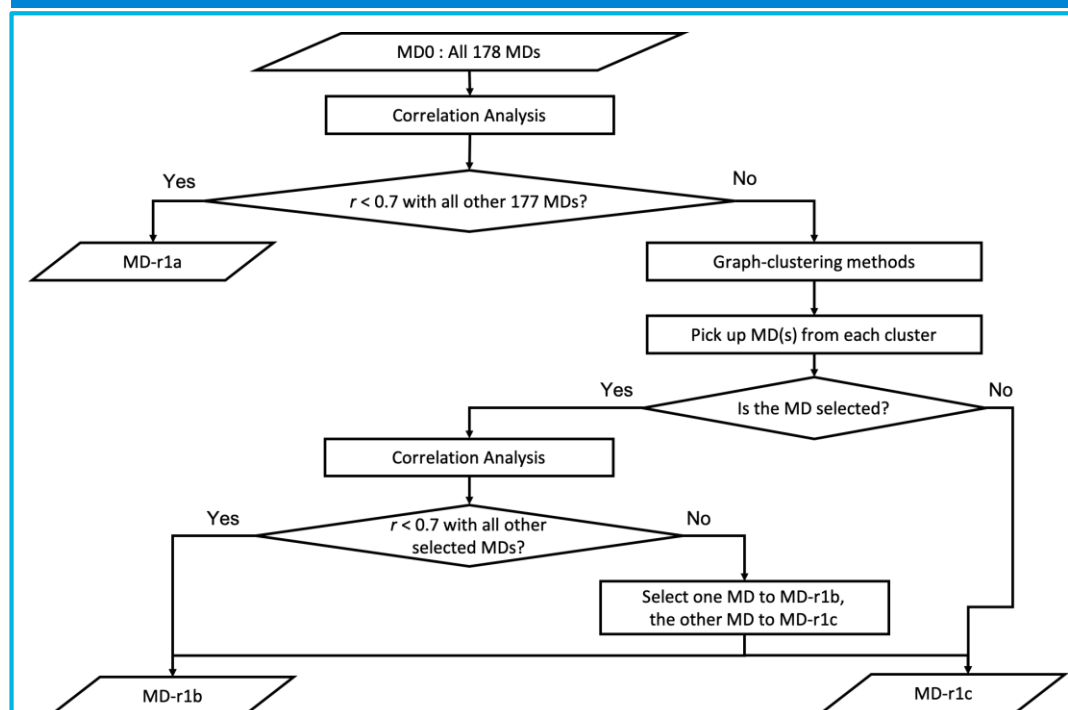


Figure 1. Process chart of selecting the optimum MDs

The 3rd step is to visualize the correlations of strongly correlated MDs by the method of graph clustering method called DPCLUS^[3] and pick up the representative MD(s) from each cluster according to the flow chart in Figure 2, based on the considerations of removal of highly correlated MDs while minimizing the loss of information. The parameters of DPCLUS software is set as in Table 3.

The 4th step is the second correlation analysis among the representative MDs picked up from each cluster. Threshold of correlation is $r > 0.7$.

The final step is to select the MD(s) based on the step 4. The MDs of weak correlation with other MDs in step 4 are grouped as “MD-r1b”, which are used for regression analysis. Other MDs in step 4 are divided into two groups, “MD-r1b” and “MD-r1c”. MDs in group MD-r1c are excluded from regression analysis.

Thus, 178 MDs are divided into three groups as listed in the Table 4 according to the process in Figure 1.

$$\text{Prediction Error (PE)} \quad PE_j = \frac{\sum_{i=1}^N (y_{obs}^{(ij)} - y_{pred}^{(ij)})^2}{\sum_{i=1}^N (y_{obs}^{(ij)} - \bar{y}^{(j)})^2} \quad (1)$$

Table 4. Molecular Descriptors selected by the correlation analysis and cluster analysis

MD group	Description of MDs	# of MDs	Selected
MD-r1a	MD of $r < 0.7$ with any of other 177 MDs	60	Yes
MD-r1b	MD of $r \geq 0.7$ with any of other 177 MDs and selected by graph-clustering method	23	Yes
MD-r1c	MD of $r \geq 0.7$ with any of other 177 MDs and excluded by graph-clustering method	95	No

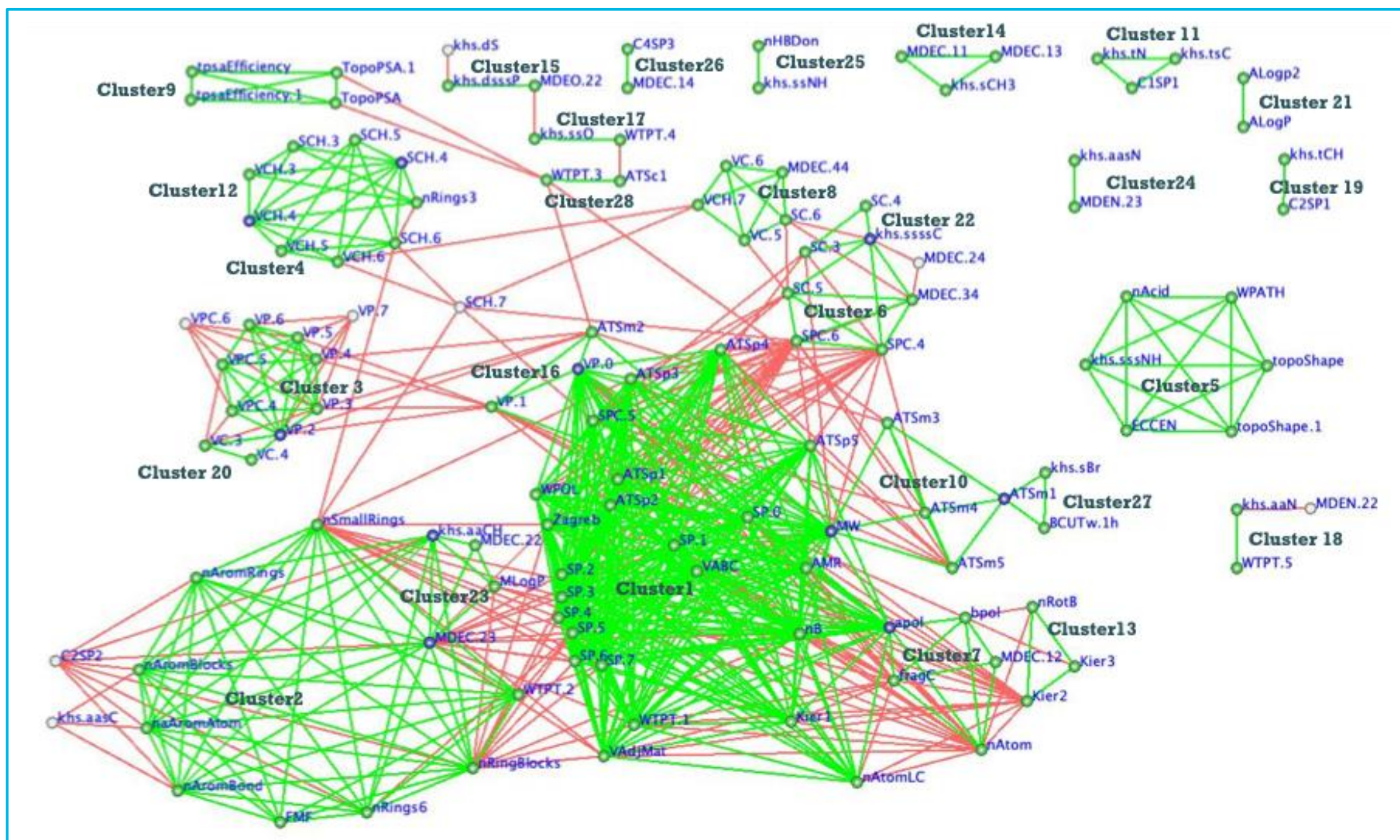


Figure 3. Result of cluster analysis result by DPCLUS

Experimental

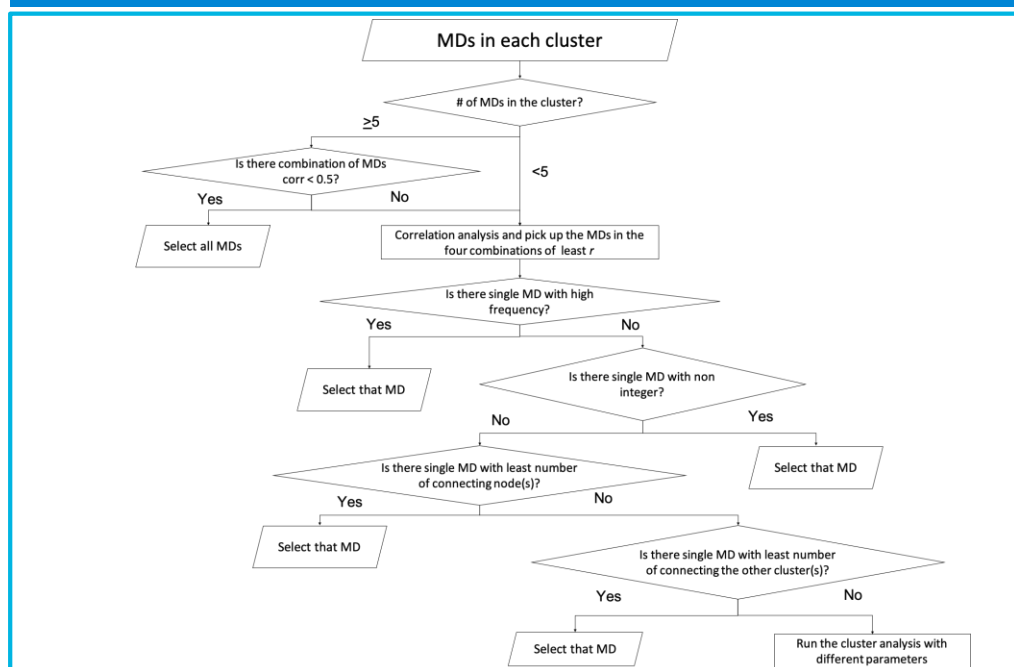


Figure 2. Process chart of selecting the optimum MDs from each cluster

Results and discussion

Correlation analysis among molecular descriptors

658 combinations consisted of 118 MDs were $r \geq 0.7$, which correlate strongly. Other 60 MDs were correlated with the other MDs at $r < 0.7$, which was classified as the MD group MD-r1a in the Table 4.

Selection of molecular descriptors by the clustering tool

Relationships of 118 MDs of strongly correlated with any other MD(s) were classified into 28 clusters according to the cluster analysis by DPCLUS, shown in Figure 3. 19 clusters are connected by red lines each other dependently and MDs in the other 9 clusters has no connection with the other clusters.

Selection of molecular descriptors for machine learning after cluster analysis

The combinations of MDs with $r > 0.7$ among them are listed in the Table 5. The MDs of the column MD-a in the Table 5 are classified to MD-1rb and MD-b are classified to MD-r1c of Table 4.

Table 5. Combination of MDs with the $r > 0.7$ after selection of cluster analysis

MD-a	MD-b	Correlation coefficient	MD-a	MD-b	Correlation coefficient
khs.aaCH	MDEC.22	0.833	nAtomLC	VP.0	0.751
ATSm1	BCUTw.1h	0.777	WTPT.4	ATSc1	0.736
VCH.4	SCH.3	0.769	SPC.5	MDEC.34	0.731

Comparison of machine learning performance between with and without selection of molecular descriptors

By selecting the MDs, 57 machine learning methods gave better PE for regression analysis and 32 methods got worse. Top and bottom 10 machine learning methods in prediction error by selecting MDs are listed in Table 6.

bagEarthGCV(LogPE -0.473 to 3.501), ppr(-1.482 to -0.824) and 4 ordinary simple liner methods (glm -0.956 to -0.397, glmStepAIC -0.918 to -0.363, lmStepAIC -0.912 to

Results and discussion

-0.397 and lm -0.930 to -0.397) got worse in prediction error by the selection of MDs with cluster analysis. lasso(LogPE 23.723 to -0.232) and lars(8.871 to -0.161) bagEarth(5.398 to -0.283) were improved by selecting the MDs with cluster analysis. Ordinary Decision trees, Ordinary Centroid and Ensemble Simple Liner show-small differences in prediction error by the selection of MDs.

Table 6. Top 10 methods of best (right) and worst (left) in differences of prediction error by selecting the molecular descriptors, sorted by the Prediction Error difference

Met	Category	MD2_PE	MD0_PE	PE Diff.	Met	Category	MD2_PE	MD0_PE	PE Diff.
bagEarthGCV	E. Spline	3.501	-0.473	3.974	lasso	O. Sparse Modeling	-0.232	23.723	-23.955
ppr	O. Others	-0.824	-1.482	0.657	lars	O. Sparse Modeling	-0.161	8.871	-9.032
glm	O. Simple Liner	-0.397	-0.956	0.559	bagEarth	E. Spline	-0.283	5.398	-5.681
glmStepAIC	O. Simple Liner	-0.363	-0.918	0.556	bridge	O. Simple Liner	-0.211	0.552	-0.762
lmStepAIC	O. Simple Liner	-0.363	-0.912	0.550	blassoAveraged	O. Sparse Modeling	-0.183	0.564	-0.747
lm	O. Simple Liner	-0.397	-0.930	0.532	Rborist	E. Decision Tree	-0.901	-0.304	-0.597
svmPoly	O. Kernel	-0.069	-0.545	0.476	xgbTree	E. Decision Tree	-0.812	-0.550	-0.262
bayesglm	O. Simple Liner	-0.397	-0.798	0.401	xgbDART	E. Spline	-0.888	-0.640	-0.248
brnn	O. Newral Network	-0.364	-0.693	0.329	RRF	E. Decision Tree	-0.851	-0.694	-0.158
gaussprPoly	O. Kernel	-0.163	-0.445	0.282	rf	E. Decision Tree	-0.860	-0.708	-0.152

Conclusions

The procedure to remove the highly correlated explanatory variables of molecular descriptors with correlation analysis and graph clustering tool are developed for the data set of residual pesticide recovery. Correlation analysis is applied on all 178 molecular descriptors and finally 83 molecular descriptors were selected for regression analysis of 89 machine learning methods. Prediction error of machine learning methods in the ordinary sparse model improved by removal of highly correlated molecular descriptors. On the other hand, prediction error of the methods of ordinary simple liner got worse by the selection of molecular descriptors.

References

- 1 Takeshi Serino, et al. 67th American Society for Mass Spectrometry TP-298. *Comprehensive Machine Learning Prediction of GC/MS Pesticide Recovery Based on the Molecular Fingerprinting for Food QA/QC*. Atlanta, GA. June, 2019.
- 2 A. Garg and K. Tai. 2013. Comparison of statistical and machine learning methods in modelling of data with multicollinearity. *International Journal of Modelling, Identification and Control(IJMIC)* **18**: 295-312.
- 3 M. Altaf-Ul-Amin, Y. Shibo, K. Mihara, K. Kurokawa and S. Kanaya. 2006. Development and implementation of an algorithm for detection of protein complexes in large interaction networks. *BMC Bioinformatics* **7**: 207

Poster Reprint

ASMS 2020

ThP 184

Black Pepper authenticity workflow using high-resolution GC/Q-TOF

Sofia Nieto, Melissa Churley

Agilent Technologies, Santa Clara, CA

Introduction

Black pepper, as a highly valued commodity, is known to be subject to economically motivated adulteration [1]. Here we present a novel workflow which utilizes a high-resolution GC-QTOF and classification modeling to be able to distinguish two pepper samples from different geographic regions as well as to identify adulteration of black pepper samples. Two tested “adulterants” to black pepper were Szechuan pepper and papaya seeds, the latter of which is known to be used in the adulteration process.

1. <https://www.sciencedirect.com/science/article/abs/pii/S0956713519300842>

Experimental

Adulteration of Malabar black pepper was studied. Black pepper from two different geographical regions (Malabar, from India, and Phu Quoc, from Vietnam), Szechuan pepper and papaya seeds were ground. In separate sample groups for each adulterant, Szechuan pepper and Papaya seeds were mixed in varying proportions to Malabar to mimic 5 – 50% adulteration. Pure samples of each material listed above were used to build the classification model. Positive controls consisted of pure samples, and negative controls consisted of Malabar mixed with either Szechuan or papaya seeds. All samples were extracted sequentially using hexane and acetone. Method blanks were prepared using the same solvent. The extracts were combined and filtered through 0.45 μm nylon filters and analyzed in random order using a 7890 GC coupled to a high-resolution Q-TOF MS in full acquisition mode.

GC and MS Conditions:	Q-TOF (7250)
GC	7890
Column	30-5MS UI, 15 m, 0.25 mm, 0.25 μm
Inlet	MMI, 4-mm UI liner single taper w wool
Injection volume	1 μL
Injection mode	Split, 10:1
Inlet temperature	280°C
Oven temperature program	50°C for 2 min; 10°C/min to 300°C, 10 min hold
Carrier gas	Helium
Column flow	1.2 mL/min
Transfer line temperature	300°C
Quadrupole temperature	150°C
Source temperature	200°C
Electron energy	70 eV
Emission current	5 μA
Spectral acquisition rate	5 Hz
Mass range	45 to 650 m/z

Table 1. GC/Q-TOF acquisition parameters.

Experimental

The retention indices were calculated based on the alkane ladder to ensure correct compound identification. The GC/Q-TOF data were processed using the Unknown Analysis tool of MassHunter Quantitative Analysis Software 10.1, Mass Profiler Professional 15.1 and Classifier 1.1. The conditions are described in detail in Table 1.

Results and Discussion

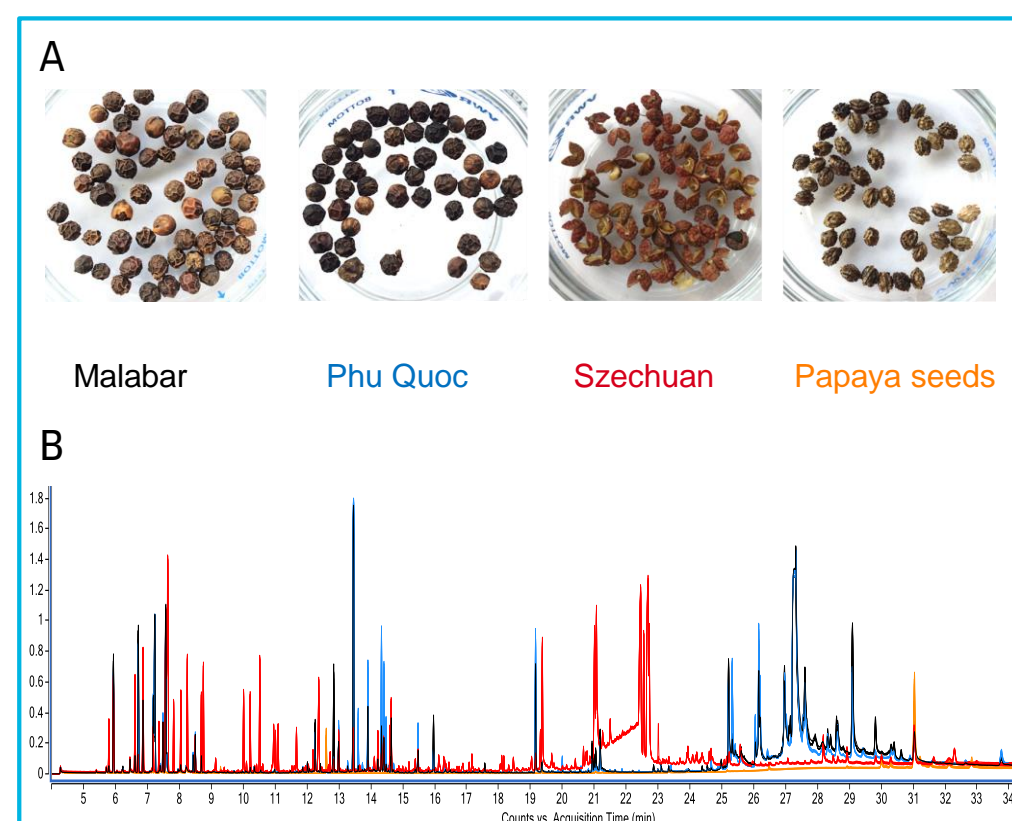


Figure 1. A) Pepper and papaya seeds samples B) Chromatogram overlay of 6 replicates of each extract. The colors in the chromatogram in B correspond to the colors shown in A. Papaya seeds extract (orange color trace) was found to be relatively clean versus the more complex pepper samples.

Classification Model Building

Six replicate extracts of each type of pepper – Malabar, Phu Quoc, Szechuan, as well as papaya seeds were used to build the classification model in Mass Profiler Professional (MPP). General workflow for building a classification model and processing unknown samples is shown in Figure 2. The first step involves data acquisition for the pure unadulterated samples as well as positive and negative controls. The accurate mass GC/Q-TOF data were processed in the Unknowns Analysis to perform chromatographic deconvolution and NIST17 library search (Figures 2 and 3). Next, the data were exported from Unknowns Analysis to MPP.

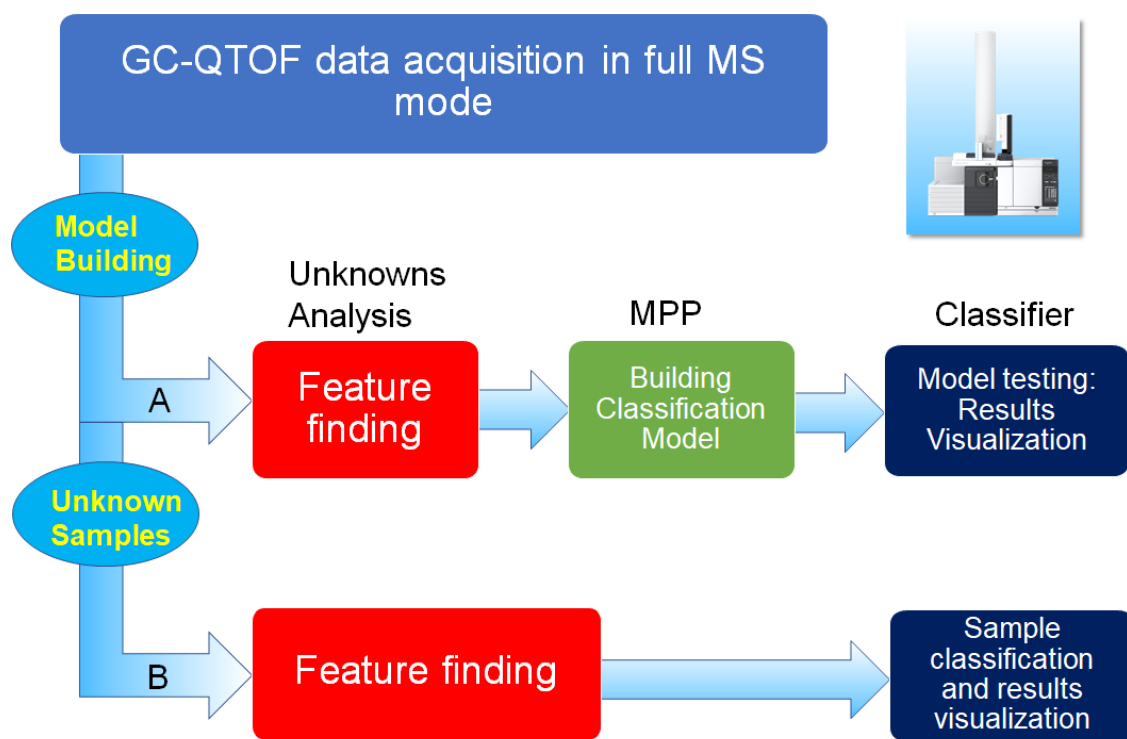


Figure 2. Workflow overview for a classification study using GC/Q-TOF. A) Building classification model. B) Analysis of unknown samples.

MPP is then used to build, test and validate the classification model. An example of such workflow in MPP is outlined in Figure 4. Then, the data are exported to Classifier that allows for easy results visualization and reporting that facilitate model testing. After the model is finalized, the unknown samples are processed in Unknowns Analysis and Classifier, bypassing data processing in MPP (Figure 2B).

The classification models were built using two different algorithms: PLSDA (Partial Least Square Discrimination) and SIMCA (Soft Independent Modeling of Class Analogy).

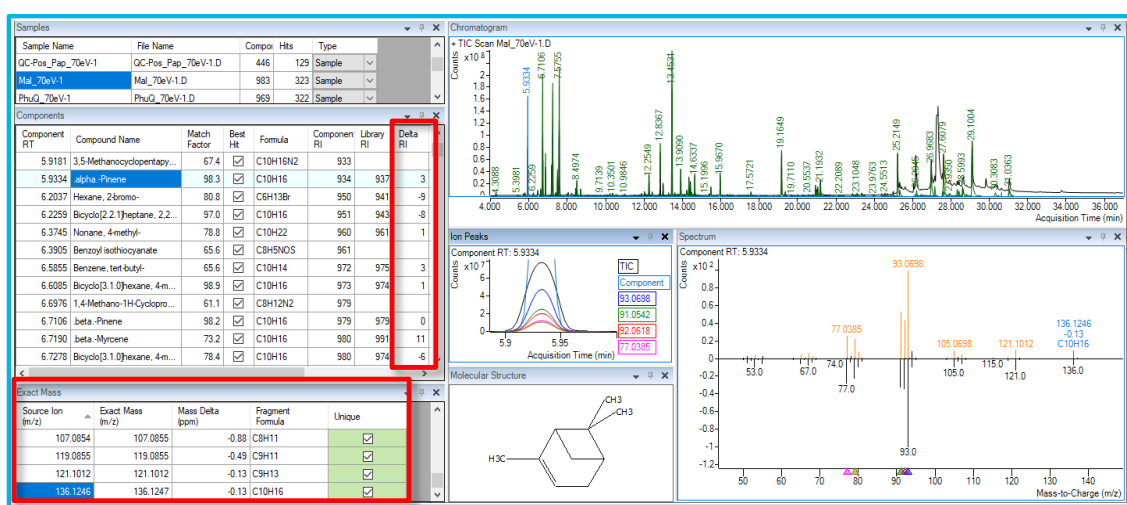


Figure 3. Feature finding in Unknowns Analysis. Highlighted in red boxes: RI calibration function helps confirm compound ID. ExactMass feature provides additional confirmation of compound identification using accurate mass spectral information.

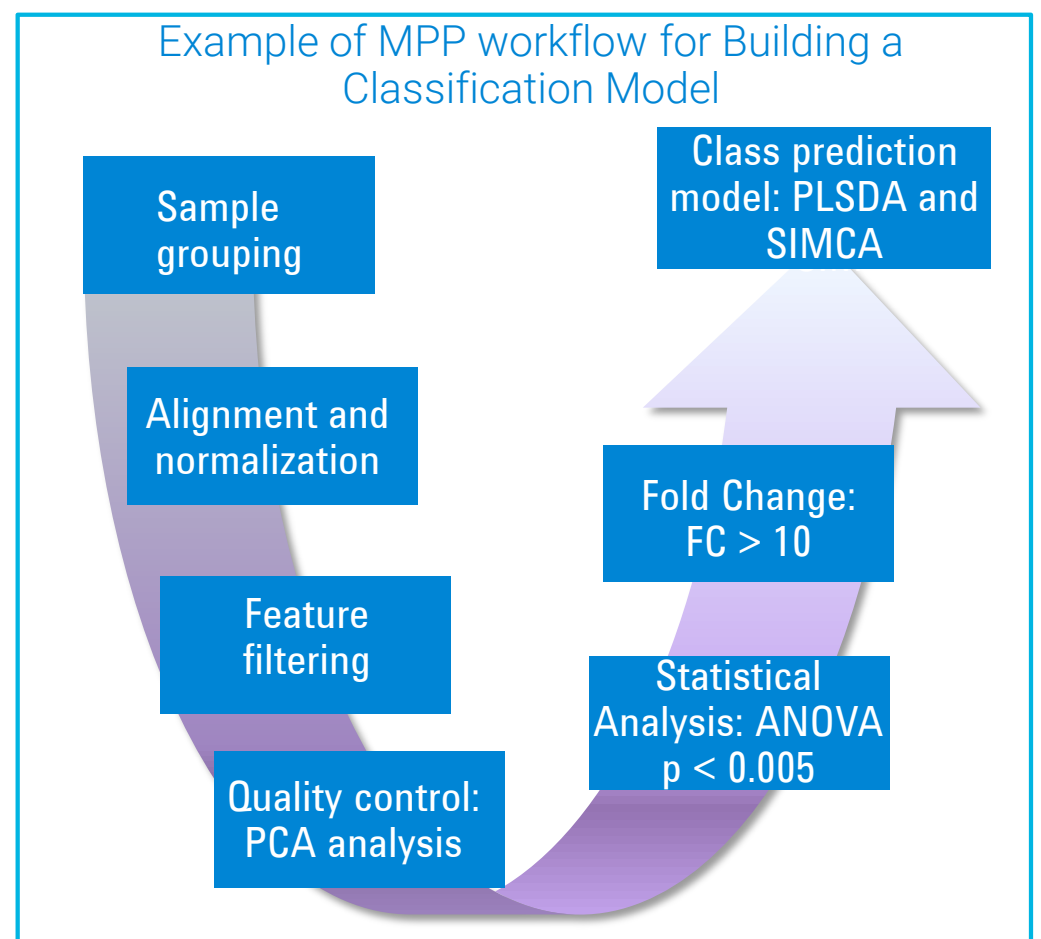


Figure 4. MPP workflow summary.

Closer Look at Model Compounds

	Malabar	Phu Quoc	Szechuan	Papaya seeds
	% base peak			
α -Pinene	21.7	16.9	8.4	
Sabinene			16.7	
β -Pinene	37.0	31.3		
β -Myrcene	1.3	2.0	19.4	
α -Phellandrene	4.5	10.6		
β -Carene	64.5	86.6		
α -Cymene	2.1	1.7		
D-Limonene	23.9	21.4	22.1	
Eucalyptol	23.7	1.6	100	
β -cis-Ocimene			3.2	
γ -Terpinene			4.5	
4-Thujanol			4.0	
Terpinolene		1.0		
Linalool			2.1	
Benzyl nitrile				2.8
L-4-terpineol			2.8	
L- α -Terpineol			2.5	
δ -Elemene		1.1		
α -Terpinyl acetate			10.3	
Benzyl isothiocyanate				80.7
Copaene	4.1			
β -Cubebene		1.4		
Caryophyllene	24.9	59.6		
α -Guaiane		1.6		
Humulene	1.1	3.4		
β -Eudesmene		4.4		
α -Selinene		3.3		
β -Bisabolene		1.5		
δ -Cadinene			2.2	
Caryophyllene oxide		1.7		
Pellitorin	5.4	4.8		
9,12-Octadecadienoic acid (Z,Z)-			5.3	
Kalecide		1.1		
Hydroxy-sanshool 2			4.3	
Hexadecanoic acid, octyl ester				
Piperanine	18.6	3.7		
Piperlonguminine		3.8		
(2E,4E)-N-Isobutyloctadeca-2,4-dienamide		2.9		
Squalene				2.4
Piperlyline	4.4	3.7		
Piperine	100	100		
Pipersintenamide	2.2	11.0		
Kusunokinin		2.3		
Piperoleine B	8.3	5.1		
γ -Sitosterol	1.6	1.5	1.6	100
Stigmastanol				8.1
4-Campestene-3-one				2.9
Sitostenone (Stigmast-4-en-3-one)				7.8

Table 2. Major compounds included in PLSDA model. Relative amounts in each of the extracts (% base peak on the chromatogram) are shown. Percent of base peak was calculated after averaging across all the replicates from each group (<1% if not indicated).

Fragment formula annotated compound spectra for two predominant, unique compounds identified in Szechuan pepper and papaya seeds extracts are shown in Figure 5. Note, that Hydroxy-sanshool does not have a spectrum in NIST17. However, a tentative ID can still be assigned based on published information [2].

2. Yue Ji, Shiming Li, Chi-Tang Ho. *Food Science and Human Wellness*. 8 (2019) 115–125

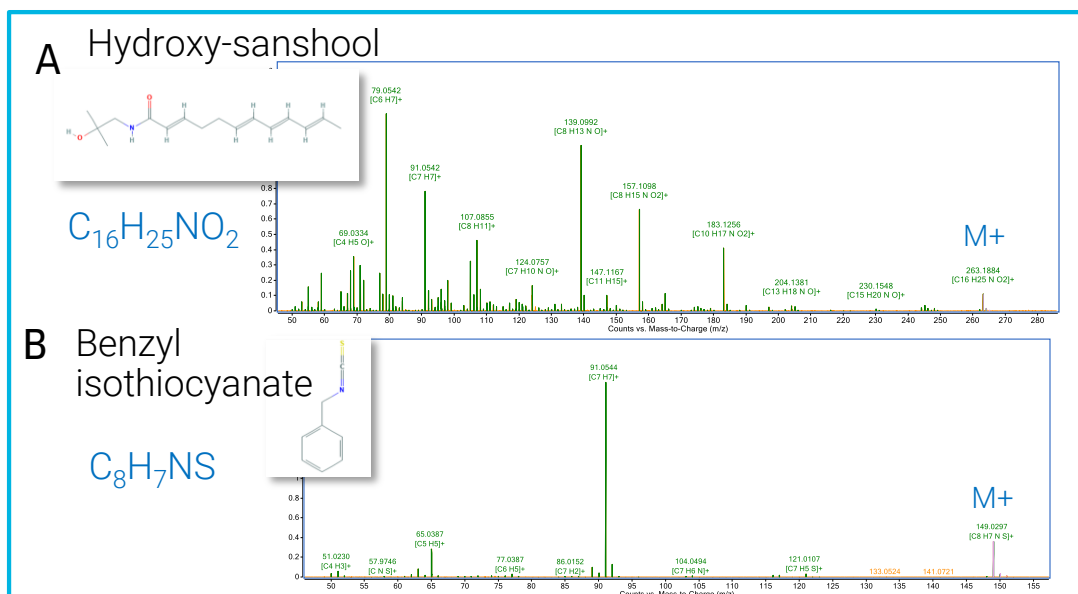


Figure 5. Example spectra for two unique and predominant compounds identified in “adulterants”: A) in Szechuan pepper and B) in Papaya seeds. Structures were exported from PubChem database.

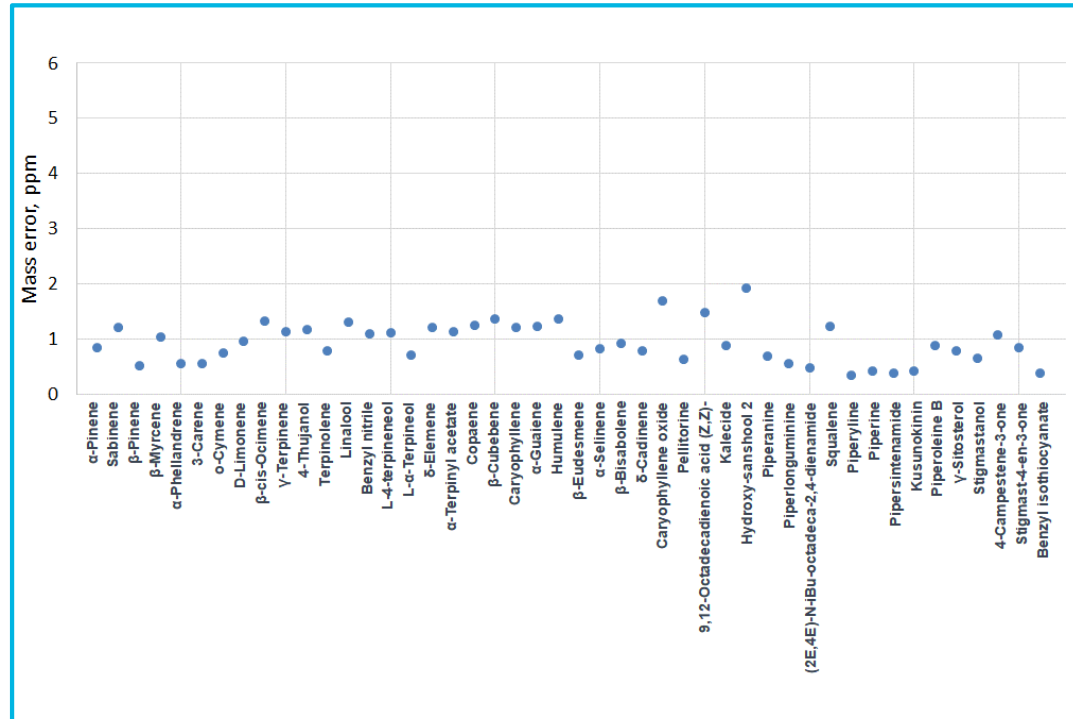


Figure 6. Mass accuracy of the major model compounds.

Analysis of “Unknown” Samples in Classifier

The models were exported to the Classifier software for further validation using both positive and negative controls. Finally, the models were evaluated using the samples “adulterated” with 5-50% of either papaya seeds or Szechuan pepper (Figure 7).

For the PLSDA model to effectively determine adulteration with papaya seeds, papaya seeds samples needed to be included in the model. The SIMCA model was able to distinguish as low as to 5% dilution (adulteration) with Szechuan and papaya seeds even when papaya seeds were not included in the classification model. (Figure 8).

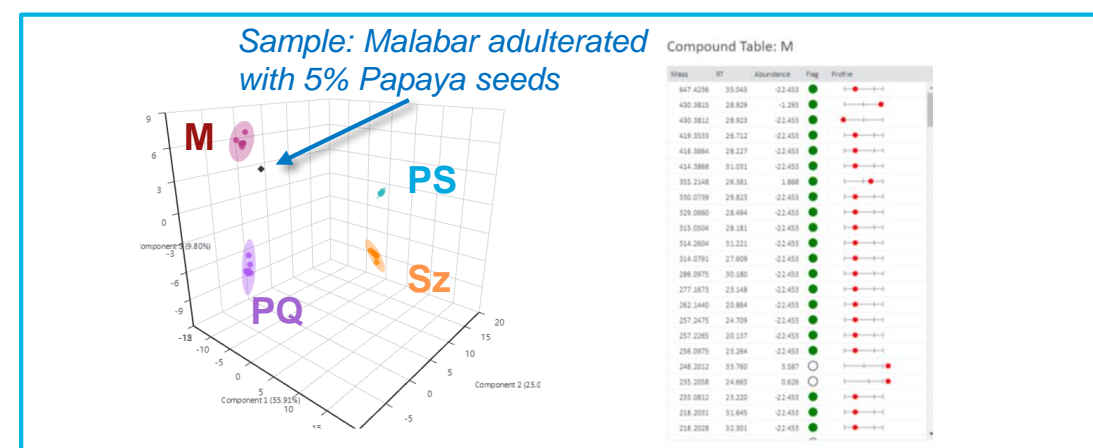


Figure 7. Results visualization in Classifier.

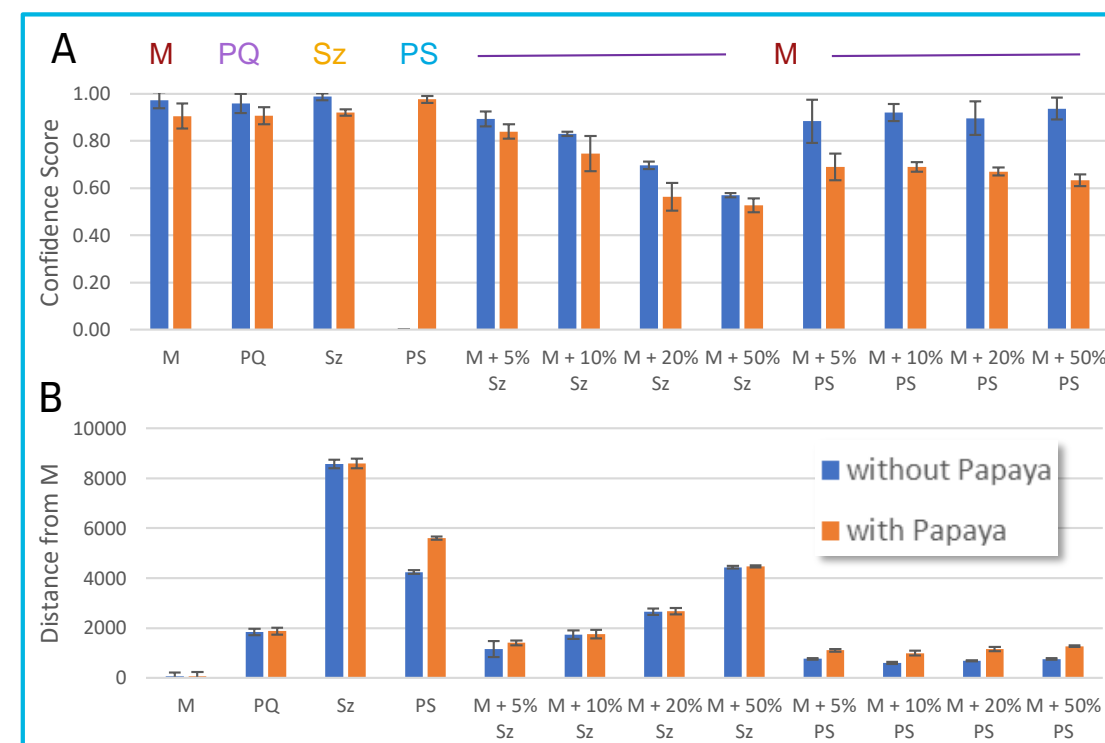


Figure 8. Results of PLSDA vs SIMCA model comparison, both with and w/o papaya seeds extracts included in the model. A) PLSDA, classification category for the confidence score given on the y-axis is annotated above the bars. B) SIMCA

Conclusions

- Novel classification workflow for black pepper authenticity using high-resolution GC/Q-TOF and Classifier software has been demonstrated.
- The model was able to better distinguish between pure and adulterated black pepper when adulterant was included in a model in which case, as low as 5% adulteration with both papaya seeds or Szechuan pepper can be detected.

Poster Reprint

ASMS 2020

ThP 187

Rinse and Shoot: Rapid Pesticide Screening Workflow by GC/MS in Under Five Minutes

Anastasia Andrianova and Bruce Quimby
Agilent Technologies Inc., Wilmington, DE
19808 USA

Introduction

Trace-level pesticide and environmental pollutants in the food supply continue to be a worldwide concern and are driving the demand for more rapid and reliable methods of analysis. Part of the challenge is to find technologies that can search for hundreds of pesticides with **simple sample preparation** and **a quick turnaround time**.

Simple sample preparation was accomplished with a “rinse and shoot” approach. The solvent rinsate collected from the fruit surface has a favorable pesticide-to-matrix ratio. Because of the limited interferences, the rinsates can be screened with GC coupled with a single quadrupole mass spectrometer (GC/MSD) in full scan mode.

Custom-created and commercial spectral libraries were used for comprehensive screening of the rinsates [1,2]. Confidence in identification was further increased with mass spectral deconvolution and time-filtering.

Quick turnaround time was achieved with a ramp rate of 250 °/C available with the Intuvo 9000 GC.

In this work, the Agilent Intuvo/5977B GC/MSD system was used for a rapid (3.4 min) analysis of fruit rinsates, followed by compound identification based on deconvoluted mass spectral search and time-filtering using linear retention indices (RIs).

Experimental

The system used here was configured to enable the shortest cycle time, avoid carryover and maximize throughput.

The important techniques employed are:

- A 10 m x 0.18 mm x 0.18 µm HP-5MS UI used as column 1 and 1.3 m 0.15 mm deactivated fused silica restrictor as column 2
- Oven ramp rate of 250 °C/min achieved with the Intuvo 9000 GC enabling 3.4 min run time
- Mid-column backflushing to extend the life of the columns and the guard chip. During backflushing, the carrier gas flow through the first column and the guard chip is reversed to carry any high boilers that were in the column and the guard chip at the end of data collection out into the split vent trap
- The Intuvo 9000 GC enables self-configuration when setting up backflush and columns, which are equipped with the column information keys, that significantly simplifies method setup

Experimental, cont.

- The Intuvo PSD Module is a pneumatics module optimized for backflushing. During backflushing, it significantly reduces the flow of helium used compared to previous configurations
- The Intuvo 9000 MMI guard chip prevents high boiling matrix compounds from contaminating the head of the column
- The spectral deconvolution feature in MassHunter Quant 10.1 Unknowns Analysis (MH UA) enables automatic compound identification even in high matrix samples in the presence of coeluting compounds using library match score
- Time filtering using RIs increased compound identification accuracy



Fig. 1. Intuvo 9000/5977B GC/MSD system with a 50-vial capacity 7650A Automatic Liquid Sampler

Sample preparation

The fruits were placed into a glass funnel and rinsed with acetone. The rinsate was collected into a 4 mL amber vial and injected into the GC/MSD system.

This sample prep maximized pesticide-to-matrix ratio.



Fig. 2. Simple sample preparation to accompany fast chromatography for quick screening

Pesticides Found on the Surface of Fruits in 3.4 minutes

The scan files for fruit rinsates were analyzed using MH UA with the deconvoluted components searched against a custom pesticide library that included mass spectra and linear retention index (RI) information for 1,081 entries.

The use of RI makes the screening strategy independent of chromatographic conditions such as the flow path, column flow, and oven ramp rate. When time-filtering is performed with RIs, the library RI values are recalculated to retention times (RTs) using a RI-to-RT calibration. Component RTs are compared with calculated library RTs. RT tolerance range is specified in the method.

RI calibration was performed with a C₈-C₃₄ n-alkane ladder.

Below is an example of the pesticide reported in the strawberries, fenhexamid. The deconvoluted mass spectrum (on top) is compared with the library spectrum and the extracted spectrum before deconvolution is shown on the bottom right.

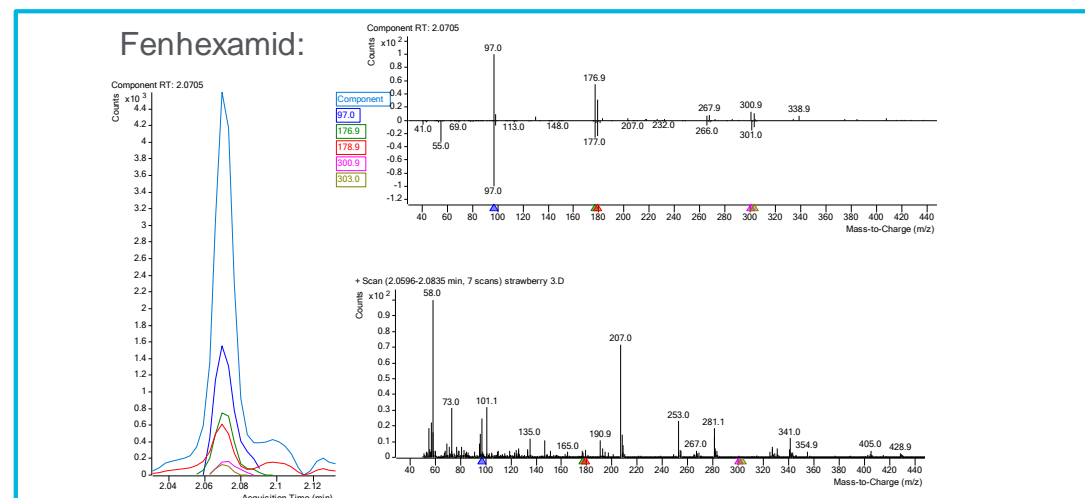


Fig. 3. Identification of fenhexamid in the strawberry rinsate with MassHunter Unknowns Analysis.

Pesticides identified in the fruit rinsates are highlighted in red in the chromatograms and in blue in the tables. Screening results for lemon, strawberry, banana, cherry, and peach are shown in Figs. 4-6.

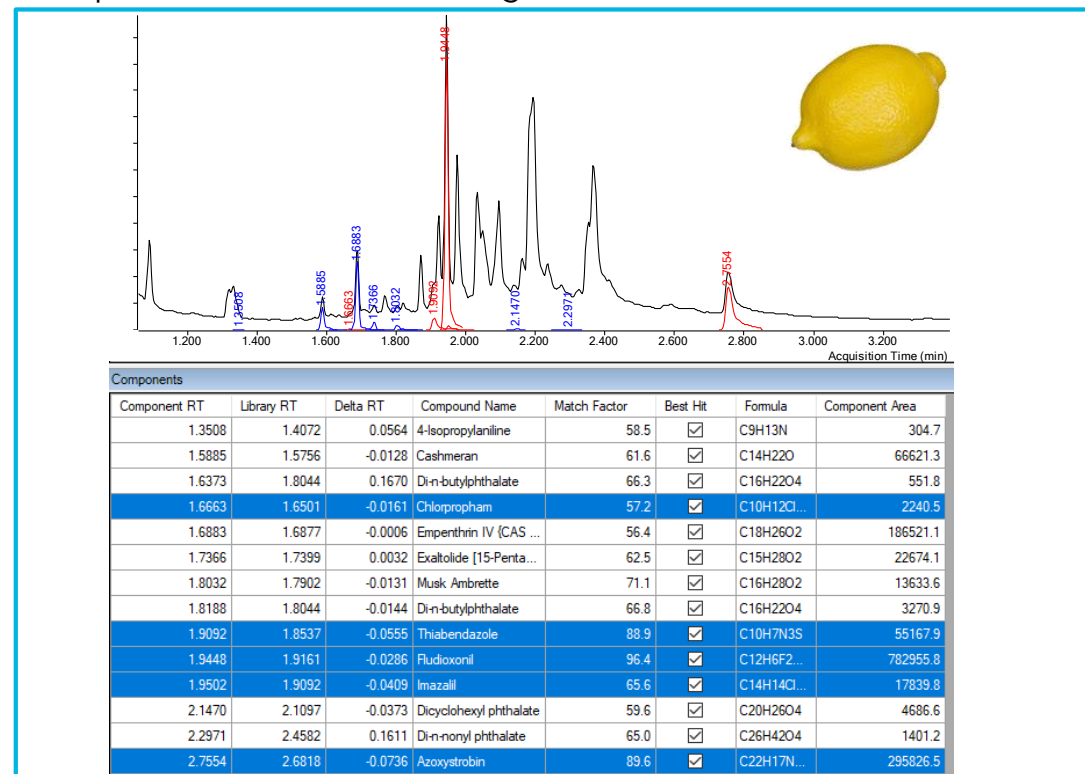


Fig. 4. Screening results for a lemon rinsate.

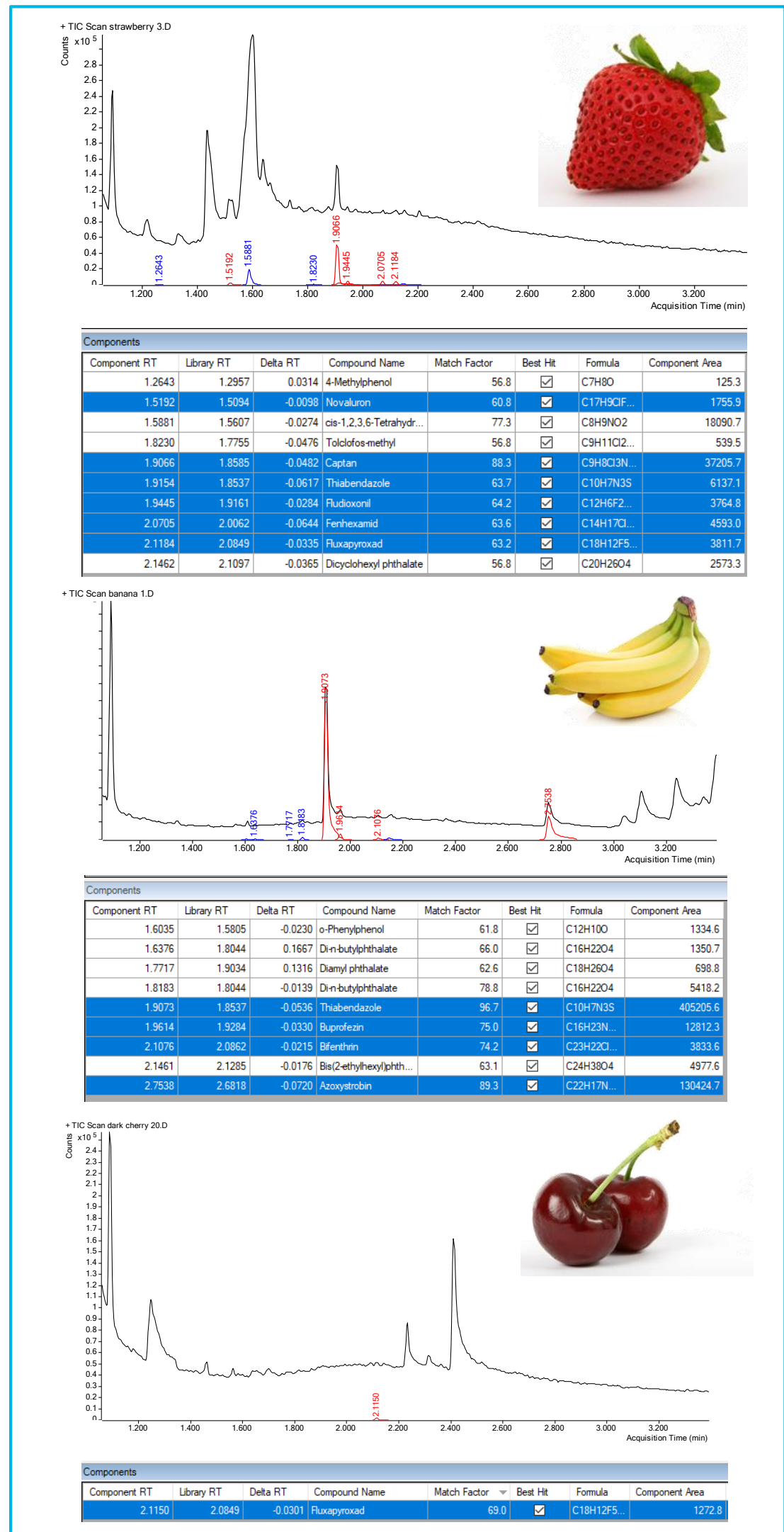


Fig. 5. Screening results for banana and cherry rinsates identified against the pesticide library.

MH UA can also be used to search the deconvoluted components against the NIST 17 library, which contains over 260,000 spectra. NIST 17 contains RIs experimentally determined on "Semi-standard non-polar" columns of the type used here for many of the entries.

Identity Confirmation with Increased Chromatographic Resolution

With the hardware employed, the oven ramp rate can be lowered to yield a significant increase in a chromatographic resolution. For example, to more closely evaluate a screening result and increase confidence in compound identification, chromatographic and spectral interference can be reduced by using the slower oven ramp.

If the rapid screening analysis finds compounds of high concern, the confirmation analysis can be used to confirm the results. Fig. 6 shows the utility of this optional capability.

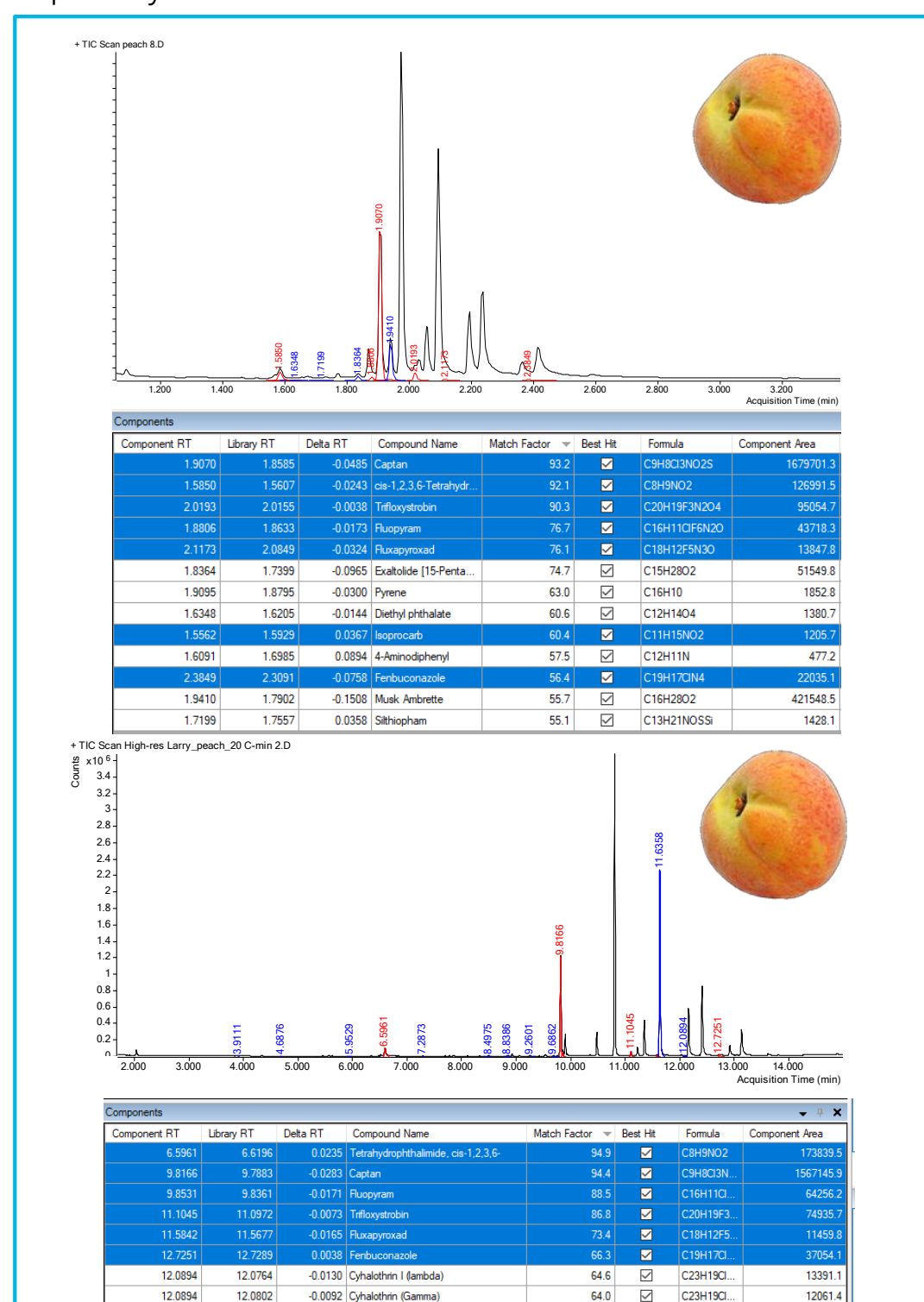


Fig. 6. Screening results for a peach rinsate with a rapid 3.4 min analysis (top) and a 15-min confirmation run (bottom).

As expected, LMS for some compounds like fluopyram and fenbuconazole were improved from 76.7 to 88.5 and from 56.4 to 66.3, respectively, with a slower oven ramp rate due to the decreased interferences.

System Robustness with 210 Injections of Peach Rinsate

To demonstrate the robustness of the system, 210 injections of a peach rinsate were performed.

These injections of sample led to a response loss, especially for high-boiling compounds, and a small RT shift towards earlier times.

System maintenance was performed, including liner, septum, and guard chip replacement. Next, the electron multiplier gain was updated and an alkane ladder (C₉-C₃₄) was analyzed to update the RI calibration.

This restored the system response and corrected for the small RT shift.

Conclusions

The Agilent Intuvo 9000/5977B GC/MSD system enables rapid screening for pesticides found on the surface of fruits and berries in 3.4 minutes.

The Intuvo 9000 GC provides oven ramping at a rate of 250 °C/min without requiring special electrical service (V or A) at the bench.

Rapid and reliable identification of pesticides is achieved by library searching of deconvoluted spectra coupled with time-filtering using RIs.

The Intuvo 9000 guard chip extends column lifetime and its replacement does not alter RI calibration.

Backflushing allows for extending maintenance-free uptime and ensures no carryover is observed, eliminating the need for extended column bakeout.

The screening workflow described herein provides the means for identifying those pesticides that should be included in subsequent quantitative targeted analysis.

References

¹Andrianova, A.; et al. Agilent Technologies Application Note, publication number 5994-0915EN, 2019

²Churley, M.; et al. Agilent Technologies Application Note, publication number 5994-1505EN, 2019.

Acknowledgements

The authors would like to thank Rebecca Veeneman for her help with this work.

Poster Reprint

ASMS 2020

ThP 219

Unambiguous di-sulphide bond assignment in synthetic peptides Linaclotide and Plecanatide using Agilent 6546/6550 LC-QTOF High Resolution Mass Spectrometer

S. Polisetty¹, V. Reddy¹, L. K. Reddy¹, S. Banerjee², A. Pargaonkar² and S. Nagpal^{2*}

¹ MSNL R&D Center Pashamylaram, Medak (Dist), Telangana, India

² Agilent technologies India Pvt. Ltd., Delhi, Bangalore and Hyderabad, India

Introduction

Disulphide linkages and functionality

Di-sulphide bridges are critical for secondary structure and functionality of the peptide/protein. Identification of the Cysteines involved in di-sulphide bond formation is a challenge. Close spacing of cysteines esp. in small peptides poses further challenges.

Disulphide locations in Linaclotide and Plecanatide

- Linaclotide is 14 amino-acid long peptide with 3 di-sulphide bridges involving 6 Cys residues viz. Cys1-Cys6, Cys2-Cys10 and Cys5-Cys13.
 - The sequence is CCEYCCNPACTGCV
- Plecanatide is a 16 amino acid peptide with two di-sulphide bridges between Cys4-Cys12 and Cys7-Cys15
 - The sequence of Plecanatide is NDECELCVNVACTGCL

Ensuring correct di-sulphide linkages during the synthesis of these molecules is very important as some participating Cysteines are closely located.

Experimental

Di-sulphide peptide cleavage.

The Peptide were subjected to partial reduction of di-sulphide bridges by Tris(2-carboxyethyl)phosphine hydrochloride TCEP.

The methodology used by Go'ngora-Beni'tez et al.¹ was followed for linaclotide however peptide concentration and the TCEP ratios were optimized further for Plecanatide.

The reduced peptides were Cyanylated by using CDAP and these cyanylated peptides were separated on HPLC and collected as separate fractions.

Fractionated peptides were cleaved at Cyanylated Cysteines by incubating with 1 M Ammonia and 6M Gdn-Hcl at 25°C for 25 minutes.

Mass-spectrometric analysis

All the samples were analyzed on Agilent 6550 or 6546 LC/Q-TOF platform coupled with Agilent 1290 Infinity II HPLC

The same instrument was used to monitor the partial reduction, cyanylation and cleavage steps. The sequence of the peptide fragments were confirmed by MS/MS data.

Peptide fractionation was carried out on high binding capacity column and fractions were collected manually after UV detection.

Experimental



Fig1: 6546 LC/Q-TOF with 1290 Infinity II

Results and Discussion

Di-sulphide bond confirmation in Linaclotide



Fig 2a: Deconvoluted Mass-spectrum of native Linaclotide

Mass of native Linaclotide molecule was observed as 1525.39 Da which was found to increase by 2 Da on reduction of one di-sulphide bond to 1527.41 Da. Three distinct peaks with 1527.41, 1527.42, 1527.41 were observed respectively after reduction of the three di-sulphide bonds one at a time. After Cyanylation, the mass was found to be 1577.40 Da..

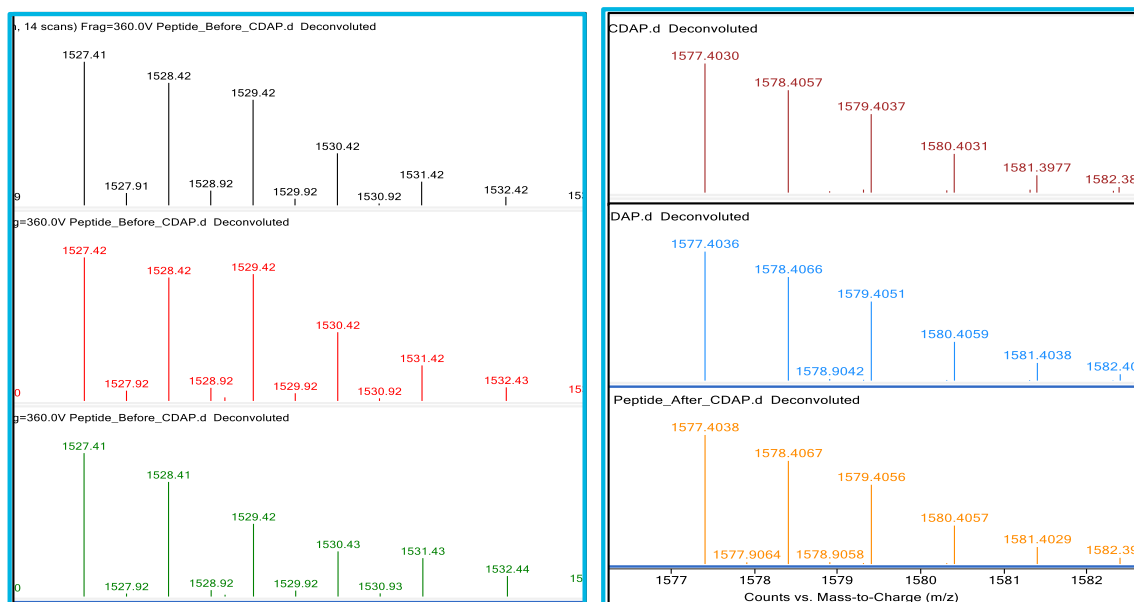


Fig 2b: Deconvoluted Mass-spectra of three reduced disulphide peaks.

Fig 2c: Deconvoluted Mass-spectra of the peaks after CDAP treatment.

Confirmation of Cys1-Cys6 bond in Linaclotide

- Cleavage of the Cys1-Cys6 bond results in the formation of two peptide fragments of CCEY C (643.16 Da) and CNPACTGCY (955.310 Da). The sequence of both fragments is confirmed with MS/MS pattern

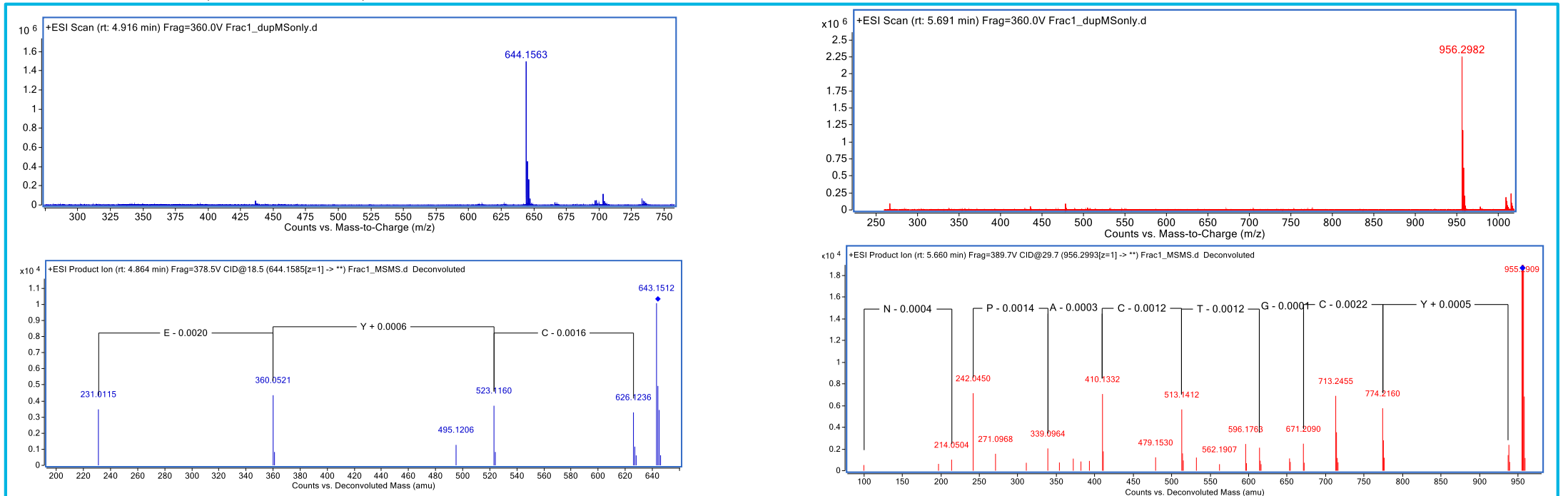


Fig 3a : MS and MS/MS spectrum of the peptide fragments (m/z 644.1563 and 956.2982) confirming the Cys1-Cys6 bond.

Confirmation of Cys2-Cys10 bond in Linaclotide

- The cleavage of Cys2-Cys10 di-sulphide bond results in three signature peptide fragments with sequence CC(120.04 Da), CTGCY(570.165 Da) and CEYCCNPA(925.29Da)

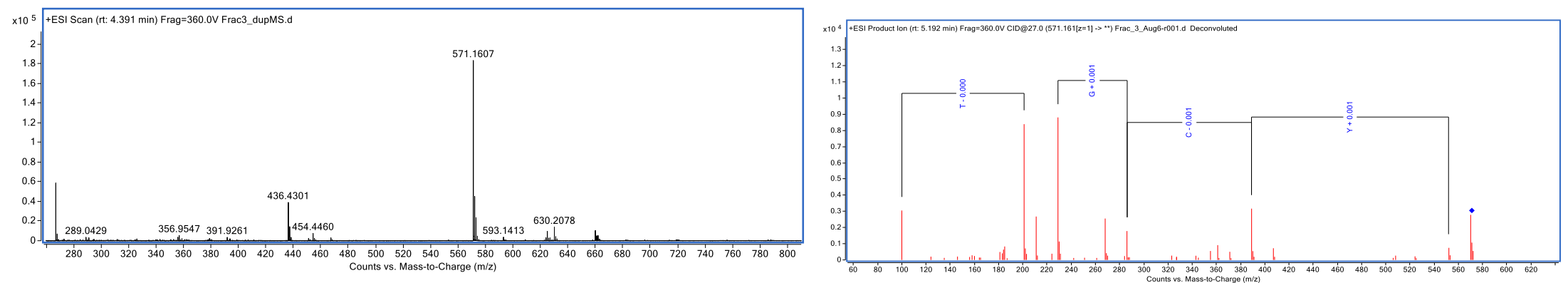


Fig 3b : MS and MS/MS spectrum of the peptide fragments m/z 571.1607 confirming the Cys2-Cys10 bond.

Confirmation of Cys5-Cys13 bond in Linaclotide

The cleavage of Cys5-Cys13 bond results in 3 fragments CCEY (516.1349 Da), CCNPACTG (791.2275 Da) and CY(309.0783 Da)

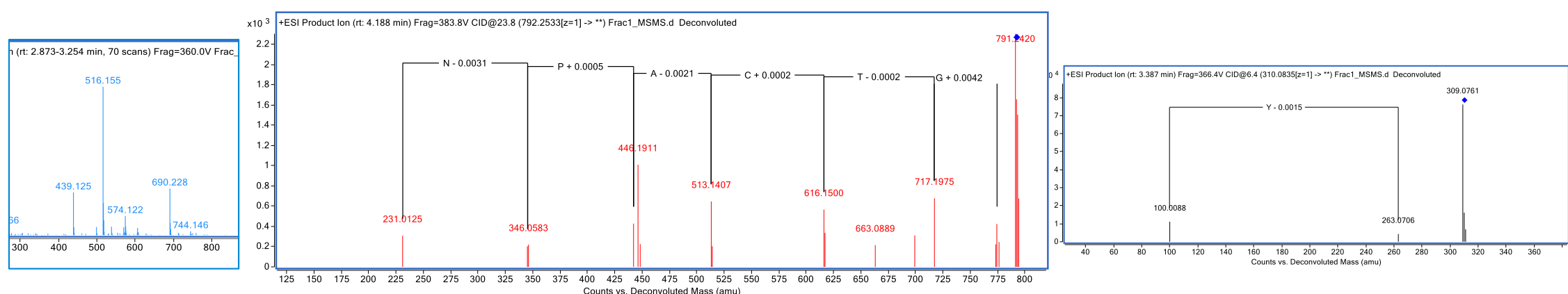


Fig 3c : Deconvoluted MS and MS/MS spectrum of the peptide fragments CCEY (516.1349 da), CCNPACTG (791.2275 da) and CY(309.0783 Da)

Di-sulphide bond confirmation in Plecanatide

The partial reduction of one of the two di-sulphide bonds in Plecanatide was obtained by optimizing TCEP to peptide ratio and was monitored on Agilent 6546 LC/Q-ToF Mass-spectrometer.

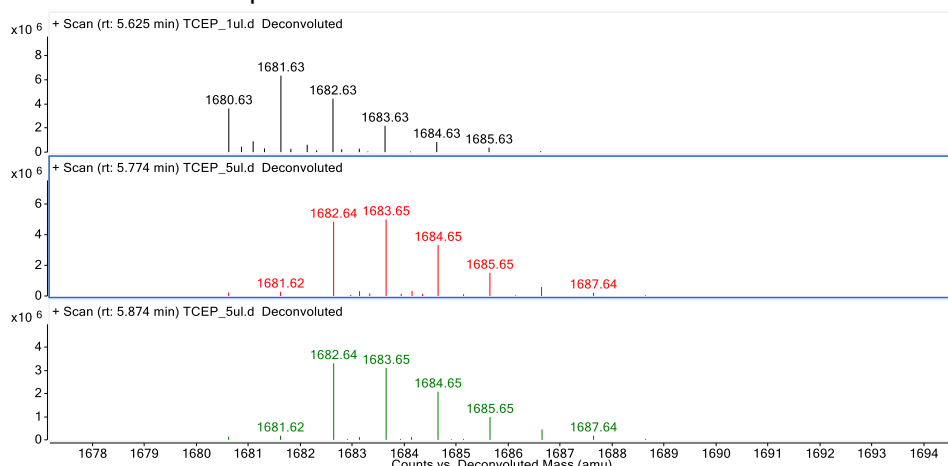


Fig 4a: Deconvoluted Mass-spectra of two separate peaks showing reduced di-sulphide linkage by increment of mass from 1680.63 Da to 1682.64 Da

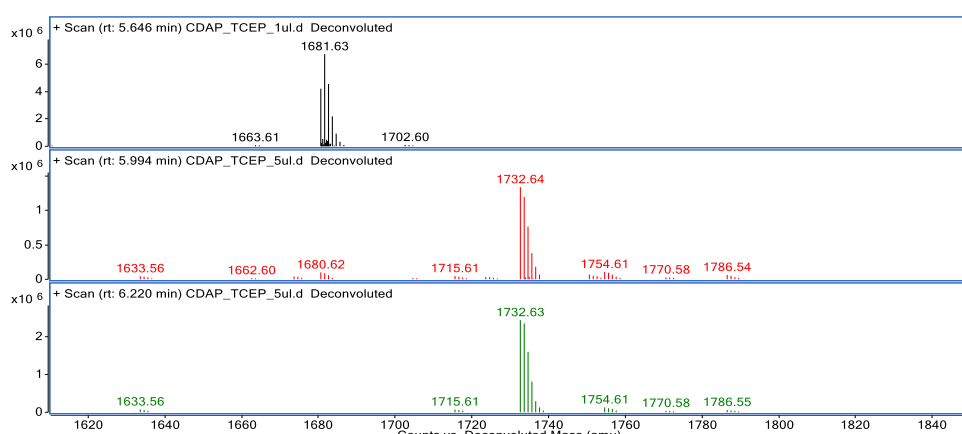


Fig 4b: Deconvoluted Mass-spectra confirming Di-Cyanylation of the reduced di-sulphide links and increasing of 50 Da by addition of two CN residues instead of H (1732.64 Da)

Confirmation of Cys7-Cys15 linkage

The cleavage of Cys7-Cys15 bond results in two fragments NDECEL (721.2589 da) and CVNVACTG (789.33 Da)

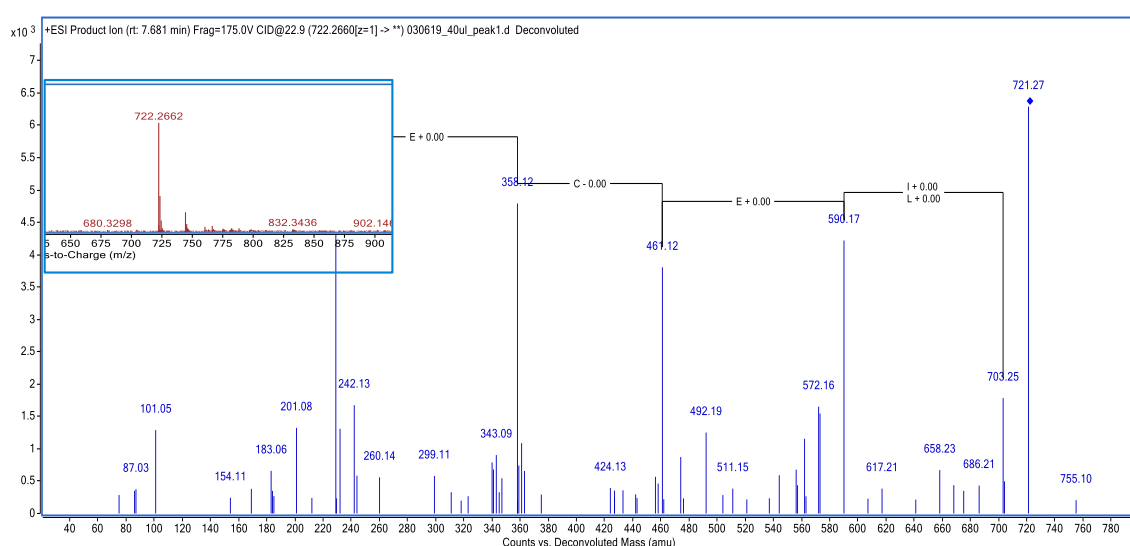


Fig 4c : Deconvoluted MS and MS/MS spectrum of NDECEL (721.2589 Da)

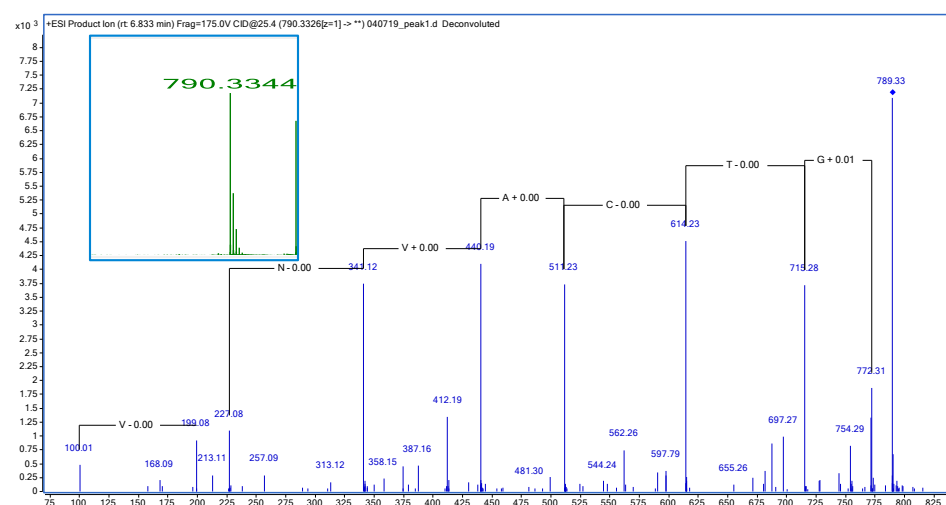


Fig 4d: Deconvoluted MS and MS/MS spectrum of CVNVACTG (789.33 Da)

Confirmation of Cys7-Cys15 linkage

The cleavage of Cys4-Cys12 bond results in two fragments viz. CTGCL (520.1774 Da) and CELCVNVA(874.3677 Da)

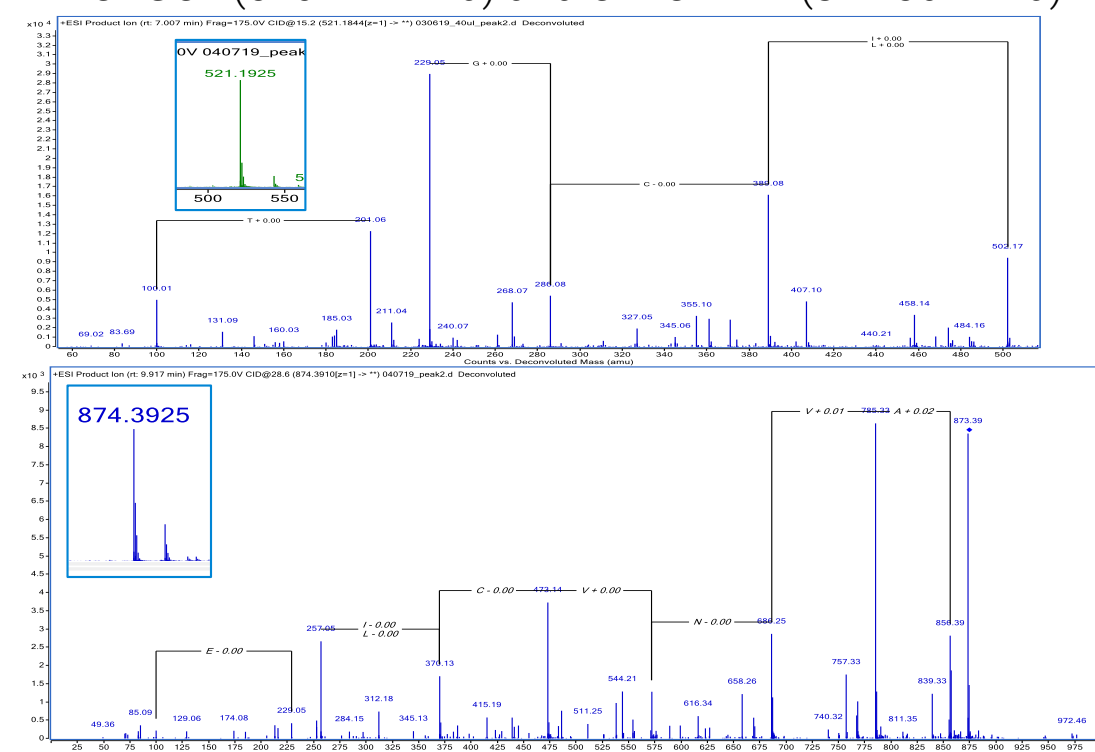


Fig 4e: Confirmation of Cys4-Cys12 with signature fragments

Conclusions

- Presence of three di-sulphide bridges was confirmed in the Linaclotide sample (C1≈C6, C2≈C10, C5≈C13) by using signature peptides resultant of differential cleavage.
- Two di-sulphide bridges at C7-C15 and C4-C12 were confirmed in Plecanatide samples.

References

- 1: Góngora-Benítez M, Tulla-Puche J, Paradís-Bas M, Werbitzky O, Giraud M, Albericio F. Optimized Fmoc solid-phase synthesis of the cysteine-rich peptide linaclotide. Biopolymers. 2011;96(1):69-80.doi:10.1002/bip.21480.Epub2010 Aug 21.

Poster Reprint

ASMS 2020

ThP 404

Identification of Therapeutic Peptide and its Impurities

S. Polisetty², V. Reddy², L. K. Reddy², Ashish Pargaonkar⁽¹⁾, Saurabh Nagpal⁽¹⁾, Kartheek Chidella Srinivas⁽¹⁾ and Saikat Banerjee⁽¹⁾

Agilent Technologies, Bangalore, INDIA.
MSN Laboratories Pvt. Ltd, Hyderabad, INDIA

Introduction

Therapeutic peptides gained a lot of interest and attention due to various advantages over protein drug therapies due their small size (< 40-50 amino acids), ease of synthesis and its biological and chemical diverse activity. There are over 60 peptide drugs that have been approved in the USA, Europe, and Japan; over 150 are in active clinical development.

Peptides tend to have additional process impurities e.g. amino acid deletion or insertion, and degradation pathways e.g., oxidation and deamidation. These modifications are critical for product quality and need to be monitored.

In this study different therapeutic peptides were used viz. Liraglutide, Teriparatide, Abaloparatide and Exenatide for identification of peptide API's based on sequence confirmation using Accurate Mass, high resolution for Intact and MSMS Fragments.



Figure 1. Agilent 6545XT AdvanceBio LC/Q-TOF

The Agilent 6545XT AdvanceBio LC/Q-TOF has several features to enhance the sensitivity and dynamic range of the analysis. Agilent AJS Source improves analytical sensitivity and SWARM tuning help to improve resolution and applications based sensitivity.

Experimental

All the peptide samples were provided by MSN Laboratories Pvt Ltd and was analyzed on Agilent 6545XT AdvanceBio LC/Q-TOF. The LC separation method was developed using the AdvanceBio Peptide Mapping column to separate the impurities. Identification and confirmation of the peptide and impurities based on sequence matching algorithms of MassHunter BioConfirm B.07 Software using its Synthetic peptide workflow. This workflow has all the features to detect the intact mass and related missing/additional amino acids, oxidation and deamidation.

Workflow

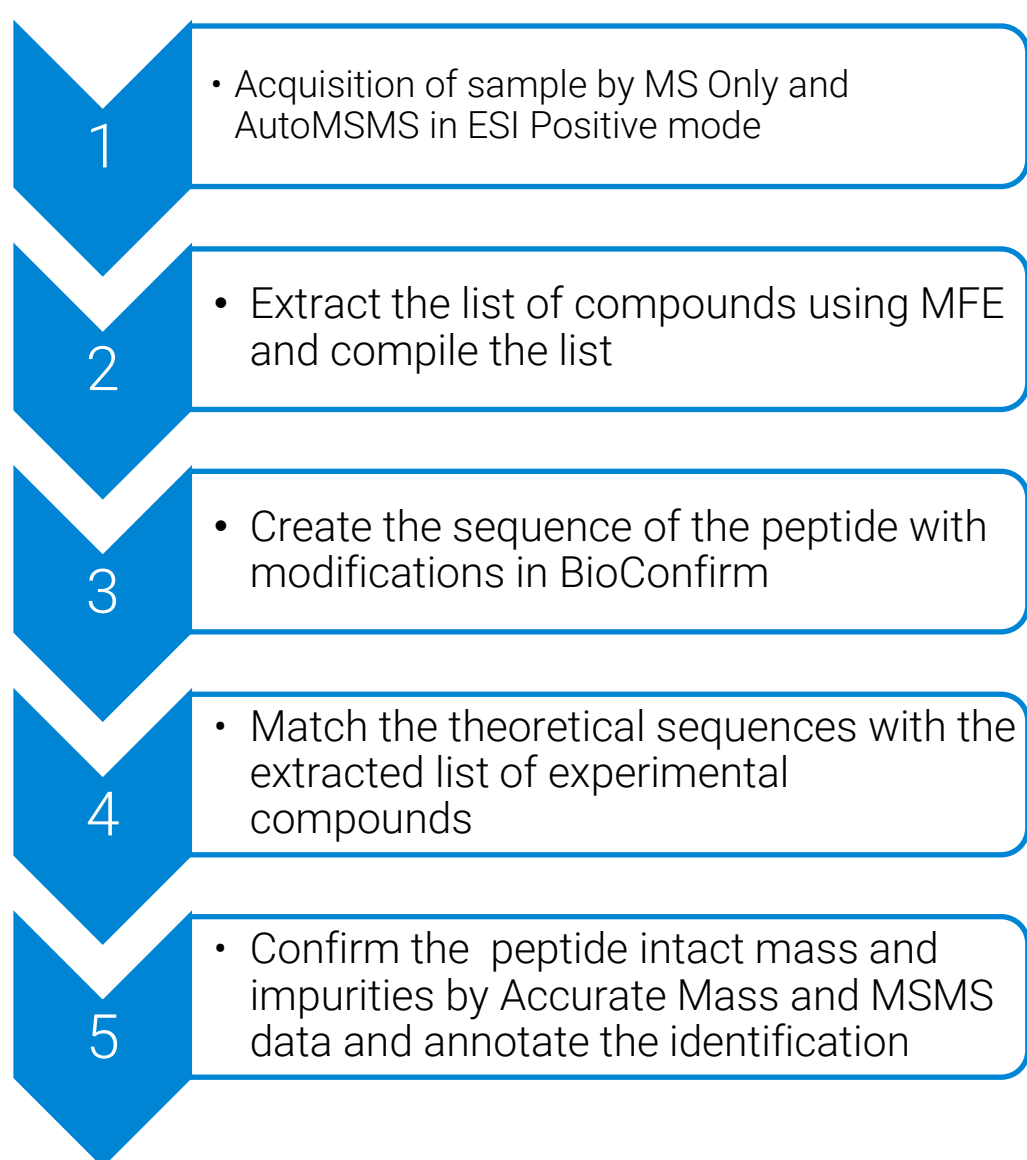


Figure 2. Agilent BioConfirm Synthetic Peptide Workflow

The peptide drugs are unique with certain chemical modification to the amino acids e.g. Lysine of Liraglutide is modified with Palmitoyl-Glut, presence of an unnatural amino acid Aib at position 29 of Abaloparatide. These modifications are defined in the sequence manager of the BioConfirm B.07 software tool.

Results and Discussion

The therapeutic peptides were identified by accurate mass and sequence matched with less than 5 ppm error and the related impurities were identified based on the corresponding mass differences, which are due to either missing or additional amino acids, or oxidation and deamidation of specific amino acids

The high resolution and mass accuracy provides very good isotopic fidelity to confirm the peptide and its impurities at intact levels with multiple charge states. The data was deconvoluted and matched with theoretical sequence input in the BioConfirm B.07 Software to get the identification and confirmation.

Various impurities were identified in all the samples including the oxidation and deamidation of amino acids which might lead to typical product or process related aspects.

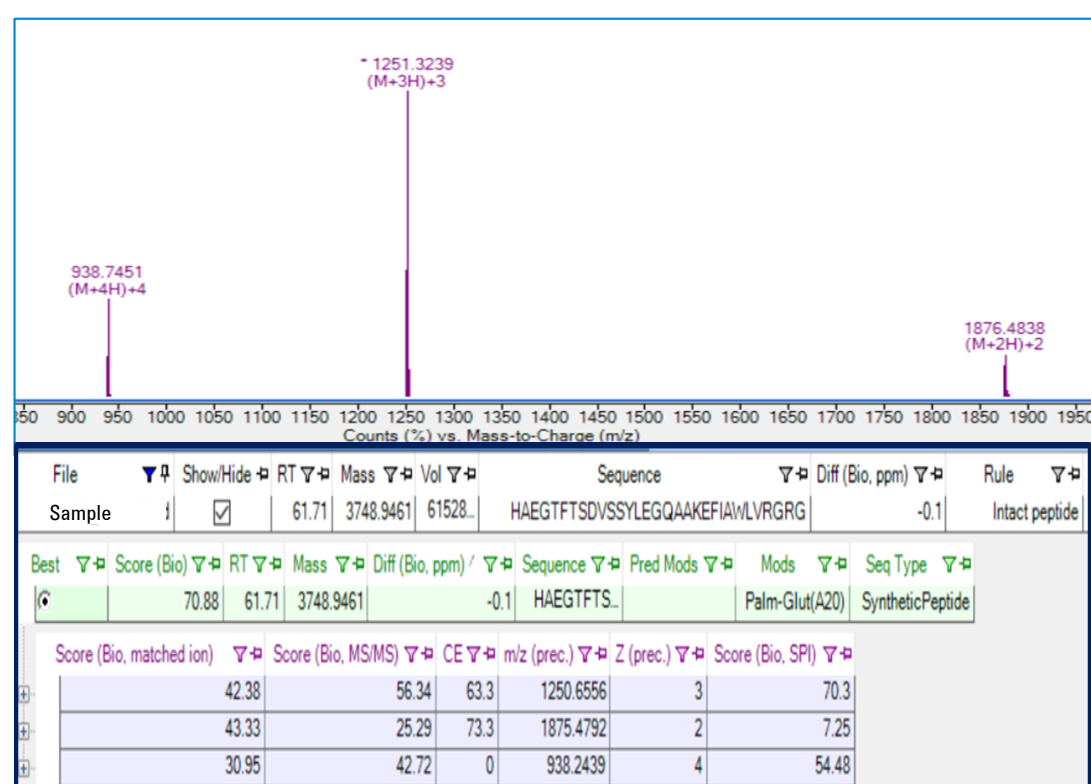


Figure 3. The intact mass and different charge states identified by BioConfirm for Liraglutide

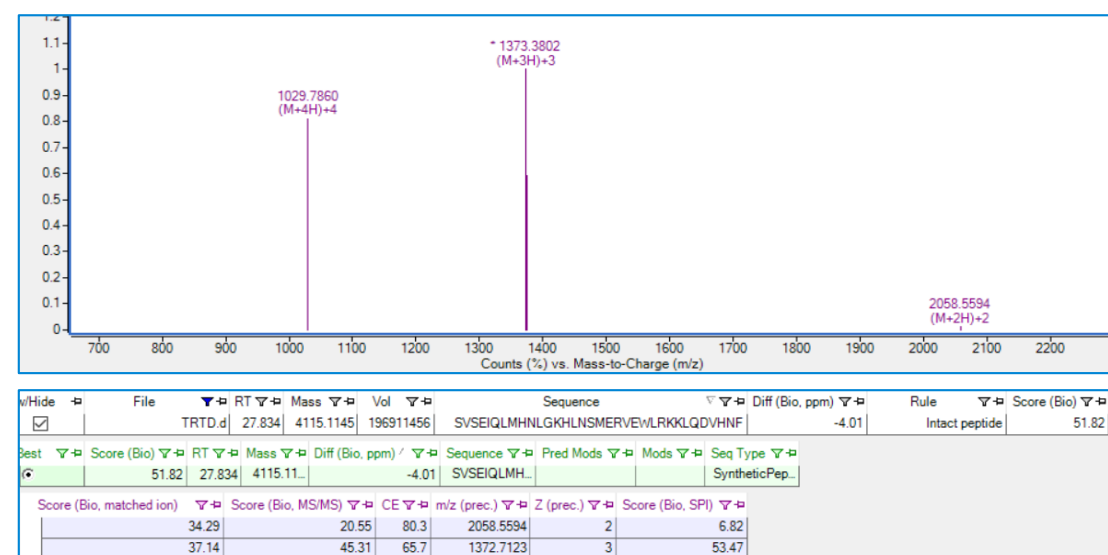


Figure 4. The intact mass and different charge states identified by BioConfirm for Teriparatide

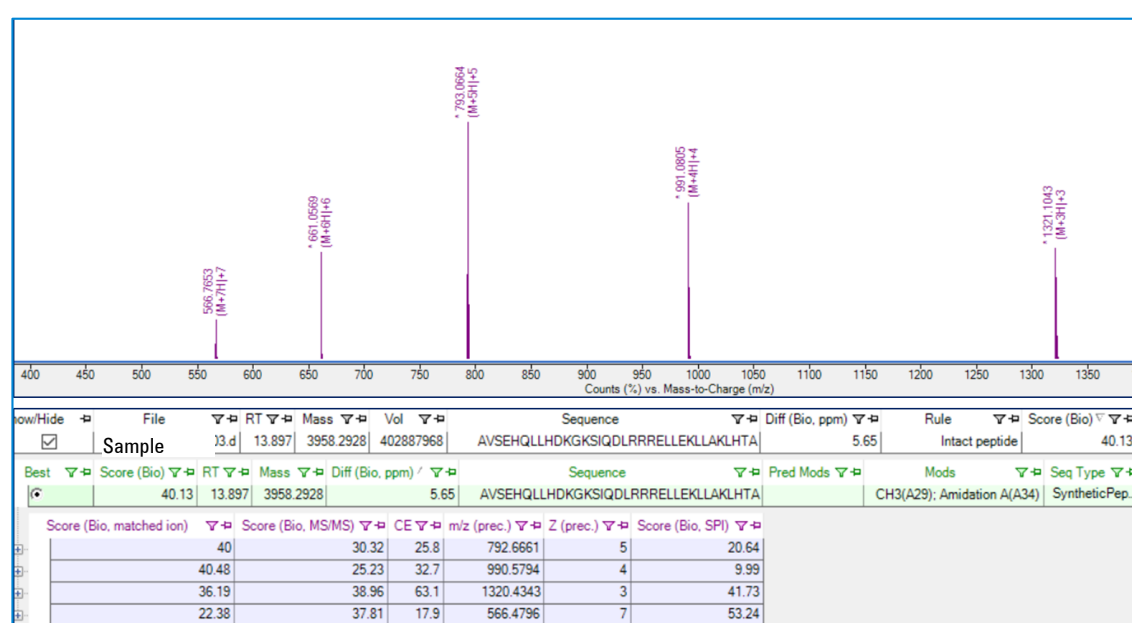


Figure 5. The intact mass and different charge states identified by BioConfirm for Abaloparatide

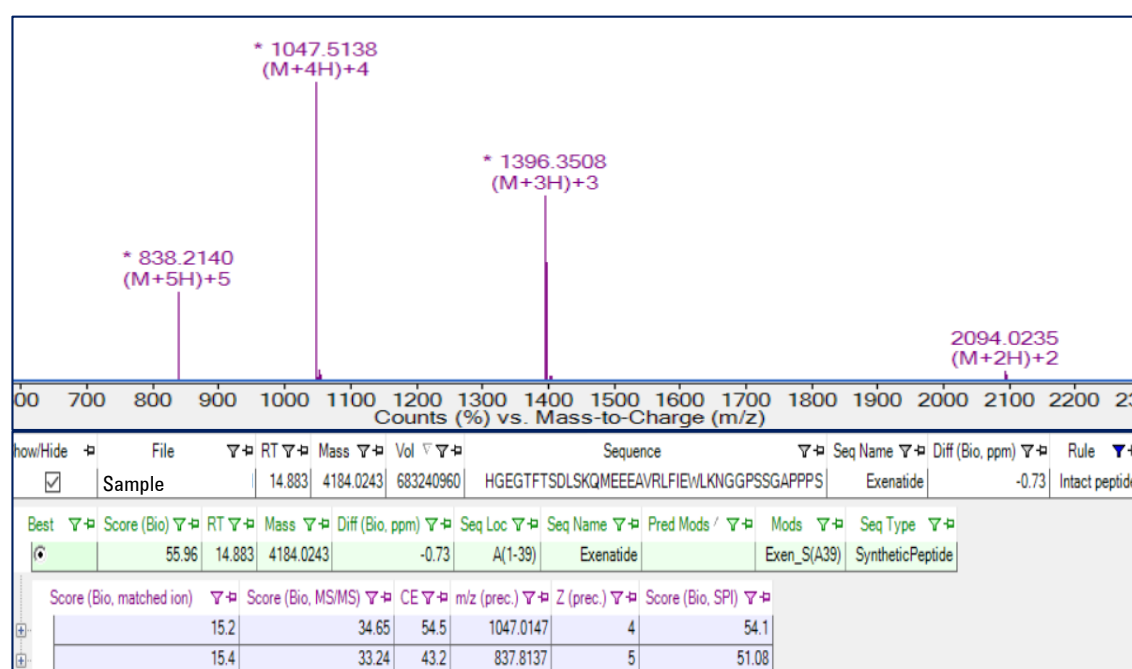


Figure 6. The intact mass and different charge states identified by BioConfirm for Exenatide

Liraglutide			
Impurity	Predicted Modification	Mass	ppm
Missing Amino Acid	T5	3647.89	0.27
Missing Amino Acid	G31	3691.91	3.26
Missing Amino Acid	E21	3619.89	2.28
Teriparatide			
Impurity	Predicted Modification	Mass	ppm
Missing Amino Acid	R20	3959.01	4.84
Missing Amino Acid	H9	3978.45	4.12
Oxidation	M8	4131.106	4.63
Deamidation	N10	4116.1	3.97
Abaloparatide			
Impurity	Predicted Modification	Mass	ppm
Extra Amino Acid	K27	4086.36	1.17
Missing Amino Acid	A1	3887.23	0.03
Exenatide			
Impurity	Predicted Modification	Mass	ppm
Extra Amino Acid	M15	4315.06	0.08
Missing Amino Acid	Q13	4055.973	1.28
Oxidation	M14	4200.028	1.39

Figure 7. Summary of few impurities identified in different samples

Results and Discussion

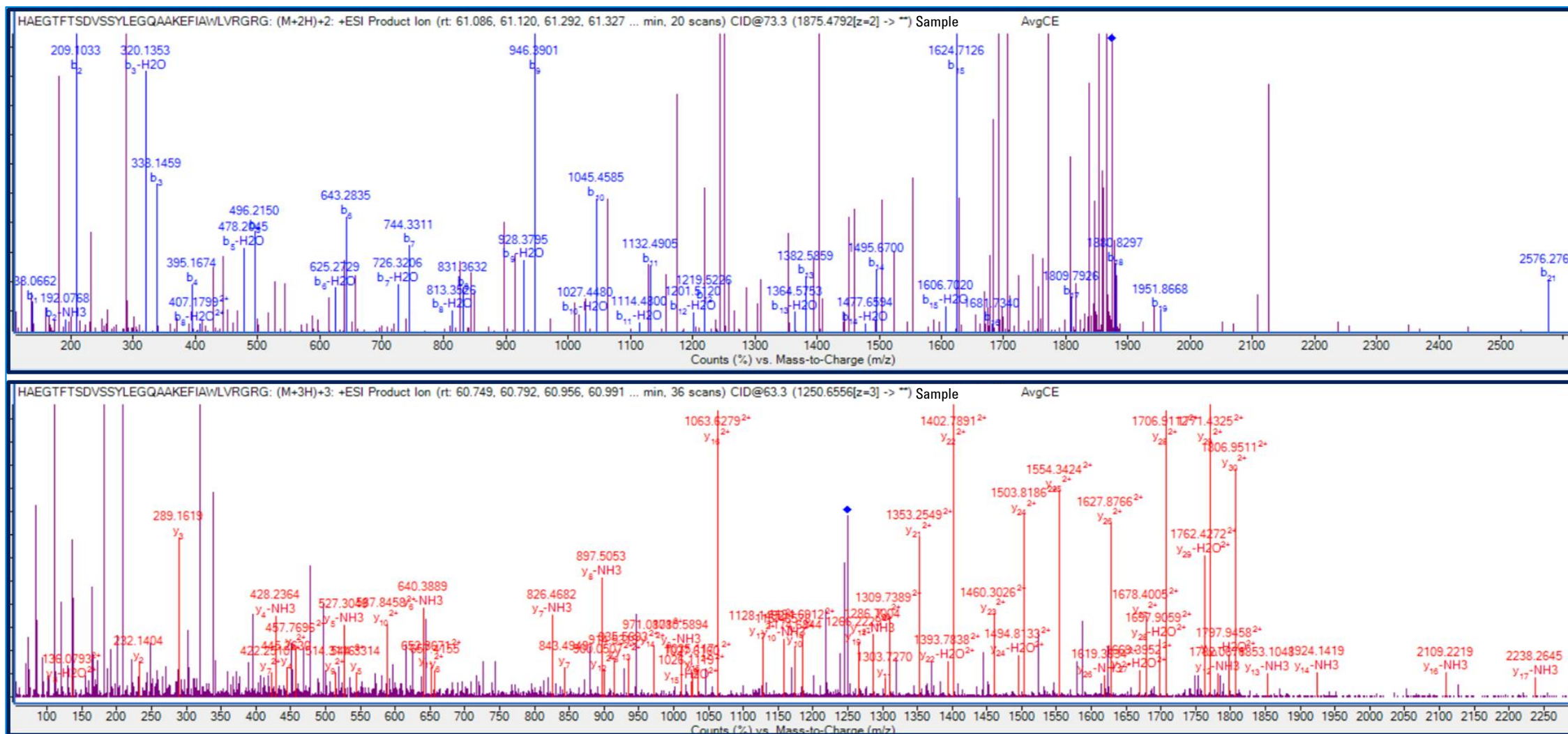


Figure 8 . The MSMS Fragmentation pattern for Liraglutide peptide with coverage of both b and y ion series

INTACT					Missing T5					Missing T(5)				
RT	Mass	Diff (ppm)	Pred Mods	Mods	RT	Mass	Diff (ppm)	Pred Mods	Mods	RT	Mass	Diff (ppm)	Pred Mods	Mods
61.71	3748.9461	-0.1		P-Glut(A20)	61.029	3647.8978	-0.27	T	P-Glut(A20)					
m/z (prec.)	Z (prec.)	File			m/z (prec.)	Z (prec.)	File			m/z (prec.)	Z (prec.)	File		
1250.6556	3	Sample			1216.9724	Sequence	Sample							
Ion	Sequence	Diff (ppm)	m/z (prod.)	Z (prod.)	Ion	Sequence	Diff (ppm)	m/z (prod.)	Z (prod.)	Ion	Sequence	Diff (ppm)	m/z (prod.)	Z (prod.)
b3	HAEG	-4.4	338.1459	1	b3	HAEG	-3.7	338.1459	1	b3	HAEG	-3.7	338.1459	1
b4	HAEG	-4.2	395.1674	1	b4	HAEG	1.2	395.1674	1	b4	HAEG	1.2	395.1674	1
b5	HAEGT	-3.4	496.215	1	b5	HAEGF	-2.1	542.2358	1	b5	HAEGF	-2.1	542.2358	1
b6	HAEGTF	-3.8	643.2835	1	b6	HAEGFT	-6.2	643.2835	1	b6	HAEGFT	-6.2	643.2835	1
b8	HAEGTFS	-9.7	831.3632	1	b8	HAEGTSD	-7.4	845.3424	1	b8	HAEGTSD	-7.4	845.3424	1
y25	TSDVSSYLEGQAAKEFIWLVRGRG	-3.9	1554.3424	2	y25	TSDVSSYLEGQAAKEFIWLVRGRG	-3.4	1554.3424	2	y25	TSDVSSYLEGQAAKEFIWLVRGRG	-3.4	1554.3424	2
y27	TFTSDVSSYLEGQAAKEFIWLVRGRG	-4.7	1678.4005	2	y28	EGFTSDVSSYLEGQAAKEFIWLVRGRG	-7.1	1720.9087	2	y28	EGFTSDVSSYLEGQAAKEFIWLVRGRG	-7.1	1720.9087	2
y28	GTFTSDVSSYLEGQAAKEFIWLVRGRG	-3.3	1706.9112	2	y29	AEGFTSDVSSYLEGQAAKEFIWLVRGRG	4.2	1756.4272	2	y29	AEGFTSDVSSYLEGQAAKEFIWLVRGRG	4.2	1756.4272	2



Figure 9. Missing T(5) impurity in Liraglutide : Comparison of the b/y ions from the MS/MS spectrum for modified b5 and y27 ions shows an effective change over those ions in unmodified peptide, suggesting that Threonine, T is missing at position 5.

The Accurate mass MSMS data provides the ion series and the effective difference of mass due to shifts/modifications of amino acids, as annotated by the BioConfirm Software.

Conclusions

Using Accurate Mass MS, Therapeutic peptides and impurities can be detected and confirmed

The MSMS data of the peptides confirms the site of modifications

Excellent resolution and isotopic fidelity provides accurate data for confirmation and sequence matching

Several peptide drugs were identified and impurities characterized using this workflow

References

Zeng K, Geerlof-Vidavisky I, Gucinsky A, Jiang X, Boyne MT II. Liquid chromatography-high resolution mass spectrometry for peptide drug quality control. AAPS J. 2015;17(3):643–51

Lau, J.L.; Dunn, M.K. Therapeutic peptides: Historical perspectives, current development trends, and future directions. Bioorg. Med. Chem. 2017

For Research Use Only. Not for use in diagnostic procedures.

Poster Reprint

ASMS 2020

ThP 412

Development of an automated MHC-associated peptide enrichment method for immunopeptidomics analysis using AssayMAP large capacity cartridges

Samuel Pollock¹, Shuai Wu², Jerry Han², Steve Murphy²

¹ Genentech, South San Francisco, CA, USA

² Agilent Technologies Inc., Santa Clara, CA, USA

Introduction

Immunopeptidomics is generally considered more challenging than conventional proteomics workflows for a number of reasons: First, the MHC-associated peptides are extremely low in abundance compared to other cellular peptides (or proteins), which makes their enrichment and detection very difficult. Second, the mechanism of generating the mature peptide-MHC complex is unclear as it involves multiple proteases and peptidases. The peptides that bind with MHC complex have similarity in terms of length and sequence which are different from proteolytic digested peptides.

In this workflow, we used the AssayMAP Bravo for automated immunoaffinity purification and peptide clean-up that provided users with a high throughput and reproducible method for MHC peptidomics.

Experimental

Antibody Cross-link with PAW Cartridge

1 mg of anti-human MHC-I antibody (w6/32) was loaded on new AssayMAP 25 μ L PAW cartridges in parallel (x6) using the Affinity Purification application (Figure 1). Dimethyl pimelimidate (DMP) was used to cross-link the antibody to protein A, before being washed away with TBS. The just-crosslinked cartridges were then washed with 1% acetic acid to remove unbound antibody, equilibrated in TBS, and stored at 4 °C until use.

Immunoaffinity Purification of MHC-I Complex

GRANTA-519 cell pellets were lysed in non-denaturing buffer as previously described. The MHC-I complexes were immunoprecipitated with the antibody cross-linked cartridges. About 3 mg GRANTA lysate was loaded on each of 6 cartridges and the MHC complex was enriched out of the lysate and combined to give sample 1. The same experiment was repeated on different days to give samples 2 and 3. The MHC-associated peptides were separated from MHC protein and desalted on C18 cartridges using Peptide Cleanup Application. The AssayMAP protocols are summarized in Table 1.



Figure 1. AssayMAP Bravo platform with new AssayMAP 25 μ L PAW cartridge (Right)

Experimental

LC/MS Analysis

The Agilent 1290 Infinity II LC system was converted to nanoflow LC with the Agilent Infinity UHPLC Nanodapter. This nanoflow LC was connected to the Agilent nanoESI source and coupled to the 6550 iFunnel Q-TOF (Figure 2).

Peptide samples were analyzed with a 90-min gradient using data-dependent acquisition (Table 2). The tandem MS results were analyzed with Byonic software using human UniProt database with no enzyme specificity. Methionine oxidation, deamidation, were used as variable modifications for database search.

Table 2. Nano-LC Parameters

LC Conditions				
Trap-Column	PepMap C18, 75 μ m x 2 cm, at 60 °C			
Analytical Column	PepMap C18, 75 μ m x 25 cm, at 60 °C			
Solvent A	0.1% Formic Acid in Water			
Solvent B	0.1% Formic Acid in 90 % Acetonitrile			
Flow rate	0.085 mL/min primary flow			
	300 nL/min on-column flow rate			
	Time (min)	B (%)	Time (min)	B (%)
Gradient	0	3	97	70
	90	35	100	3
	95	70	120	3
Injection volume	5 μ L			

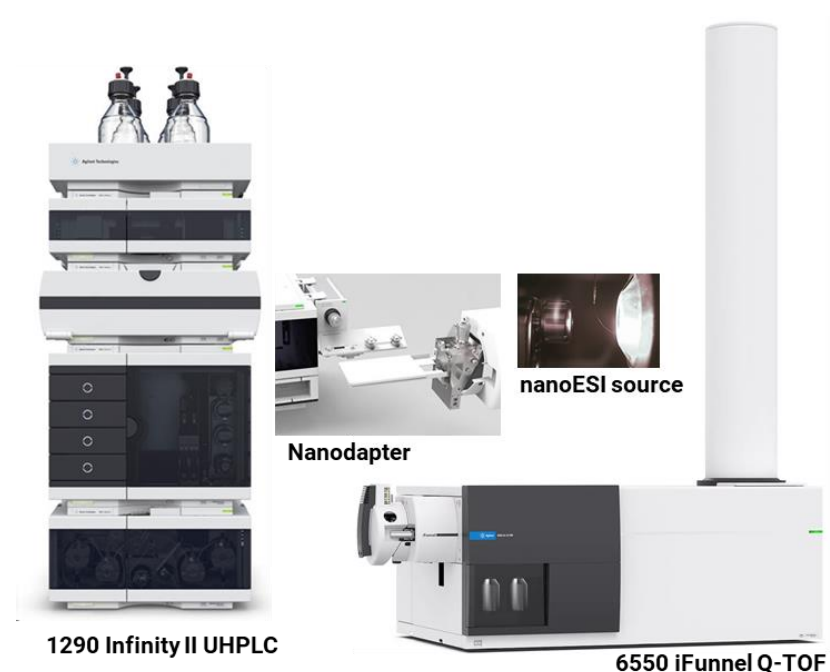


Figure 2. Nanodapter converts standard flow LC to nanoflow LC coupled with Q-TOF

Table 1. AssayMAP Bravo protocols

	Affinity Purification	Cross-linking	Immunoaffinity purification	Peptide Clean-up
Resin volume	25 μ L	25 μ L	25 μ L	5 μ L
Affinity Medium	Protein A	Protein A + antibody	Protein A +Xlinked antibody	C18
Prime buffer	PBS, pH=7.4	0.2 M triethanolamine, pH=8.1	TBS, pH=7.4	70% ACN, 0.1% TFA in water
Equilibration buffer	PBS, pH=7.4	0.2 M triethanolamine, pH=8.1	TBS, pH=7.4	2% ACN, 0.1% TFA in water
Loading buffer	Antibody storage buffer	5mM DMP in 0.2M TEA	3 mg/mL GRANTA lysate	1% Acetic Acid
Loading volume	1000 μ L	250 μ L	1000 μ L	100 μ L
Loading flow rate	20 μ L/min	10 μ L/min	20 μ L/min	5 μ L/min
Washing buffer 1	PBS, pH=7.4	TBS, pH=7.4	TBS, pH=7.4	2% ACN, 0.1% TFA in water
Washing volume 1	250 μ L	250 μ L	250 μ L	50 μ L
# washes 1	1	3	3	1
Washing buffer 2	NA	1% Acetic Acid	25mM Tris, pH=8.0	NA
Washing volume 2	NA	100 μ L	250 μ L	NA
# washes 2	NA	3	3	1
Elution buffer	NA	TBS, pH=7.4	1% Acetic Acid	30% ACN, 0.1% TFA in water
Elution volume	NA	250 μ L	100 μ L	100 μ L

MHC Peptide Identification and Quantitation

Figure 3 is the total ion chromatogram (TIC) of the three samples using a 90-minute gradient. The TIC shows reproducible retention time and peak abundance between the samples. The tandem MS data were analyzed by Byos workflow with Byonic for peptide identification and Byologic for peptide quantitation (Figure 4). In Byonic, both singly and multiply charged ions were considered as precursor ions. A manual score cut, 150, was used for filtering identified peptides.

The identified peptides were imported into Byologic with their sequences. Byologic extracted each identified peptide with its peak area and further filtered peptides with certain number of decoys defined by user. The final

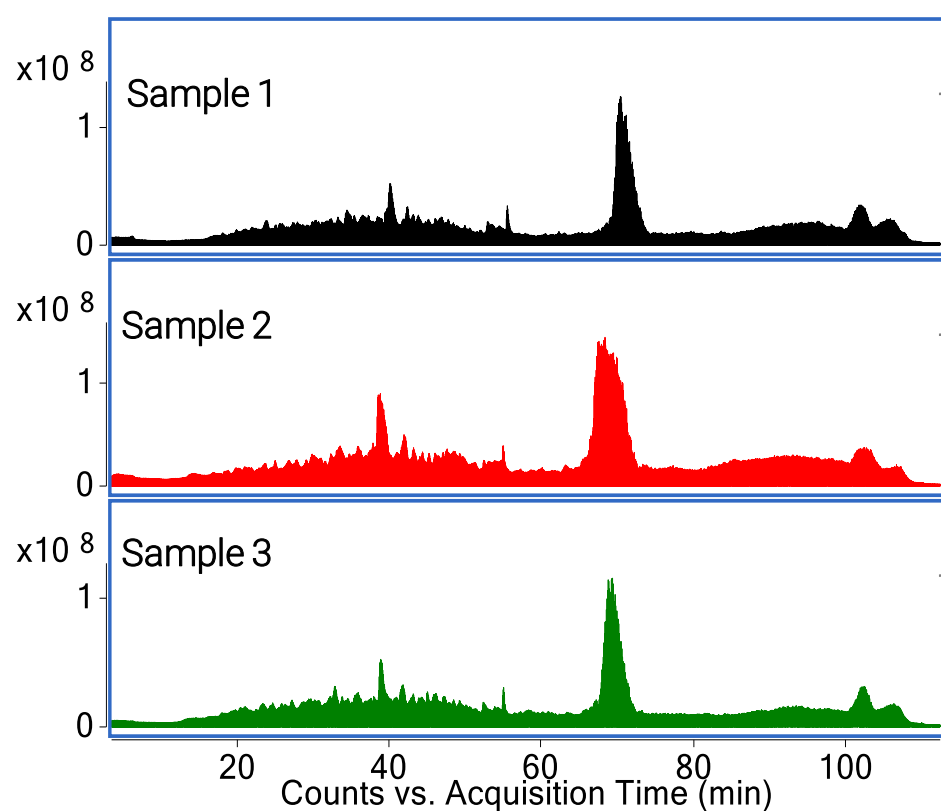


Figure 3. TIC of MHC peptides using 90 minute gradient

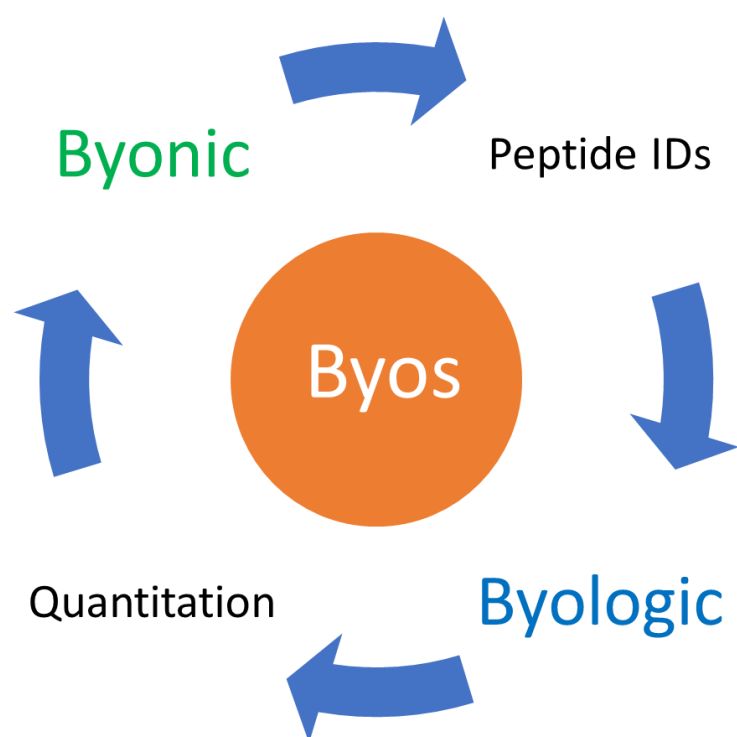


Figure 4. Byos workflow for peptide analysis

peptide IDs are summarized in Figure 5. The unique MHC class I peptides identified in each sample ranged from 2282 to 2424 with a CV% at about 3.0%. The number of unique peptides identified across all three samples is 3604.

The total peptide abundances in each sample are summarized in Figure 6 with a CV% at about 11.1%. Considering multi-steps were used including GRANTA lysate loading on PAW cartridges at different days with a following C18 cleanup, the CV% calculated from the three samples are within a good range, which showed a good reproducibility from the automated sample preparation.

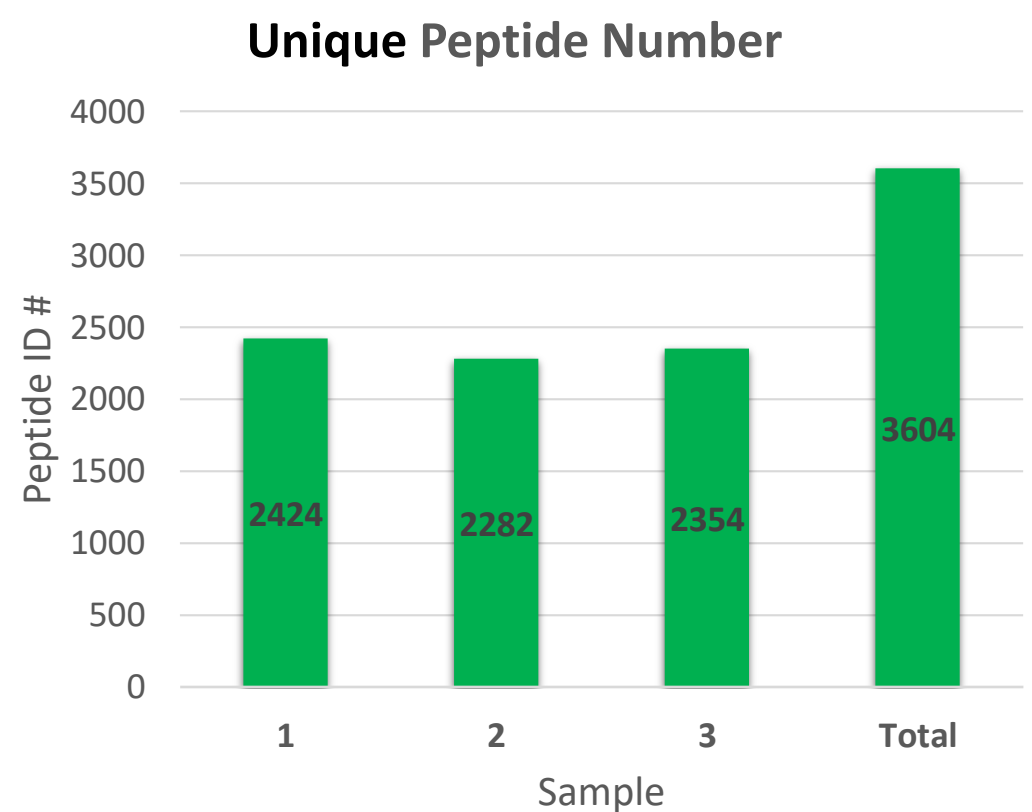


Figure 5. The unique peptide number identified using 6550 iFunnel Q-TOF LC/MS

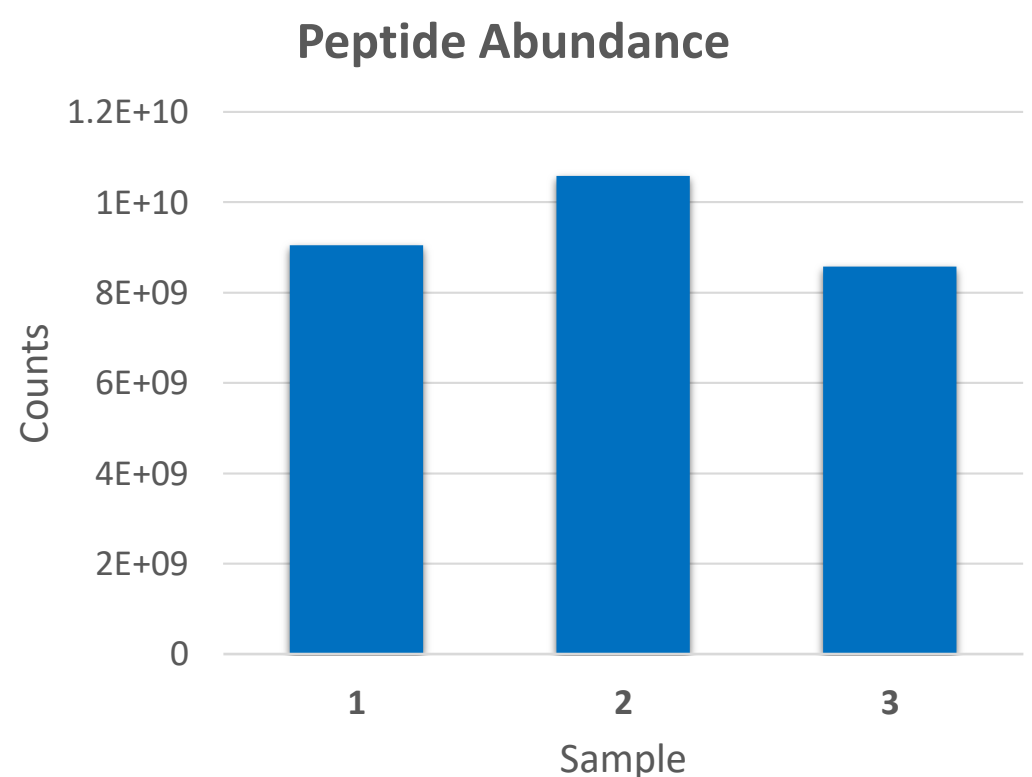


Figure 6. MHC Class I peptide abundance for each sample with CV% at about 11.1%

Peptide Length Distribution

The frequency distribution of peptide length is plotted in Figure 7 to further confirm the identification of MHC Class I peptides. Data shown in figure 7 are compiled from the overall peptide identified after Byos workflow analysis. The 3604 unique peptides (Figure 5) spanned peptide lengths from 3 to 17 residues. However, the vast majority of peptides (94%) were 8 to 11 residues long, with most (75%) at 9 residues. This is well in line with what has been reported in literature.

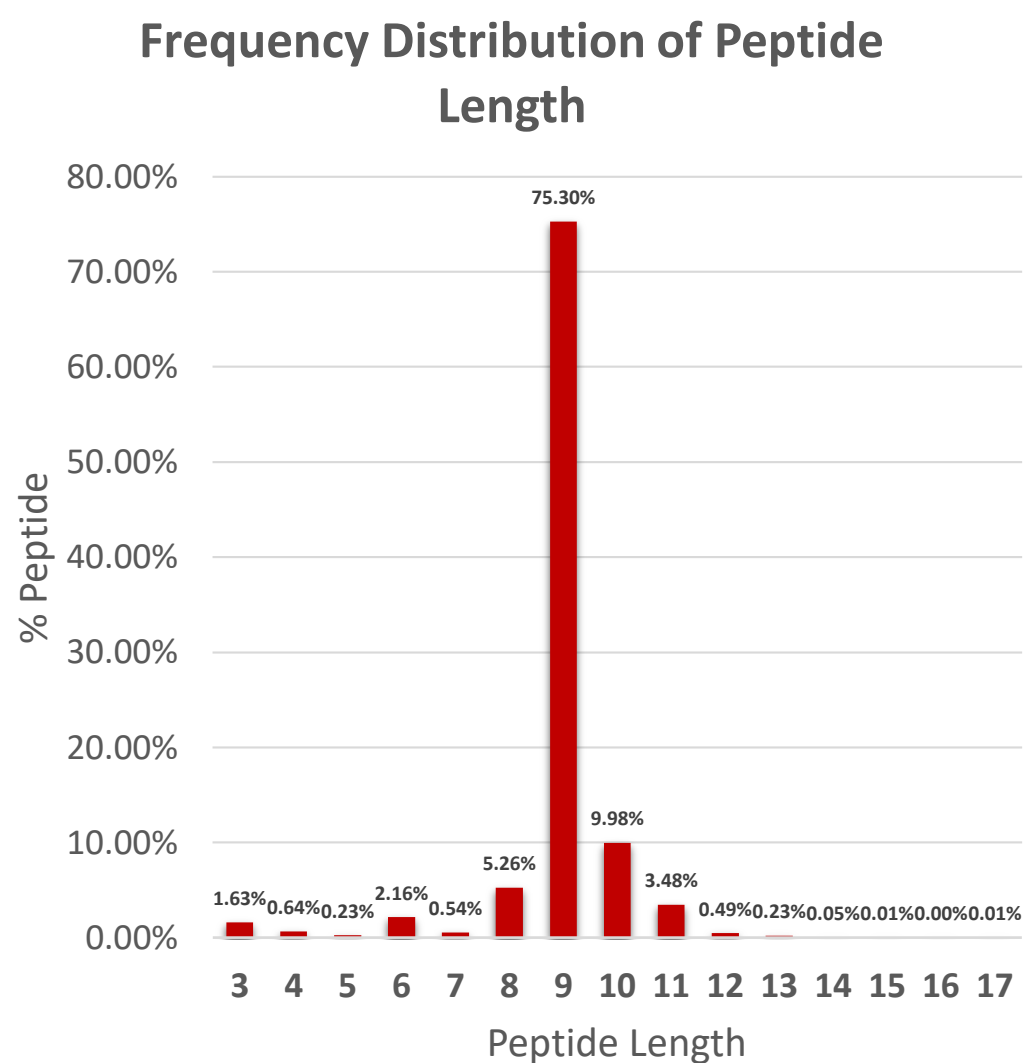


Figure 7. The frequency distribution of the peptide length of MHC class I peptides from the average of 3 samples

Peptide-binding Motif Analysis

It is critical to carefully evaluate the HLA-bound peptide data to ensure the quality of the results. One popular method is to visualize positions of residue preference within the immunopeptidomic datasets. This can be achieved using online tools such as Seq2Logo. <http://www.cbs.dtu.dk/biotools/Seq2Logo/>

Since the majority of the peptides identified were 8-, 9-, 10- and 11-mers with 9-mers being the most abundant peptides (> 75%), all 9-mer sequences were uploaded to the Seq2Logo website and generated the HLA peptide-binding motif in Figure 8. The analysis of the HLA motif showed a strong preference for L or V at position 9 (C terminus) and at position 2.

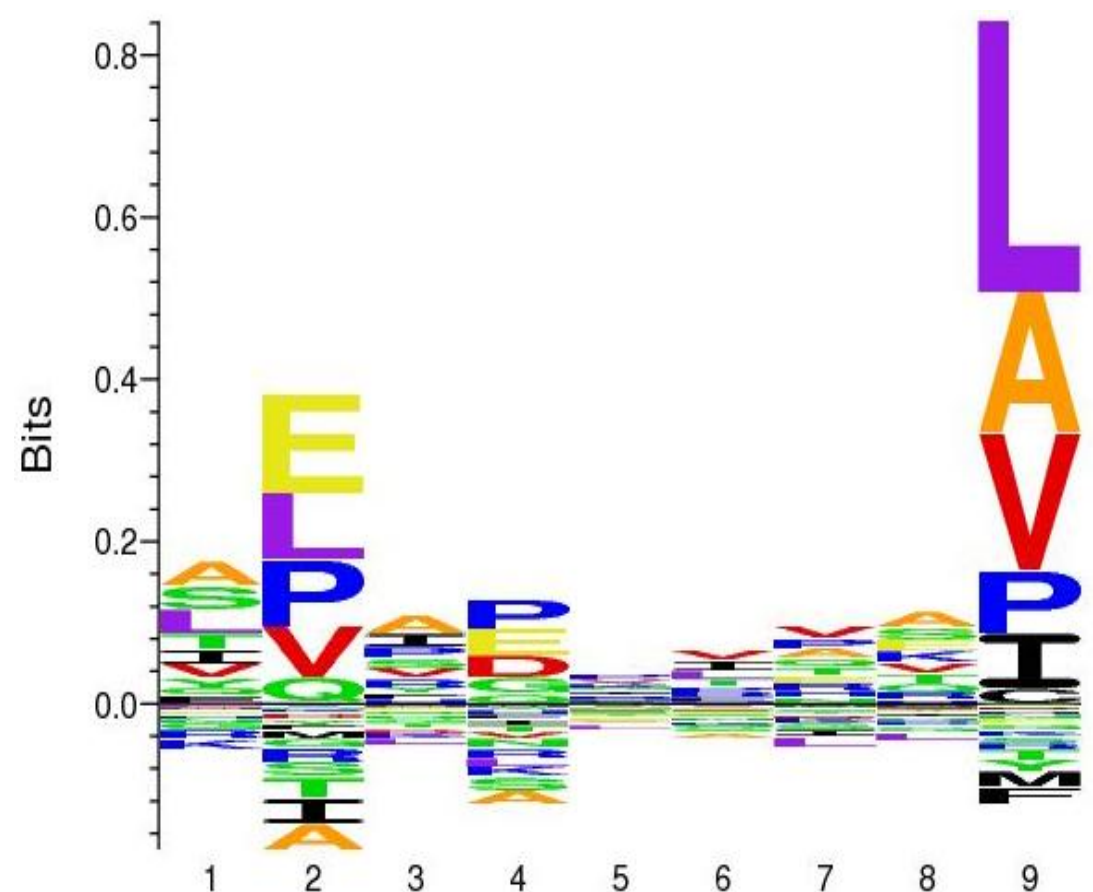


Figure 8. HLA peptide-binding motif was constructed on the basis of nonamer peptides (created by Seq2Logo)

Conclusions

An automated MHC-associated peptide enrichment for immunopeptidomics analysis has been developed. This workflow provides a high throughput, reproducible and easy-to-use enrichment for MHC peptide analysis.

- AssayMAP 25 μ L PAW cartridges are well suited for low concentration MHC-complex enrichment. 5 μ L C18 cartridge provides an efficient peptide separation and cleanup from protein complexes.
- The number of unique peptides identified from the samples are highly consistent.
- The peptide abundance between the samples showed good reproducibility with predominantly 9-mer peptides.

For Research Use Only. Not for use in diagnostic procedures.

Poster Reprint

ASMS 2020

ThP 466

Purity and Identity Characterization of Adeno- Associated Virus Capsid Particles by Intact and Bottom- Up Based Liquid Chromatography-Mass Spectrometry Methods

Wendi A. Hale¹, Dominique Garceau²,
Tristan Cano², Caitlin Jaeger², Roy
Hegedus², William Hermans², Norman
Garceau², Christopher M. Colangelo¹

¹Agilent, Lexington, MA

²LakePharma, Worcester, MA

Introduction

Adeno-associated viruses (AAVs) are the main viral vectors for gene therapy and have been successful in treating inherited retinal diseases and spinal muscular atrophy. AAV is composed of an icosahedral protein shell with a single-stranded genome of approximately 4.7 kb. The intact AAVs act as a vehicle to protect and deliver oligonucleotide therapeutics. There are 11 known serotypes that transduce different cell types, allowing for increased selectivity for therapeutics. As AAVs continue to be explored as therapeutic delivery platforms, it is vital to ensure that all the critical quality attributes (CQAs) of the therapeutic product are maintained.

Characterizing viral capsid proteins yields several challenges. The protein shell is composed of three capsid proteins, VP1, VP2 and VP3, that assemble into a 3.9 megadalton structure in a ratio of 1:1:10 with 60 capsids per virion. In addition to the low molar ratios of VP1 and VP2, all three proteins have overlapping sequences at the C-terminus. Traditionally, SDS-PAGE is used to establish the molecular weight of the capsid proteins, however, this technique provides an approximate molecular weight and may not be able to distinguish between different serotypes. Mass spectrometry is a promising method to overcome these challenges and determine CQAs of the capsid proteins.

Experimental

Materials:

AAV8 was produced by Lake Pharma (Worcester, MA). Molecular weight cutoff filters and (tris(2-carboxyethyl)phosphine) (TCEP) were purchased from Millipore Sigma. Trypsin and rAsp-N were purchased from Promega.

Sample Preparation:

For intact analysis, AAVs underwent a buffer exchange three times at 10,000 g with a 10 kDa molecular weight filter. The buffer contained 5 mM TCEP, 20% H₂O and 80% acetonitrile with 0.1% formic acid (v/v). After the sample was collected, it was incubated at room temperature prior to injection. For peptide mapping, the AAVs underwent denaturation, reduction, alkylation and digestion. Enzymes utilized in this experiment were trypsin and rAsp-N.

Experimental

LC/MS Analysis:

LC/MS analysis was performed on a 1290 Infinity II LC coupled to a 6545XT AdvanceBio LC/Q-TOF system with a dual Agilent Jet Stream source. Agilent MassHunter Acquisition (B.09.00) workstation software with the large molecule SWARM autotune feature was used for intact analysis. The instrument was further calibrated and operated in standard mass mode. The iterative MS/MS feature was used for the peptide mapping workflow. All MS data was processed with Agilent MassHunter BioConfirm 10.0 software.



Figure 1: 6545XT AdvanceBio LC/Q-TOF

	Intact Analysis	Peptide Mapping Analysis
Column	Zorbax Diphenyl RRHD 300Å, 2.1 x 150 mm. 1.8 µm	AdvanceBio Peptide Mapping, 2.1 x 150 mm. 2.7 µm
Flow Rate	0.4 mL/min	0.4 mL/min
Injection Volume	20 µL	40 µL
Column Temperature	60°C	60°C

Table 1: Column and LC Conditions for Both Analyses

Intact Analysis of AAV8 on the 6545XT AdvanceBio LC/Q-TOF

The spectral clarity provided by the improved vacuum on the AdvanceBioLC/Q-TOF in combination with the large molecule SWARM autotune feature show all three viral capsid proteins with their post-translational modifications (PTMs) with high mass accuracy, under 10 ppm for all proteoforms. While it is not shown, VP1 and VP2 are chromatographically separated which can be challenging. While mass spectrometry can separate these proteins by mass, having chromatographic separation allows for less ion suppression of these two low abundant proteins.

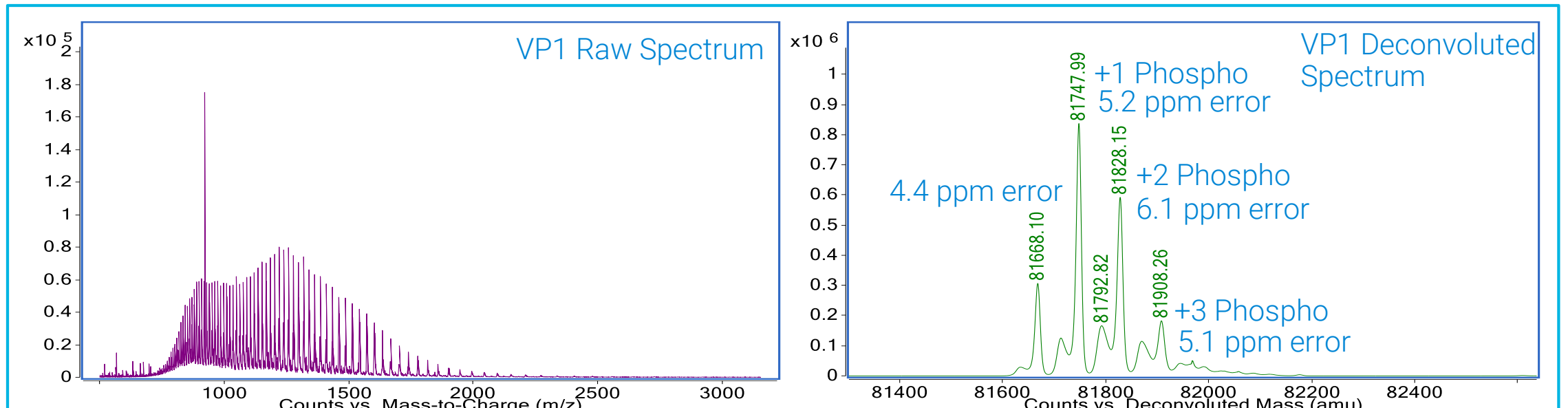


Figure 2: VP1 raw and deconvoluted mass spectra. Three phosphorylation sites were detected on VP1 with less than 10 ppm error. The accurate mass data confirmed that VP1 is missing its N-terminal amino acid residue and that the new N-terminus is acetylated.

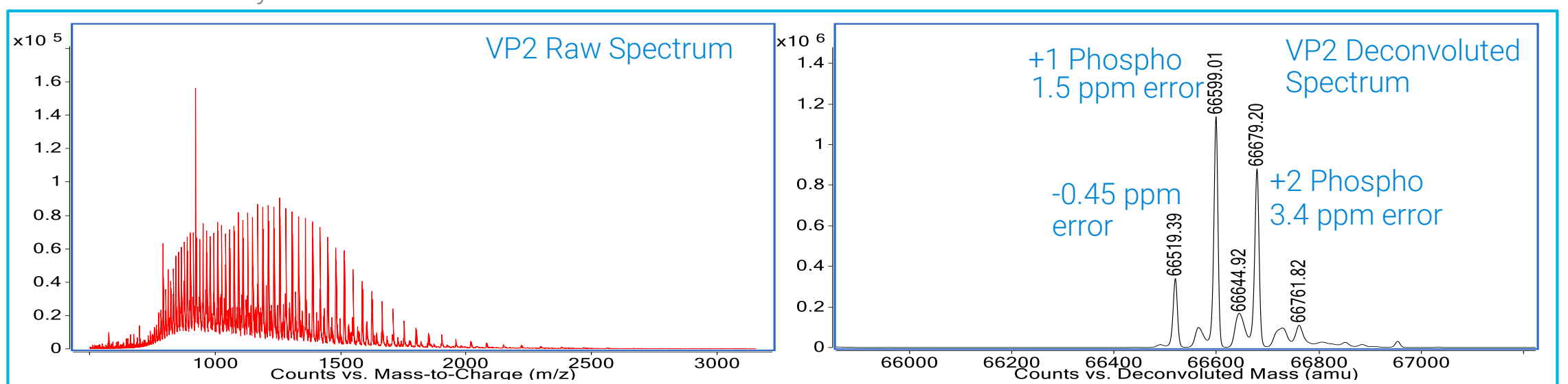


Figure 3: VP2 raw and deconvoluted mass spectra. The accurate mass data confirms at least two phosphorylation sites on VP2.

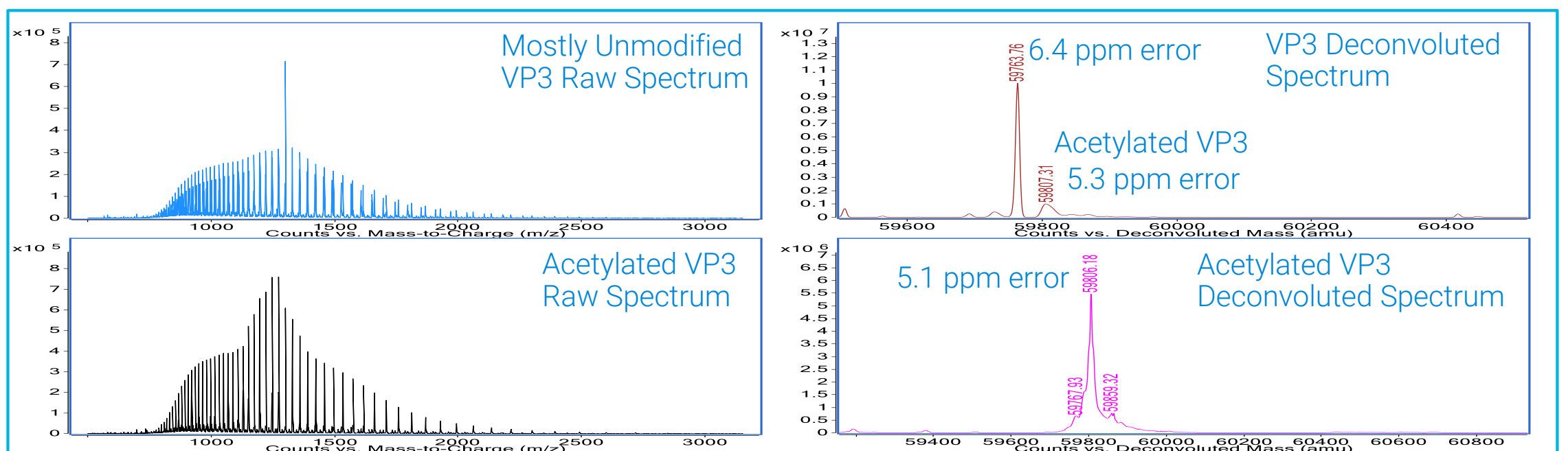


Figure 4: VP3 raw and deconvoluted mass spectra. The unmodified form of VP3 is mostly chromatographically separated from acetylated VP3. While VP1 was fully acetylated, about 70% of VP3 was acetylated.

Peptide Mapping of VP1, VP2, and VP3 on the 6545XT AdvanceBio Q-TOF.

Peptide mapping of biotherapeutics is an essential method to determine protein sequence and post-translational modifications, required by the ICH, FDA and other regulatory agencies. As of January 2020, the FDA recommends providing information regarding primary and secondary structure including PTMs for human gene therapy drug substances. Peptide mapping with the iterative MS/MS feature excludes peptides from all previous runs for isolation and fragmentation, allowing for selection and detection of low abundant peptides. In addition, BioConfirm 10.0 allows for multiple runs to be selected to provide a total sequence coverage. This feature is useful for combining results from iterative MS/MS runs as well as using multiple enzymes.

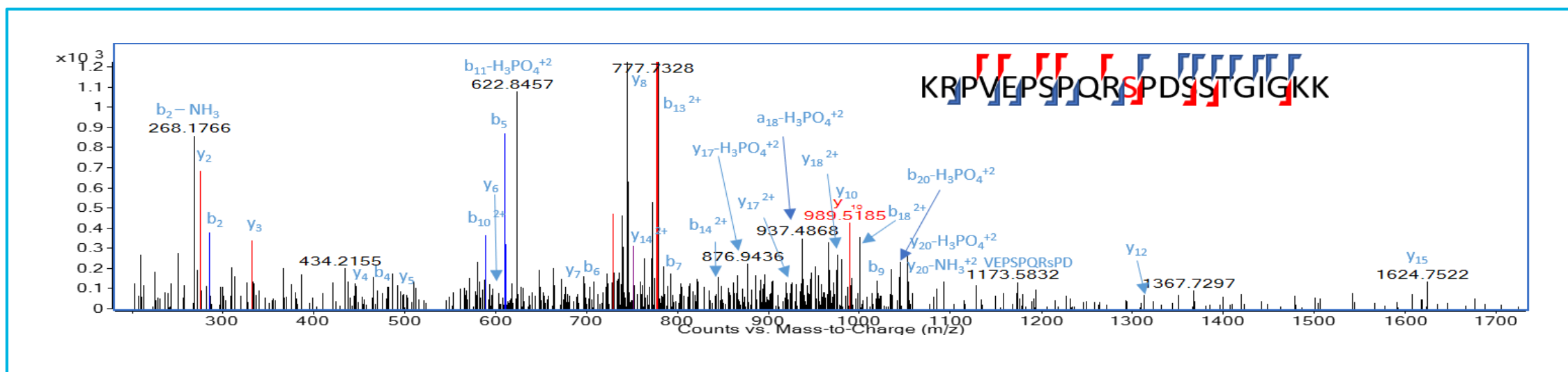


Figure 5. Example of MS/MS spectrum confirming site-specific phosphorylation of a serine residue.

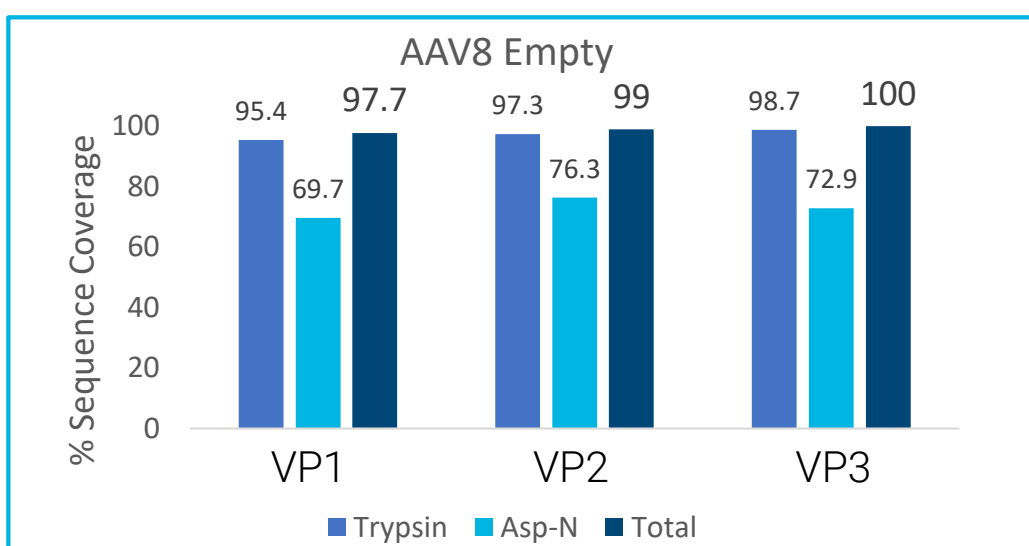


Figure 6. Peptide mapping results of each of the viral capsid proteins. Each protein has 100% or nearly 100% sequence coverage with MS/MS confirmation.

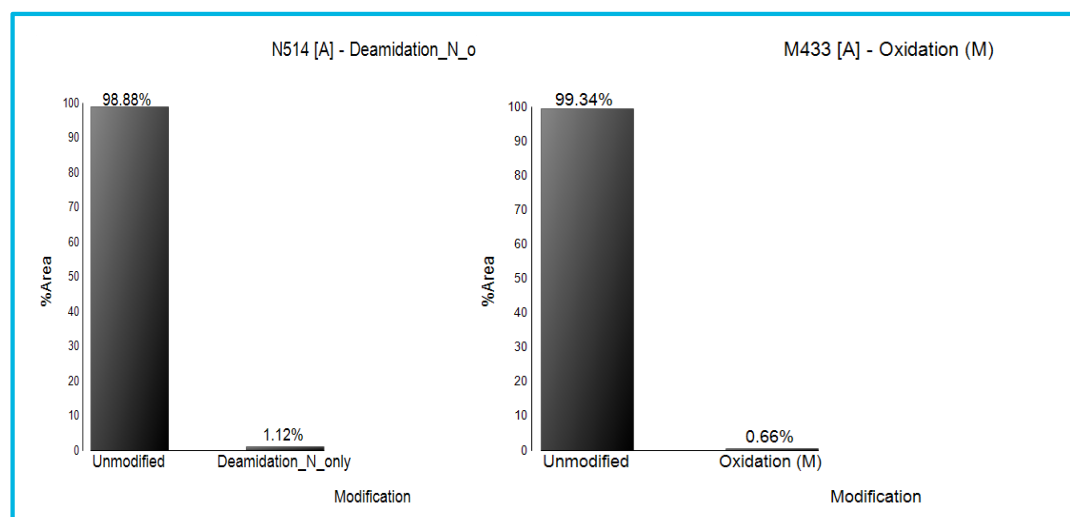


Figure 7. Examples of common PTMs. Low levels of deamidation and oxidation indicate this protein has not degraded.

Conclusions

- All three capsid proteins were chromatographically separated.
- The intact protein data has clear spectra and all proteoforms have less than 10 ppm error.
- The peptide mapping data gives between 97.7-100% sequence coverage with MS/MS confirmation.
- Site specific phosphorylation was localized.
- Relative quantitation of PTMs was performed.

References

- 1 Dalkara, D. et al. *Sci. Transl. Med* **2013**. 5(189), 189ra76-189ra76.
- 2 Moore, N. A. et al. *Expert Opin. Biol. Ther.* **2018**. 18(1), 37-49.
- 3 Wu, Z. et al. *J. Mol. Ther.* **2006**. 14(3), 316-327.
- 4 Jin, X. et al. *Hum. Gene Ther. Methods* **2017**. 28(5), 255-267.
- 5 Giles, AR. et al. *Mol. Ther.* **2018**. 26(12), 2848-2862.

For Research Use Only. Not for use in diagnostic procedures.

Poster Reprint

ASMS 2020

ThP472

Impact on Glycan profile caused by media components as a critical quality attributes on in-house produced mAb

Rohan Shah¹, Saurabh Nagpal² and Anurag S. Rathore¹

¹Indian Institute of Technology, New Delhi, India

²Agilent Technologies, Manesar, India

The glycan structure contributes to the protein half-life in plasma and also possesses an ability of the mAb to trigger the immune response, which is required for efficacy. Regulatory authorities consider glycosylation to be one of the critical quality attributes of biomolecules. Therefore, it must be characterized and quantified, with acceptable ranges determined, as part of the development process for a glycoprotein innovator, biosimilar, or biobetter pharmaceuticals. Any changes in glycan profile has shown to be associated with various inflammatory diseases and cancer. One of the most common PTM's related to protein glycosylation that involves in controlling of various biological processes like such as molecular recognition, cell adhesion, fertilization and signal transduction. These variations in glycosylation pattern affect the therapeutic proteins in board biological process, therefore regulatory approvals are closely monitored for observing consistency in glycosylation pattern. Hence, the acceptable limits for mAb glycosylation variability are provided by the regulatory bodies, for High Mannose 3-10%, Afucosylated 2-13%, Galactosylation 10-40%, Sialic Acid 0-2%.

Vitamins are essential for growth and maintenance of cells and hence are integral part of cell culture media.

Methods and Materials

We have used 6 different vitamins in this study to investigate the effect of vitamins on glycosylation. The control in this experiment is Trastuzumab Innovator Batch1 and Standard refers to the prelabelled glycan from mAb provided with the GX96-IPCGly-X™ N-Glycan Rapid Release and InstantPC™ Kit . Herein, 17 different runs were performed having different levels of vitamins under investigation. Higher and lower levels were determined by analyzing the concentration of vitamins in basal media. During the culture process the different concentration of vitamins based on DOE (design of experiment) were supplemented. N-linked glycans were released from the protein backbone using peptide-N-glycosidase F (PNGase F) in a single replicate. The released glycans were derivatized with instant mass tag (InstantPC from Prozyme Inc, now Agilent Technologies) that permits detection using both fluorescence and mass spectrometry (MS) at the reducing terminal N-acetylglucosamine (GlcNAc). The glycoprotein samples of concentration 50µg was used in 50mM of HEPES buffer with pH 7.9. The deglycosylation protocol was provided with the kit and was modified based on the nature of study. This unique strategy of the dye enhances the labelling speed and also improves the sensitive identification by UHPLC-FLD-QToF. The labeled oligosaccharides were separated by HILIC column using Agilent 1290 Infinity II UPLC coupled to Agilent 6546 LC/Q-TOF. The bound oligosaccharides were eluted, and relative area under the curve of the oligosaccharides were calculated. Vitamins were supplemented at three levels wherein the lower level corresponds to basal media and upper level corresponds to 10 – 100 times higher than lower level. The middle level was used as per design developed by software JMP.

Results and Discussion

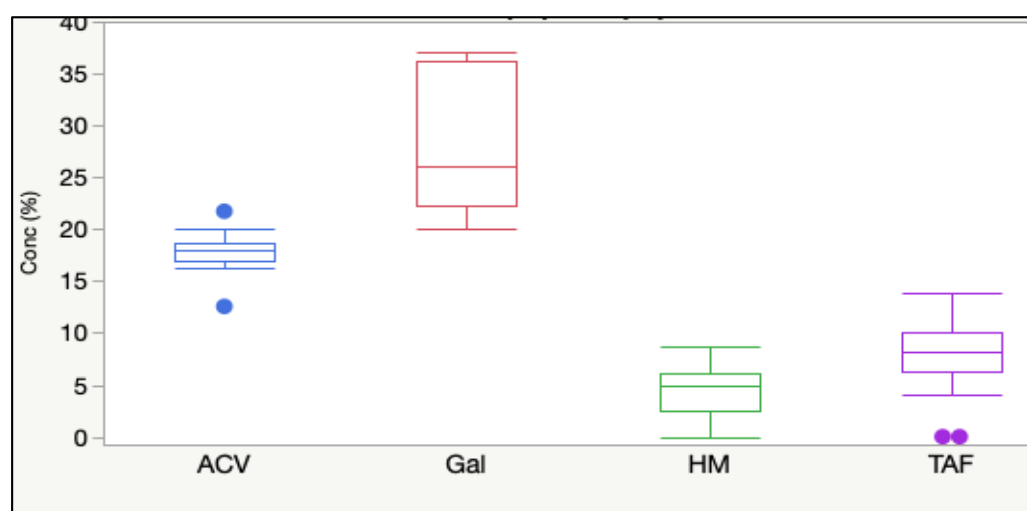


Figure 1a: Total glycan distribution profile from DOE.

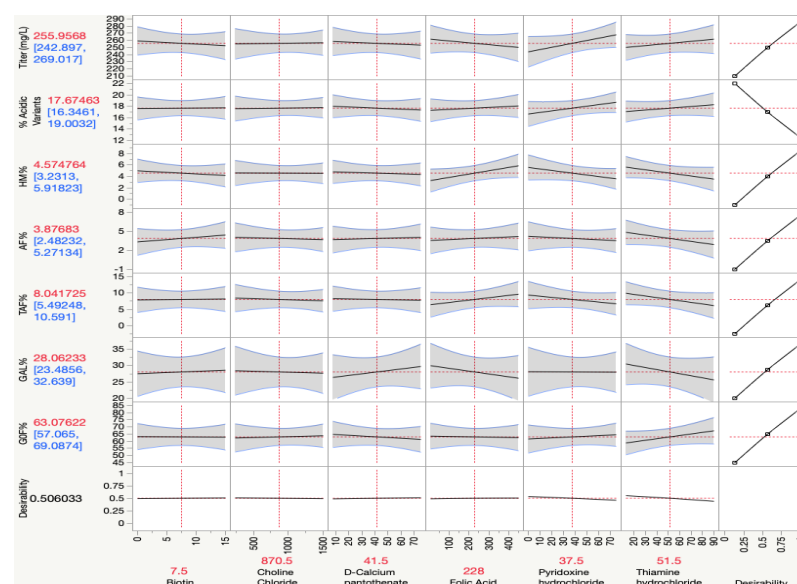


Figure 1b: Prediction profile for vitamin supplementation.

Impact of vitamin supplementation on glycan profile:

The Figure 1a and 1b refers to the prediction of total glycan distribution and the effect of vitamin on glycan. The glycoforms are compared between the innovator, vitamin supplemented sample and the Glycan library. The final area under the curve was grouped under AF%, GAL%,TAF%, GOF% and HM% is shown in Figure 2. The glycosylation pattern of the major abundant glycans, such as the GOF and AF% were comparable between the innovator and Vitamin samples (Figure 2). In the vitamin supplemented samples, differences in the HM% (Man5). of the glycoforms were observed, as shown in Fig. 2. A significant impact was observed in HM% upon the supplementation of vitamins in media during the mAb production. The Gal% can be improved to 40% as compared to innovator, which can be achieved with such supplementation. While, TAF% and AF% are in alignment with the innovator. More than 50% of variation is observed in prediction profile Figure 1b.

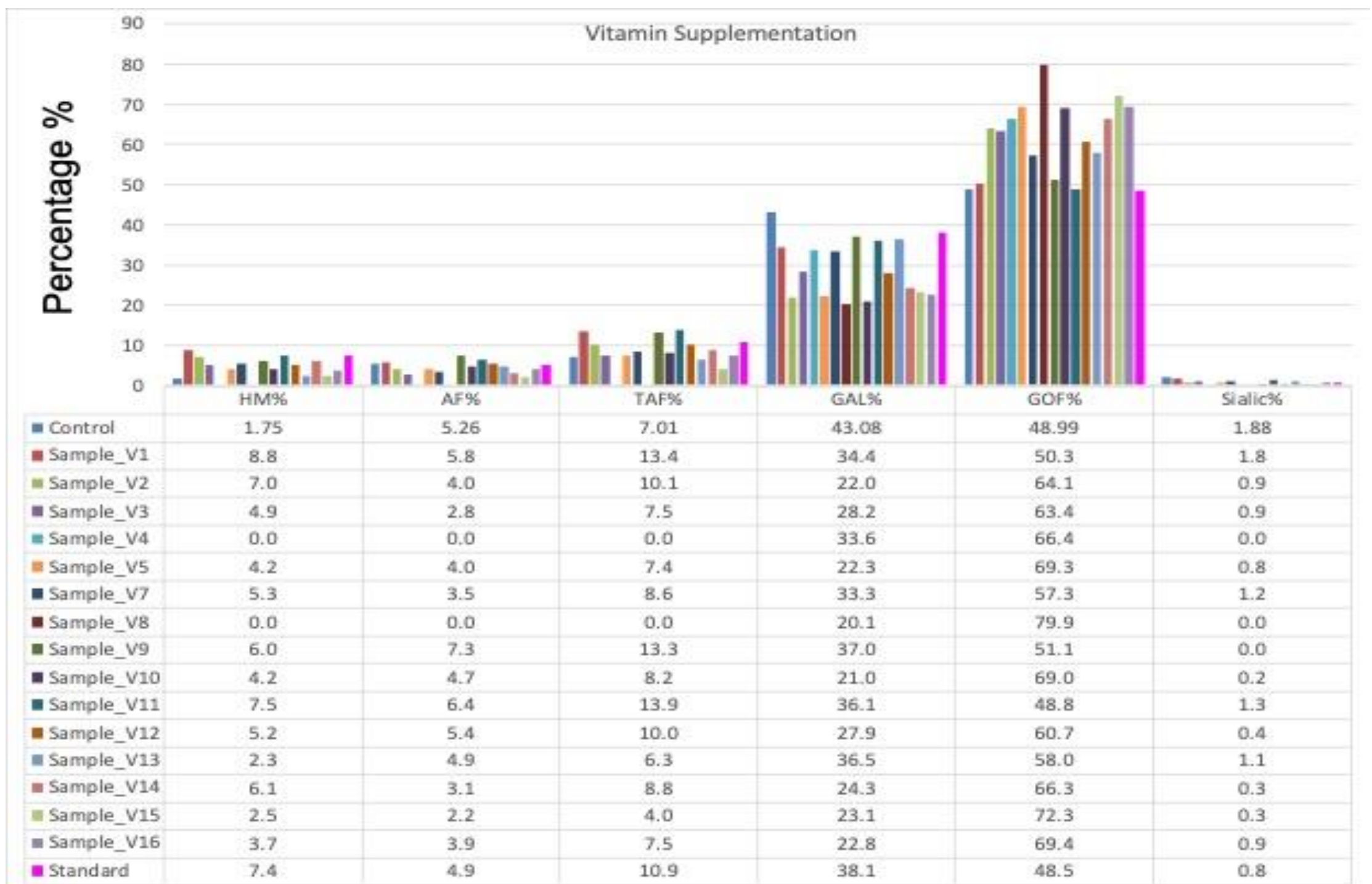


Figure 2. Glycan area percentage between innovator and vitamin supplemented samples. The percentage of glycoforms are showed for various supplemented vitamin samples. The Control represents the innovator of trastuzumab, V1-V16 different concentration of vitamin supplemented samples and Standard represents the Glycan library.

Conclusions

1. Vitamin supplementation can help to control the CQA to greater extent in achieving optimum DOE.
2. Different media supplementation needs to be added for establishing optimal media component and creating a list of components, which possess a significant impact on the glycan and HCP profile.
3. Different supplementation of media components are required to construct an optimal DOE for achieving higher product yield. While Vitamin supplementation has clearly shown a significant effect on HM% and Gal% this possesses a significant effect on CDC (Complement Dependent Cytotoxicity)

References

1. Morelle, W. A et. Al. Rapid Mass Spectrometric Strategy for the Characterization of N-and O-glycan Chains in the Diagnosis of Defects in Glycan Biosynthesis. *J. Biol. Chem.* 277 (11), 1800–1813.
2. Batra, J.; Rathore, A. S. Glycosylation of Monoclonal Antibody Products: *Biotechnol. Prog.* 2016, 32 (5), 1091–1102.

Acknowledgement

Authors are thankful to Indian Institute of Technology for the Lab facilities.

R Shah would like to thank Agilent University relations office for the fellowship grant.

For Research Use Only. Not for use in diagnostic procedures.



Poster Reprint

ASMS 2020

ThP487

Robust and Reproducible Protein Quantification in Plasma using Evosep One and Agilent 6495 Triple Quadrupole LC/MS

Linfeng Wu¹ and Nicolai Bache²

¹Agilent Technologies, Santa Clara, CA;

²Evosep Biosystems, Odense, Denmark

Introduction

In clinical research applications, it is commonly necessary to analyze low abundance protein biomarkers from large sample cohorts, which therefore requires the LC/MS platform to be highly sensitive, rapid, and robust for analytical analysis. Nanoflow LC separation has often been used to separate complex biological samples prior to MS analysis owing to the sensitivity requirement. However, nanoflow LC/MS is usually neither fast nor robust. Conversely, conventional flow LC/MS setups are faster and much more robust but requires more sample loading.

This study was performed to evaluate the robustness, reproducibility and analytical sensitivity of a new low flow solution, Evosep One, using a preformed gradient and disposable trap columns when coupled to an Agilent nanospray source and a high-performance 6495 Triple Quadrupole (TQ) LC/MS for high throughput quantitative proteomics.

Experimental

Instrumentation

Evosep One (EV1000) coupled to an Agilent Nanospray source (G1992A) and 6495 triple quadrupole LC/MS (G6495B) (**Figure 1**).

Materials

The Human plasma was purchased from Bioreclamation (catalog no. HMPLEDTA2). The PeptiQuant Biomarker Assessment Kit (BAK-A6495-76) was purchased from Cambridge Isotope Laboratories.

Data processing

Data analysis for targeted peptide quantification was carried out using Agilent MassHunter workstation software (v10.0) and Skyline software (v19.1.0.193).

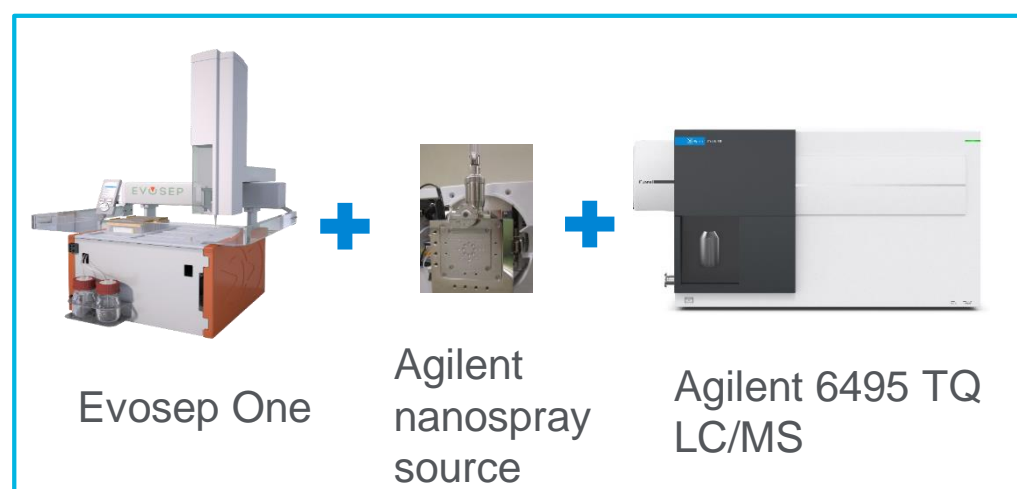


Figure 1. Evosep One coupled to an Agilent 6495 triple quadrupole LC/MS system with Nanospray source.

Experimental

Sample preparation

Human plasma was prepared by denaturation, reduction, alkylation, and trypsin digestion; then lyophilized using SpeedVac. The plasma digest was reconstituted and spiked with the balanced Stable Isotope-labeled Standard (SIS) peptide mixture from the Biomarker assessment Kit followed by serial dilution for standard curve analysis. In addition, a large stock of plasma digest sample spiked with 0.7 nmol/mL of the SIS peptide mixture was also prepared for robustness test. All the SIS-spiked plasma digest was directly loaded on the Evotips with ~1 µg digest per Evotip without further SPE cleanup.

LC/MS analysis

Peptide samples were separated using a standardized 60 SPD method which is a pre-formed 21-min gradient on a 100 µm x 8 cm C18 column from Evosep (Table 1). A stainless-steel emitter was implemented into the needle holder (clamshell) for the Agilent nanospray source. LC/MS data was acquired using the Agilent 6495 Triple Quadrupole LC/MS in dMRM mode for 33 pairs of heavy and endogenous peptides matching to 31 protein biomarkers.

Evosep One LC system	
Analytical Column (length/ID/C18 bead size)	8 cm/100 µm/3 µm
Flow rate	1 µL/min
Gradient length	21 min
Cycle time	24 min
Throughput (samples/day)	60
Agilent 6495 Triple Quadrupole mass spectrometer	
Ion mode	nanoESI, Positive
Gas temperature	200 °C
Drying gas flow	11 L/min
Capillary voltage	1750 V
High/Low Pressure RF voltage	200/110 V
Delta EMV	200 V
Q1 and Q3 resolution	Unit/Unit
Cycle time	500 ms
Min. / Max. dwell Time	5.90 ms/80.59 ms
Total MRMs	198

Robustness of LC Retention Time

To assess system robustness, replicate injections of SIS peptide-spiked human plasma digest were carried out with 10fmol SIS peptides in $\sim 1\mu\text{g}$ plasma matrix on column per injection. A total of 574 injections was performed consecutively on the same column without any adjustment on spray needle or mass spectrometer.

The retention time of all the targeted peptides show excellent reproducibility across the test (Figure 2), with the RSD ranging from 0.43%~2.75%. The back pressure of the analytical column did not change over the entire duration of the experiment.

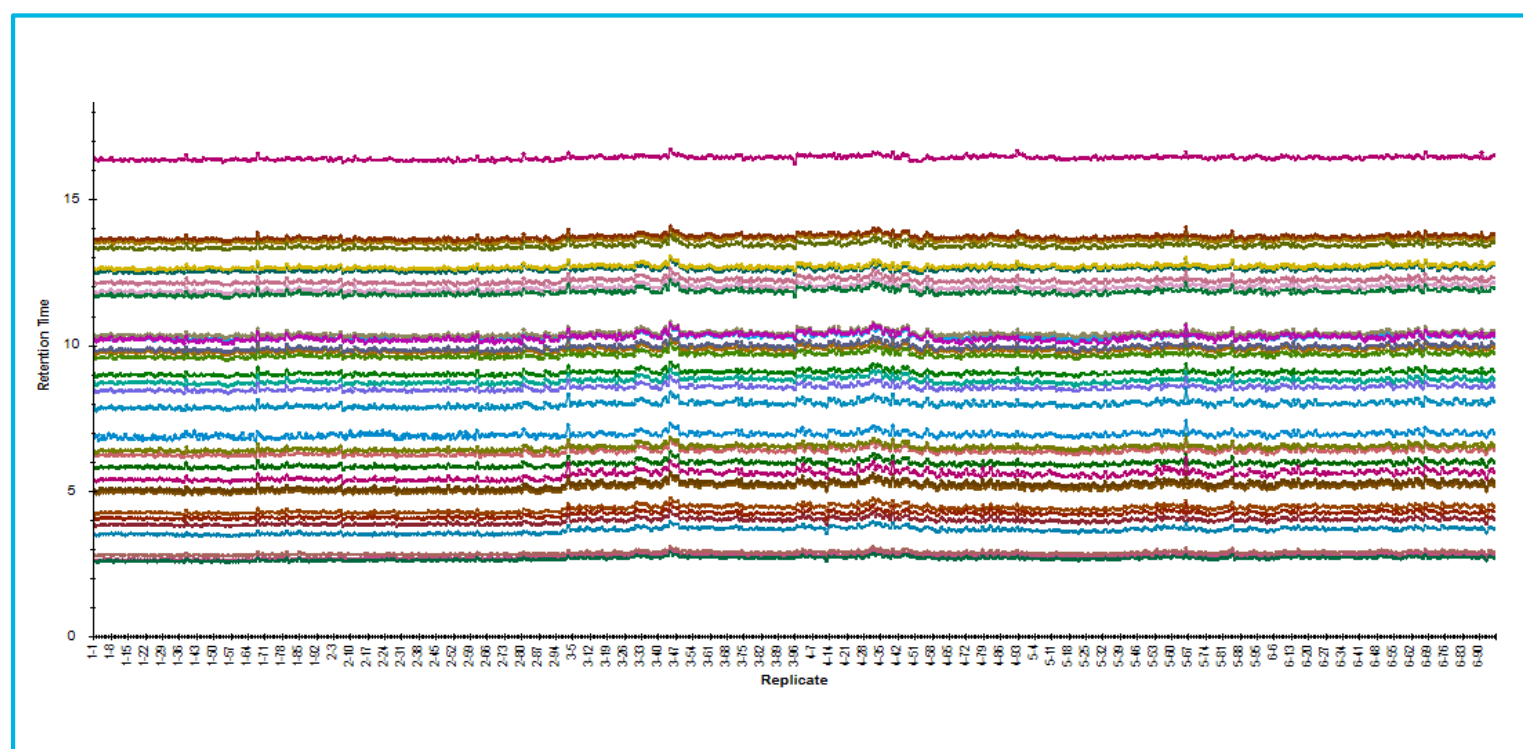


Figure 2. Retention time distribution of all the targeted peptides from 574 replicate injections during robustness test. The different peptides were color-coded.

Reproducibility of MS Signal Response

The relative standard deviation (RSD) of MRM peak area of each targeted peptide is displayed in a histogram plot (Figure 3). The median RSD is 8.5%, with 62 out of the 66 peptides (93.9%) showing an RSD below 16%. Only two pairs of heavy and endogenous peptides show an RSD greater than 16%. One pair is hydrophilic peptides and unstable in solution. The other pair shows severe matrix interference, causing variation in peak integration. Therefore, the high RSD of these two pairs of peptides was not due to instrument variation

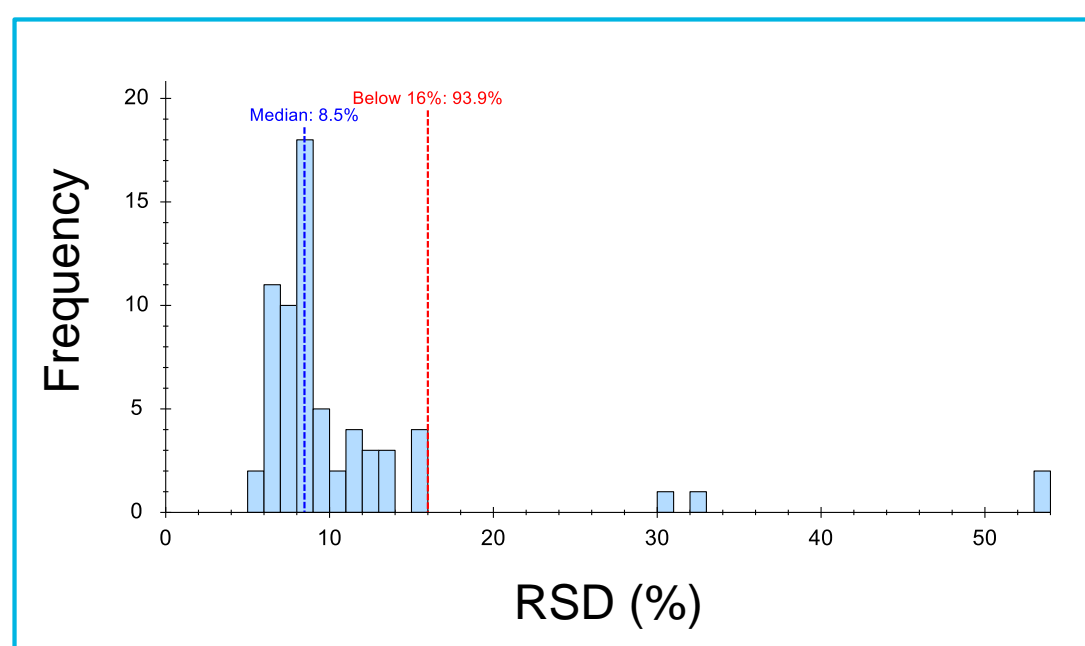


Figure 3. Histogram of peak area RSD for all the targeted peptides during robustness test. The blue dash line labels the median RSD of 8.5%. The red dash line marks the 93.9% of the peptides having an RSD below 16%.

Reproducibility of Four Selected Peptides

The MS signal response of four selected peptides matching to four protein biomarkers shows outstanding stability for the 574 replicate injections (Figure 4):

- Very stable MS response (MRM peak area RSD = 6.5, 7.0, 7.9, and 6.0%, respectively, for n=574)
- Good RT reproducibility (RSD = 0.69, 0.80, 1.04, and 0.59%, respectively, for n=574)

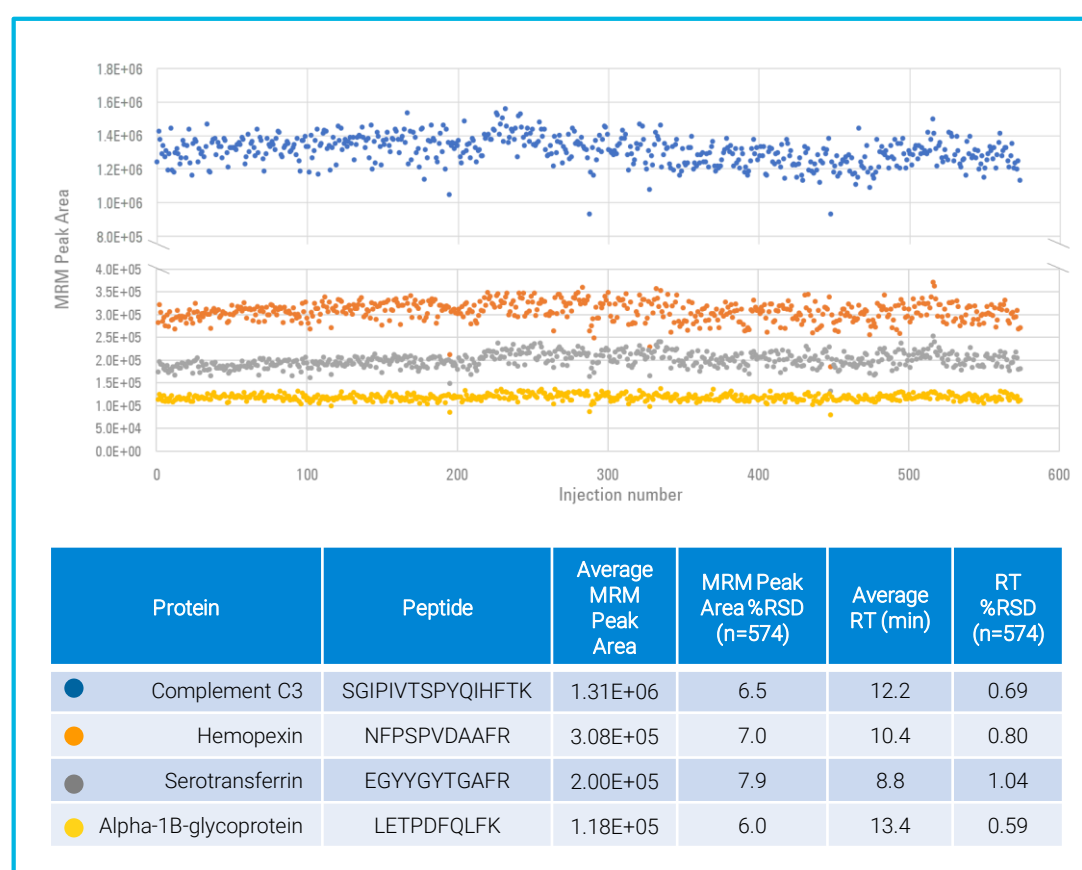


Figure 4. MRM peak area of four selected SIS peptides from 574 replicate injections for robustness Test.

Standard Curve Analysis

To evaluate analytical sensitivity for protein quantification in heavy matrix, the SIS peptide mixture was spiked into human plasma digest at eight different concentrations. Replicates (n=5) of each calibration sample was directly loaded onto Evotip with ~1 µg plasma digest on column per injection. Standard curve analysis was carried out both before and after robustness test on the same column for robustness test. The two standard curves for the SIS peptide SGPIVTSPYQIHFTK from Complement C3 in plasma were very similar with LLOQ of 10 amol on column (Figure 5).

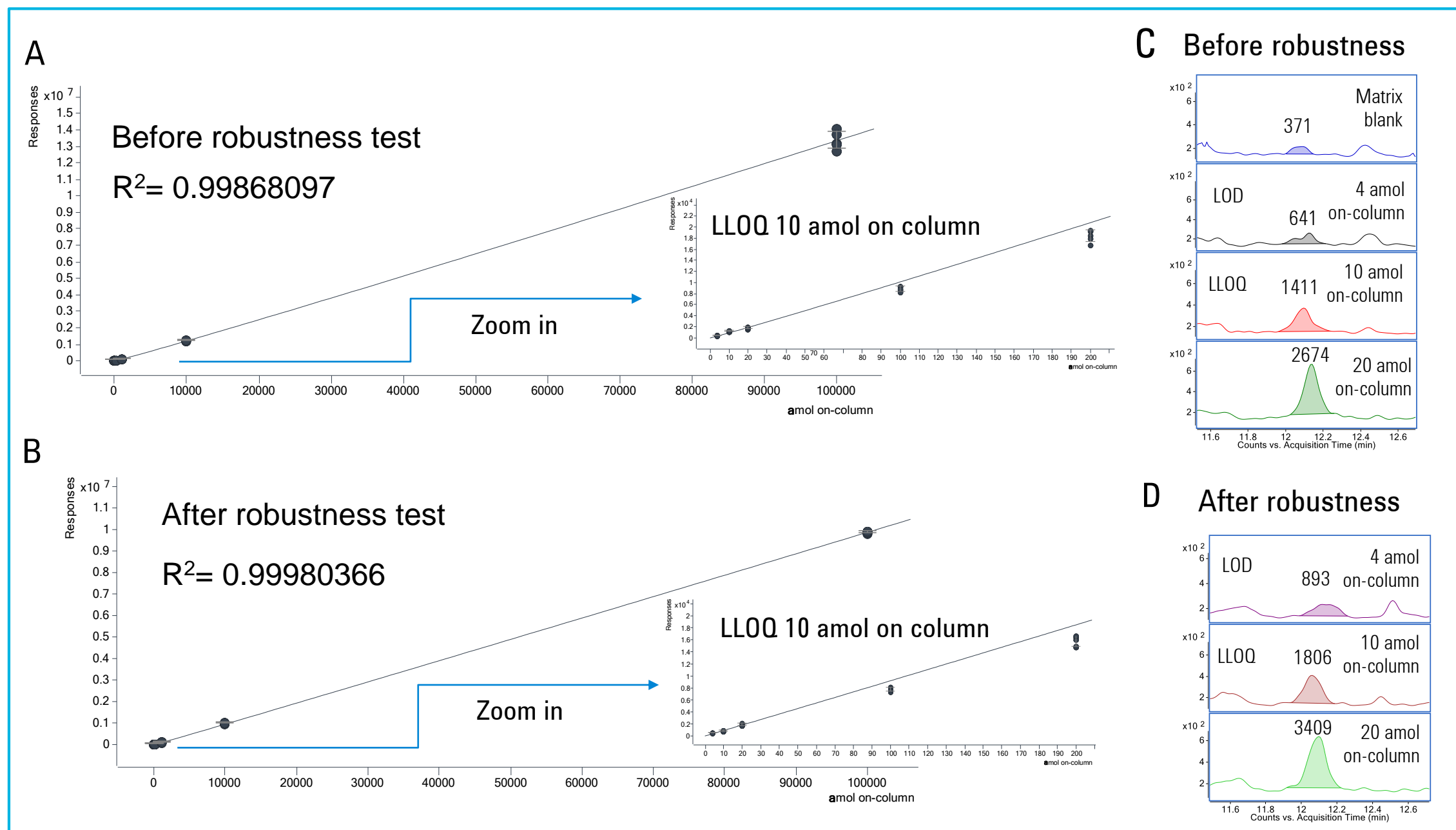


Figure 5: Standard curve analyses of SIS peptide SGPIVTSPYQIHFTK from Complement C3 in plasma both before and after robustness test. A,B) standard curves before and after robustness test. C,D) Stacked extracted ion chromatograms showing the LOD of 4 amol and LLOQ of 10 amol on-column.

Conclusions

The excellent reproducibility, robustness and analytical sensitivity of a low flow LC/TQ system, including Evosep One LC system, Agilent Nanospray source and Agilent 6495 TQ LC/MS were demonstrated for high throughput protein quantification:

- Reproducible LC retention time for all targeted peptides across over 600 injections on the same analytical column
- MRM signal response shows outstanding stability during consecutive analysis of complex plasma samples over twelve days without any adjustment on spray needle or mass spectrometer
- Similar standard curves were achieved for the example SIS peptide both before and after robustness test
- Robust and reproducible storage of samples loaded on the Evotips

For Research Use Only. Not for use in diagnostic procedures.

Poster Reprint

ASMS 2020

ThP564

Extractables Detection in Rubber Plug Products

Chang Jiang¹, Pei-bin Hu¹, Lv Lei², Chan Jimmy³

¹ Agilent, Chengdu, China; ²Agilent, Wuhan, China, ³Agilent, Taipei, Taiwan

Introduction

For E&L researchers, injections and injectable suspensions are high & medium risk products, for which the most complex components are thermoplastic elastomers. A rubber plug is commonly used in cillin bottles, manufactured with polyisoprene rubber, butyl rubber, halogenated butyl rubber and many other rubber-like materials.

There is no doubt that HRMS is more commonly used for E&L compound screening and identification, partially simplified with AET value (Analytical Evaluation Threshold), which is based on the SCT and is the threshold *at-or-above* which a chemist should begin to identify a particular leachable or extractable for potential toxicological assessment.

Considering the regulatory detection requirements and applicable coverage, an LC/TQ system is the gold standard for targeted compound detection and quantitation where a MRM method can be used for E&L research.

In this study, we investigated the detection of 35 compounds in rubber plugs using an Agilent 6470 triple quadrupole LC/MS system (LC/TQ). These compounds include antioxidants, slip agents, and vulkacits, which are the most conventional and widely used additives in the manufacture for elastomers.

This method aims to test the feasibility of LC/TQ technology for the measurement of E&L, to help manufacturers to evaluate their elastomer products and set up quality control standards – at relatively lower cost than HRMS platforms.



The 6470 triple quadrupole LC/MS coupled to the 1290 Infinity II HPLC

Experimental

Sample preparation

For 1g of rubber stopper sample,

1. Cut into pieces with a diameter of about 5mm
2. Microwave extract with 10ml of dichloromethane at 40 ° C for 45min,
3. Dry with nitrogen then dissolve with 1ml of isopropanol
4. Solvent extracts are injected directly into the LC-TQ system.

Agilent 1290 Infinity II UHPLC System

Column	Agilent ZORBAX RRHD Eclipse Plus C8, 3.0* 150 mm, 1.8 µm
--------	--

Column temperature	45 °C
--------------------	-------

Injection volume	2 µL
------------------	------

Autosampler temp	4 °C
------------------	------

Mobile phase	A) Water(4.5mM NH ₄ Formate + 0.5mM NH ₄ F + 0.1% formic acid)
--------------	--

	B) 80%Methanol + 20% isopropanol (4.5mM NH ₄ Formate + 0.5mM NH ₄ F + 0.1% formic acid)
--	---

Flow rate	0.4 mL/min
-----------	------------

Stop time	25min
-----------	-------

Agilent 6470 LC/TQ System

Drying gas temperature	325 °C
------------------------	--------

Drying gas flow	10 L/min
-----------------	----------

Sheath gas temperature	350 °C
------------------------	--------

Sheath gas flow	11 L/min
-----------------	----------

Nebulizer pressure	45 psi
--------------------	--------

Capillary voltage	4000 V(pos)/3500V(neg)
-------------------	------------------------

Nozzle voltage	0 V(+)/500 V(-)
----------------	-----------------

Delta EMV	200 V
-----------	-------

Polarity:	Positive/Negative
-----------	-------------------

Trap column configuration

E&L compounds, especially antioxidants, were found as contamination at very low concentrations in mobile phase solvents, which may give false positive results if not taken into account. So, the use of a C18 trap column (Agilent ZORBAX Eclipse Plus C18, 2.1* 50 mm, 1.8 μ m) should be situated between the Binary Pump and the Autosampler. The addition of a trap column is used to delay interferences from the mobile phase, which will be eluted about 0.5min later than target compounds of interest.

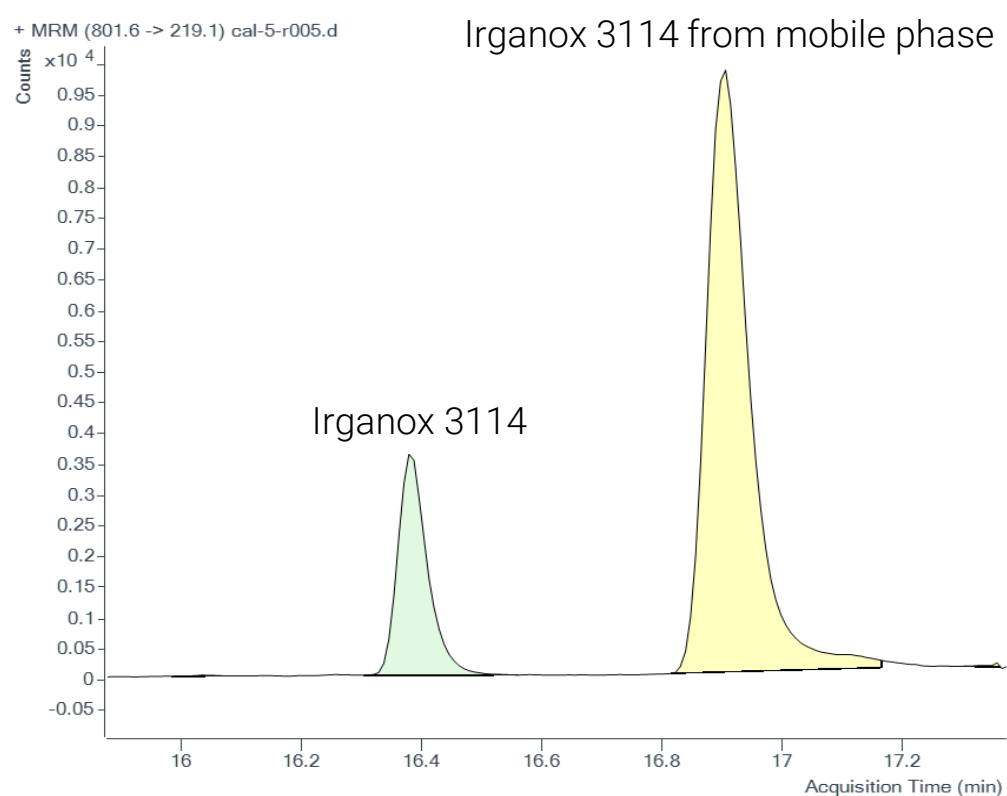


Fig 1. Delayed peak by trap column

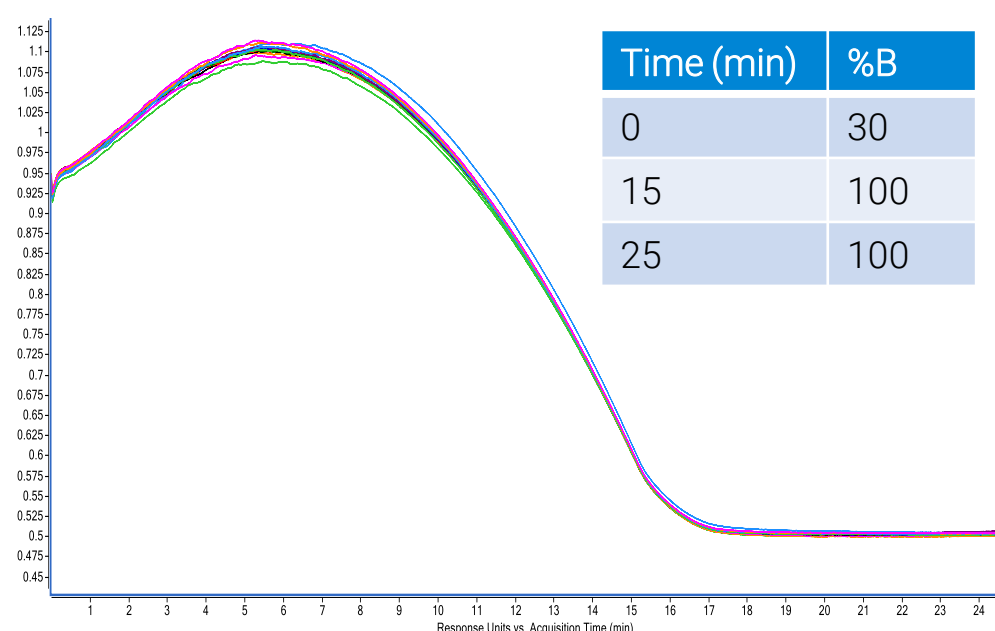


Fig 2. Reproducibility of binary pump pressure profiles

Table 1. MRM list for 35 E&L compounds

Compound Name	Precursor Ion	Product Ion	Polarity	Compound Name	Precursor Ion	Product Ion	Polarity
2,4-Di-tert-butylphenol	205.1	189.1	Negative	Irgafos 126	622.3	510.2	Positive
	205.1	173.1			622.3	223	
9-Octadecenamide	282.3	265.3	Positive	Irganox 1010	1194.8	729.3	Positive
	282.3	247.3			1194.8	563.2	
Benzothiazole	136	109	Positive	Irganox 1076	548.5	149	Positive
	136	65			548.5	107	
BHT	219.1	219	Negative	Irganox 1310	296.2	167	Positive
	219.1	203.1			296.2	107	
BHT-CHO	235.2	179	Positive	Irganox 1330	792.6	569.4	Positive
	235.2	57.1			792.6	219.1	
BHT-COOH	251.2	195	Positive	Irganox 168	647.5	441	Positive
	251.2	57.1			647.5	347	
BHT-OH	235	217.2	Negative	Irganox 245	604.4	263.1	Positive
	235	160.1			604.4	177.1	
Bis(diisobutylthiocarbamoyl) disulfide	409.2	172.1	Positive	Irganox 246	280.3	202	Positive
	409.2	116			280.3	77	
BPA	227	212.1	Negative	Irganox 259	656.5	415.2	Positive
	227	133.1			656.5	107	
Cyanox 2246	358.3	229	Positive	Irganox 3114	801.6	784.5	Positive
	358.3	121			801.6	219.1	
Cyanox 425	386.3	257.1	Positive	MBT	168	109	Positive
	386.3	191.1			168	77	
Dipentamethyl enethiuram disulfide	321	160	Positive	MBTS	333	166.9	Positive
	321	128			333	123	
Dipentamethyl enethiuram tetrasulfide	385	204	Positive	N,N'-(1,3-Phenylene)dimal eimide	286.1	269	Positive
	385	172			286.1	241	
Disulfiram	297.1	116	Positive	Palmitic acid	255.2	255	Negative
	297.1	88		Stearic acid	283.2	283	Negative
Erucamide	338.3	321	Positive	Tetrabutylthiuram disulphide	409.2	172.1	Positive
	338.3	303			409.2	116	
Ethanox 702	442.4	219.1	Positive	Thiram	241	119.9	Positive
	442.4	163.1			241	88	
Ethanox 703	264.2	219.1	Positive	Tinuvin 770	481.4	140.1	Positive
	264.2	203.1			481.4	123.1	

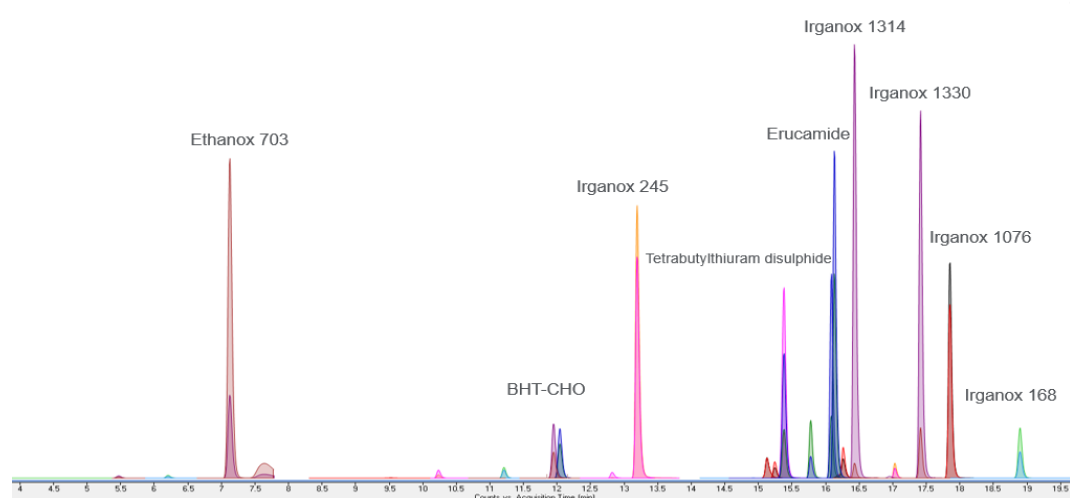


Fig 3. MRM chromatogram for 35 E&L compounds listed

Sample test result

We have tested 3 samples of rubber plugs sold in the market. With the extraction conditions described here, all samples were found to leech antioxidants, slip agents and vulkacits.

Table 2. Sample concentrations of E&Ls found in rubber plug products

Compound	Sample A (µg/kg)	Sample B (µg/kg)	Sample C (µg/kg)
Ethanox 703	14.3	ND	9.6
Disulfiram	ND	ND	98.8
BHT-OH	183.6	ND	ND
BHT-COOH	454.7	152.1	35.8
BHT-CHO	3012.6	890.8	517.4
Irganox 1310	15	101.9	3062.7
Irganox 246	ND	ND	62830
9-Octadecenamide	80.6	109.7	12866.1
Cyanox 2246	ND	41.7	140.2
Palmitic acid	16660.9	3820.8	10307.8
Stearic acid	12354.5	10506.8	9873.2
Erucamide	ND	ND	6303.8
Irganox 3114	20.6	3.6	13.4
Irganox 1010	ND	213.5	23649.7
Irganox 1330	ND	ND	12.1
Irganox 1076	329.6	11941.3	5324.5
Irganox 168	ND	ND	28481.5

Discussion

Antioxidants 1010, 1076, BHT-CHO, palmitic acid, and stearic acid exist in isopropanol at lower concentration than methanol (Table 3), so we suggest isopropanol as the dissolved solvent for extracted samples. Besides that, pipette tips also will release compounds such as Erucamide in organic solvents. It is highly recommended that clean tips with dichloromethane 2 to 3 times before pipetting.

Even with above precautions, for party of the antioxidants and slip agents, positive response can also be observed in MRM chromatogram when injecting different blanks, coupling with multiple solvent washing for needle and needle seat. It suggests those carry over response leached from rubber seal in valve system of autosampler module.

Table 3. Peak area of contaminants found in various solvent blanks

Blank Respond	BHT-CHO	Palmitic acid	Stearic acid	Erucamide	Irganox 1010	Irganox 1076	Irganox 168	Irganox 1310
Methanol	2187	2136	4625	23667	640	3911	322	426
Isopropanol	658	931	1031	79312	613	1514	217	373
2µl of air	488	770	1015	78602	587	670	235	370
No injection	362	563	709	70997	502	282	416	305

Conclusions

- 35 E&L compounds (antioxidants, slip agents, and vulkacits) were detected in rubber plug samples.
- The use of a C18 trap column placed between the Binary Pump and Autosampler is important to avoid the quantitation of false positives.
- Further precautions must be taken when considering dilution solvents, blank solvents, and lab equipment.

Poster Reprint

ASMS 2020

ThP579

Determination of Nitrosamine impurities in Pregabalin drug substance using Triple Quadrupole Liquid Chromatography Mass Spectrometry

Chander Mani, Saikat Banerjee and Samir Vyas

(Agilent Technologies, India.)

Introduction

The announcement for the recall of ARB medicines made N-Nitroso impurities a focus for regulatory agencies including the FDA and the European Medicines Agency (EMA). Nitrosamine impurities are byproducts produced in trace amounts during the manufacturing processes of these medicines. These impurities/compounds are classified as probable carcinogens. Not only ARB drugs but there are other medicines like Pregabalin known as an anti-epileptic drug where the synthetic route or the manufacturing processes may cause the formation of some nitrosamine impurities at trace levels.

There seems to have a clear need for screening of such pharmaceuticals drugs as well for nitrosamine impurities. LCMS-based method presented here is carried out on 6470 triple quadrupole LC/MS (LC/TQ) and provides comprehensive analysis of 5 nitrosamine impurities at low detection limits. These nitrosamine impurities include: N-nitrosodimethylamine (NDMA), N-nitrosodiethylamine (NDEA), N-nitroso-methyl-4-aminopyridine (NMAP), N-nitrosopiperidine (NPIP) and N-nitrosodibutylamine (NDBA).

Instrumentation

1290 Infinity II high-speed pump (G7120A)
1290 Infinity II multisampler (G7167B)
1290 Infinity II multicolumn thermostat (G7116B)
1290 Infinity II variable wavelength detector (G7114B)
6470 triple quadrupole LC/MS (G6470A)

Table 1: Instrumentation detail



Figure 1: 6470 triple quadrupole LC/MS

Experimental

Sample Preparation

The sample preparation procedure was optimized using the following steps.

1. Weigh 100mg(\pm 2mg) Pregabalin drug substance sample in a 15 mL centrifuge tube.
2. Add 5 mL sample diluent and vortex for 2minute.
3. Now put the sample in shaker at 450rpm for 40 minutes.
4. Centrifuge the sample at 5000 rpm for 10 minutes.
5. Filter the supernatant using 0.2 μ m nylon syringe filter into an LCMS vial.
6. Inject the sample into LCMS/MS.

LC Conditions		
Needle wash	Methanol: Water/ 80:20	
Sample diluent	Water: Methanol 95:5	
Multisampler temperature	6 °C	
Injection volume	20 μ L	
Analytical column	Infinity Lab Poroshell HPH C18 3 x 150mm 4 μ m (P/N 693970-502T)	
Column temperature	40 °C	
Mobile phase A	0.2 % formic acid in water	
Mobile phase B	Methanol	
Flow rate	0.5 mL/min	
Gradient	Time (min)	%B
	0.0	5
	5.0	30
	6.2	33.5
	8	95
	11	95
Stop time	11.1	5
	14	5
Post time	14 minutes	
	1 minute	

Table 2: 1290 UHPLC conditions

Method Optimization

The 6470 LC/TQ was used for detecting the mass conditions for nitrosamine impurities in positive mode where $[M+H]^+$ species were found to be predominant precursor ions. The method was optimized using an atmospheric pressure chemical ionization (APCI) source as most of the nitrosamines give better response and low noise background using APCI source.

MRM Transitions and Conditions

Compound	Prec. Ion (m/z)	Product Ion (m/z)	Frag. (V)	CE (V)	CAV (V)	±
NDEA	103.1	75.1	80	9	3	+
NDEA	103.1	47.1	80	17	3	+
NDMA	75.1	58	60	12	3	+
NDMA	75.1	43.1	60	18	3	+
NPIP	115.1	69.1	90	12	3	+
NPIP	115.1	41.2	90	24	3	+
NMAP	138.1	108	60	6	5	+
NMAP	138.1	79.2	60	42	5	+
NDBA	159.1	57.2	90	12	3	+
NDBA	159.1	41.1	90	22	3	+

MS Conditions

Equipment	6470 LC/TQ Parameters
Gas Temperature	300°C
Gas Flow	6L/min
Capillary Voltage	3000V
Nebulizer Pressure	55psi
APCI Heater	350°C
APCI Needle Positive	4 μ A

Table 4: MS conditions

The most critical part of this method is chromatographic separation of Pregabalin from nitrosamine impurities. In this method Pregabalin peak (monitored at 200nm wavelength) is separated well from all five intended nitrosamine impurities and hence making it a very robust method in terms of avoiding high concentration drug substance contamination to mass spectrometer with the help of the diverter valve program.

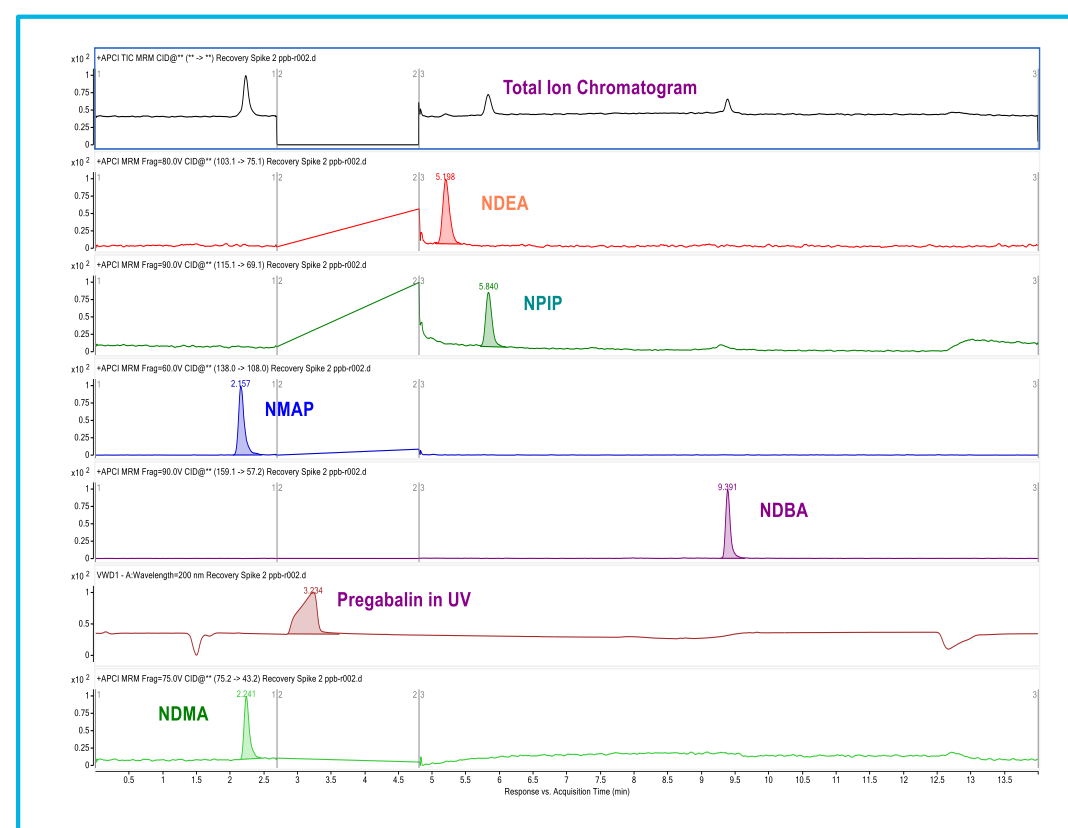


Figure 2: Representative EIC of NDEA, NPIP, NMAP, NDBA and NDMA at 0.1 ppm conc. using 20mg/mL of Pregabalin API.

The table below presents the reproducibility data at 1ng/mL standard concentration for 7 replicates including bracketing standard (# 7) showing excellent area RSD % of < 2 % for each 5 nitrosamine impurities.

Area % RSD at 1ng/mL

#	NDMA	NMA P	NDEA	NPIP	NDBA
1	102233	5515	7590	42752	23307
2	101469	5388	7720	42832	23278
3	102858	5372	7701	42798	23269
4	102147	5577	7832	42969	23224
5	103343	5382	7784	43041	23133
6	102921	5347	7705	43029	23957
7	102268	5301	7692	43226	24152
Average	102462.7	5411.	7717.	42949	23474
SD	621.69	97.86	76.24	166.9	404.1
RSD (%)	0.61	1.81	0.99	0.39	1.72

Table 5: Peak area % RSD for 7 replicates at 1ng/mL

Method Performance Characterization

Figure 3 shows the calibration curves for the standard calibration of all 5 nitrosamines. The relevant calibration range for NDEA, NPIP, NMAP, NDBA and NDMA is from 0.1 ng/mL to 100 ng/mL. The coefficient of regression achieved for each nitrosamine is > 0.990 .

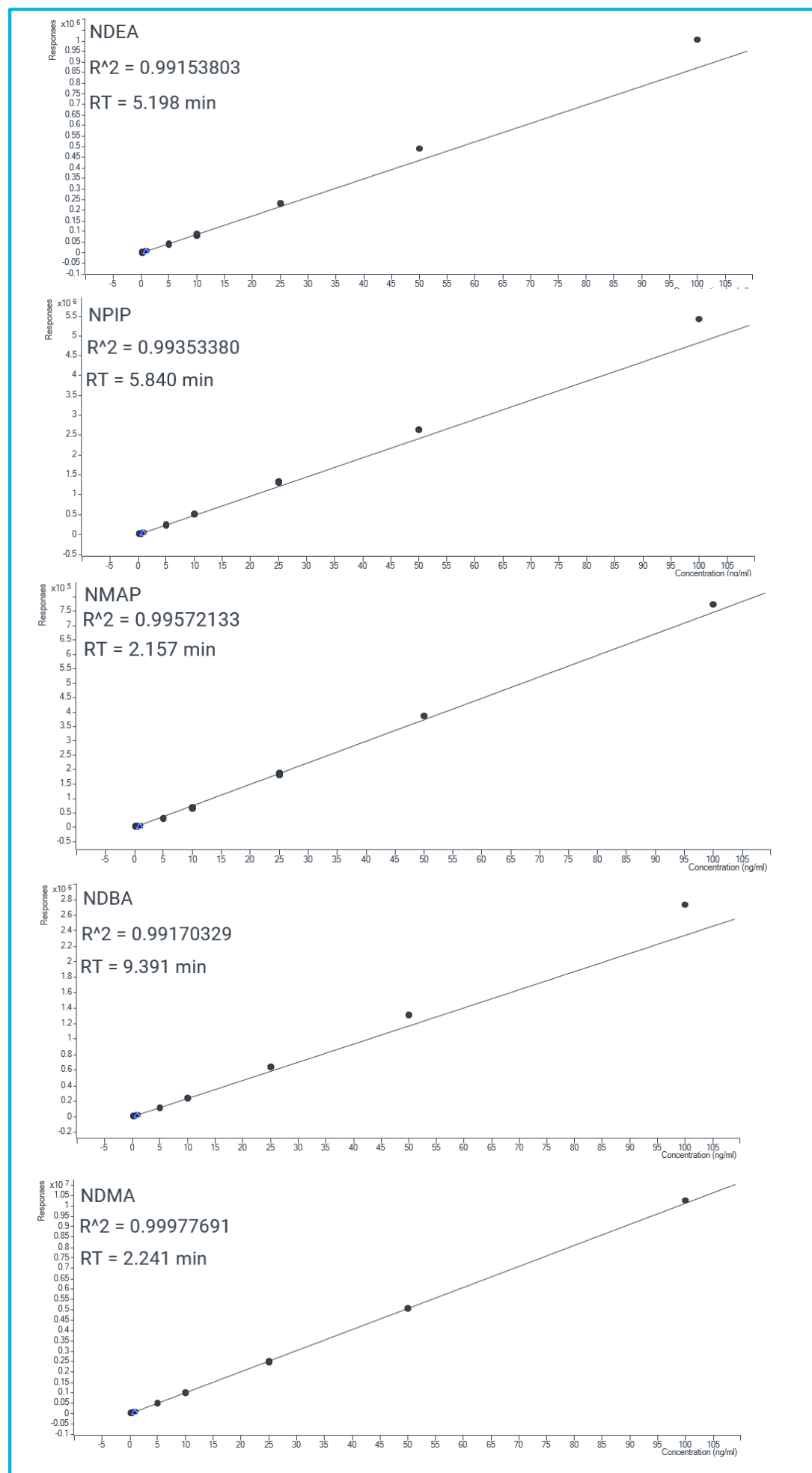


Figure 3: Calibration curves of all 5 nitrosamines

Recovery Study

The recovery experiment shows excellent recovery of $\pm 20\%$ of the spiked concentrations. In this experiment recovery study was performed at 5 different concentration levels. This recovery data makes the method ready for batch analysis of Pregabalin drug substance.

Spike Conc. (ng/mL)	Recovery %				
	NDEA	NPIP	NMAP	NDBA	NDMA
0.5	102.2	91.1	94.99	102.96	102.7
1	98.86	93.3	115	107.45	94.7
2	88.7	96.9	100.5	94.62	105.8
5	93.11	95.89	100.3	104.12	103
10	86.1	96.11	105.4	97.99	97.6

Table 6: Recovery data in Pregabalin drug substance

Conclusions

- The method provides excellent reproducibility at USFDA defined LOQ concentrations levels as it shows excellent reproducibility of $< 2\%$ with bracketing standard included in the calculations.
- The method is a ready to use method for analysis of Pregabalin drug substance batches as the method shows excellent recovery.
- As Pregabalin drug substance peak is chromatographically well separated from nitrosamine peaks so there is no contamination to mass spectrometer due to high concentration API.

References

Poster Reprint

ASMS 2020

ThP586

Development of a simple, selective and sensitive bioanalytical method for the analysis of Donepezil in plasma using LC-ESI-MS/MS

Chidella Kartheek Srinivas¹; Prasanth
Joseph¹; Arun Kumar P¹; Saikat Banerjee¹;
Samir Vyas²

¹Agilent Technologies, BENGALURU, India;

²Agilent Technologies, Mumbai, India

Introduction

Donepezil is an FDA approved drug used to treat dementia in Alzheimer's patients. It is available in generic form. It belongs to a class of cholinesterase inhibitors and comes as a tablet that dissolves quickly in the mouth.

In this work, we used a triple quadrupole LC-MS/MS equipped with an electrospray ionization source operated in positive mode to quantify Donepezil in human plasma samples. The developed method consisting of a simple liquid-liquid extraction protocol and multiple reaction monitoring-based quantification was selective and highly reproducible. Assay performance was within current pharmaceutical and regulatory guidelines.



Figure 1. 1290 Infinity II UHPLC coupled to a 6470 LC/TQ

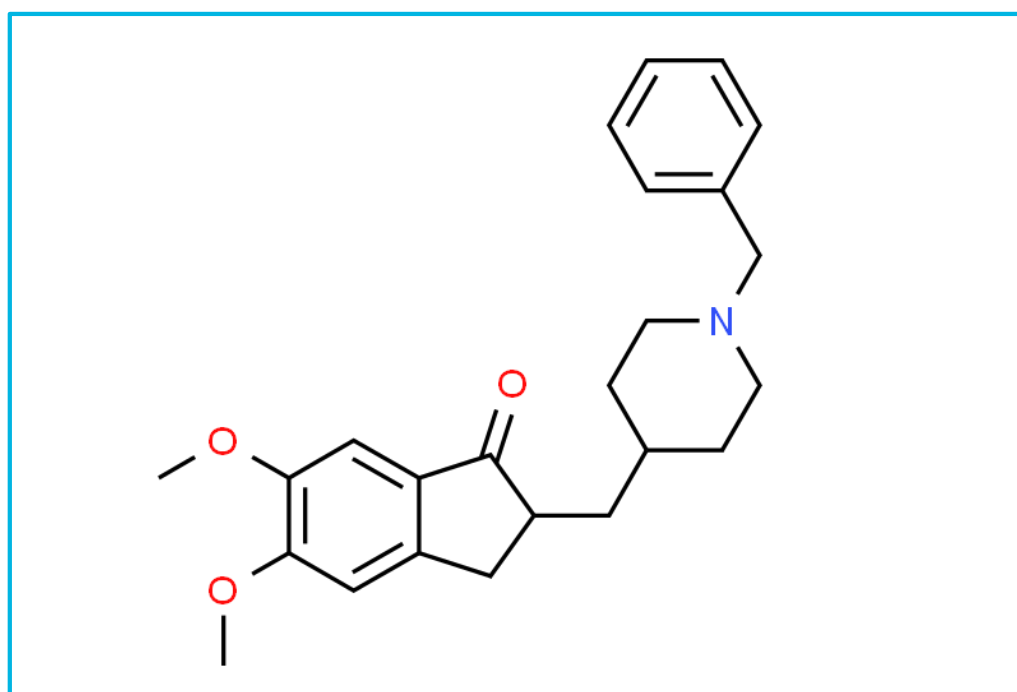


Figure 2. Chemical structure of Donepezil

Experimental

Sample Preparation

1. 0.25 ml plasma spiked with the drug (2% spiking)
2. Extracted with 1.5 ml of Ethyl Acetate: n-hexane (90:10)
3. Vortex for 5 minutes
4. Centrifuge at 5000 rpm for 5 minutes.
5. Supernatant is evaporated to dryness at 45 degrees in SpeedVac.
6. Reconstitute with 0.25 ml of mobile phase.

Figure 3. Liquid- Liquid extraction protocol for the sample preparation of Donepezil

Chromatographic conditions

Analytical column	SB C18 (100 X3.0, 1.8um)
Flow rate	0.4 ml/min
Mobile phase A	5mM ammonium formate with 0.1% formic acid
Mobile phase B	Acetonitrile
Injection volume	2 µl
Elution	Isocratic
Mobile phase ratio	20:80
Needle wash solvent	Acetonitrile: Water (60:40)

Source parameters

Ionisation: ESI	Polarity: Positive
Sheath gas temp: 275°C	Sheath gas flow: 8l/min
Drying gas temp: 200°C	Drying gas flow: 8l/min
Cap Voltage: 3500V	Nozzle voltage: 0
Nebuliser pressure: 40 psi	

Method development

The method was developed on an Agilent G6470 QQQ LC-MS/MS equipped with an Electrospray ionization source. Both Donepezil and the internal standard Donepezil-D7 were ionized in positive ionization mode.

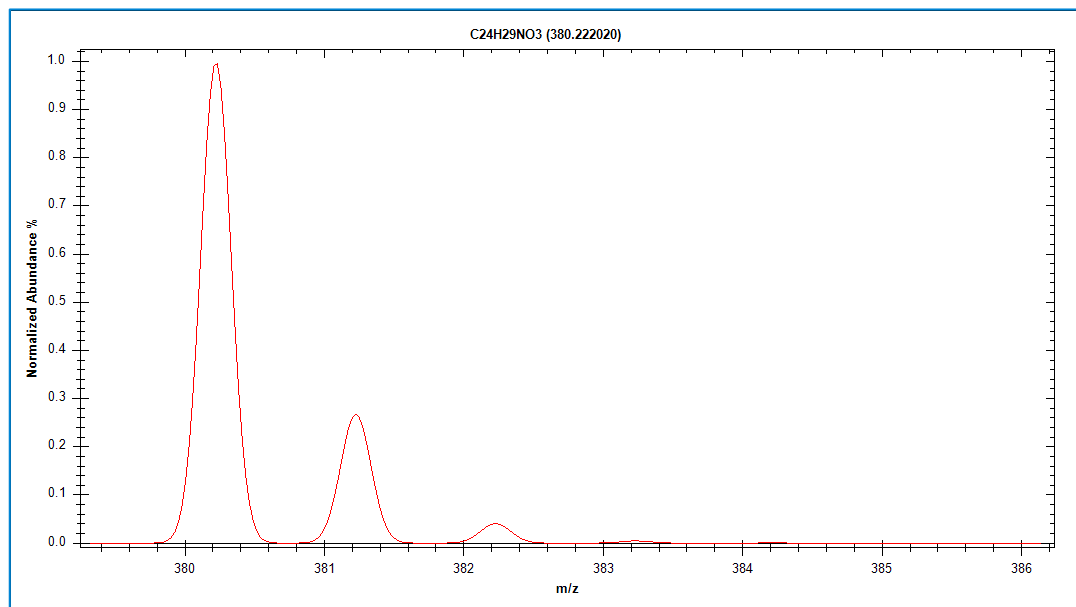


Figure 4. Isotopic pattern of Donepezil in Positive mode

Compound ID	Precursor ion m/z	Product ion m/z	Collision energy
Donepezil	380.2	91	40
Donepezil-D7	387.3	98	40

Table 1. MRM parameters for Donepezil in ESI positive mode

The calibration curve in the range of 0.1 ng/ml to 100 ng/ml was linear with weighing factor = $1/X^2$. The regression coefficient for relative response versus relative concentration of the analyte to the internal standard was 0.9993. The accuracy of the calibration standards in the linearity curve was between 96 and 106%.

As a part of the precision and accuracy batch, triplicate injections of LLOQ, LQC, MQC and HQC were performed to calculate recovery. Average recovery at LLOQ of 0.1 ppb was 107%. Average recovery at 0.5ppb (LQC), 40ppb (MQC) and 80 ppb (HQC) were 101%, 98% and 102% respectively.

Calibration curve

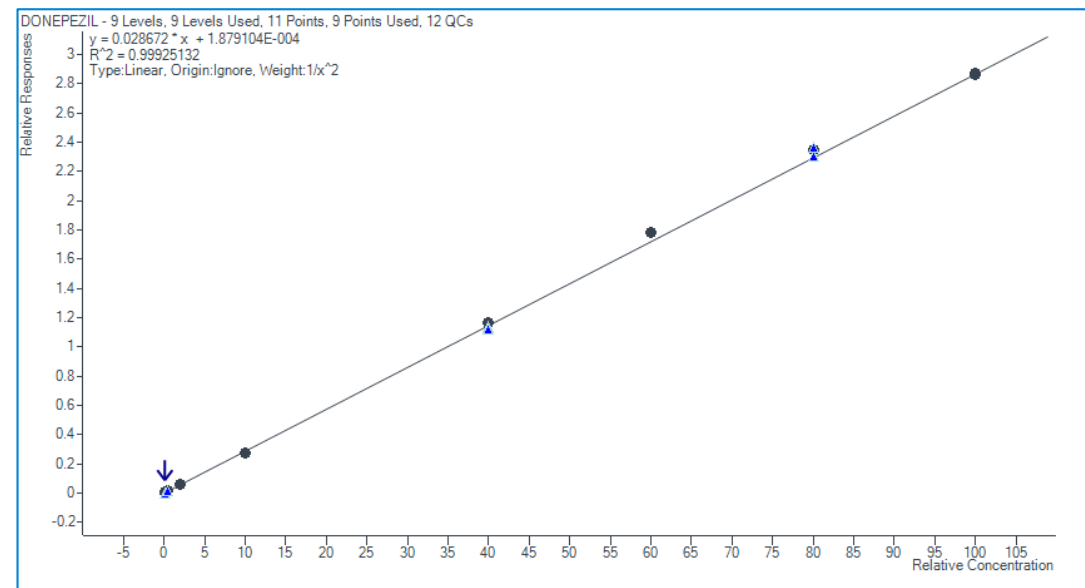


Figure 5. Calibration curve of Donepezil

Sample ID	Type	RT, min	Response	Calculated concentration	Accuracy (%)
Blank	BLANK	1.747	93		
Blank+IS	BLANK	1.747	241	0.0085	
0.1 ppb	CAL	1.747	1710	0.1058	105.8
0.2 ppb	CAL	1.747	3090	0.1993	99.7
0.5 ppb	CAL	1.747	8164	0.4928	98.6
2.0 ppb	CAL	1.747	31324	1.9417	97.1
10 ppb	CAL	1.747	156466	9.6055	96.1
40 ppb	CAL	1.747	661169	40.7788	101.9
60 ppb	CAL	1.747	1013018	62.1801	103.6
80 ppb	CAL	1.747	1333669	81.9101	102.4
100 ppb	CAL	1.747	1634651	100.0444	100
LLOQ1	QC	1.75	1959	0.1106	110.6
LLOQ2	QC	1.75	1765	0.0995	99.5
LLOQ3	QC	1.75	1960	0.1118	111.8
LQC 1	QC	1.75	9292	0.5727	114.5
LQC 2	QC	1.75	7994	0.4814	96.3
LQC 3	QC	1.75	8164	0.4731	94.6
MQC 1	QC	1.75	666329	39.5861	99
MQC 2	QC	1.75	666599	39.8187	99.5
MQC 3	QC	1.75	655234	39.138	97.8
HQC 1	QC	1.75	1335138	82.5444	103.2
HQC 2	QC	1.75	1347247	80.5089	100.6
HQC 3	QC	1.75	1319752	82.6568	103.3

Figure 6. Calibration table of Donepezil

25 injections of plasma sample prepared at the LLOQ level were carried out to evaluate the reproducibility of the response. % CV of area ratio for 25 injections was 2.5%.

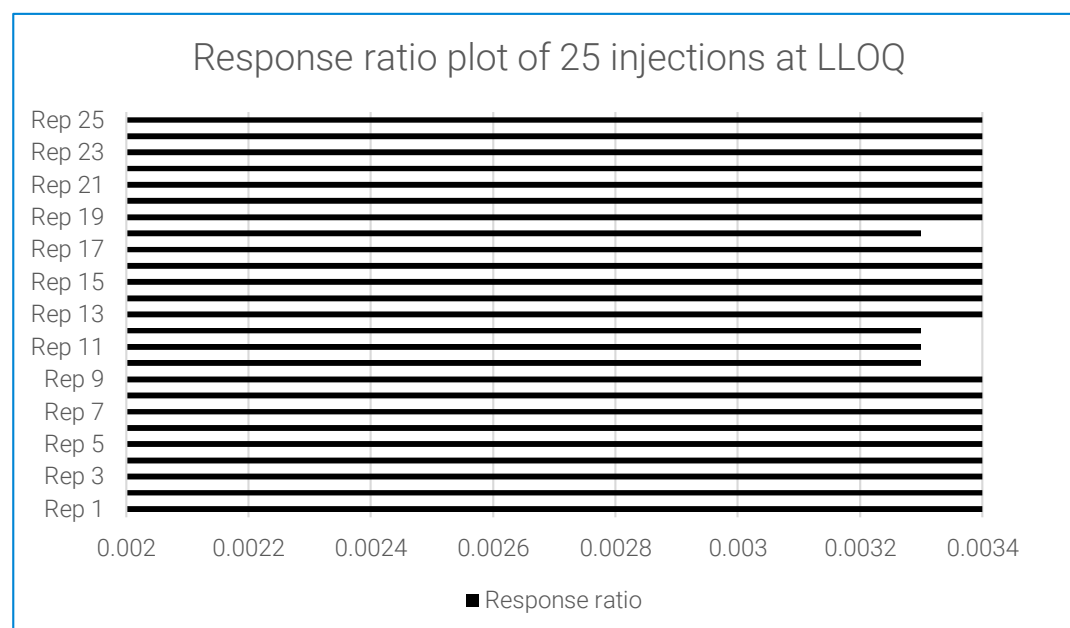


Figure 7. Reproducibility (area ratio plot) of 25 injections of Donepezil at LLOQ.

MRM chromatogram at LLOQ (0.1 ppb)

Signal to noise ratio calculated for the LLOQ level was more than 20:1, where the noise calculation was performed by the peak to peak algorithm.

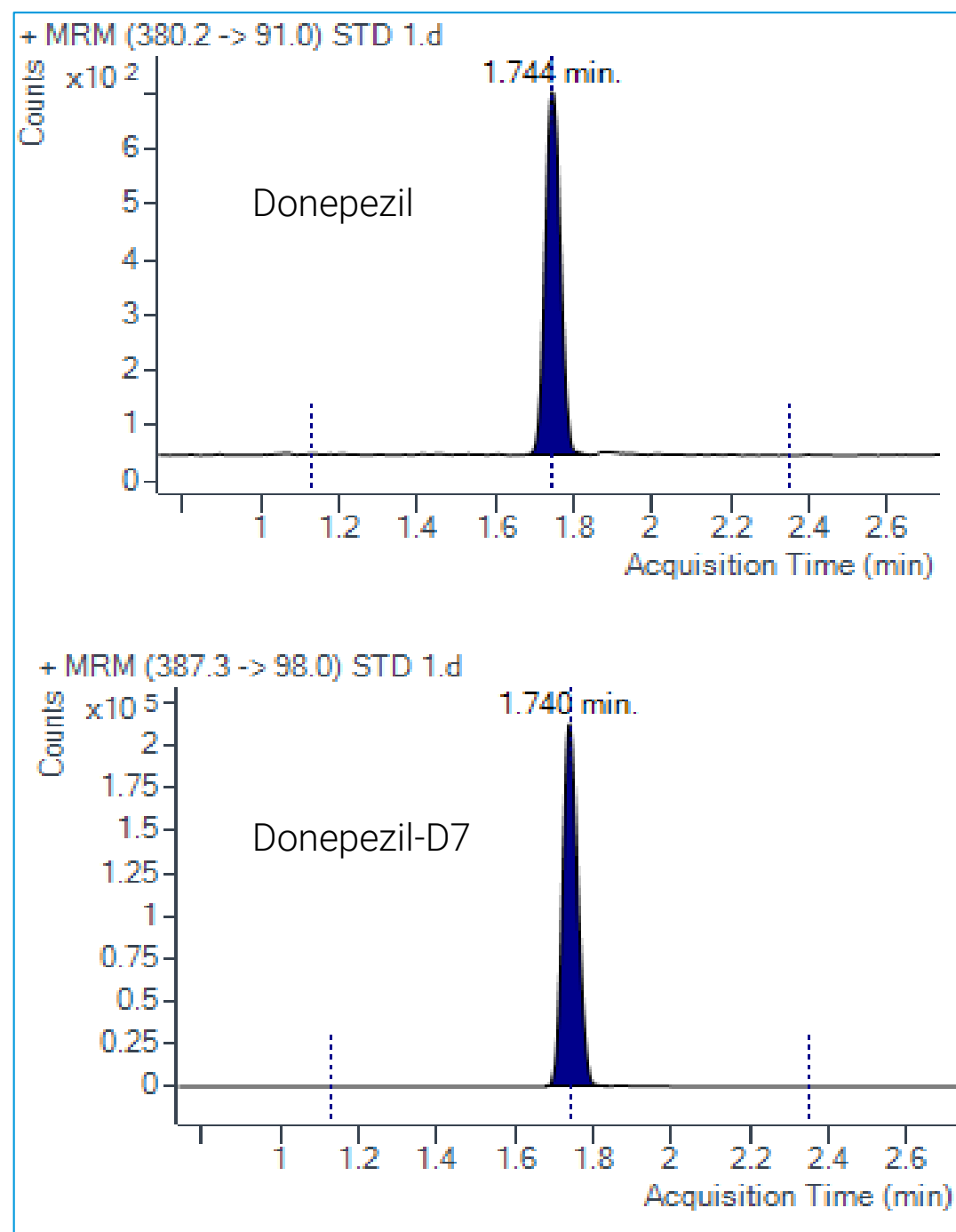


Figure 8. MRM chromatogram of Donepezil at LLOQ

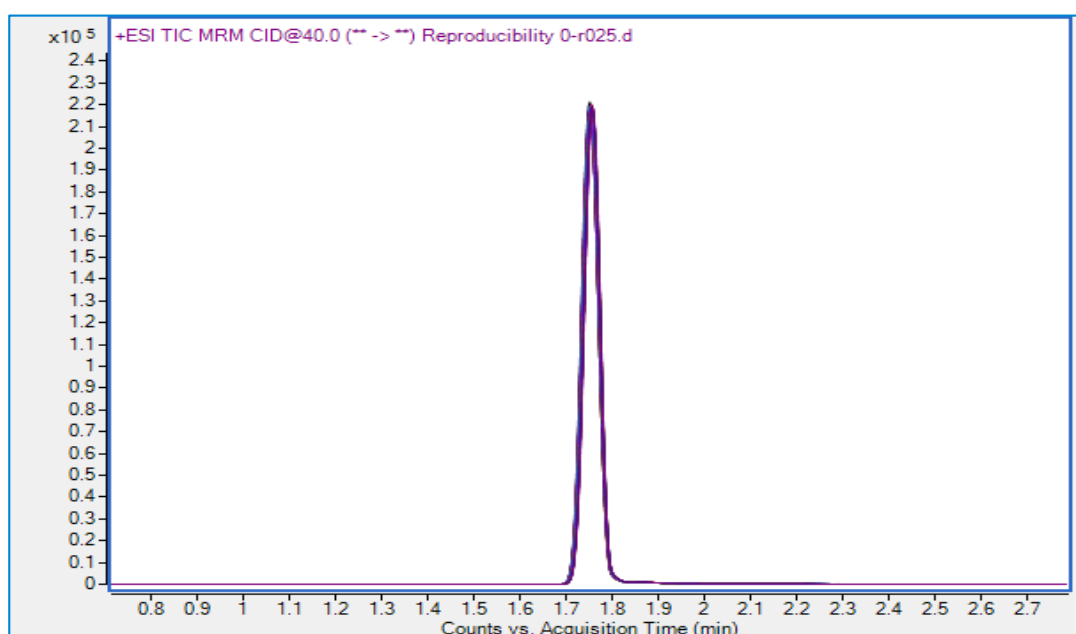


Figure 9. Overlay of 25 injections of system suitability standard of Donepezil

Recovery of QC samples

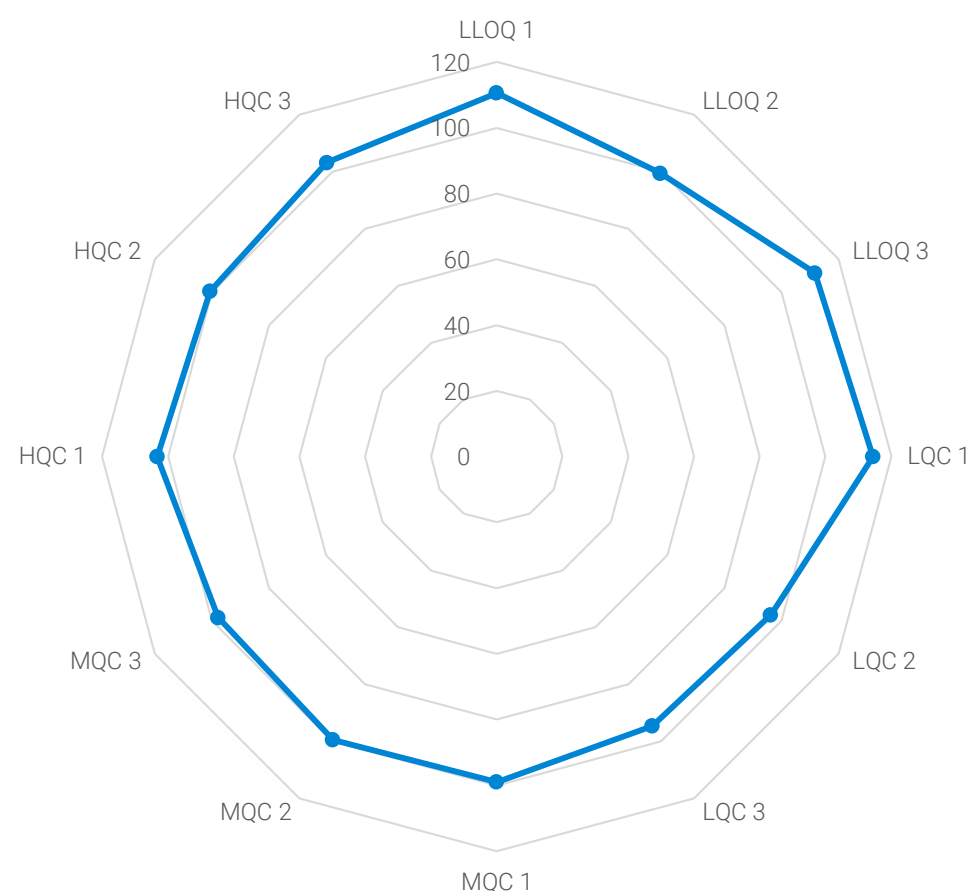


Figure 10. RADAR plot denoting recovery [%] of Donepezil in QC samples

Conclusions

- The developed MRM based method shows good sensitivity and is linear from 0.1 ng/ml to 100 ng/ml
- The developed bioanalytical method was based on a simple sample preparation that demonstrated selectivity and recovery.
- Developed method found to be highly reproducible over the precision and accuracy batch.

References

- Transl Clin Pharmacol 2018;26(2):64-72; <https://doi.org/10.12793/tcp.2018.26.2.64>
- International Journal of PharmTech Research, Vol.3, No.3, pp1667-1674, July-Sept 2011

For Research Use Only. Not for use in diagnostic procedures.

Poster Reprint

ASMS 2020

TP 129

Determination of sex hormones in human serum and plasma using a LC/TQ medical device

Suparna Mundodi, Xiaoli Dong

Agilent Technologies, Santa Clara, CA

Introduction

Sex hormones are steroid hormones synthesized from cholesterol, and many are of great clinical importance. Considerable inaccuracy of testosterone and progesterone assays via immunoassay has been well documented due to poor specificity.

Liquid chromatography coupled to tandem mass spectrometry (LC-MS/MS) has become an alternative for steroid analysis in clinical routine diagnostics due to simplified sample preparation and increased specificity and accuracy compared to immunoassays.

In this study, we demonstrate a comprehensive LC/MS method which utilizes an Agilent LC/MS medical device composed of an Infinity LC coupled with a K6460 triple quad mass spectrometer for the determination of testosterone and progesterone in human serum and plasma. Excellent robustness, precision and accuracy were achieved on this platform. Wide dynamic range and good sensitivity with this LC/MS allows accurate quantification of these sex hormones at all concentration levels in the general population.



Figure 1. Agilent K1260-6460 Class I LC/MS system

Experimental

Experimental

Sample pretreatment: Liquid-liquid extraction was performed on 200 μ L of serum (plasma) and 20 μ L of 13 C₃-testosterone (500 ng/dL) using 1000 μ L of 90:10 (v/v) hexane: ethyl acetate. The sample was vortexed and centrifuged at 4000 rpm for 10 min. The organic layer containing testosterone was pipetted off, dried under nitrogen and reconstituted with 60% methanol and water. 20 μ L is injection onto LC-MS/MS.

HPLC Conditions

Agilent K1260 Infinity HPLC series binary pump, thermostatted column compartment

Infinity HPLC Column: Agilent InfinityLab Poroshell HPH-C18, 2.1 mm \times 50 mm, 2.7 μ m

Column temperature: 40 $^{\circ}$ C

Injection Volume: 20 μ L

Autosampler Temperature: 4 $^{\circ}$ C

Needle Wash: Flush port (70%Methanol:30%Water) 3 seconds

Mobile Phase A: 0.4 mM ammonium fluoride in Water

Mobile Phase B: Methanol

Flow Rate: 0.4 mL/min

Gradient: 0min: 50%B; 3min: 98%B; 7min: 98%B; 7.1 min: 50%B.

Run time: 10 minutes

MS Conditions

K6460C triple quadrupole mass spectrometer

Ion mode: AJS Positive Mode

Gas Temperature: 300 $^{\circ}$ C

Gas Flow: 10 L/min

Nebulizer: 45 psi

Sheath Gas Temperature: 350 $^{\circ}$ C

Sheath Gas Flow: 11 L/min

Capillary Voltage: 3500V

Nozzle Voltage: 1500V

Q1/Q2 Resolution: 0.7 FWHM/0.7 FWHM

Dwell time: 50 msec

Delta EMV: +200V

Testosterone MRM: 289.2>97.0;
289.2>109.0

Progesterone MRM: 315.3>109.2

Testosterone- 13 C₃ MRM: 292.2>100.1

Linearity

Linearity in both serum and plasma were investigated. Greater than three orders of dynamic range was achieved.

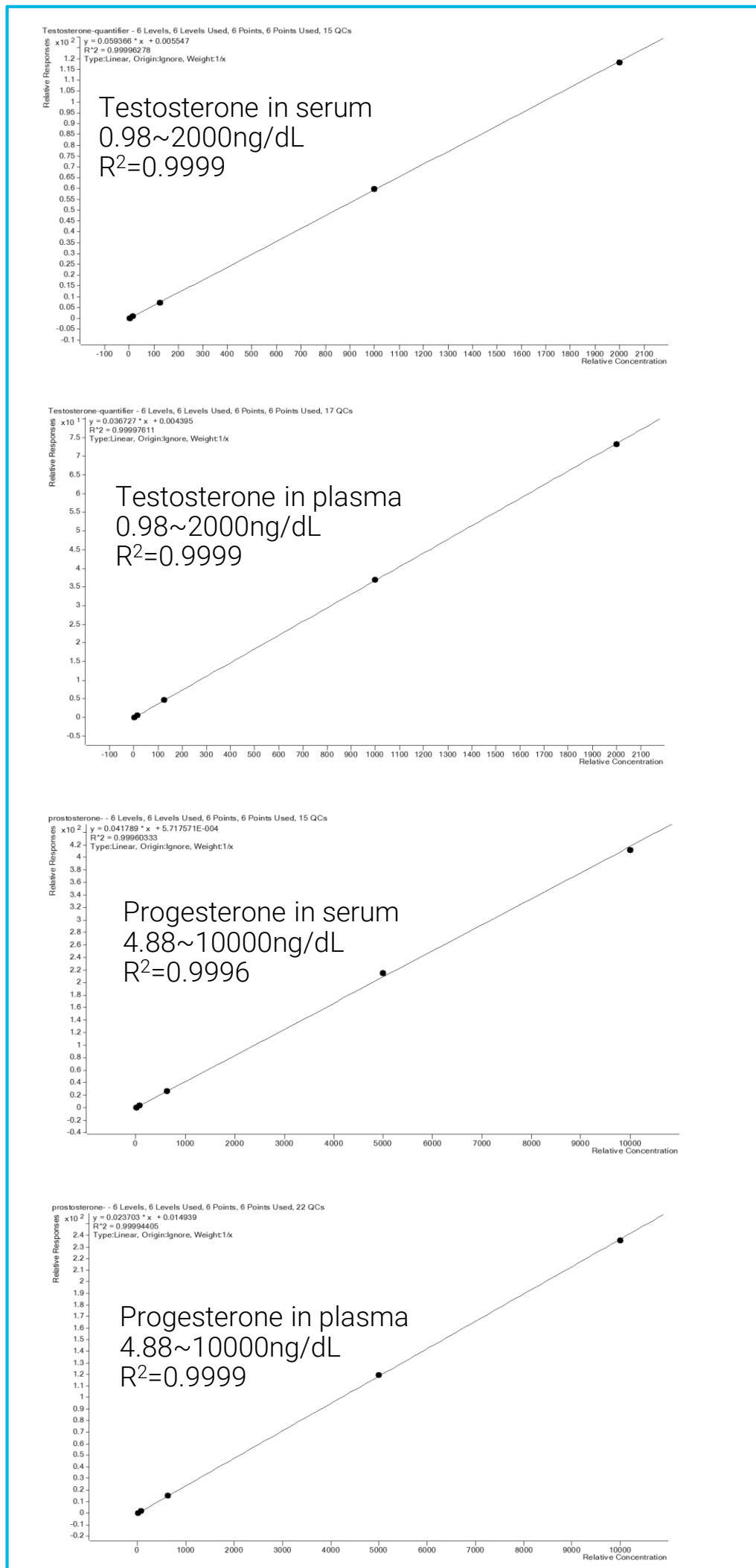
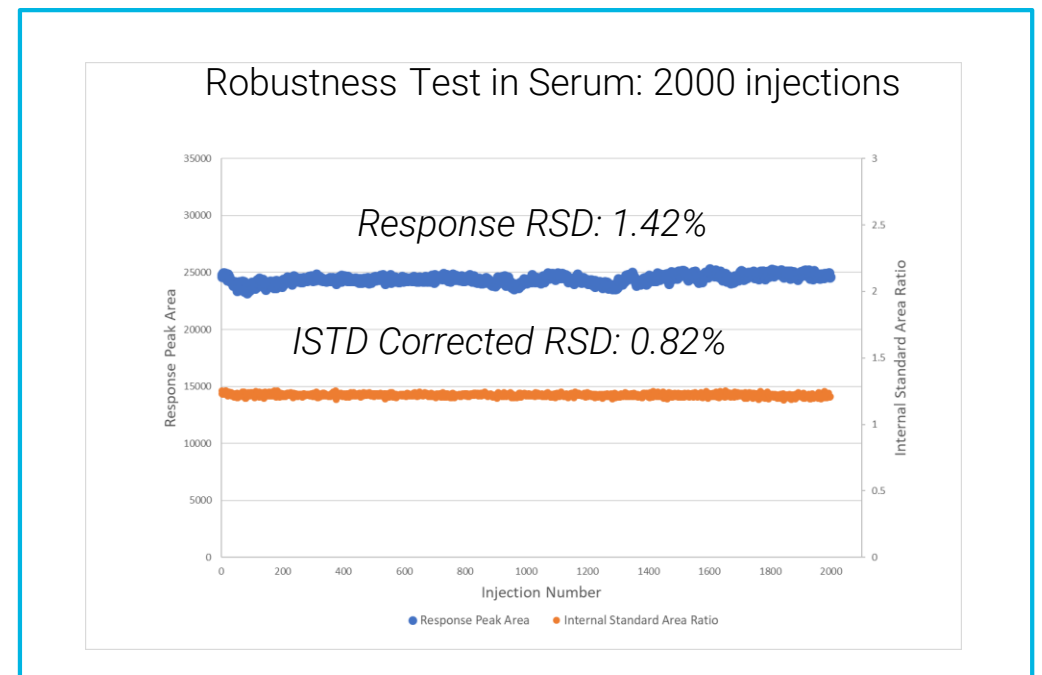


Figure 2. Calibration Curves. Weighting of 1/x was applied.

Robustness

2000 consecutive injections of testosterone in serum was done. Very low response RSD value at 1.42% and ISTD corrected RSD at 0.82% were obtained which demonstrates the excellent robustness of this LC/MS system.



Sensitivity

The mobile phase modifier was investigated to get better sensitivity of testosterone and progesterone. Testosterone responses were 12 fold higher in NH_4F than that in 0.1% FA while progesterone responses were improved 14 times in mobile phase with 0.4 mM NH_4F . See the results in Figure 2. Addition of NH_4F in mobile phase greatly improved the hormone sensitivity.

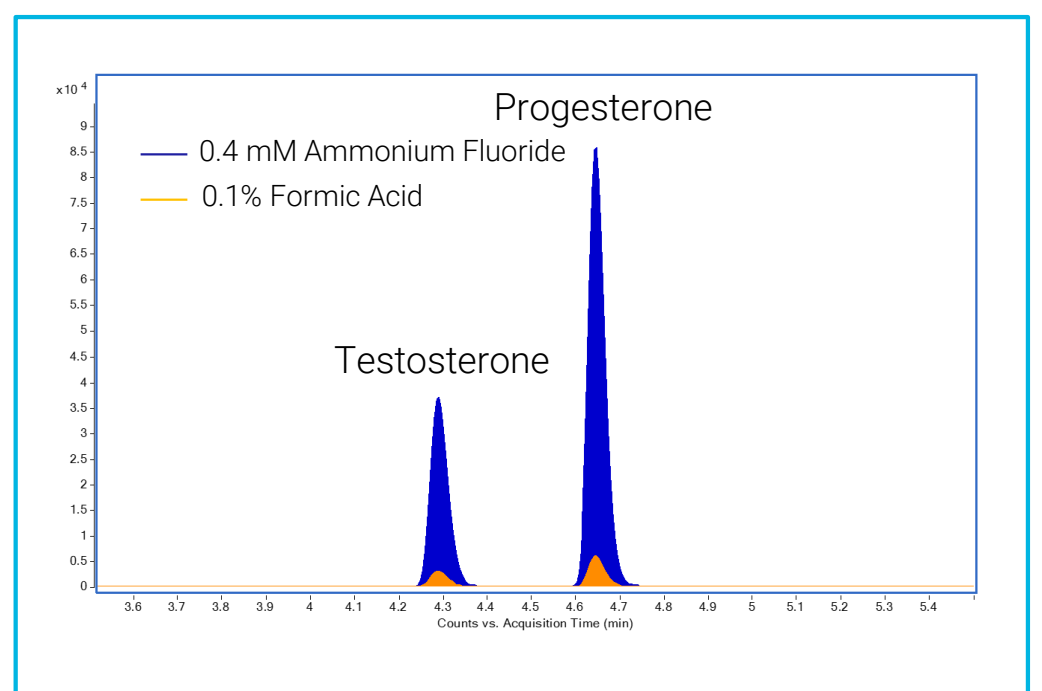


Figure 4. Response improvement using NH_4F as the mobile phase modifier instead of formic acid.

Results and Discussion

Thus, low LOQ was achieved in both serum and plasma. See result in Figure 3. Criteria for determining LOQ: $S/N > 20$, $CV < 20\%$; bias $< 20\%$.

We observed that a lower LOQ of progesterone in serum can be achieved compared to that seen in plasma, while testosterone sensitivity is comparable in both serum and plasma matrices.

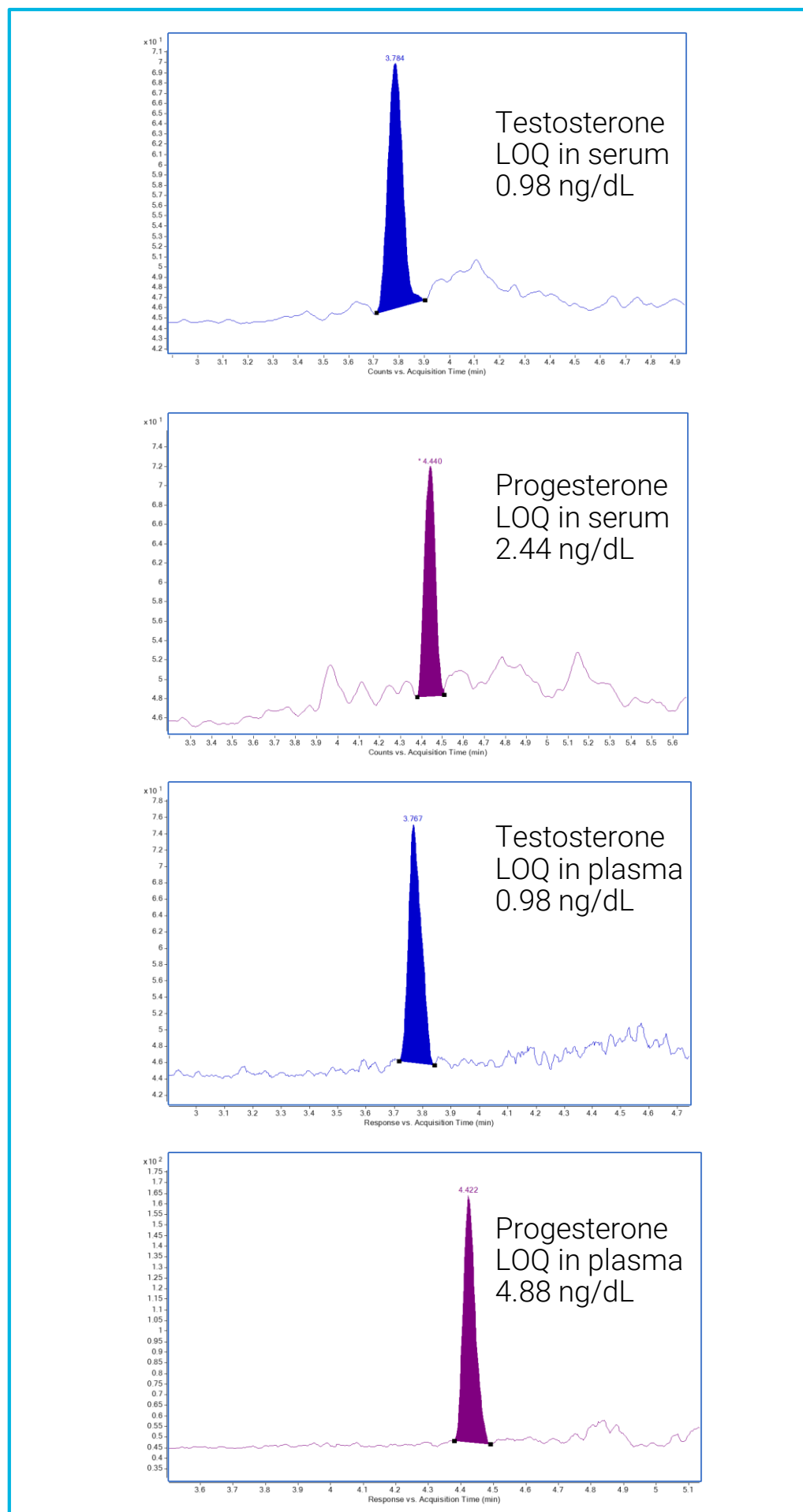


Figure 5. LOQ.(criteria: $S/N > 20$, $CV < 20\%$, bias $< 20\%$)

Precision and accuracy

Precision and accuracy testing were established by running three levels of in-house QCs in five replicates. Both serum and plasma matrix were investigated. Results are shown in Table 1 below.

Table 1. Precision and Accuracy

Hormones in Serum	QC level	Measured value (ng/dL)	Accuracy %	CV% (N=5)
Testosterone	Low	3.8	97.0	5.5
	Medium	31.4	100.2	1.6
	High	499.3	99.8	2.3
Progesterone	Low	19.4	99.4	2.2
	Medium	160.7	102.8	1.5
	High	2619.0	104.8	2.3

Hormones in Plasma	QC level	Measured value (ng/dL)	Accuracy %	CV% (N=5)
Testosterone	Low	3.9	100.8	1.1
	Medium	31.2	99.8	1.3
	High	501.4	100.3	0.8
Progesterone	Low	19.8	104.3	1.4
	Medium	158.6	101.5	1.8
	High	2646.5	105.6	0.7

The intra-assay precision was found to have a $CV\% < 10\%$ for both hormones in each matrix. The accuracy was less than 10% for all levels in either serum or plasma.

Conclusions

A robust and solid method was developed for the quantitation of testosterone and progesterone in both human serum and plasma using an Agilent LC/TQ medical device.

- Excellent linearity (>0.999) with greater than three orders of dynamic range is achieved in both matrices.
- Great robustness was observed in 2000 injections of serum testosterone sample which reached extremely low RSD at 0.82%.
- This LC/TQ platform also shows excellent accuracy and high sensitivity which is suitable for measuring sexual hormones across large reference interval in men, women and children.

For In Vitro Diagnostic Use.

Poster Reprint

ASMS 2020

TP 343

Ultra-Fast Analysis of Nitrosamines Using SPE-QQQ

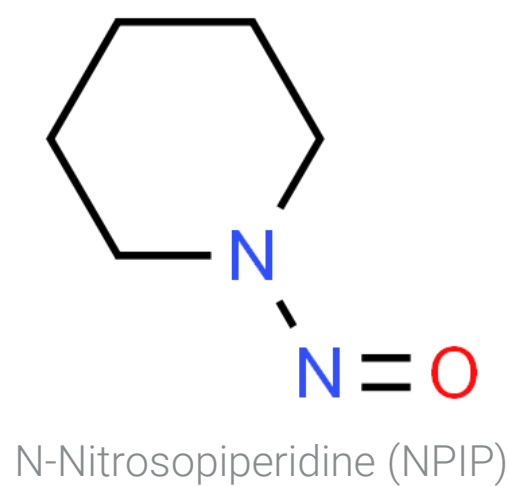
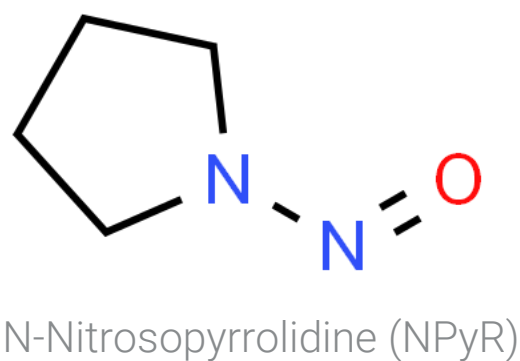
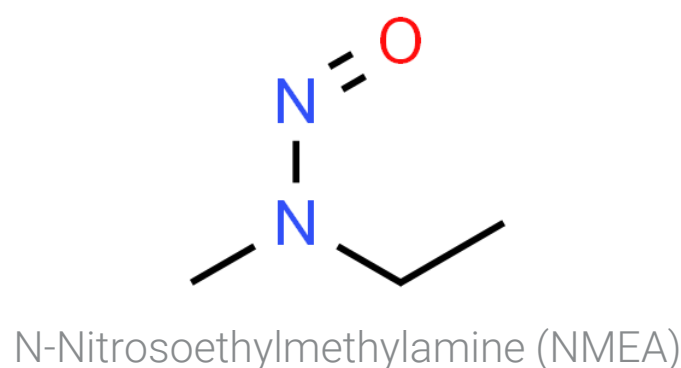
Kevin Truempi, Kevin McCann

Agilent Technologies, Santa Clara , CA

Introduction

Several highly sensitive quantitative methods have been developed for the analysis of nitrosamines using mass spectrometry¹. However, these methods rely on chromatographic separations that take several minutes per sample. Rapid, robust screening and quantitation of impurities is an essential analytical tool for a wide variety of laboratories. High-throughput environments must be able to perform these analyses in a way that ensures productivity, minimizes costs, and eliminates backlog. The use of Solid Phase Extraction Triple Quadrupole Mass Spectrometry (SPE-QQQ) allows for the ultra-fast analysis of samples without compromising analytical fidelity.

This work explores the simultaneous quantitation of a panel of nitrosamines in less than 15 seconds per injection. An existing U.S. Food and Drug Administration (US FDA) analytical method² was reproduced and then additional nitrosamines were added to assess feasibility and ease of expanding the panel.



<https://www.chemspider.com/>

Figure 1. Three nitrosamines studied as proof-of-concept additions to FDA's RapidFire method for the analysis of nitrosamine impurities.

Experimental

Instrumentation

Instrumentation for the SPE-QQQ analysis consisted of a RapidFire High-Throughput Mass Spectrometry System coupled to an Ultivo Triple Quadrupole LC/MS. Online solid phase extraction (SPE) was performed using a graphitic carbon cartridge to separate target analytes from salts and any other interferences present in the samples.



Figure 2. Agilent RapidFire 400 High-Throughput Mass Spectrometry System coupled to an Agilent Ultivo triple quadrupole LC/MS

Chemicals and Reagents

Nitrosamine standards, LC/MS grade methanol, and formic acid were purchased from Sigma-Aldrich, St. Louis, MO, USA.

Method

The automated trap, wash, and elute cycle was optimized to achieve an analysis time of less than 15 seconds per injection.

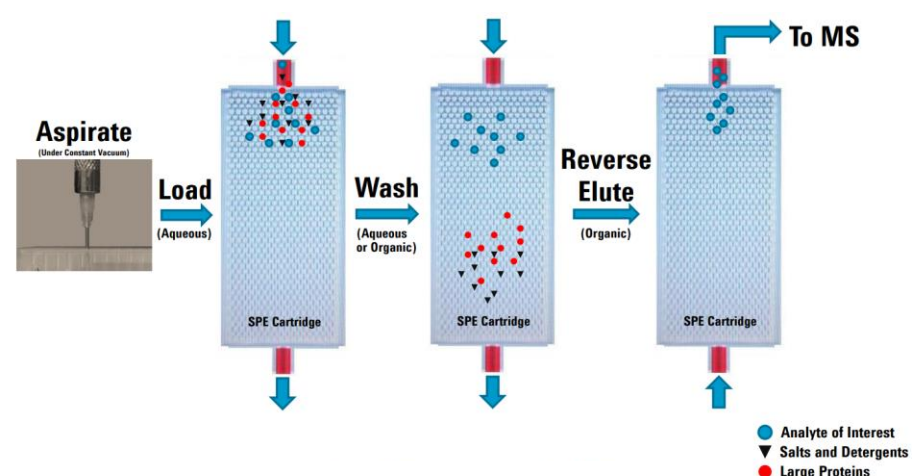


Figure 3. RapidFire injection cycle.

Instrument Settings

RapidFire Conditions

Buffer A: Water + 0.1% Formic Acid

Buffer B: Methanol + 0.1% Formic Acid

SPE Cartridge: Graphitic Carbon, Type D (G9206A)

State	Time (ms)
Aspirate	600
Load/Wash	2000
Elution	7000
Re-Equilibrate	2000

Ultivo Conditions

Parameter	Value
Ion Mode	APCI
Polarity	Positive
Drying Gas Temp	300 °C
Drying Gas Flow	6 L/min
Nebulizer	55 psi
APCI Heater	350 °C
APCI Needle	4 μ A
Capillary Voltage	3000 V

Results and Discussion

Ultra-Fast Data Acquisition

Injections were made at a rate of approximately 12.5 seconds per sample while data was acquired by triple quadrupole mass spectrometry. Figure 4 shows 72 injections acquired in under 15 minutes; several blanks were run between calibration levels to assess carryover.

Reproducible and Accurate Results

Triplicate injections of each calibrator demonstrated excellent reproducibility. Coefficients of variation range from 4.5 to 9.0% for NPIP (Figure 4) and are representative of all analytes. Excellent linearity is also observed, with R^2 ranging from 0.997 to 0.999 (Figure 5).

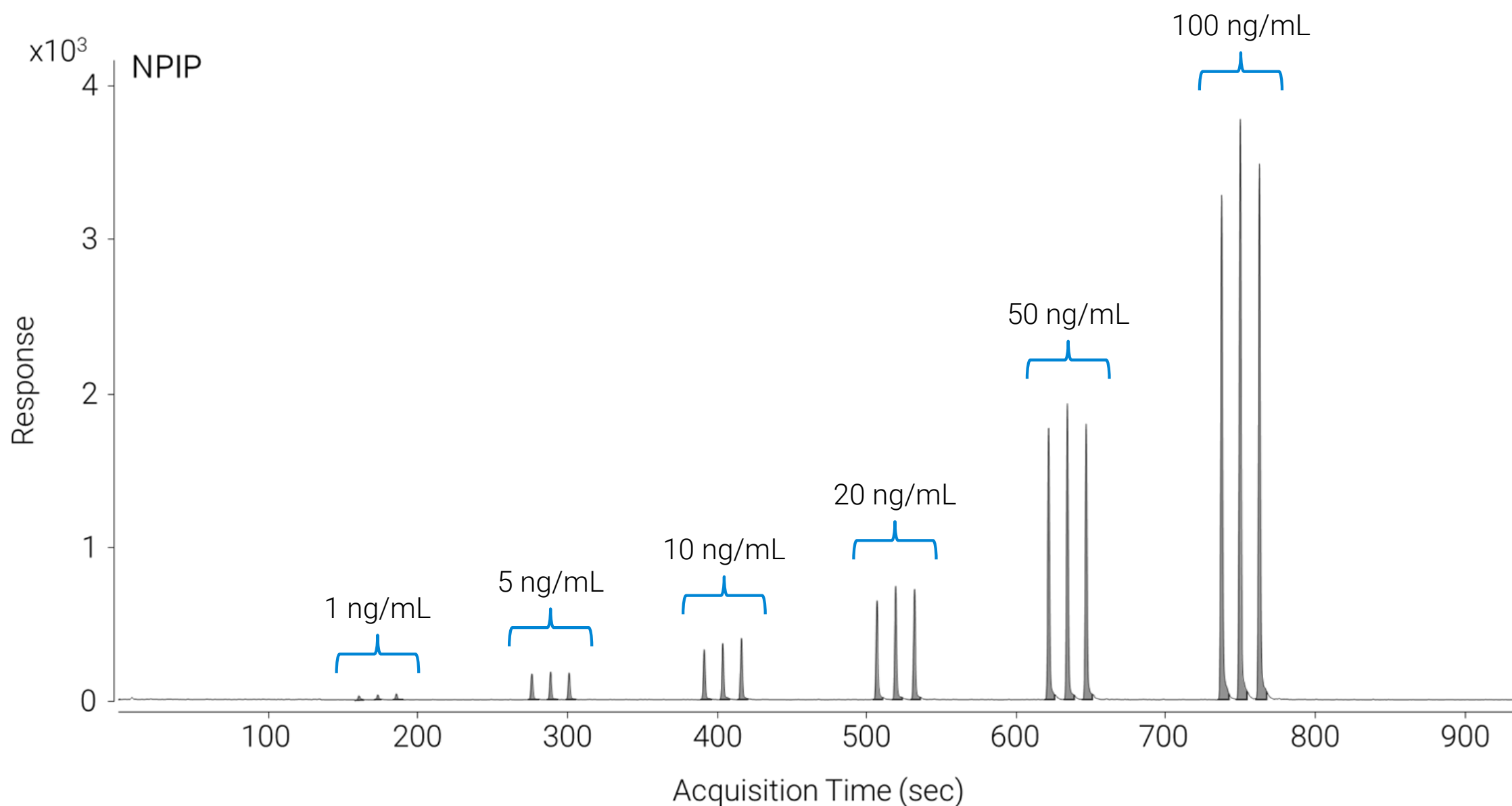


Figure 4. Triplicate injections of a 6-point calibration curve for NPIP. Six blank injections were made between each calibration level to evaluate carryover.

Results and Discussion

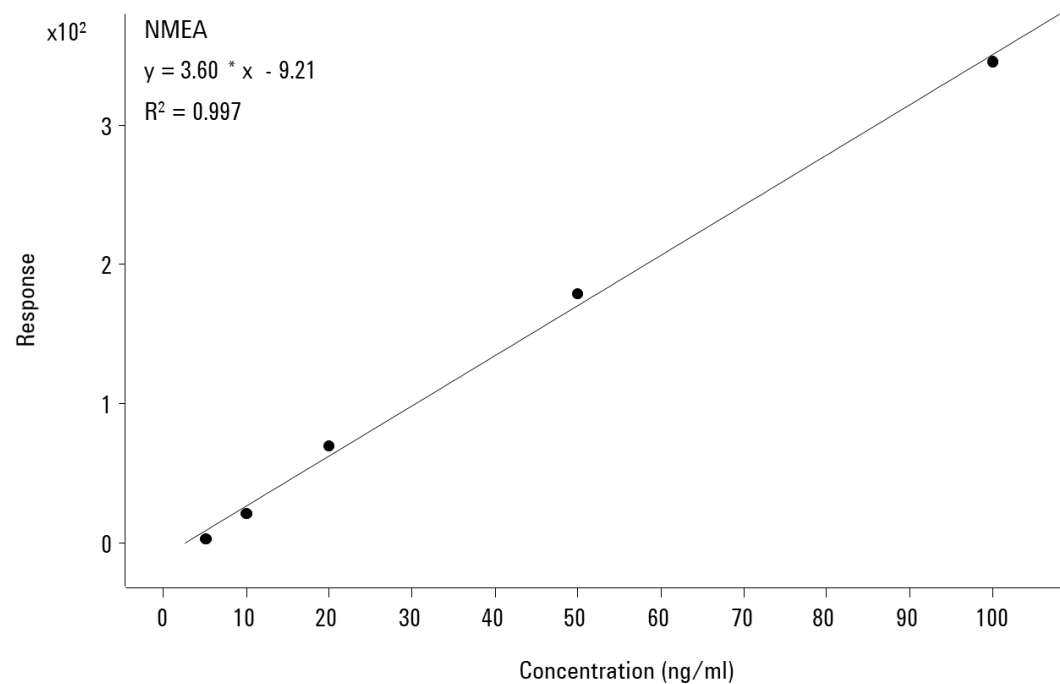
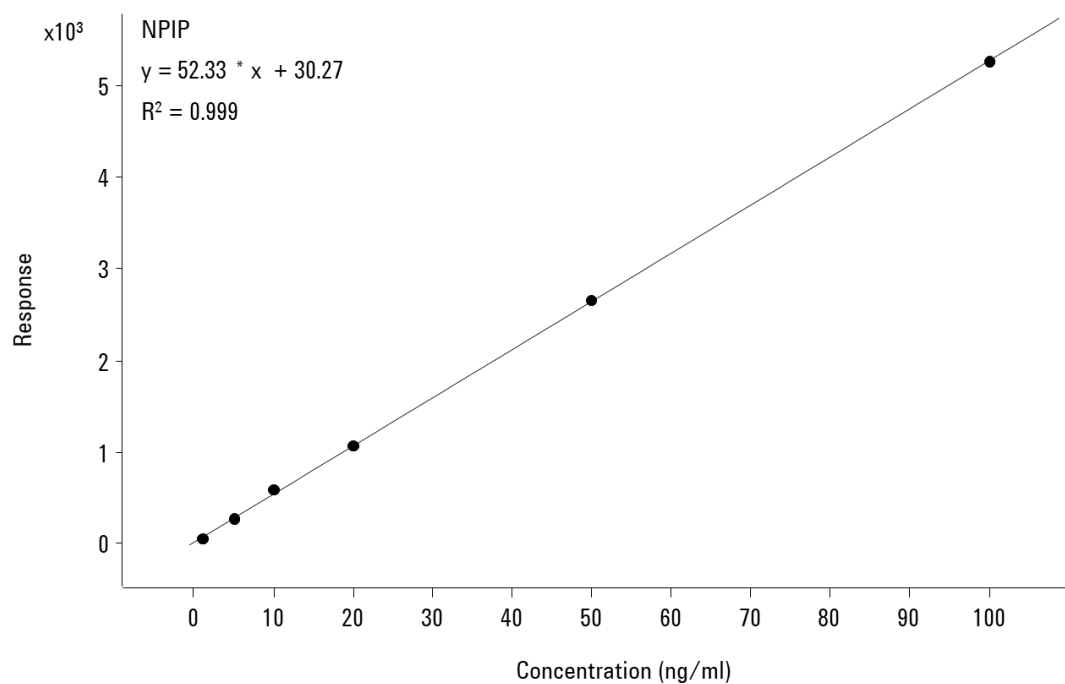
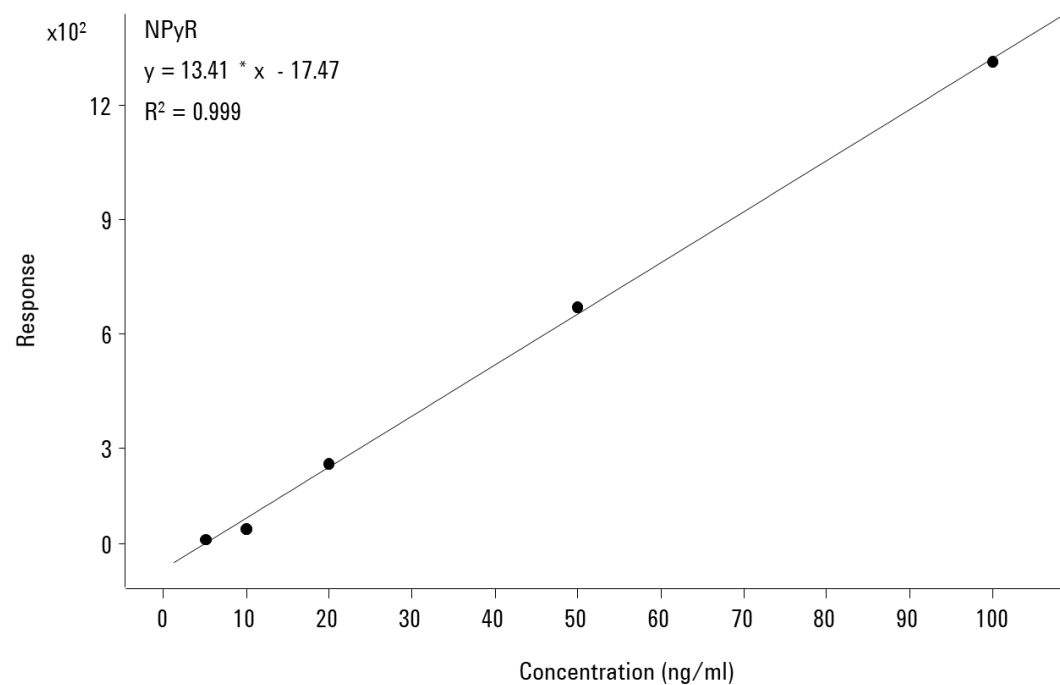
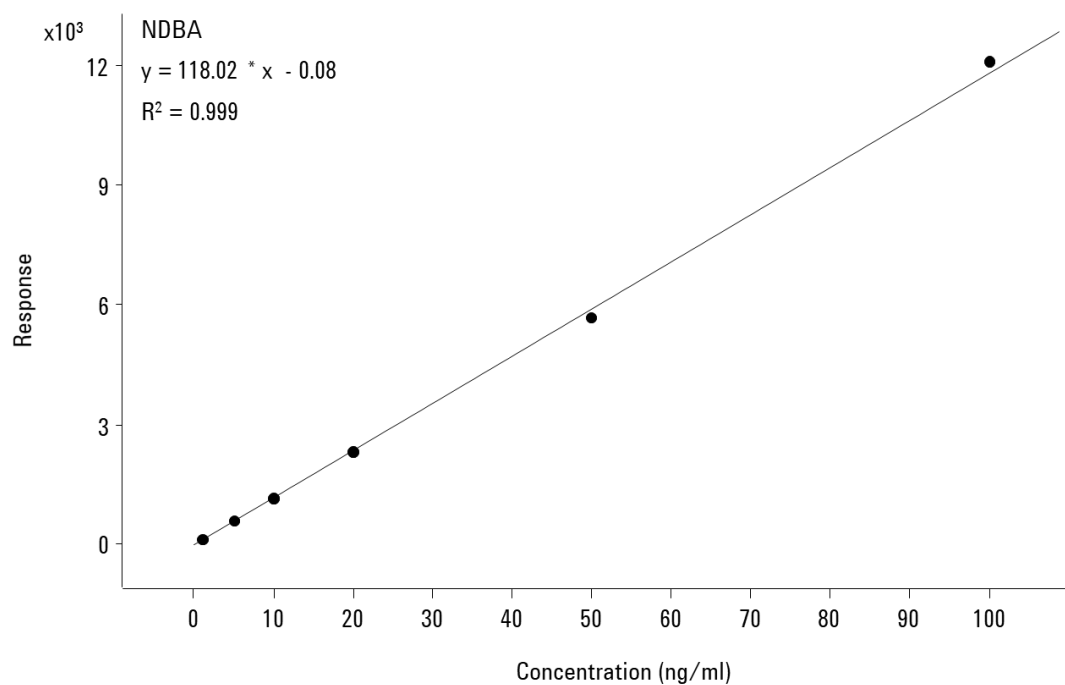


Figure 5. Calibration from 1-100 ng/mL for NDBA and NPIP. Calibration from 5-100 ng/mL for NPyR and NMEA.

Conclusions

The US FDA's method for rapid analysis of nitrosamine impurities has been replicated with consistent results. Further proof-of-concept work demonstrates the simplicity of adding additional nitrosamine analytes, without any significant method development.

References

- ¹ FDA Updates and Press Announcements on Angiotensin II Receptor Blocker (ARB) Recalls. (2019, November 13). FDA. Retrieved April 15, 2020. <https://www.fda.gov/drugs/drug-safety-and-availability/fda-updates-and-press-announcements-angiotensin-ii-receptor-blocker-arb-recalls-valsartan-losartan>
- ² Development and validation of a RapidFire-MS/MS method for screening of nitrosamine carcinogen impurities...in ARB drugs. (2019, July 24). FDA. Retrieved April 15, 2020. <https://www.fda.gov/media/125477/download>
- ³ Information about Nitrosamine Impurities in Medications. (2020, February 3). FDA. Retrieved April 15, 2020. <https://www.fda.gov/drugs/drug-safety-and-availability/information-about-nitrosamine-impurities-medications>

Poster Reprint

ASMS 2020

TP 434

High-throughput Mass Spectrometry Analysis of Synthetic Oligonucleotides: A Comparison of Data from Fast LC and RapidFire Methods

Peter Rye, Ph.D. and Yanan Yang, Ph.D.

Agilent Technologies

Introduction

Liquid chromatography (LC) and mass spectrometry (MS) play a vital role in the characterization of synthetic oligonucleotides (oligos), and the appetite for higher throughput analytical methods has increased in the past years alongside the acceleration of oligo production and use. Traditional LCMS of oligos, where separation is desired, can necessitate run times of many minutes. However, not all applications require chromatographic separation and desalting prior to MS measurement can be sufficient. This work describes and compares two methods, Fast LC and RapidFire, for the high-throughput sampling and desalting of oligos. Each method was optimized for speed on 18mers, and then characterized for performance on a range of synthetic DNA and RNA, 18 to 100mer in length.

Experimental

Fast LC Method



LC Conditions, Agilent 1290 Infinity II Binary pump, Multisampler with Dual Needles			
Column	AdvanceBio Oligo UHPLC Guard column, 1.7 μ m, 2.1 x 5mm pn: 821725-921		
Column temperature	room temperature		
Injection volume	10 μ L		
Smart Overlap	Enabled, alternating needle		
Autosampler temp	5 $^{\circ}$ C		
Needle wash	Methanol:Water 50:50		
Mobile phase	A = Water + 15 mM TEA + 400 mM HFIP B = Methanol		
Flow rate	1.75 mL/min		
Gradient program	Time (min)	Time (sec)	B (%)
	0.00	0.00	20
	0.03	1.80	20
	0.24	14.4	50
	0.25	15.0	100
	0.30	18.0	100
	0.31	18.6	20
	0.59	35.0	20
Stop time	0.60 min		
Post time	0.00 min		

6545LC/Q-TOF Conditions	
Ion Polarity	Dual AJS Negative
Data Storage	Both (Centroid and Profile)
Gas temperature	350 $^{\circ}$ C
Drying gas flow	13 L/min
Nebulizer gas	60 psi
Sheath gas temperature	350 $^{\circ}$ C
Sheath gas flow	12 L/min
Capillary voltage	3500V
Nozzle voltage	2000V
Fragmentor	200 V
Skimmer	65 V
Oct 1 RF Vpp	750 V
Mass Range	400 – 3200 m/z
Acquisition Rate	10 spectra/sec

RapidFire Method



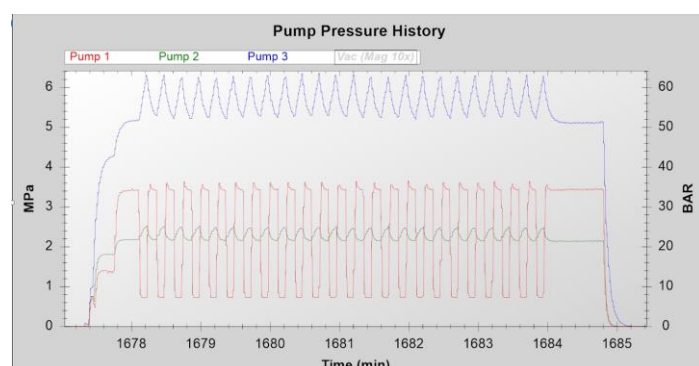
RapidFire Conditions		
Cartridge	PLRP-S, 30 μ m 1000A, 4 μ l bed volume	
Cartridge Temperature	room temperature	
Injection volume	10 μ L	
Pump 1	Water + 7.5 mM TEA + 200 mM HFIP	1.2 ml/min
Pump 2	50% Methanol + 7.5 mM TEA + 200 mM HFIP	0.6 ml/min
Pump 3	50% Methanol + 7.5 mM TEA + 200 mM HFIP	0.6 ml/min
State 1	Aspirate sample (sip sensor on)	600 msec
State 2	Load/wash (desalt)	6,000 msec
State 3	Extra wash	0 msec
State 4	Elute (inject)	6,000 msec
State 5	Reequilibrate	500 msec

6545LC/Q-TOF Conditions	
Ion Polarity	Dual AJS Negative
Data Storage	Both (Centroid and Profile)
Gas temperature	275 $^{\circ}$ C
Drying gas flow	11 L/min
Nebulizer gas	35 psi
Sheath gas temperature	325 $^{\circ}$ C
Sheath gas flow	11 L/min
Capillary voltage	3500V
Nozzle voltage	2000V
Fragmentor	200 V
Skimmer	65 V
Oct 1 RF Vpp	750 V
Mass Range	400 – 3200 m/z
Acquisition Rate	4 spectra/sec

For the Fast LC method, an Agilent 1290 Infinity II multi-sampler was equipped with dual injection needles that alternated between samples with smart overlap, providing analysis from one needle at the same time as sample draw from the other. The run time was further optimized by a fast gradient at high flow running through a guard column attached directly to the analytical nebulizer of the MS. The high flow rate for the Fast LC method was required to desalt the oligos quickly. In turn, the Fast LC acquisition rate was set to 10 spectra/sec to ensure at least 15 points across all chromatographic peaks (which were \sim 2 seconds wide, vs \sim 5 seconds for the RapidFire method). For the RapidFire method, the system performed a six second desalting (Pump 1, State 2) followed by a six second elute (Pump 3, State 4) on each sample. All resulting data were analyzed using MassHunter Bioconfirm B07.

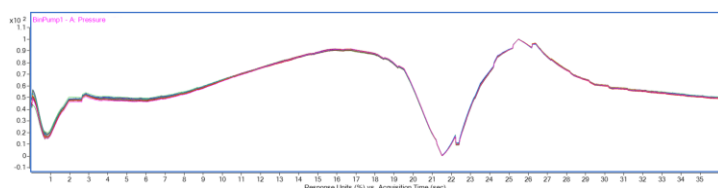
Results and Discussion

Throughput and Reproducibility – RapidFire



The throughput of the RapidFire method is determined by the sum of the five states (\sim 13 seconds, see experimental) plus \sim 1.5 seconds for plate stage motion, and was just under 15 seconds per sample. For RapidFire MS, to circumvent the delay times associated with MS acquisition start/stop, a single data file is acquired per sample set and parsed post-acquisition. This figure shows the pressure for all three RapidFire pumps as one continuous file for a set of 24 replicate injections. For each pump, the pressure peaks and valleys were steady, and in the range between 0.5 and 10 MPa, consistent with a stable method.

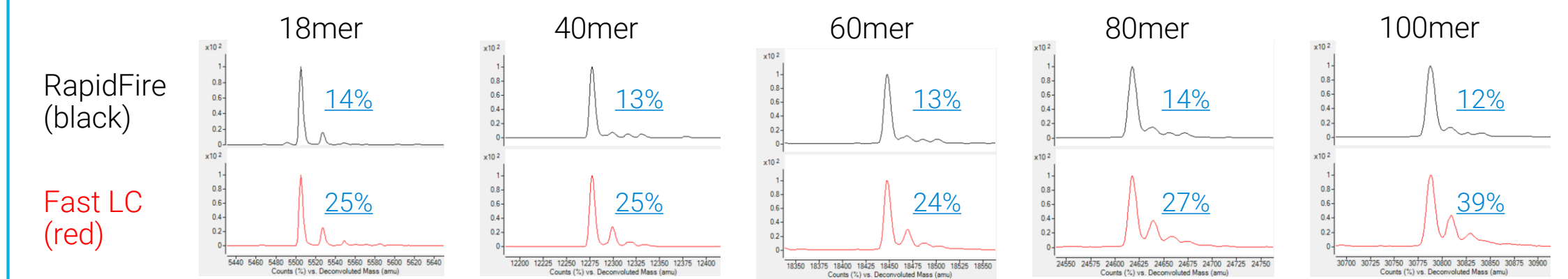
Throughput and Reproducibility – Fast LC



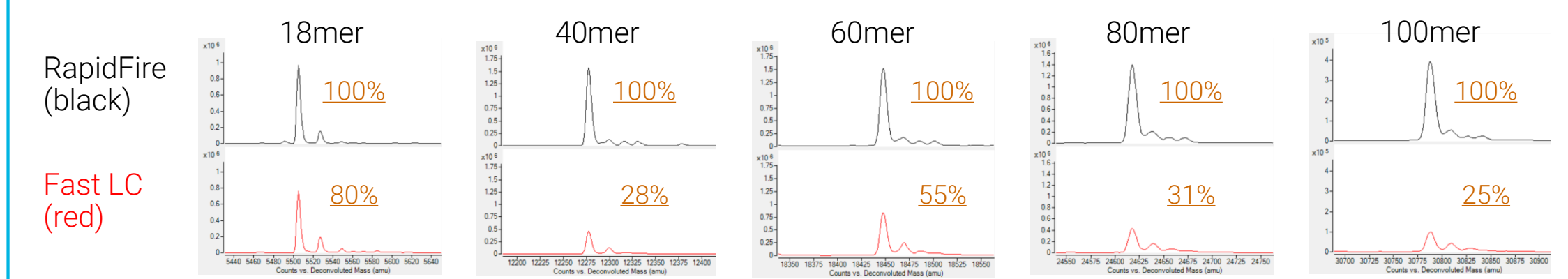
The throughput of the Fast LC method is determined by the gradient program (~35 seconds, optimized within the time of next sample draw) plus MS acquisition stop/start (~5 seconds), and was 40 seconds per sample. This figure shows the overlaid pump pressure traces from 24 injections. The traces are superimposed, revealing good gradient reproducibility.

Desalting and Signal Intensity

Scaled to largest peak in each spectrum. The percent salt adducts, relative to target peak, are in [blue](#).



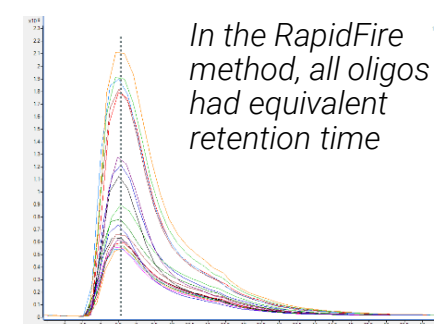
Linked Y-axis. The intensity of the target peaks for each oligo size are indicated in [brown](#).



The panels above show the deconvoluted spectra from unpurified 18, 40, 60, 80, and 100mer oligos acquired using the RapidFire method (black) and the Fast LC method (red). The top figure represents the data scaled to the largest peak in each spectrum, and shows that the RapidFire method was more efficient than Fast LC at decreasing salt adducts, which appear as peaks +22 (Na) and +38 (K) Da. The relative percent of adducts, to the target peak, for each spectrum are indicated in [blue](#). Very efficient desalting by the RapidFire method derives from the 6 second State 2 (see experimental) on the 4 ul bed volume cartridge, which results in 15 cartridge volumes of wash. The bottom figure shows the same data as on top but with the Y-axis for each oligo size linked. Comparison of the absolute peak heights shows the Fast LC method provides less abundant target MS signals, which are indicated for each oligo in [brown](#). Despite the separative characteristics of Fast LC (see below) which can decrease ion suppression and thereby increase signal, the lower signals from Fast LC are the combined result from higher pump flow rate (1.75 vs 0.6 ml/min for RapidFire), faster acquisition rate (10 vs 4 spectra/sec for RapidFire), and less efficient desalting.

Oligo Retention - RapidFire

To evaluate oligo separation by the two methods, nineteen unique DNA and RNA samples ranging from 18 to 100mer in length were measured. In the RapidFire method, all of the oligos eluted from the cartridge at the same retention time. This result was expected as the RapidFire is specifically designed to prevent separation by switching from low to high organic conditions instantly (by valving), utilizing cartridges with a small resin volume (4 ul), and eluting in the reverse direction to minimize analyte/cartridge interactions. This figure shows the overlaid total ion chromatograms (TIC) for all nineteen samples.



Oligo Retention – Fast LC

In contrast to the RapidFire method, variable retention times were observed with the Fast LC method. Figure A shows the overlaid TIC for nineteen unique DNA and RNA samples ranging from 18 to 100mer in length. For these samples, the retention times varied within a 7 second window. Figure B shows overlaid extracted ion chromatograms for a 20, 40, 60, 80, and 100mer that were injected as a single mixture, illustrating resolution of these products by a combination of chromatography and mass.

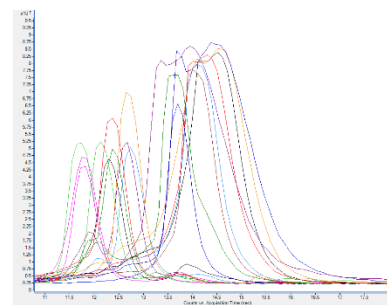


Figure A. Differential RT from the Fast LC method

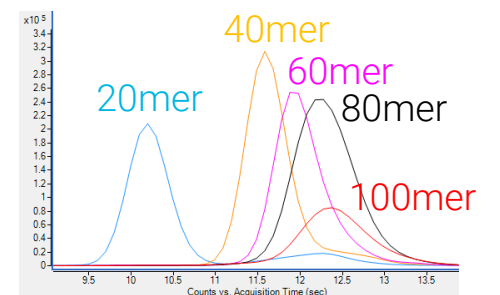


Figure B. Overlaid EIC from an oligo mixture

To evaluate the ability of the Fast LC method to separate and produce distinct deconvolution results for two oligos that were close in size, a 1:1 mixture of 18mer and 20mer was run. Figure C shows the TIC, revealing the oligos produced peaks which the software integrated separately. Figure D shows the resulting deconvoluted spectra, revealing the two species, and their respective impurities. This separation could be easily improved by small changes to the gradient program (not shown).

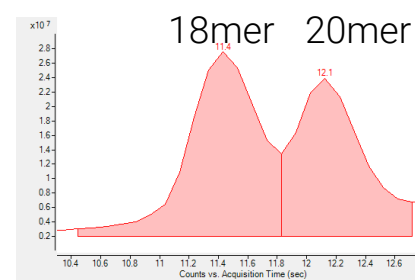


Figure C. Separation of 18 and 20mer by Fast LC

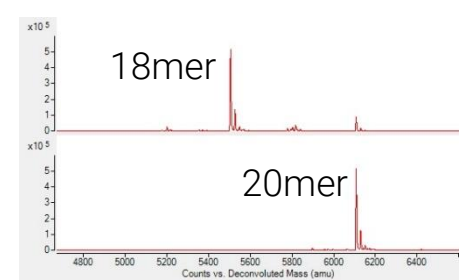
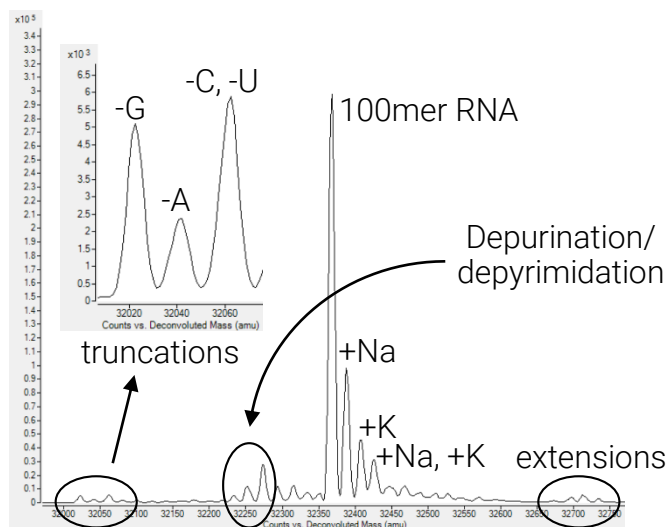


Figure D. Deconvoluted spectra showing how oligo separation can simplify data interpretation

Low Abundance Impurity Analysis



High-throughput purity assessment of oligos can be done by mass resolving the products from a single chromatographic peak. Oftentimes, there are many low abundance impurities coeluting with the highly abundant target, making MS measurement with a wide dynamic range, as well as software that can deconvolute complicated spectra, critical. To evaluate the detection of low abundance impurities in the same chromatographic peak as the main product, the RapidFire method was used to analyze a 100mer guide RNA. This figure shows that despite zero chromatographic separation, the deconvolution results reveal 100mer RNA as well as numerous impurities, many with a relative area as low as ~0.5%. As expected, this dynamic range was even better with separative/lower throughput methods (data not shown).

Conclusions

- Both the RapidFire TOF and Fast LC TOF methods produced reproducible and high quality data for synthetic oligos.
- The RapidFire method sustained a throughput of 15 seconds per sample (240 samples an hour, 5760 a day) while the Fast LC method sustained a throughput of 40 seconds per sample (90 samples an hour, 2160 a day).
- The RapidFire method desalted oligos more efficiently than Fast LC, about 2- to 3-fold as oligo size increased.
- The Fast LC method produced less intense target signal than RapidFire, from 80 to 25% as oligo size increased.
- Small changes to the Fast LC method, with some compromise to throughput, further improved its performance.
- The Fast LC method afforded some separation of oligo species, a characteristic that could simplify the interpretation of data from mixtures and could also be adjusted to balance the throughput and separation needs of the application.
- In spite their speed over separation approach, both high-throughput systems provided excellent oligo data by mass resolving large numbers of low abundance impurities.

Poster Reprint

ASMS 2020

TP 582

Monitoring Enzymatic Reactions by LC/Single Quad to Gain Insights on Reaction Mechanisms

Kyle J Covert¹; Carim Van Beek²; 1Agilent
Technologies, Santa Clara, CA; 2University of
the Pacific, Stockton, CA

Introduction

Reaction monitoring is important during a synthesis process to identify intermediates and products, as well as track the completion of a reaction. Obtaining fast and reliable results is paramount for making quick decisions. Typically, reactions are monitored using an LC method, but a single quadrupole (SQ) mass spectrometer can be added to increase productivity, sensitivity and selectivity. With the addition of a single quadrupole, co-eluting compounds can be detected separately, and ionizable compounds that do not contain a chromophore or absorb poorly can be detected. With a single quadrupole, compounds that may not have standards, such as reaction intermediates, can be identified. For this study, an enantioselective enzymatic hydrolysis of butyric ester derivatives was monitored using an LC/MSD iQ and a Diode Array Detector.

A 13-minute LC/MS method was developed with UV and mass detection. Several ions, based on the expected products, were monitored on the SQ using selected-ion-monitoring (SIM) and a scan between 100-500 m/z was collected in parallel to detect any reaction intermediates to gain insights on reaction mechanisms.



Figure 1. Agilent LC/MSD iQ coupled to a 1290 Infinity II LC System

Experimental

Instrumentation

- 1290 Infinity II Binary Pump (G7120A)
- 1290 Infinity II Vialsampler (G7129B)
- 1290 Infinity II MCT (G7116B)
- 1290 Infinity II DAD (G7117B)
- LC/MSD iQ (G6160A)

Data acquisition and analysis was performed using Agilent's OpenLab CDS 2.4 Software. OpenLab CDS provides full compliance features that support data integrity with US FDA 21 CFR Part 11, EU Annex 11, and other similar regulations.

LC Method		
Column	Poroshell 120 EC-18 2.1x100 mm, 1.9 μ m at 40°C	
Flow rate	0.500 mL/min	
Solvent A	0.1% Formic Acid in H ₂ O	
Solvent B	0.1% Formic Acid in ACN	
Gradient	Time	%B
	0.0	5
	10.0	90
	11.0	90
	11.2	5
	13.2	5 (post time)
UV Signal	210, 254, 275 nm	
Inj. Vol.	1 μ L	

Table 1. 1290 Infinity II LC Method

MS Parameters		
Scan (200 ms)	100-500 m/z	
SIM (15 ms/ion)	177 m/z	247 m/z
	194 m/z	264 m/z
	199 m/z	269 m/z
		159 m/z
Fragmentor	70 V	
Gas Temperature	325 °C	
Gas Flow	11 L/min	
Nebulizer Pressure	35 psi	
Capillary Voltage	4500 V	

Table 2. LC/MSD iQ Mixed Scan/SIM Mode Method

Enantioselective Enzymatic Hydrolysis

The reaction monitored was an enantioselective enzymatic hydrolysis as shown in Figure 2. The starting reactants are a racemic mixture from a previous step in a larger reaction. Two different enzymes (L3 and E2) were selected and reactions were monitored across several days after the start of the reaction. Aliquots at different time points were taken directly from the reaction vessel and passed through a C18-SPE cartridge with cold ether, effectively trapping the enzyme and stopping the reaction.

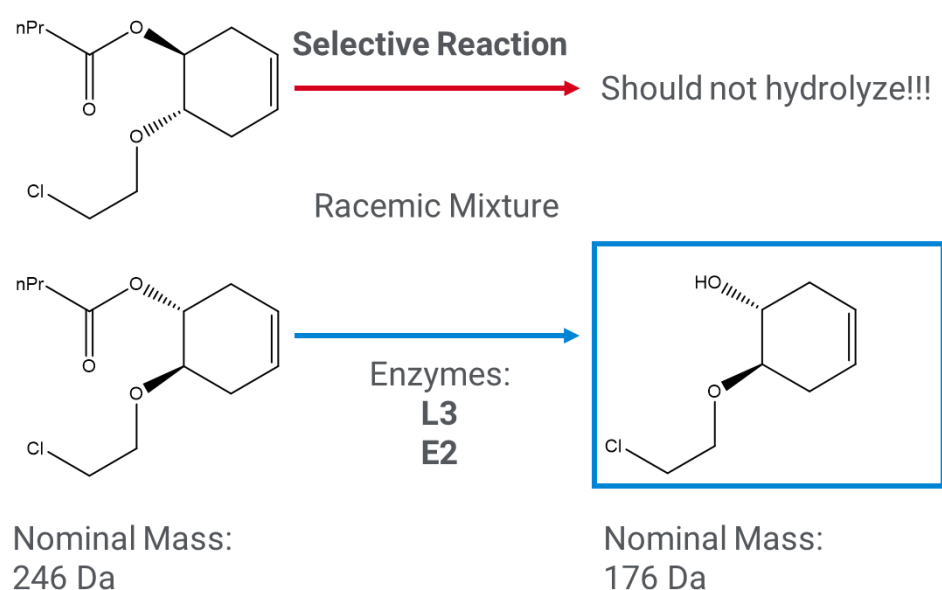


Figure 2. Enantioselective enzymatic hydrolysis reaction carried out in this study

No Compounds Detected in the UV

The reaction compounds most likely do not contain a chromophore, necessitating the need for mass detection. Figure 3 shows a UV isoabsorbance plot of the reaction at 115.5 hours. No compounds were detected across the entire UV range. The wide band is from the absorption of the organic solvent, acetonitrile. Figure 4 shows MS scan and SIM TIC chromatograms of the same sample where both the reactant and product are clearly detected, along with a number of byproducts.

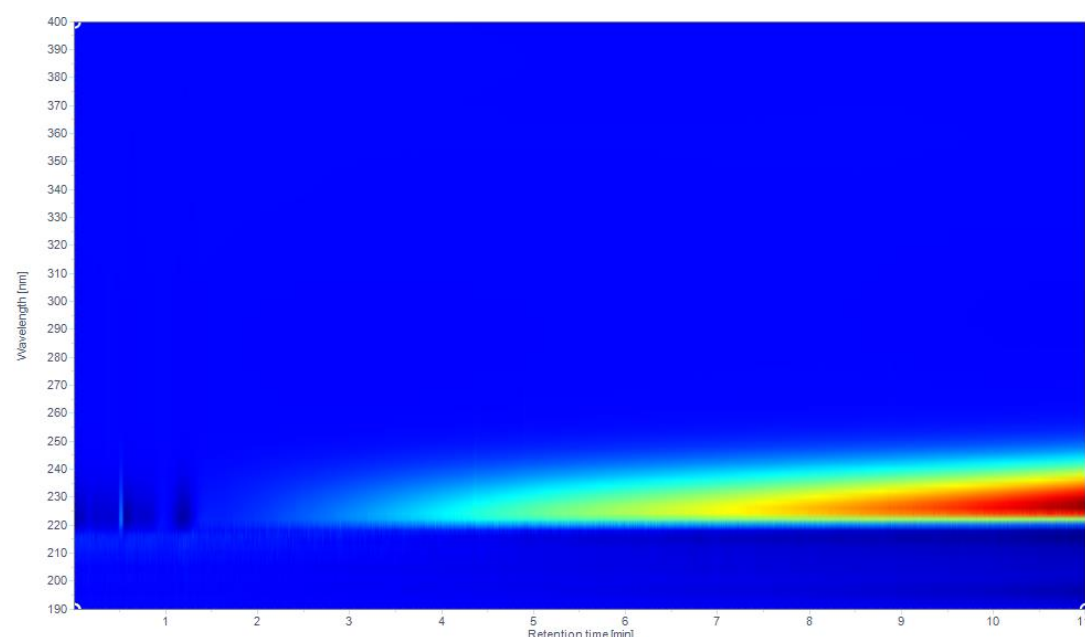


Figure 3. UV isoabsorbance plot of the reaction vessel contents after 115.5 hours

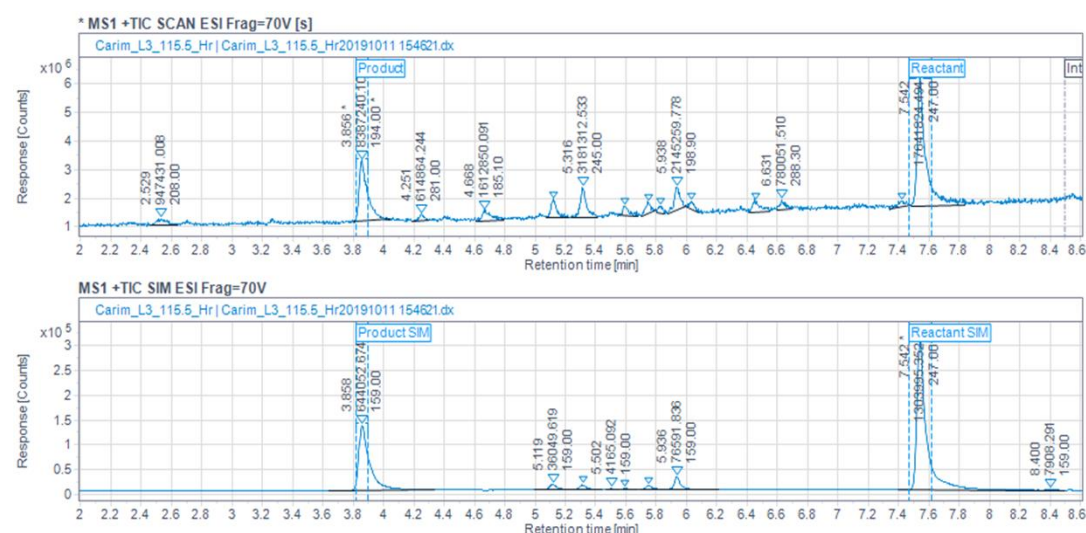


Figure 4. MS scan and SIM TIC chromatograms of the reaction vessel contents after 115.5 hours.

The reactant and product peaks were also monitored in SIM mode with an additional ion at m/z 159 which corresponds to a water loss from the product. Several peaks were detected between the product and reactant that contained m/z 159, indicating that they are coming from the reaction; possibly as intermediates to the product.

Mass Detection Can Lead to Insights in Reaction Mechanisms

Figure 5 shows MS spectra of the product and reactant peak before and after the addition of NH_4F to the mobile phase. The reactant was detected at m/z 247 $[\text{M}+\text{H}]^+$ and 269 $[\text{M}+\text{Na}]^+$ while the product was detected at m/z 194 $[\text{M}+\text{NH}_4]^+$ and 199 $[\text{M}+\text{Na}]^+$. A fragment ion was detected at m/z 159 with the product and is formed by a water loss from the unstable $[\text{M}+\text{H}]^+$ ion. This was confirmed by adding 0.5 mM of NH_4F to the aqueous phase which shows only the $[\text{M}+\text{NH}_4]^+$ ion, thus stabilizing the product.

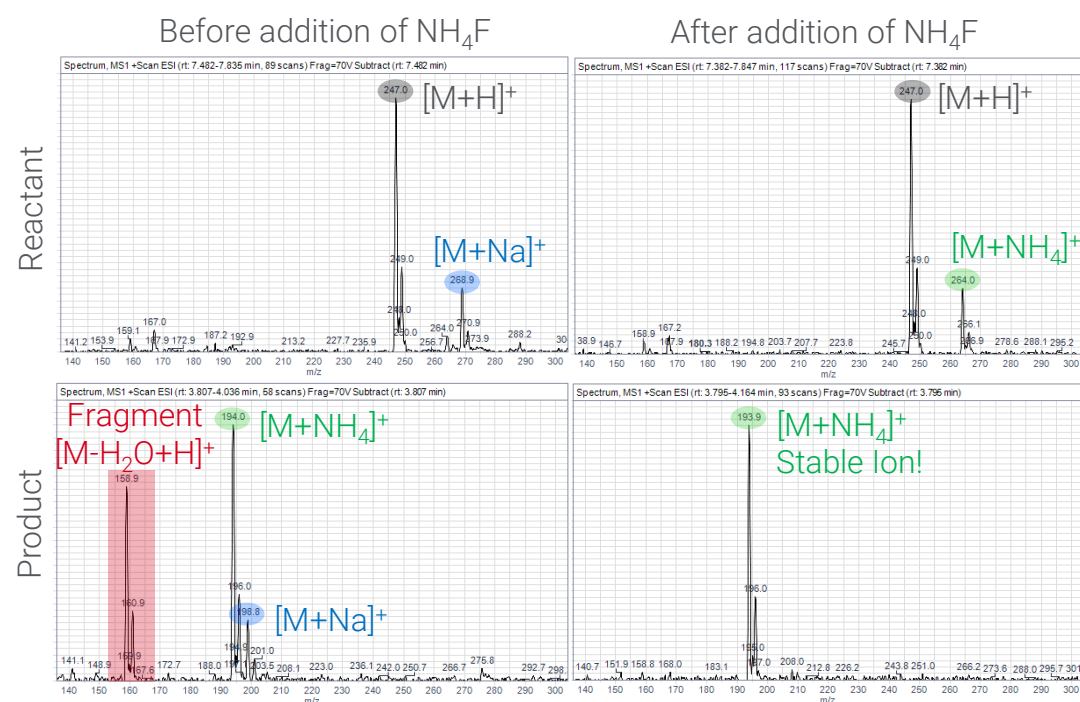


Figure 5. MS Spectra of the reactant peak (7.542 min) and product peak (3.856 min), before (left side) and after (right side) the addition of 0.5 mM NH_4F to the aqueous solvent

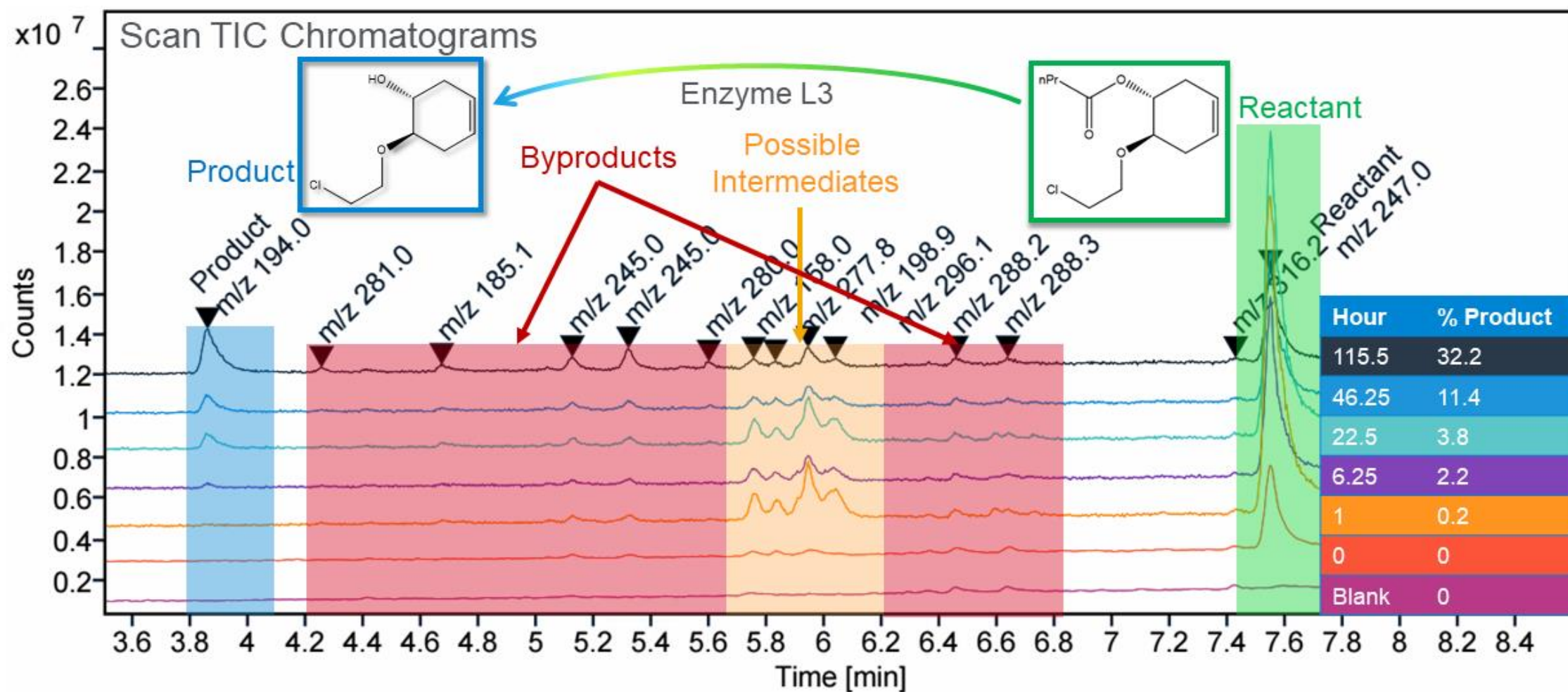


Figure 6. Stacked scan TIC chromatograms of aliquots from the reaction vessel for enzyme L3 during the course of the reaction. Highlighted regions indicate peaks corresponding to: product in blue, byproducts in red, possible intermediates in orange, and reactant in green. A table color coding the TIC to time points of the reaction is inlayed on the right.

Identifying Byproducts and Intermediates from Scan MS Chromatograms

Scan TIC chromatograms at various time points during the reaction with enzyme L3 can be seen in Figure 6. Before 6.25 hours, no product was detected but several peaks appeared between 5.7 and 6.2 minutes. These peaks were classified as intermediates because their abundance begins to decrease and fluctuate with the detection of the product and they all contain an ion at m/z 159. Several other peaks whose abundance increased overtime with the product were classified as byproducts.

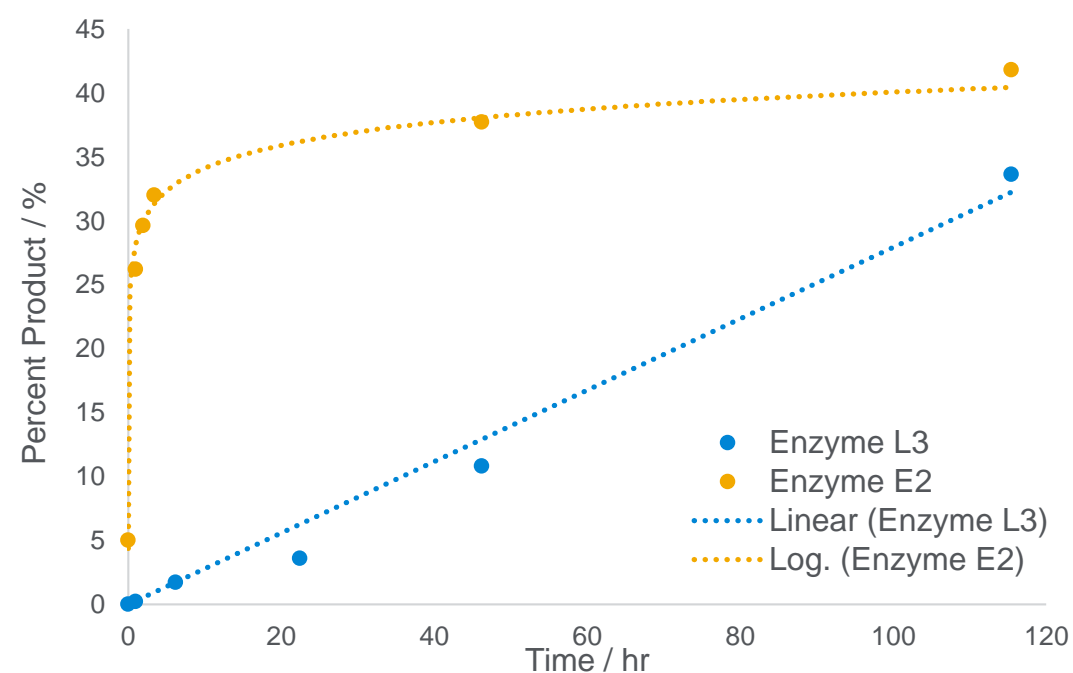


Figure 7. Percent product during reaction for enzymes L3 (blue) and E2 (orange)

Reaction Rates lead to Quick Decisions

A plot of percent product as a function of time for each enzyme can be seen in Figure 7. The percent product should only reach 50% due to the enantioselective nature of the reaction. Within 24 hours it can be seen that the E2 enzyme is much faster than L3 with a relatively logarithmic reaction rate versus linear, respectively.

Conclusions

- An enantioselective enzymatic hydrolysis reaction was monitored for two different enzymes, L3 and E2
- No compounds were detected in the UV signal, necessitating the need for mass detection
- The LC/MSD iQ detected compounds using a mixed mode scan/SIM method
- Products and reactants were detected along with several unknown byproducts and intermediates
- The L3 enzyme produced products much faster than the E2 enzyme

Poster Reprint

ASMS 2020

WP 004

Mass Spectrometric Characterization of Antibody-RNA Conjugates using the Agilent 6545XT AdvanceBio LC/Q-TOF

David L. Wong

Agilent Technologies, Inc., Santa Clara, CA,
USA

Introduction

Antibody-RNA Conjugates have drug-like properties comparable to antibodies and allow delivery of oligonucleotide payloads to non-hepatic tissues. The oligonucleotide payloads enable efficient treatment of previously undruggable targets. However, the use of such conjugates as therapeutic drugs is still under investigation and development. In this study, a LC/MS-based analytical method for identifying the intact antibody-RNA conjugates was developed and demonstrated. This workflow features various AdvanceBio columns for sample separation, and the 6545XT AdvanceBio LC/Q-TOF system with large molecule SWARM autotune feature and extended mass range of up to 30,000 m/z for sample analysis.



Figure 1. Analytical components of the native protein analysis workflow.

Experimental

The antibody was partially reduced with reducing agent and was then reacted with the activated RNA molecule (with linker). The unreacted free thiol groups ($-SH$) of mAb were capped with chemical reagent. The reaction mixture was further purified by ion exchange column. Unreacted antibody, DAR=1, DAR=2, and unreacted RNA were separated. The purified DAR=1 sample was then used for mass spectrometry analysis under denaturing and native conditions. Prior to the native MS analysis, sample desalting and buffer exchange with 100 mM ammonium acetate buffer (pH 7) were performed using the Bio-Rad Bio-Spin P-30 cartridge. Proteins were denatured under the traditional LC/MS analysis condition where organic and acid solvents were used.

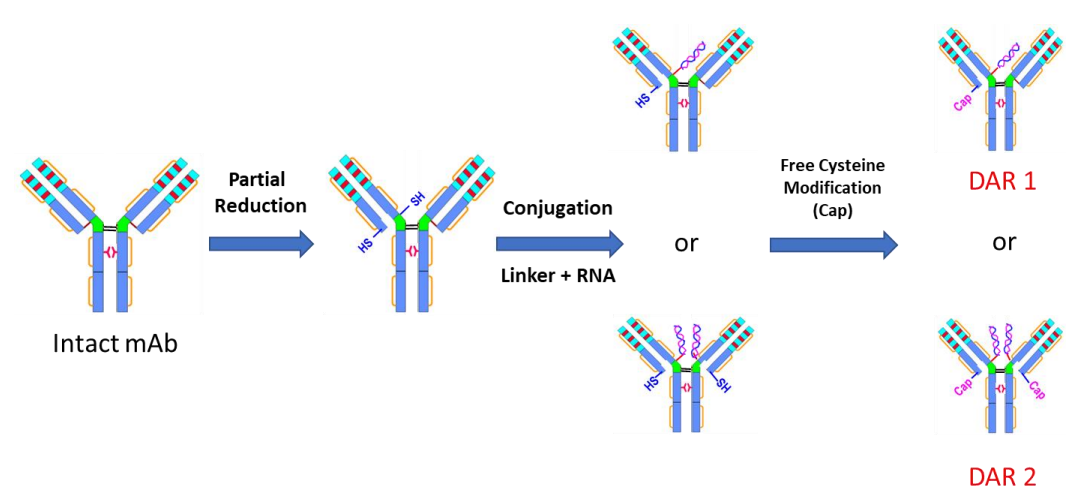


Figure 2. General Scheme of Antibody-RNA (mAb-RNA) Conjugate Synthesis.

LC/MS Analysis (Denaturing Condition) of Intact mAb (left) and mAb-RNA Conjugate (DAR1) (right):

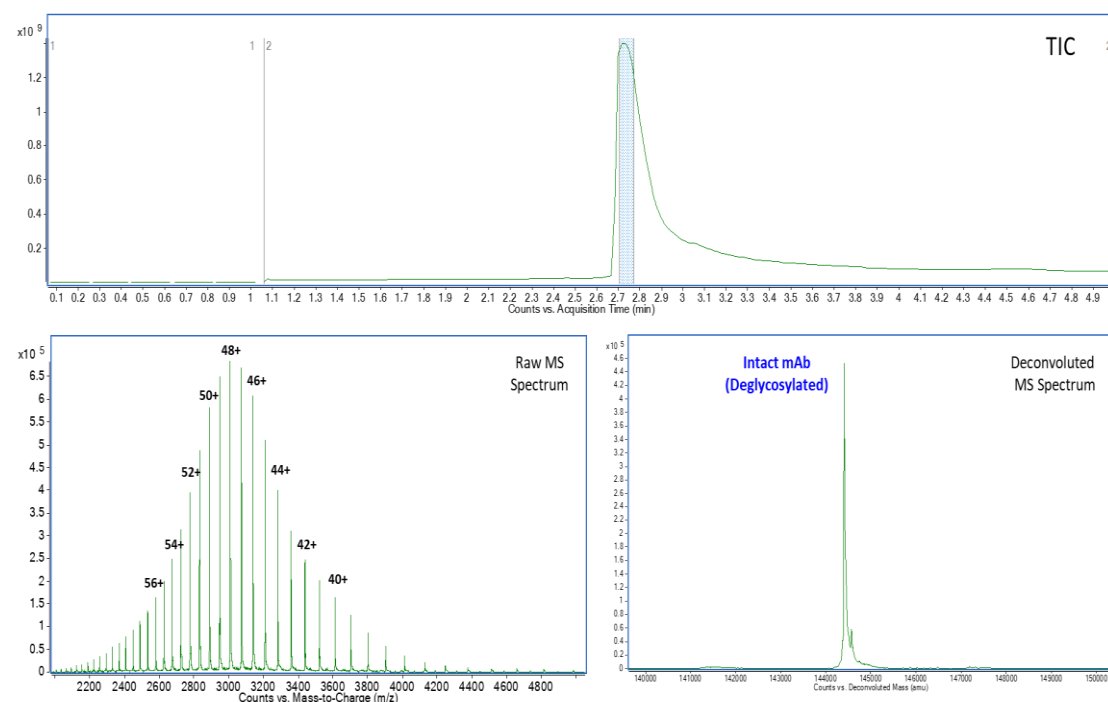


Figure 3. LC/MS analysis of intact deglycosylated mAb under denaturing condition (PLRP-S column was used). The charge state distribution of denatured mAb spanned in the mass range of m/z 2,000 to 5,000 (30+ to 75+).

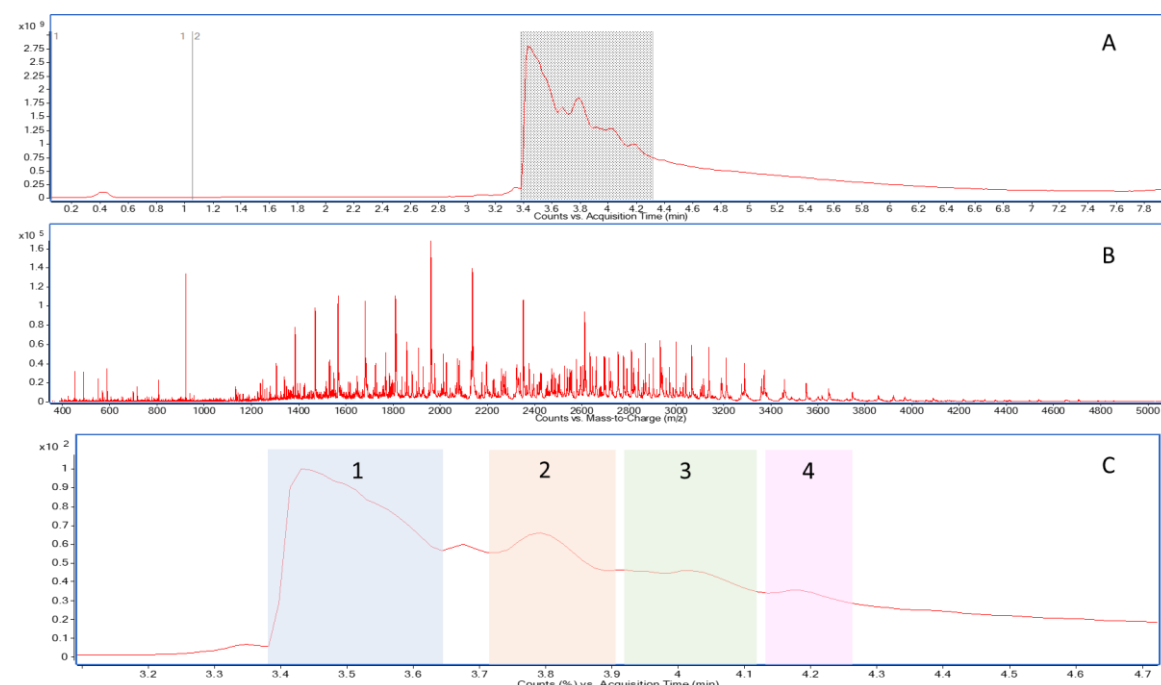


Figure 4. A) MS TIC of intact mAb-RNA conjugate (DAR1). B) Extracted Ion Chromatogram (EIC) of the chromatographic separated peaks over retention time of 3.4 – 4.3 min. C) Zoom-in chromatogram of the highlighted peaks (gray area in A). The MS data from each HPLC peaks (1-4) were deconvoluted and analyzed.

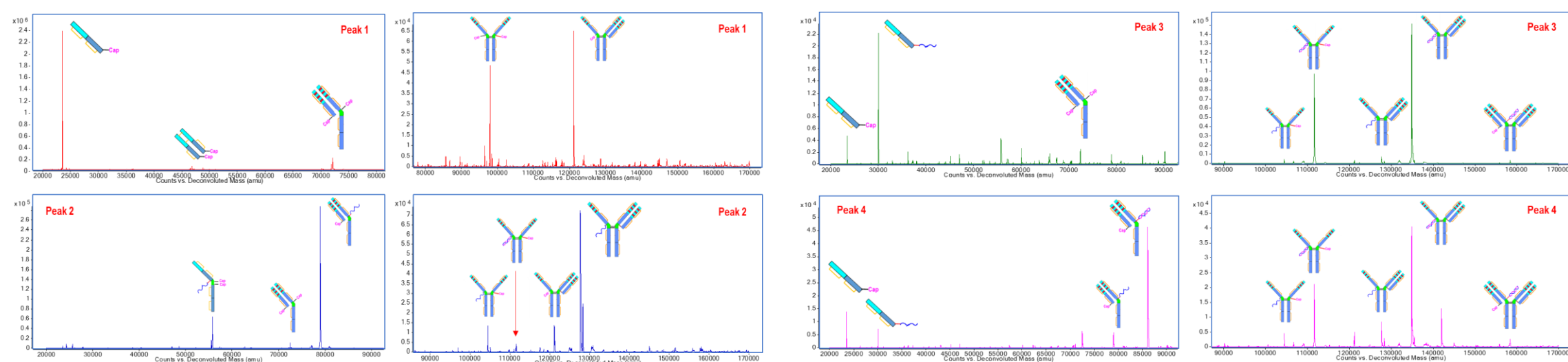


Figure 5. MS deconvoluted spectrum of HPLC peaks (1-4) of deglycosylated mAb-RNA sample (DAR1). LC/MS analysis was under denaturing MS conditions. Many dissociated molecules from mAb-RNA conjugate were observed in all 4 LC peaks mainly due to the weak electrostatic interaction of non-covalent mAb-RNA complexes. They were: mAb light chain (with Cap or RNA), mAb heavy chain (with Cap or RNA), half of conjugate, conjugates without 1 or 2 LCs, etc.

Native LC/MS Analysis of Intact mAb (top) and mAb-RNA conjugate (DAR1)(bottom):

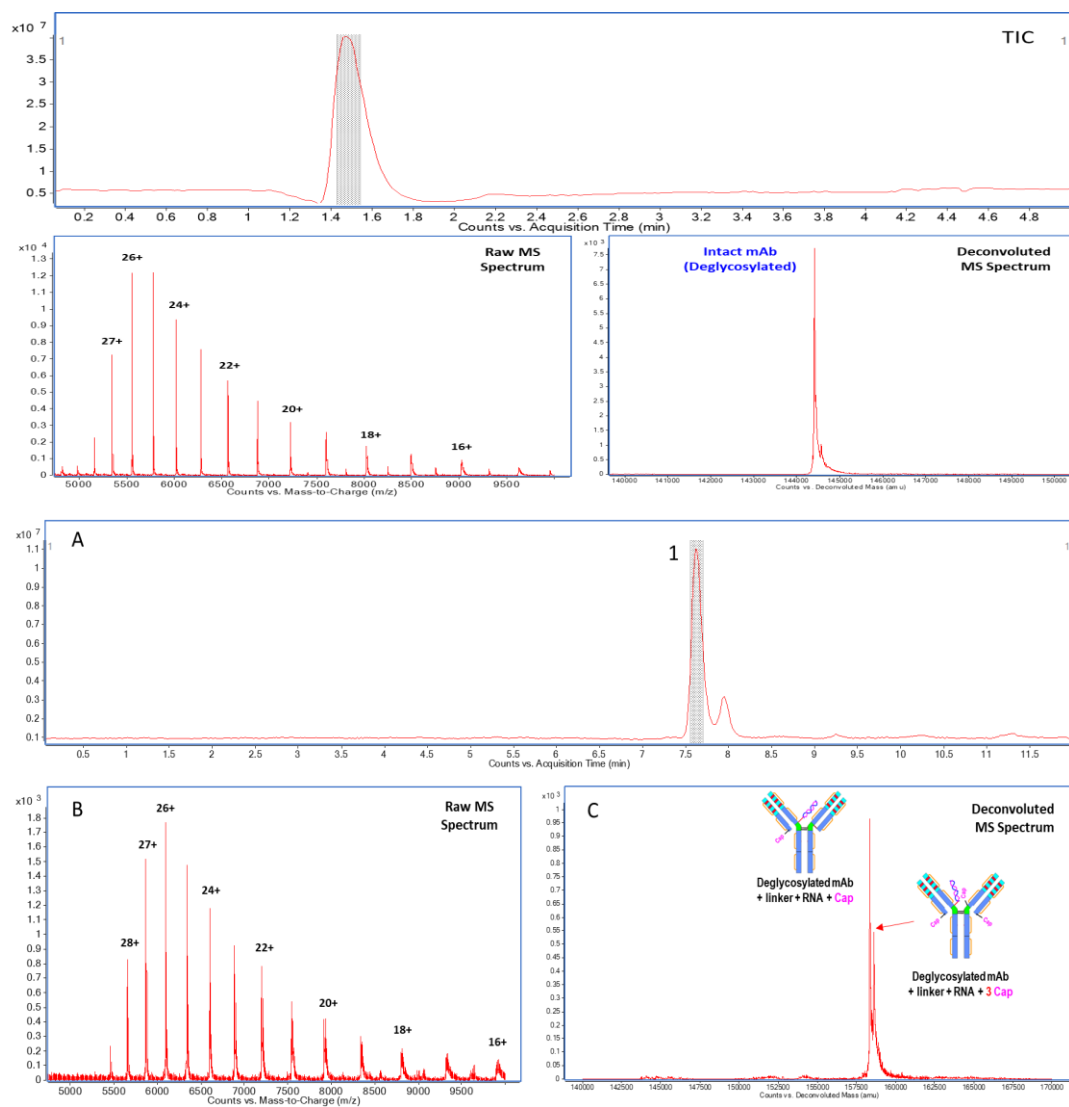


Figure 6. LC/MS analysis of intact deglycosylated mAb under native condition (SEC column was used). The native mAb had a charge envelope in the mass range of m/z 5,000 to 10,000 (15+ to 30+).

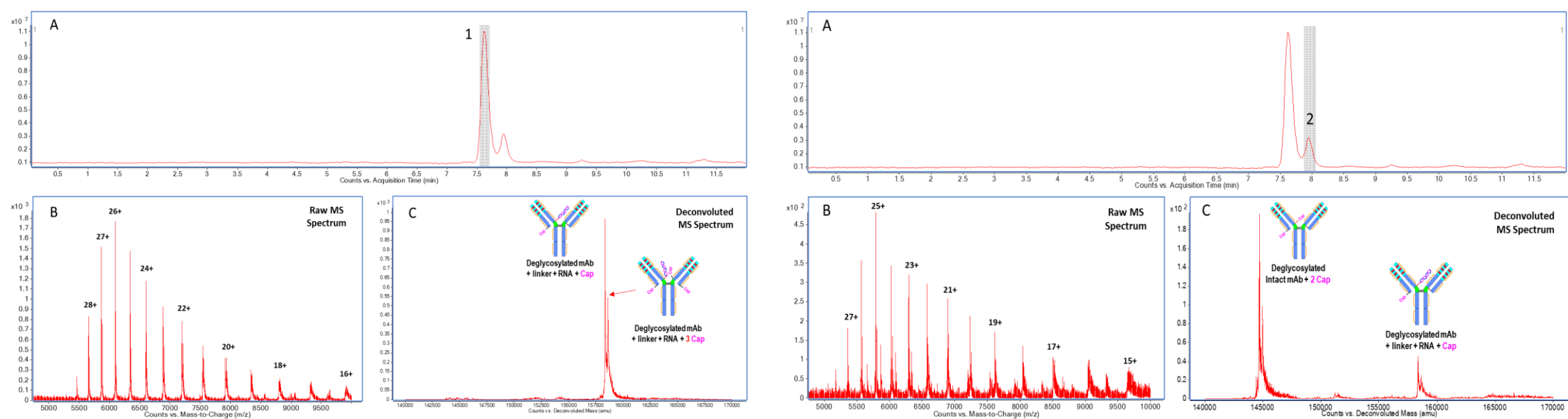


Figure 7. Native SEC LC/MS analysis of Antibody-RNA Conjugate (DAR1): A) HPLC chromatogram of SEC column separated conjugates. B) raw MS spectrum of intact mAb-RNA conjugates (peak 1 & 2). C) The deconvoluted MS spectra of intact mAb-RNA conjugates indicating two forms of conjugates were detected in peak 1: DAR1 with 1 or 3 cysteines modified by Cap, and unconjugated mAb with 2 Caps as well as DAR1 with 1 Cap in peak 2.

Conclusions

- Development of a novel method for characterization of mAb-RNA conjugates under native MS condition that overcomes the conjugate dissociation/stability issues caused by denaturing LC/MS condition.
- Native MS analysis of mAb-RNA conjugates can provide accurate mass information for conjugate structural assignment, and chromatographic separation enables relative quantitation on various types of mAb-RNA conjugates.
- Optimized workflow with the AdvanceBio SEC column, the 6545XT AdvanceBio LC/Q TOF, and MassHunter BioConfirm software.

References

1. Crooke, S. T. et al. RNA-targeted therapeutics. *Cell Metab.* 2018, 27(4), 714-739.
2. Cuellar, T. L. and Siebel, C. W. et al. Systematic evaluation of antibody-mediated siRNA delivery using an industrial platform of TH10MAB-siRNA conjugates. *Nucleic Acids Res.* 2015, 43(2), 1189-203.
3. Sugo, T., Terada, M., Oikawa, T. and Matsumoto, H. et al. Development of antibody-siRNA conjugate targeted to cardiac and skeletal muscles. *Journal of Controlled Release.* 2016, 237, 1-13.

For Research Use Only. Not for use in diagnostic procedures.

Poster Reprint

ASMS 2020

WP 165

Classifying the pesticides in foods between GC-amenable and LC-amenable using the prediction model with molecular descriptors

Sadao Nakamura¹, Takeshi Serino^{1,2},
Takeshi Otsuka¹, Yoshizumi Takigawa¹,
Tarun Anumol³, Shigehiko Kanaya²

¹ Agilent Technologies, Hachioji, Tokyo, Japan

² Nara Institute of Science and Technology,
Ikoma, Nara, Japan

³ Agilent Technologies, Wilmington, DE,
United States

Introduction

One of the frequently asked questions by food analysis chemists who are currently using GC/MS or LC/MS for residual pesticides in foods is whether that pesticide is "GC-amenable" or "LC-amenable". This is because neither LC/MS nor GC/MS can analyze all pesticides by any single technology, comparisons of the pesticides with both LC/MS and GC/MS have been researched^[1,2]. There are several guidelines for the selection between LC-amenable and GC-amenable for pesticides based on the physical and chemical properties^[3], and experienced chemists can predict the answer to this question based on the experiences for some degree. A prediction model for classifying the amenabilities of pesticides between GC-amenable and LC-amenable is developed by the quantitative structure-property relationship (QSPR) approach for answering to this question.

Experimental

Preparation of the pesticide list by validated report

Pesticide information for classification model were obtained from two validation reports of residual pesticide analysis in foods^[4,5] as below. Details of the pesticides and technologies are listed in the Table 1.

- U.S. Food and Drug Administration(FDA) List^[4]

The validation report of 136 pesticides analysis in Avocado using both LC/MS and GC/MS.

- EU Reference Laboratories for Residues of Pesticides(EURL)^[5]

The validation report of 127 pesticides analysis in Olive Oil using both LC/MS and GC/MS.

202 pesticides in total are included in both literatures. For improving the classification capability of machine learning, 8 pesticides were excluded from the machine learning which were analyzed differently between both, i.e. by GC/MS in EURL while by LC/MS in FDA as shown in Figure 1. 194 pesticides listed in the Table 1 were used.

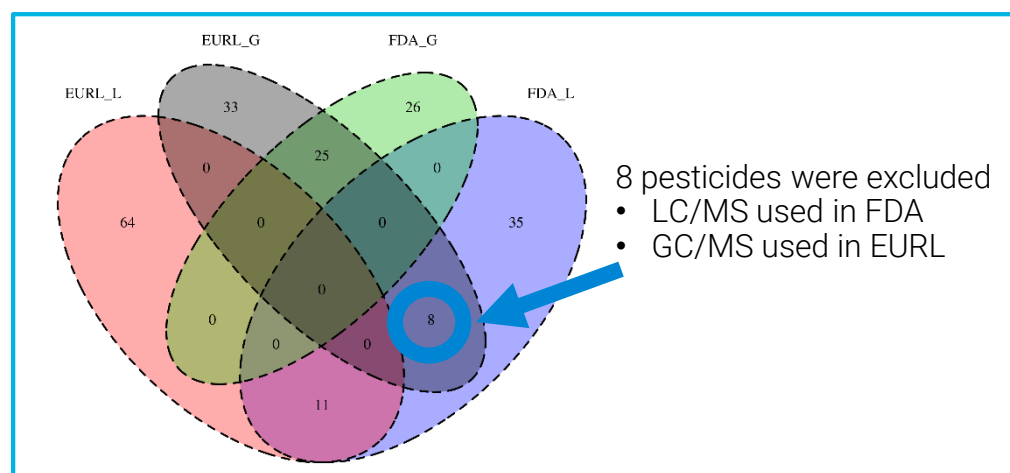


Figure 1. Venn diagram to describe the number of pesticides by the list(FDA or EURL) and the technology used for analysis (L:LC/MS and G:GC/MS).

Experimental

Molecular descriptors of the pesticides

The canonical SMILES of 194 pesticides were obtained from the PubChem website as listed in the Table 2. 224 molecular descriptors (MDs) of these pesticides were obtained by rcdk package of R program. The MDs with the zero variance among 194 pesticides were removed in order to avoid the errors in machine learning execution, 176 MDs were eventually obtained for machine learning. Each molecular descriptor was standardized for comparison as expressed by the Equation (Eq.1), where z_i is the standardized value to be used for machine learning, x_i is the raw value from rcdk, μ_i is the average of 194 pesticides and σ_i is the standard deviation of 194 pesticides for i th molecular descriptor.

$$z_i = \frac{x_i - \mu_i}{\sigma_i} \quad (\text{Eq.1})$$

Classification of pesticides by the machine learning

Either G(GC/MS) or L(LC/MS) of technology flag is assigned on the 194 pesticides based on the literatures as Table 1. 119 machine learning methods of the classification in caret package listed in the Table 3^[6] are evaluated in the present study.

Table 1. Pesticides and technologies used in the list. Technology “L” is analyzed by LC/MS, “G” is GC/MS. List of “E” is EURL list, “F” is FDA list and “Both” is both EURL and FDA list.

Pesticide	Tech	List	Pesticide	Tech	List	Pesticide	Tech	List	Pesticide	Tech	List
alpha-BHD	G	Both	Deltamethrin	G	E	Flusilazole	G	E	Pendimethalin	G	E
alpha-endosulfan	G	Both	Desmedipham	L	F	Jutolanil	L	F	pentachloroaniline	G	F
acetamiprid	L	Both	Desmethyl Pirimicarb	L	E	Flutriafol	L	E	pentachlorobenzene	G	F
Aldicarb	L	E	dichloruanid	L	F	Fluvalinate	G	Both	permethrin	G	F
Aldicarb Sulfone	L	E	dichlorvos	L	F	Forchlorfenuron	L	E	Pethoxamid	L	E
Aldicarb Sulfoxide	L	E	Dicloran	G	E	Furalaxyl	G	E	Phenthoate	G	E
ametryn	L	F	dicrotophos	L	Both	heptachlor epoxide	G	F	phosalone	G	Both
aminocarb	L	F	dieldrin	G	F	hexachlorobenzene	G	F	phosmet	L	Both
amitraz	G	F	difenoconazole	L	Both	hexaconazole	L	F	Picolinafen	G	E
azinphos-methyl	L	F	Diufenican	G	E	Hexythiazox	L	E	Prooxystrobin	L	E
Azoxystrobin	L	E	Dimofuron	L	E	Imazalil	L	F	piperonyl butoxide	L	F
b-endosulfan	G	Both	Dimethachlor	L	E	imidacloprid	L	E	Piridafenthion	G	E
Benalaxyl	G	E	Dimethenamid	L	E	iprodione	G	Both	pirimiphos-methyl	G	F
bendiocarb	L	F	dimethoate	L	Both	iprovalicarb	L	E	prochloraz	L	F
Benuralin	G	Both	dimethomorph	L	Both	isocarbophos	G	E	procymidone	G	Both
Bifenox	G	E	Dimoxystrobin	L	E	iso-fenphos-Methyl	G	E	profenofos	G	Both
bifenthrin	L	F	Diniconazole	L	E	linuron	L	Both	prometryn	L	F
boscalid	L	F	dinutramine	G	F	Malaaxon	L	E	pronamide	G	Both
bromopropylate	G	Both	dioxacarb	L	F	Mepanipyrim	G	E	propachlor	L	F
Bupirimate	G	E	Dmst	L	E	Metaxyl	G	E	propanil	G	F
cadusafos	G	F	endosulfan sulphate	G	Both	Metamitron	L	E	propargite	L	F
Carbendazim	L	E	endrin	G	F	Metconazole	L	E	pymetrozine	L	E
Carbofuran	L	E	EPN	G	F	methamidophos	L	F	Pyraclostrobin	L	E
Carbofuran 3-Oh	L	E	epoxiconazole	L	Both	Methidathion	G	E	Pyrazophos	G	E
Carfentrazone Ethyl	L	E	Etaconazol	L	E	Methiocarb	L	E	Pyridaben	G	E
Chlofenvinphos	G	E	ethiolate	L	F	Methiocarb Sulfone	L	E	pyriproxifen	G	Both
chlordimeform	L	F	ethofumesate	L	F	Methiocarb Sulfoxide	L	E	quinalphos	G	Both
Chlorfenapyr	G	E	Ethoprophos	G	E	Methomyl	L	E	Tebuconazole	G	E
Chloridazon	L	E	Etridiazole	G	F	methyl parathion	G	Both	Teuthrin	G	E
chlorothalonil	G	F	Fenamiphos	L	E	metolachlor	L	F	Terbufos	G	E
Chloroxuron	L	E	Fenamiphos Sulfone	L	E	metolcarb	L	F	Terbutryn	L	E
chlorpyrifos-methyl	G	Both	Fenamiphos Sulfoxide	L	E	Metosulam	L	E	Tetraconazole	G	E
Chlorthiophos	G	E	fenanimol	G	Both	mevinphos	L	F	tetradifon	G	F
Chlozolinate	G	E	fenbuconazole	L	F	MGK-264	G	F	Thiabendazole	L	E
Clortoluron	L	E	Fenitrothion	G	E	monocrotophos	L	Both	Thiacloprid	L	E
Clothianidin	L	E	Fenobucarb	L	E	monolinuron	L	F	Thiamethoxam	L	E
coumaphos	L	F	fenoxycarb	L	F	napropamide	G	F	tolclof-methyl	G	Both
cyanazine	L	F	Fenprophathrin	G	E	Neburon	L	E	Triadimefon	L	E
cycluron	L	F	fenpropimorph	L	F	o-phenylphenol	G	Both	Triadimenol	L	E
Cyuthrin	G	E	Fenpyroximate	L	E	o,p-methoxychlor	G	F	triallate	G	F
cyhalothrin	G	Both	Fenuron	L	E	omethoate	L	Both	Triazophos	G	E
Cymoxanil	L	E	fenvalerate	G	Both	oxadixyl	G	F	Trioxystrobin	L	E
cypermethrin	G	Both	Flazasulfuron	L	E	Oxaryl	L	E	Triumazole	L	E
cyproconazole	L	F	fludioxinil	L	F	Oxyurufen	G	E	Triuralin	G	Both
dachal	G	Both	Flufenacet	L	E	Paclbutrazole	L	E	Triticonazole	L	E
DDE(4,4)	G	F	Fluopicolide	L	E	Paraoxon Methyl	L	E	Vinclozolin	G	Both
DDT(2,4)	G	F	Fluoxastrobin	L	E	parathion	G	F	Zoxamide	L	E
DDT(4,4)	G	F	luquinconazole	L	Both	penconazole	L	F			
DEF	G	F	Flurtamone	L	E	Pencycuron	L	E			

These machine learning methods are expected to classify the 194 pesticides between G(GC/MS) or L(LC/MS) using the 176 molecular descriptors. Prediction performance of classification is measured by the accuracy of resamples from the 10-fold cross-validation(CV10) iterations and execution time. Execution time is obtained by the “System.time()” command of R package.

Table 2. 176 molecular descriptors in present study

Descriptor Class	Descriptor (Description)
ALOGP Descriptor (2)	ALOGP (Ghose-Crippen LogKow), ALOGP2 (Square of ALOGP)
APol Descriptor (1)	APol (Sum of the atomic polarizabilities (including implicit hydrogens))
Aromatic Atoms Count Descriptor (1)	nAromAtom (Number of aromatic atoms)
Aromatic Bonds Count Descriptor (1)	nAromBond (Number of aromatic bonds)
Atom Count Descriptor (2)	nAtom (Number of atoms), nB (Number of boron atoms)
Autocorrelation Descriptor Charge (5)	ATSs1, ATSs2, ATSs3, ATSs4, ATSs5 (ATS autocorrelation descriptor, weighted by charges)
Autocorrelation Descriptor Mass (5)	ATSm1, ATSm2, ATSm3, ATSm4, ATSm5 (ATS autocorrelation descriptor, weighted by scaled atomic mass)
Autocorrelation Descriptor Polarizability (5)	ATSp1, ATSp2, ATSp3, ATSp4, ATSp5 (ATS autocorrelation descriptor, weighted by polarizability)
BCUT Descriptor (6)	BCUTw.11 (nhigh lowest atom weighted BCUTs), BCUTw.1h (nlow highest atom), BCUTc.11 (nhigh lowest partial charge), BCUTc.1h (nlow highest partial charge) BCUTp.11 (nhigh lowest polarizability), BCUTp.1h (nlow highest polarizability)
BPoLDescriptor (1)	bpol (Sum of the absolute value of the difference between atomic polarizabilities of all bonded atoms in the molecule (including implicit hydrogens))
Carbon Types Descriptor (9)	C1SP1 (Triply bound carbon bound to one other carbon), C2SP1 (Triply bound carbon bound to two other carbons), C1SP2 (Doubly bound carbon bound to one other carbon), C2SP2 (Doubly bound carbon bound to two other carbons), C3SP2 (Doubly bound carbon bound to three other carbons), C1SP3 (Singly bound carbon bound to one other carbon), C2SP3 (Singly bound carbon bound to two other carbons), C3SP3 (Singly bound carbon bound to three other carbons), C4SP3 (Singly bound carbon bound to four other carbons)
Chi Chain Descriptor (10)	SCH.3-7 (Simple chain, orders 3-7), VCH.3-7 (Valence chain, orders 3-7)
Chi Cluster Descriptor (8)	SC.3-6 (Simple cluster, orders 3-6), VC.3-6 (Valence cluster, orders 3-6)
Chi Path Cluster Descriptor (6)	SPC.4-6 (Simple path cluster, orders 4 to 6), VPC.4-6 (Valence path cluster, orders 4-6)
Chi Path Descriptor (16)	SP.0-7 (Simple path, orders 0-7), VP.0-7 (Valence path, orders 0-7)
Eccentric Connectivity Index Descriptor (37)	ECCEN (A topological descriptor combining distance and adjacency information), khs.sCH3 (Count of atom-type E-State: -CH3), khs.dCH2 (=CH2), khs.ssCH2 (-CH2-), khs.tCH (#CH), khs.dCH (=CH), khs.aCH (CH-), khs.sssCH (-CH-), khs.tC (#C), khs.dsc (=C-), khs.aac (C-), khs.aaaC (-C-), khs.ssssC (-C-), khs.sNH2 (-NH2), khs.ssNH (-NH2+), khs.aanH (NH-), khs.tN (#N), khs.dnN (=N-), khs.aaN (N-), khs.ssnN (-N-), khs.ddnN (-N<-), khs.aaN (N-), khs.sOH (-OH), khs.dO (=O), khs.ssO (-O-), khs.aao (O-), khs.sF (-F), khs.sssSi (>Si<), khs.dssp (>P=), khs.dS (=S), khs.sSS (-S-), khs.aS (aS), khs.dSS (-S=), khs.ddSS (-S=>), khs.sCl (-Cl), khs.sBr (-Br)
Fragment Complexity Descriptor (1)	fragC (Complexity of a system)
Ghose Crippen Molecular Refractivity Descriptor (1)	AMR (Molar refractivity)
H Bond Acceptor Count Descriptor (1)	nHBAcc (Number of hydrogen bond acceptors)
H Bond Donor Count Descriptor (1)	nHBDon (Number of hydrogen bond donors)
KappaShape Indices Descriptor (3)	Kier1-3 (First, Second, Third kappa (k) shape indexes)
Largest Chain Descriptor (1)	nAtomLC (Number of atoms in the largest chain)
Longest Aliphatic Chain Descriptor (1)	nAtomLAC (Number of atoms in the longest aliphatic chain)
Mannhold LogP Descriptor (1)	MLogP (Mannhold LogP)
MDEDescriptor (19)	MDEC.11 (Molecular distance edge between all primary carbons), MDEC.12 (between all primary and secondary carbons), MDEC.13 (between all primary and tertiary carbons), MDEC.14 (between all primary and quaternary carbons), MDEC.22 (between all secondary carbons), MDEC.23 (between all secondary and tertiary carbons), MDEC.24 (between all secondary and quaternary carbons), MDEC.33 (between all tertiary carbons), MDEC.34 (between all tertiary and quaternary carbons), MDEC.44 (between all quaternary carbons), MDEC.11 (between all primary oxygens), MDEC.12 (between all primary and secondary oxygens), MDEC.22 (between all secondary oxygens), MDEN.11 (between all primary nitrogens), MDEN.12 (between all primary and secondary nitrogens), MDEN.13 (between all primary and tertiary nitrogens), MDEN.22 (between all secondary nitrogens), MDEN.23 (between all secondary and tertiary nitrogens), MDEN.33 (between all tertiary nitrogens)
PetitjeanNumberDescriptor (1)	PetitjeanNumber (Petitjean number)
RotatableBondsCountDescriptor (1)	nRotB (Number of rotatable bonds, excluding terminal bonds)
RuleOfFiveDescriptor (1)	LipinskiFailures (Number failures of the Lipinski's Rule Of 5)
TPSA Descriptor (19)	TopoPSA (Topological polar surface area)
VAdjMatDescriptor (1)	VAdjMat (Vertex adjacency information (magnitude))
WeightDescriptor (1)	MW (Molecular weight)
WeightedPathDescriptor (5)	WTPT.1 (Molecular ID), WTPT.2 (Molecular ID / number of atoms), WTPT.3 (Sum of path lengths starting from heteroatoms), WTPT.4 (Sum of path lengths starting from oxygens), WTPT.5 (Sum of path lengths starting from nitrogens)
WeinerNumbersDescriptor (2)	WPATH (Weiner path number), WPOL (Weiner polarity number)
XLogPDescriptor (1)	XLogP (XLogP)
ZagrebIndexDescriptor (1)	Zagreb (Sum of the squares of atom degree over all heavy atoms i)
Petitjean Shape Index Descriptor (1)	topoShape (Petitjean topological shape index)
Others (16)	nBase (Basic group count descriptor), nSmallRings (the number of small rings from size 3 to 9), nAromRings (the number of aromatic rings), nRingBlocks (total number of distinct ring blocks), nAromBlocks (total number of "aromatically connected components"), nRings3, 5, 6, 7 (individual breakdown of small rings), tpsaEfficiency (Polar surface area expressed as a ratio to molecular size), VABC (Atomic and Bond Contributions of van der Waals volume), HybRatio (the ratio of heavy atoms in the framework to the total number of heavy atoms in the molecule), tpsaEfficiency.1 (Polar surface area expressed as a ratio to molecular size), TopoPSA.1 (Topological polar surface area), topoShape.1 (A measure of the anisotropy in a molecule)

Table 3. Machine Learning methods for regression analysis used in present study

Algorithm	Methods in caret
(a) Ordinary learning methods	
Kernel (17)	dwdPoly, dwdRadial, gaussprRadial, kernelpls, lssvmRadial, stepQDA, svmLinear, svmLinear2, svmLinear3, svmLinearWeights, svmLinearWeights2, svmPoly, svmRadial, svmRadialCost, svmRadialSigma, svmRadialWeights, widekernelpls
Simple Linear (12)	bayesglm, CSimca, glm, glmStepAIC, multinom, ordinalNet, plr, pls, regLogistic, rrida, RSimca, simpls
Sparse modeling (2)	glmnet, sdwd
Neural Network (11)	avNNet, dnn, mlp, mlpML, mlpWeightDecay, mlpWeightDecayML, monmlp, msaenet, nnet, pcanNet, rbfDDBA
Decision Tree (18)	C5.0, C5.0Cost, C5.0Rules, C5.0Tree, ctree, ctree2, deepboost, evtree, J48, JRip, LMT, OneR, PART, rpart, rpart1SE, rpart2, rpartCost, rpartScore
Centroid,kNN (6)	knn, kkn, lvq, ownn, pam, snn
Spline (4)	earth, gamLoess, gamSpline, gcvEarth
Naive Bayes (2)	naive bayes, nb
Others (13)	dwdLinear, fda, hdda, null, pda, pda2, rda, rocc, sda, slda, sparseLDA, stepLDA, xyf
(b) Ensemble learning methods	
Decision Tree (26)	ada, AdaBag, adaboost, AdaBoost.M1, blackboost, bstTree, cforest, extraTrees, gbm, nodeHarvest, ORFpls, ORFridge, ORFsvm, parRF, ranger, Rborist, rf, rFerns, rFRules, rotationForest, rotationForestCp, RRF, RRFglobal, treebag, wsrif, xgbTree
Simple Linear (3)	glmboost, LogitBoost, xgbLinear
Spline (4)	bagEarth, bagEarthGCV, bagFDA, xgbDART

Results and Discussion

Classification Performance (Accuracy of CV10 resample)

The box plot in the Figure 2. shows the distribution of accuracy for each machine learning method category. The overall accuracy of CV10 is calculated by the Eq. 2.

$$CV10\ Accuracy(\%) = \frac{\sum_{i=1}^{10} (\text{Number of accurate classification of } i\text{th test})}{\sum_{i=1}^{10} (\text{Total number of } i\text{th test})} \times 100 \quad (\text{Eq. 2})$$

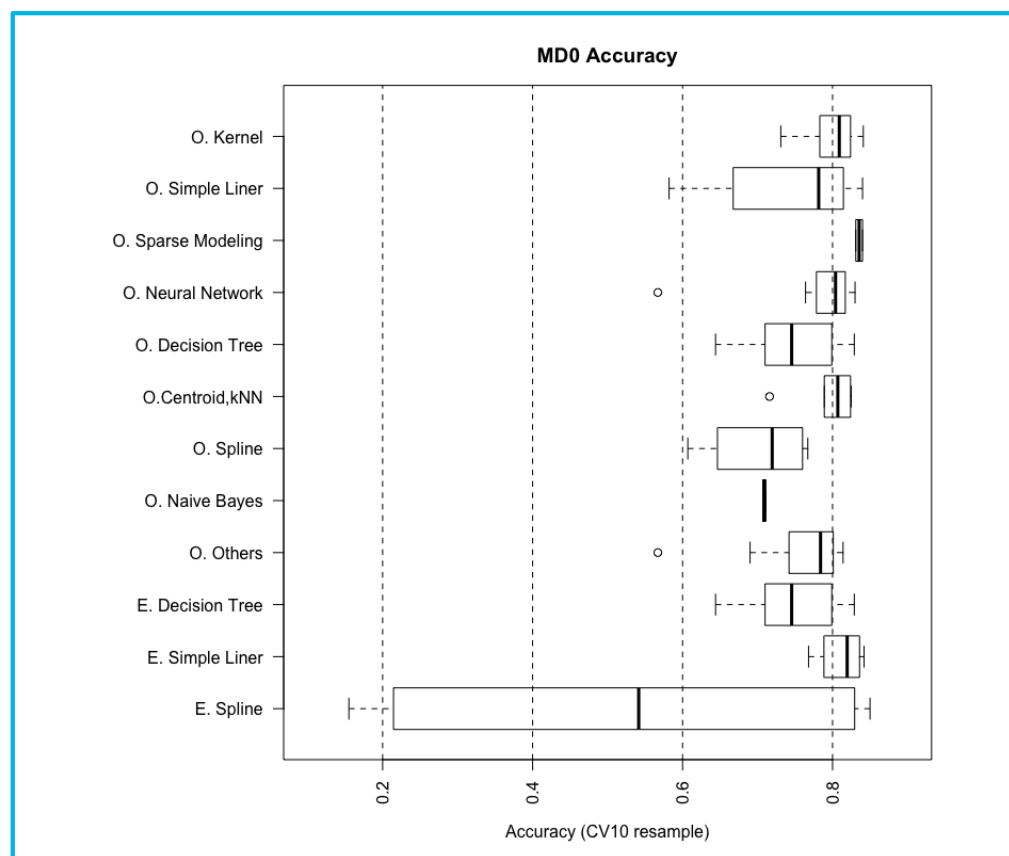


Figure 2. Accuracy of classification (CV10 resample) for 119 machine learning methods

Overall accuracy across the 119 methods was 77%. According to Figure 3, machine learning methods in the ensemble spline method category show larger variability in accuracy than the others. Four machine learning methods, bagEarth (Bagging Earth, 27%), bagEarthGCV (Bagging Earth generalized cross validation, 16%), bagFDA (Bagging flexible discriminant analysis, 81%) and xgbDART (eXtreme Gradient Boosting Dropouts Additive Regression Trees, 85%) were included on this category. According to this result, two methods of bagging earth were not suitable in classifications for this data set.

Execution time(ET)

The result of ET of each the machine learning method is shown in the Figure 3. Methods of ordinary neural network(ranged LogET 1.08 to 2.36) and ensemble spline categories(LogET 1.63 to 2.71) require more execution time than the other categories. The machine learning method with the maximum ET is glmStepAIC(Generalized Linear Model with Stepwise Feature Selection) with the LogET 4.12, i.e. 3 hours and 41 minutes.

Results and Discussion

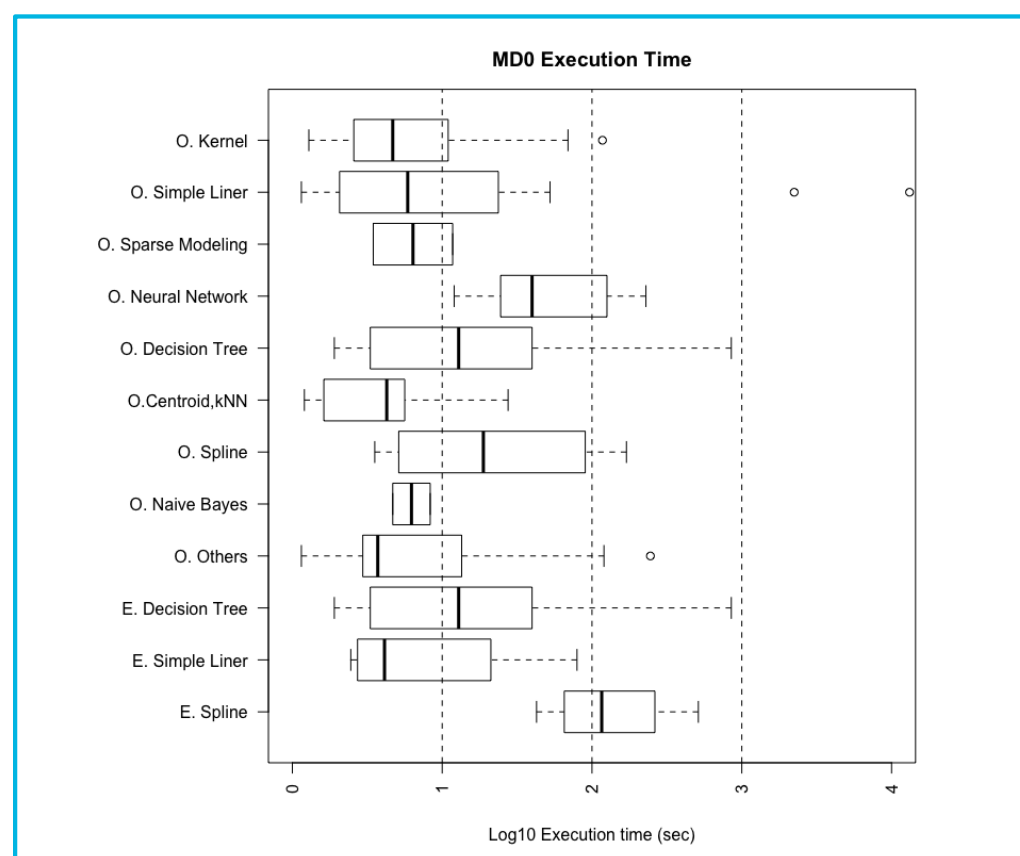


Figure 3. Execution Time for 119 machine learning methods

Total performance - both Accuracy and Execution Time

The results of Accuracy and ET by the machine learning method are shown in the Figure 4.

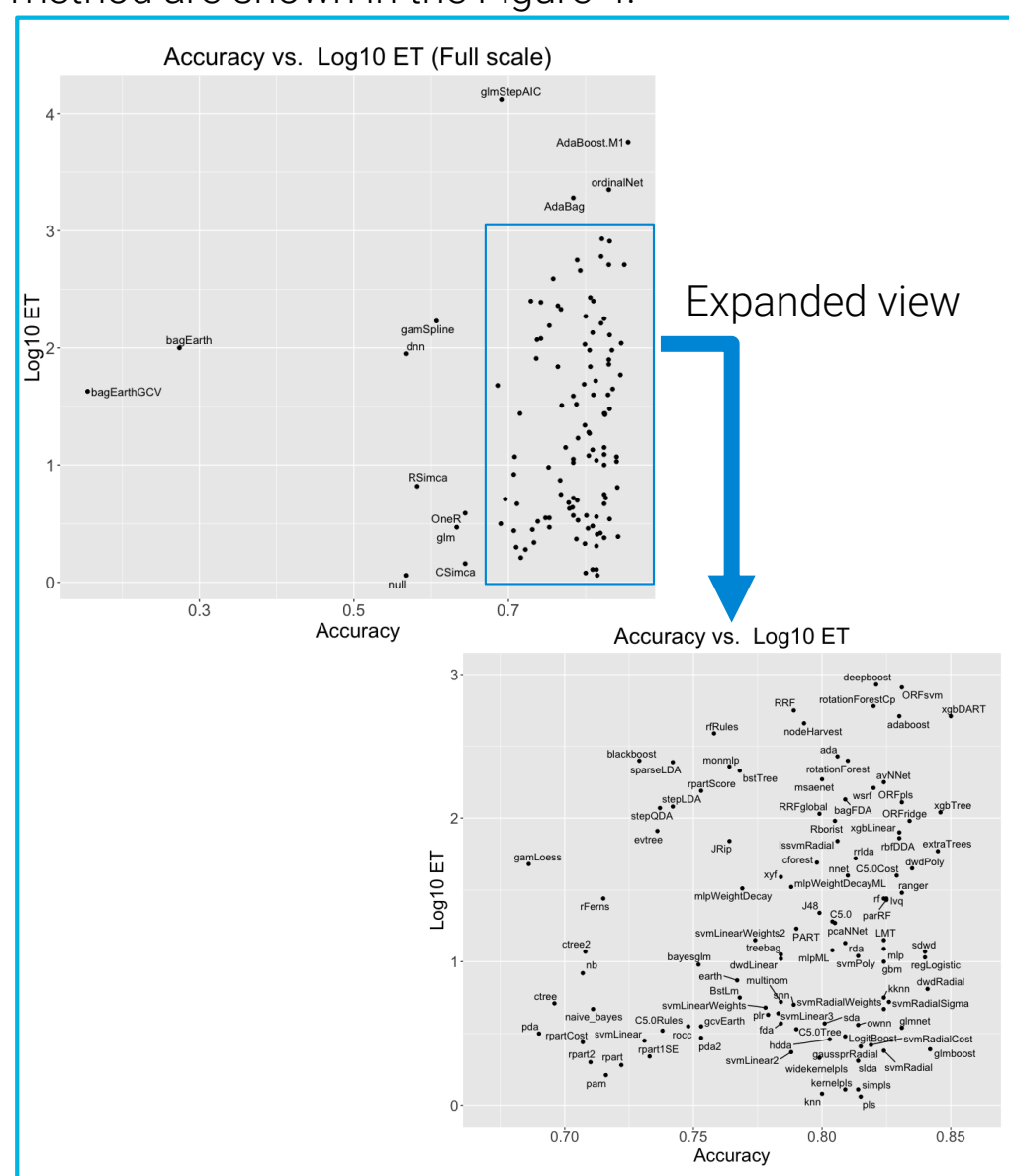


Figure 4. Accuracy and Execution time for 119 machine learning methods

Best 20 machine learning methods in accuracy ranged from 85.5%(AdaBoost.M1) to 83% (svmRadialSigma). Six methods of Ensemble Decision Tree showed higher accuracy for the present data set of GC/MS and LC/MS amenability. The best machine learning method of accuracy is AdaBoost.M1, but it requires 5,600 seconds (1 hour and 34 minutes). The method with higher accuracy with shorter ET is xgbTree, 84.6% within 2 minutes. xgbDART (85.0% accuracy with 8 minutes 33 seconds) was higher accuracy with the moderate ET. xgbDART is highly recommended among 119 methods for the present study with higher accuracy and reasonable execution time for classification.

Conclusions

The classification method of pesticides amenability between LC and GC is developed using the QSPR approach, 119 machine learning methods for classification using 176 molecular descriptors obtained by the 194 pesticides of two validation reports. Prediction accuracy and execution time are the measure of the machine learning method performance.

The recommended machine learning method for the present study is xgbDART with 85.0 % accuracy that requires less than 9 minutes for execution.

References

- 1 Z. Barganska, P. Konieczka and J. Namiesnik. 2018. Comparison of Two Methods for the Determination of Selected Pesticides in Honey and Honeybee Samples. *Molecules* **23**: 2582.
- 2 C. Anagnostopoulos and G.E.Miliadis. 2013. Development and validation of an easy multiresidue method for the determination of multiclass pesticide residues using GC-MS/MS and LC-MS/MS in olive oil and olives. *Talanta* **1121**: 1-10.
- 3 Pesticide Analytical Manual Vol. I, Appendix II, Food and Drug Administration. 1999.
- 4 N. Chamkasem, L. W. Ollis, T. Harmon, S. Lee and Greg Mercer. 2013. Analysis of 136 Pesticides in Avocado Using a Modified QuEChERS Method with LC/MS/MS and GC/MS/MS. *J. Agric. Food Chem.* **61**: 2315 - 2329.
- 5 EURL-FV(2012-M6) Validation Data of 127 Pesticides Using a Multiresidue Method by LC/MS/MS and GC/MS/MS in Olive Oil, EU Reference Laboratories for residues of pesticides. 2012.
- 6 M. Kuhn. 2008. Building Predictive Models in R Using the caret Package. *J. Statistical Software* **28**: 1 - 26.

Poster Reprint

ASMS 2020
WP 171

An End-to-End Workflow Solution For Quick and Easy Quantitative Analysis of Multiclass Veterinary Drug Residues in Meat Using LC- MS/MS

Siji Joseph^a, Aimei Zou^a, Limian Zhao^b,
Ruben Garnica^b, Dan-Hui-Dorothy Yang^c,
Patrick Batoon^c, Chee Sian Gan^a

a: Agilent Technologies, Singapore, b: Agilent
Technologies, Wilmington, Delaware, United
States

c: Agilent Technologies, Santa Clara,
California, United States

Introduction

Veterinary drugs are commonly used to improve the growth and health outcomes of farm animals. Improper use of vet-drugs in animal farming can result in accumulation of these drugs in animal-derived foods, causing adverse effects to consumers. Global regulations define limits for vet-drugs in food of animal origin to ensure Food Safety.

LC-MS/MS is a widely accepted technique for this analysis; however laboratories traditionally run individual analyses based on compound class. This can be inefficient and result in high operating costs. In this poster, we describe a comprehensive veterinary drug dMRM workflow solution (Figure 1) for highly sensitive, reproducible screening and /or quantitative analysis of >200 multi-class veterinary drugs in various animal origin food matrices using LC-MS/MS.



Figure 1:
Agilent Comprehensive Veterinary Drug dMRM Solution

Experimental

Target Selection

The 210 targeted veterinary drugs included in the workflow solution are from >28 different chemical classes. These targets were selected based on combinatory study of recommendations by AOAC¹, US FDA-CFR², US FSIS³, and EU⁴.

A Venn diagram of 210 target distribution across various organizations is given in Figure 2. Out of 210 targets, 168 of them have Maximum Residue Limits (MRL) established in three muscle matrices defined by the AOAC, EU, or US regulation/guidelines.

Workflow Solution Protocol

The analytical workflow utilized for this work is summarized in Figure 3.

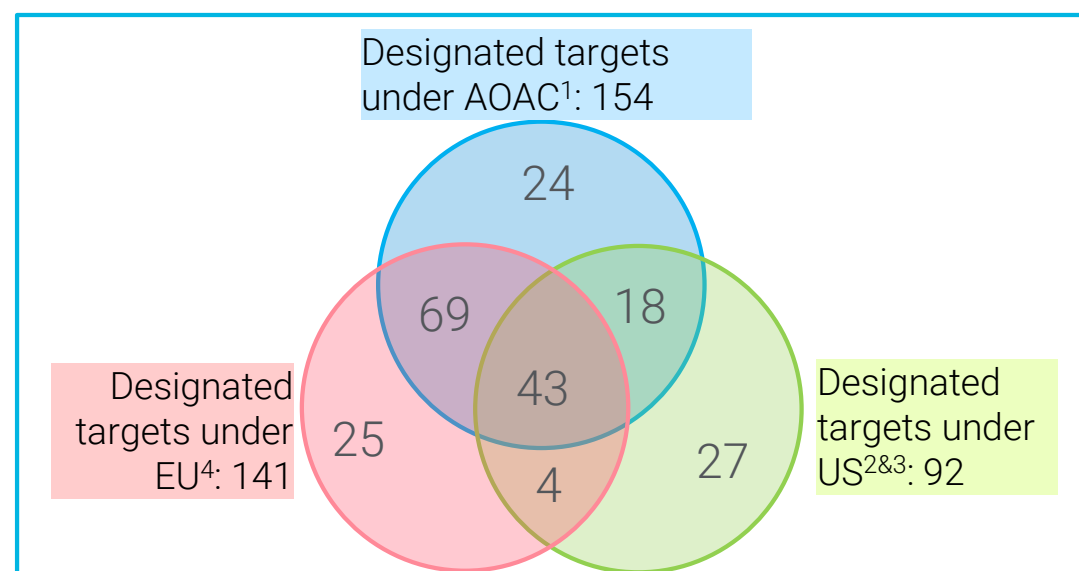


Figure 2: Venn Diagram of 210 targets distribution across various regulations.

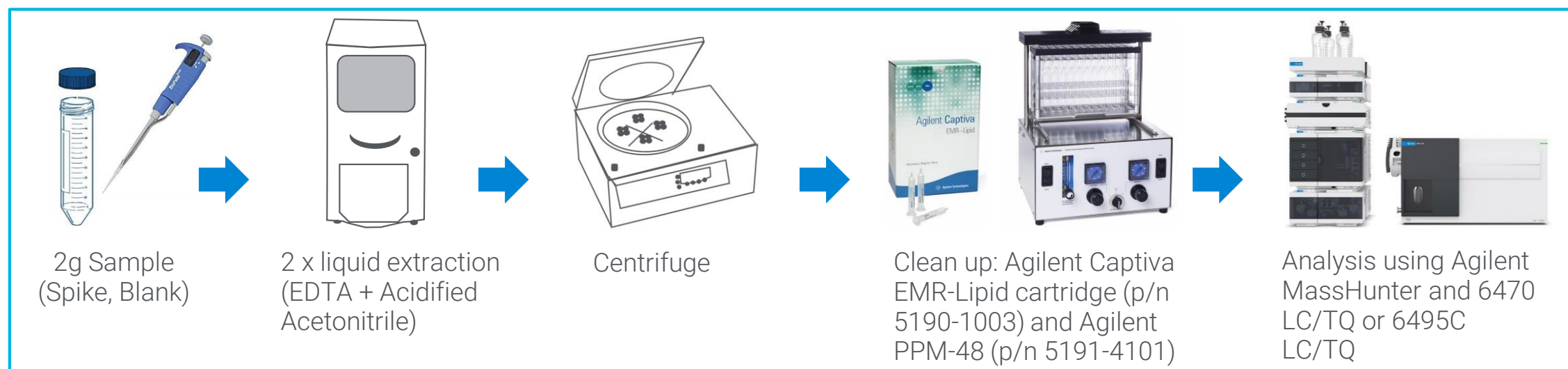


Figure 3: Analytical flow-chart

LC-MS/MS MRM Overlay

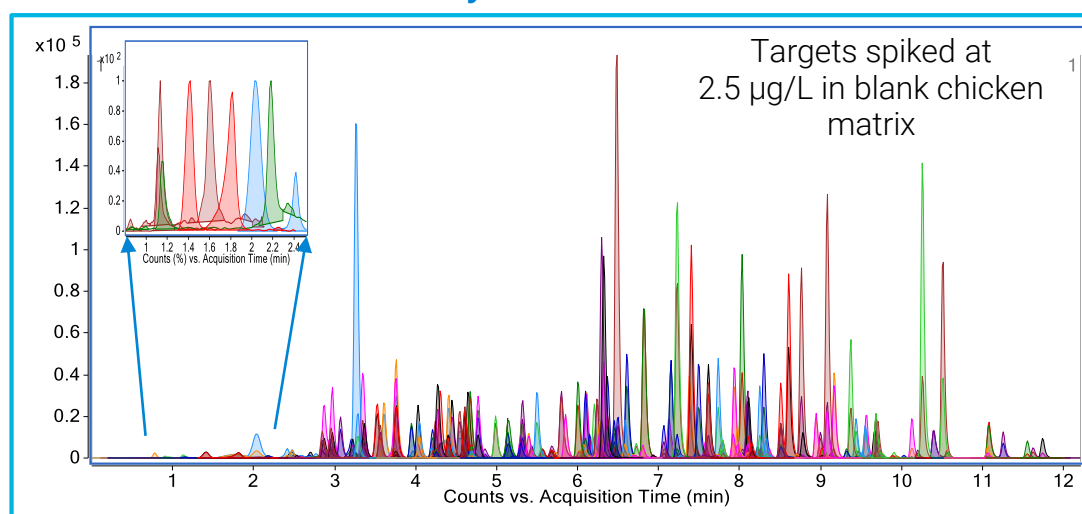


Figure 4: MRM chromatogram of 210 veterinary drug targets with zoom view of six early-eluting targets.. Column: Agilent InfinityLab Poroshell 120 EC-C18 column (p/n: 695575-302).

LC-MS/MS Method Performance Evaluation

Method sensitivity, linearity, accuracy, and precision data were measured using matrix-matched spike samples from 0.1 to 100 µg/kg. Method recovery analysis was performed using matrix-spiked samples at 1 (Low QC), 10 (Mid QC), and 25 (High QC) µg/kg concentrations.

The limit of detection (LOD) of all targets ranged between 0.1 -10 µg/kg. Calibration curves for all targets were plotted from limit of quantitation (LOQ) to 100 µg/Kg. The sensitivity and linearity results are summarized in the below table.

# of Targets	LOD (µg/kg)	Linear calibration curve Range with R2> 0.99 (µg/kg)
42	0.1	0.25 - 100
53	0.25	0.5 - 100
49	0.5	1.0 - 100
26	1	2.5 - 100
20	2.5	5.0 - 100
15	5	10.0 -100
5	10	25.0 - 100

Instrument Method Accuracy and Precision

The average accuracy was calculated from triplicate injections and observed results were well within the range of 70–120%.⁵

Precision was determined as %RSD of target response and retention time (RT) using triplicate injections of matrix sample. Response %RSD for all targets in the chicken matrix was <20% and RT %RSD of all targets was within 0.5%.

Applicability For Routine Screening

Applicability for routine veterinary drug screening is verified by performing recovery analysis using QC samples. The target recoveries from chicken muscle matrices are shown in Figure 5. The successful application of this workflow solution to screen all MRL established targets in chicken matrix as per AOAC guidelines is demonstrated in Agilent publication 5994-1932EN.⁶

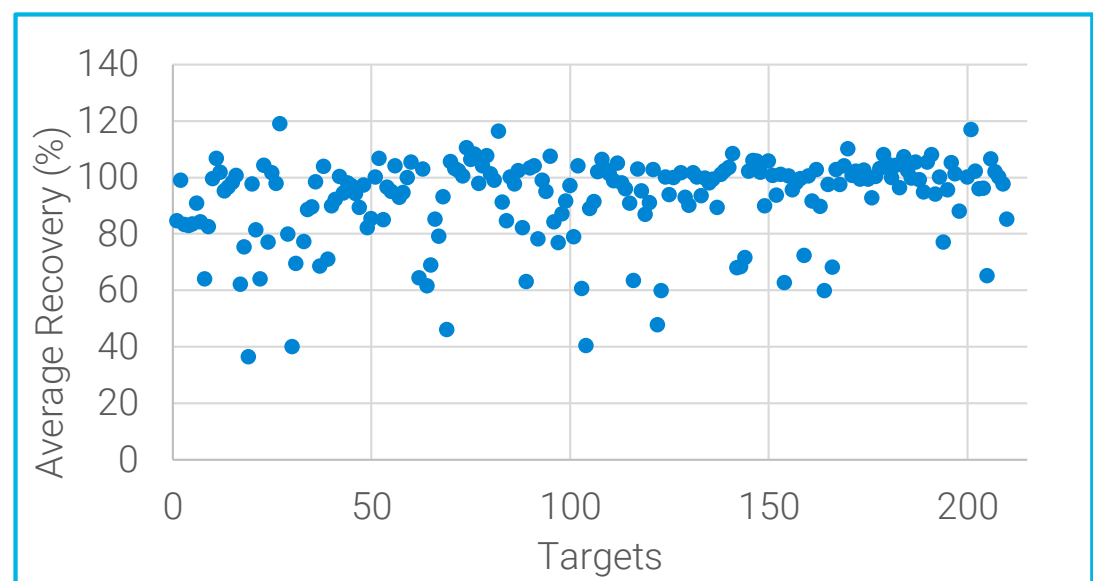


Figure 5: Target recoveries from chicken muscle spiked with 10 µg/kg standard

Intrabatch Recovery Repeatability

The intrabatch recovery repeatability of all targets were evaluated by running n=3 replicates of spiked chicken samples within a batch (Figure 6). The recovery value of a few targets was less than 60%; however, the recovery reproducibility for these targets was within 10% RSD.

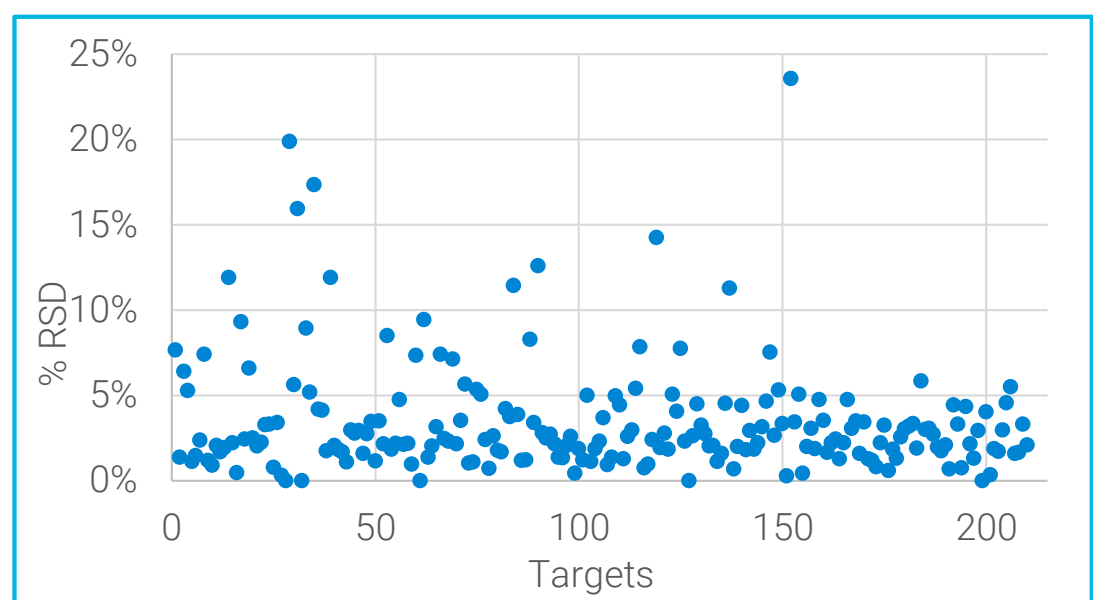


Figure 6: Intrabatch recovery repeatability of all targets using chicken matrix. Recovery repeatability of >98% targets were within 15% RSD.

Interbatch Recovery Reproducibility

Interbatch recovery reproducibility was evaluated by running n=3 replicates of spiked chicken samples prepared in different days and run in different batches (Figure 7).

Consistent and reproducible results on intrabatch repeatability and interbatch reproducibility confirmed the workflow solution applicability for confident day-to-day screening analysis.

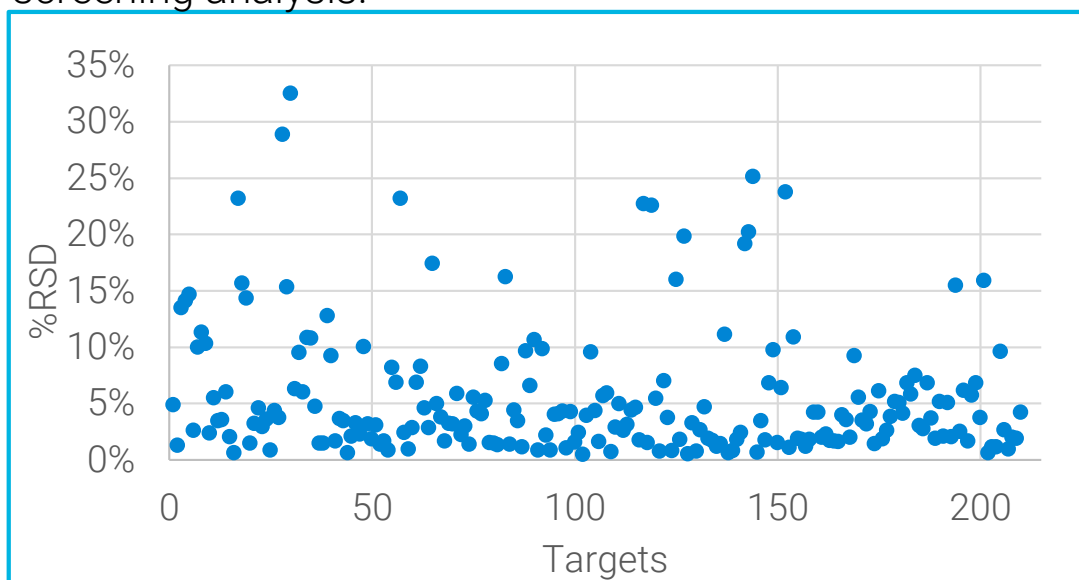


Figure 7: Interbatch reproducibility of 210 targets using prespiked QCs. All 210 targets met the limit of <32% RSD. Reproducibility of 194 targets were <15%.

Workflow Performance in Other Matrices

The workflow solution applicability in beef and pork muscles were also evaluated and results were in good agreement with that of chicken matrix.⁶

Conclusions

- Demonstrates a rapid, sensitive, and robust end-to-end LC/MS-MS workflow solution to analyze >200 multi-class veterinary drug residues in meat using Agilent LC/TQ.
- The applicability of the workflow solution for routine veterinary drug screening is demonstrated by performing screening of AOAC-listed targets in chicken matrix.
- The performance of Agilent Comprehensive Veterinary Drug dMRM Solution (G5368A) is verified using two different triple quadrupole models (6470 LC/TQ and 6495C LC/TQ).
- Workflow applicability verified for beef and pork muscle, and will extend to seafood, milk products, etc. in future.

VetDrug dMRM Database for Easy Sub-methods

A dMRM database was created that includes all the settings for acquisition of 210 targets. The database helps to easily customize dMRM sub-methods based on target list of interest or regulation in a region (Figure 8).

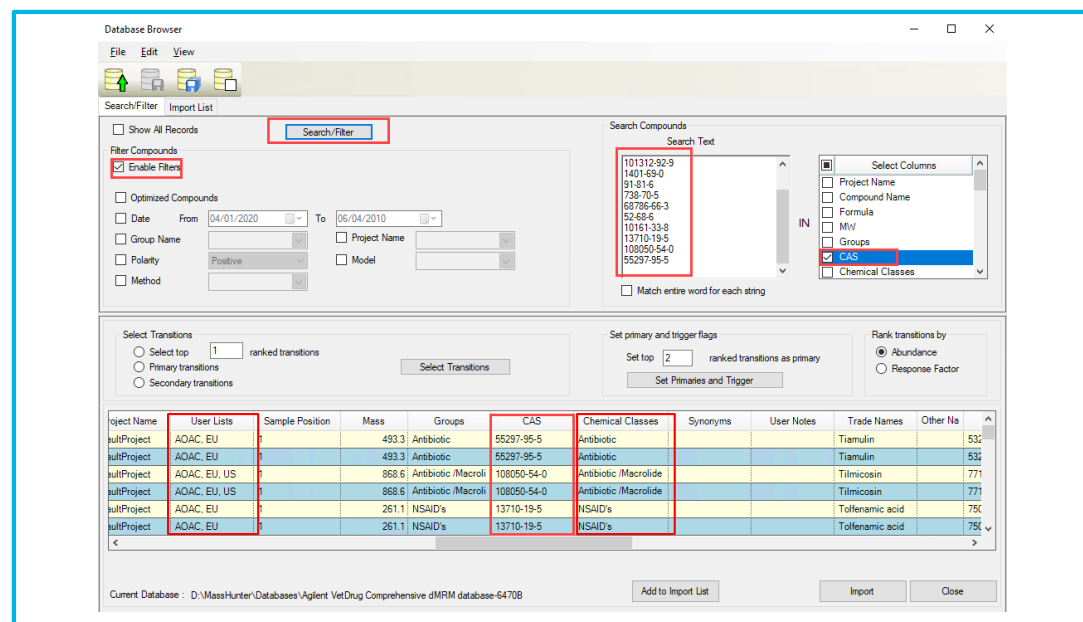


Figure 8: VetDrug dMRM database in Data Browser.

System Suitability STD Mix for Confident Performance

Vet drug System Suitability Test-Mix (Agilent p/n: 5799-0015) is available to support the workflow solution. The 25 targets are from 10 different chemical classes, with broad range of molecular weight, eluted evenly across the elution time, and covers both positive and negative polarity ionization. This standard simplifies installation verification and, when used as a regular QC sample, ensures confident day-to-day operation of workflow solution.

References

1. AOAC guidelines on "Screening and identification method for regulated veterinary drug residues in food", Version 7; June, 2018.
2. The United States, Code of Federal Regulations (CFR) - Title 21, Tolerance of Residues in New Animal Drugs in Food, Part 556, volume 6, April 1, 2019.
3. The United States, Chemical contaminants of public health concern used by the Food Safety and Inspection Service (FSIS), 2017.
4. Official Journal of the European Union, Pharmacologically active substances and their classification regarding maximum residue limits (MRL), Commission Regulation (EU) No 37/2010.
5. Guidelines for Standard Method Performance Requirements, AOAC Official Methods of Analysis (2016) Appendix F.
6. Agilent App Note, "An End-To-End Workflow for Quantitative Screening of Multiclass, Multiresidue Veterinary Drugs in Meat Using the Agilent 6470 Triple Quadrupole LC/MS", 5994-1932EN

Poster Reprint

ASMS 2020

WP 174

Characterization of Hemp-Based Products Using HS-GC/MS

Jennifer Sanderson,

Agilent Technologies, Inc. 2850 Centerville
Rd, Wilmington, DE 19808



The legalization of hemp¹ is driving the partnership between private sector agencies, regulating bodies and the state and federal governments to work together to create common sense guidelines that will provide the framework for methodologies and reporting requirements surrounding the hemp and medicinal cannabis industry. Products made from hemp have and will continue to come under scrutiny not only for the cannabinoid potency, but also for residual solvents, residual pesticides and terpene profiles. Presented here is a complete workflow for residual solvents using headspace gas chromatography-mass spectrometry (HS-GC/MS) for several hemp based consumer products.

Instrumentation

The Agilent 7697A Headspace, was coupled to the 8890/5977B GC/MS. The GC was equipped with a Agilent VF-35MS UI column and the MSD with an inert electron ionization (EI) Ion Source and was run in full scan mode.



Figure 1: Agilent 7696A Headspace and 8890 Gas Chromatograph

Calibration Preparation

For universal calibration, a saturated brine solution was made by adding 6 grams of sodium chloride to 18.2 MΩ water and shaken rigorously until a cloudy solution formed. With the use of analytical standards listed in Table 1, 5 calibration levels were created by spiking the appropriate aliquot into a 10mL headspace vial containing brine solution to bring each calibrator to a total liquid volume of 3mL. Class I residual solvents calibrator ranged from ~0.15ppm to 50ppm. Class II residual solvents ranged from ~10ppm-1,000ppm.

Analytical Standards

USP 467 Class 1	USPM-467J-1
USP 467 Class2B	USPM-467-L-1
California Residual Solvent Mix	SCA-300-1



Table 1: Analytical Standards used for calibration and matrix spikes

Sample Preparation

Five replicates of hemp bath ball, hemp cream, hemp gummies and hemp oil were prepared by dissolving 200mg of homogenized sample into 5mL of 18.2 MΩ water, shaken for 2 hours. After the samples were shaken, 500μL of each sample was transferred into 2.5mL of saturated brine solution in a 10mL headspace vial and sealed for analysis.

Matrix Spikes

For each hemp matrix tested, two of the five replicates were spiked with the analytes of interest to determine spike recoveries. This will allow multiple matrices to be analyzed using a single set of calibrators, which will increase sample throughput.

Method Precision

To evaluate the precision of this method, 8 replicate standards were created by spiking the lowest calibrator concentration into brine solution and analyzed. The %RSD was calculated for each analyte.

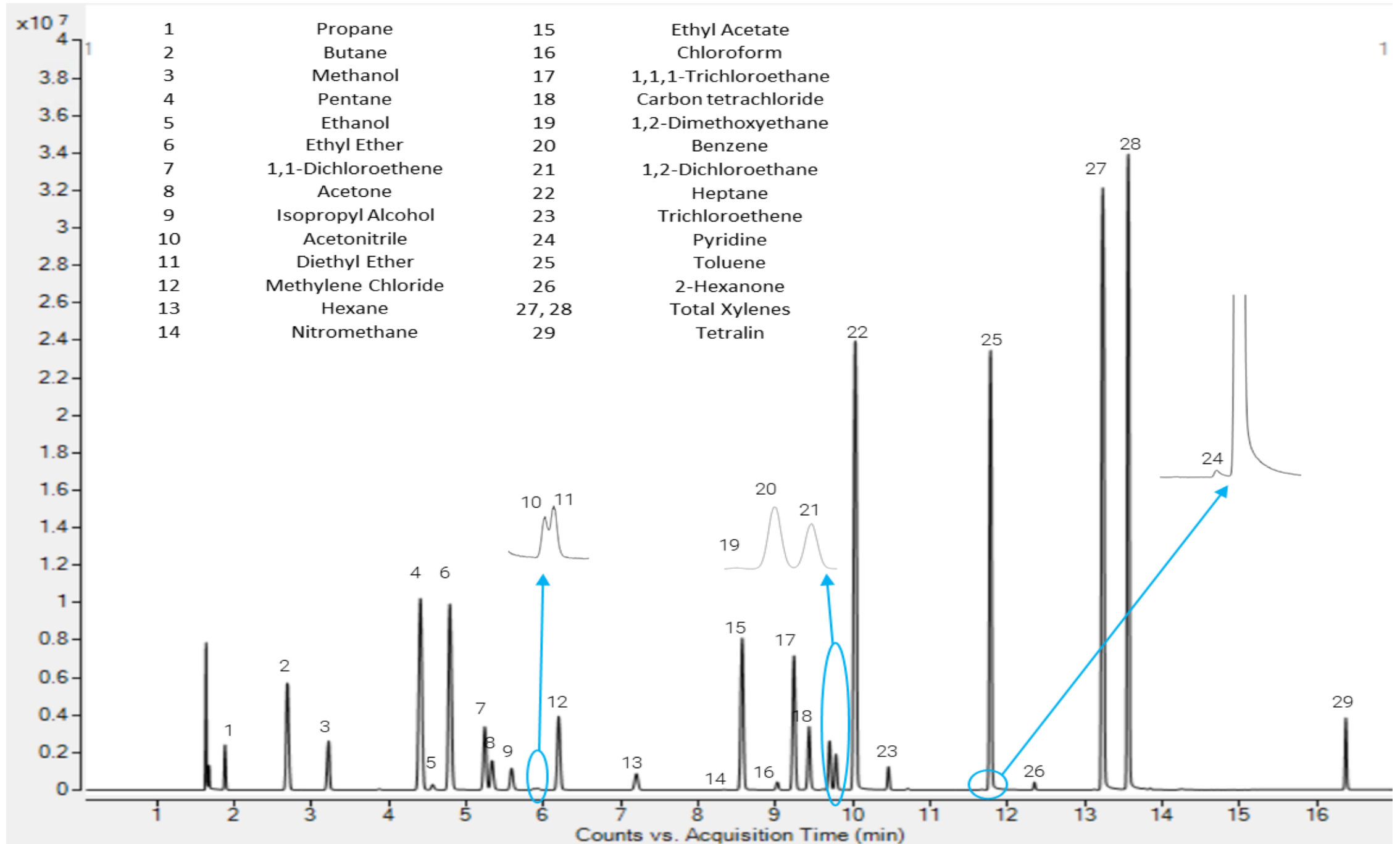


Figure 2: Chromatogram of Residual Solvent Calibrator extracted from brine matrix.

Chromatographic Separation and Linear Calibration

Chromatographic separation of 29 residual solvents is shown in figure 2. With a total sample cycle of 23 minutes, ultra light hydrocarbons, chlorinated solvents, alcohols and nitrogen containing compounds are well resolved with excellent run to run reproducibility. Each of the analytes were analyzed at 5 levels to create linear calibration curves. Sample calibrations can be seen below in figure 3. Reproducibility of the select analytes at the lowest calibrator level is shown in figure 4.

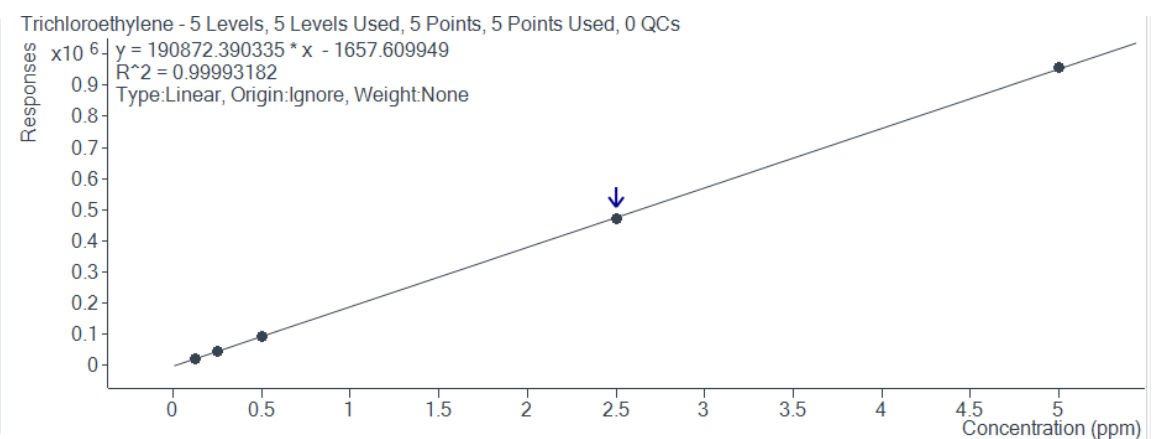
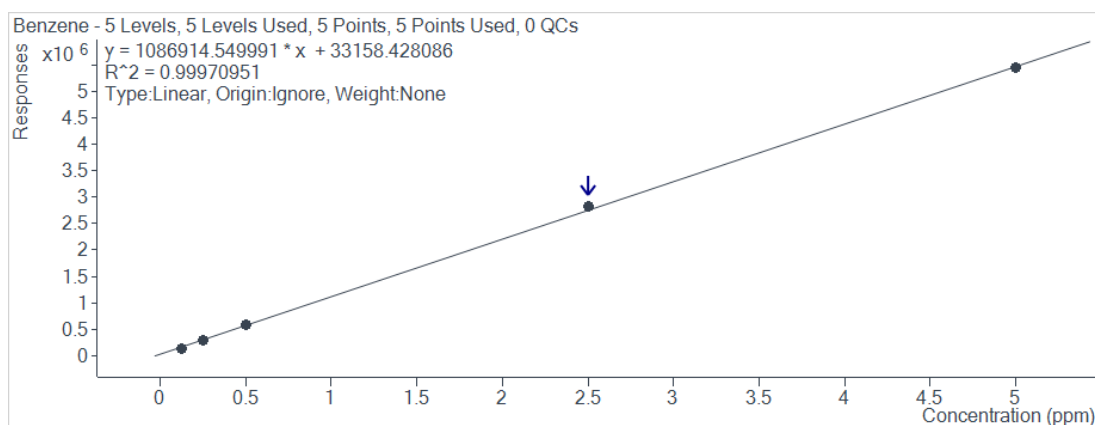
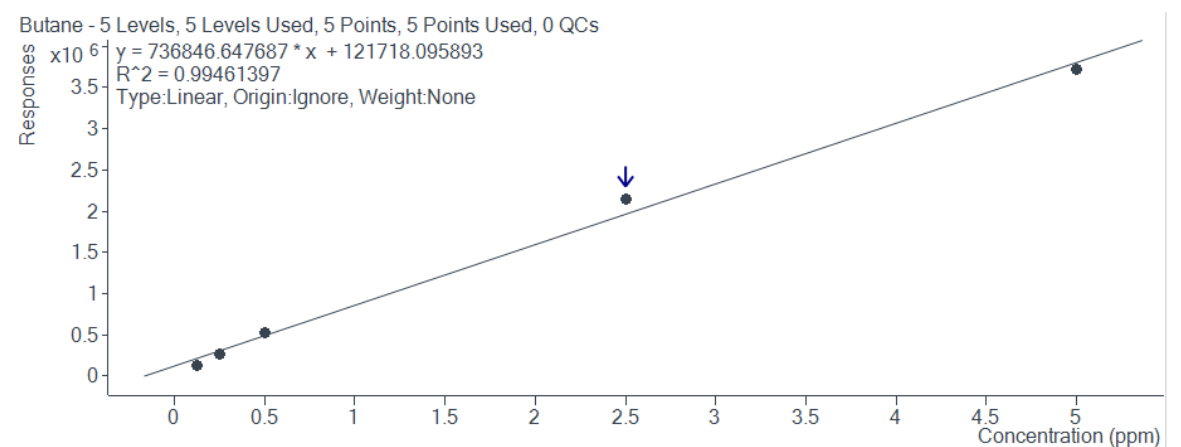


Figure 3: Calibration curves for Butane, Benzene and Trichloroethylene

Matrix Spike Recoveries

Analyte	Spike Level (ppm)	Hemp Bath Ball Rec. (%)	Hemp Cream Rec. (%)	Hemp Gummies Rec. (%)	Hemp Oil Rec. (%)
Propane	63	110	107	96	88
Butane	63	107	103	96	89
Methanol	75	99	101	95	90
Ethanol	63	90	92	94	86
Isopropyl Alcohol	63	91	93	90	85
Nitromethane	1	92	96	80	75
Ethyl Acetate	63	105	104	102	94
Chloroform	1	99	96	95	79
Benzene	3	102	99	97	79
1,2-Dichloroethane	6	99	96	95	81
Heptane	63	119	114	113	95
Trichloroethene	1	101	96	95	73

Table 2: Matrix Spike Recoveries of select analytes.

Sample Analysis and Matrix Spike Recoveries

The Hemp cream showed trace amounts of isopropyl alcohol that was detectable, but below the LOQ. All other products were negative for all residual solvents calibrated for.

Each of the hemp products were spiked in duplicate to evaluate the recovery of analytes from their respective matrix with a range of 70-130% recovery. Hemp oil showed lower recoveries of all analytes. Hemp cream, bath balls and hemp gummies all had recoveries well within the criteria for all analytes.

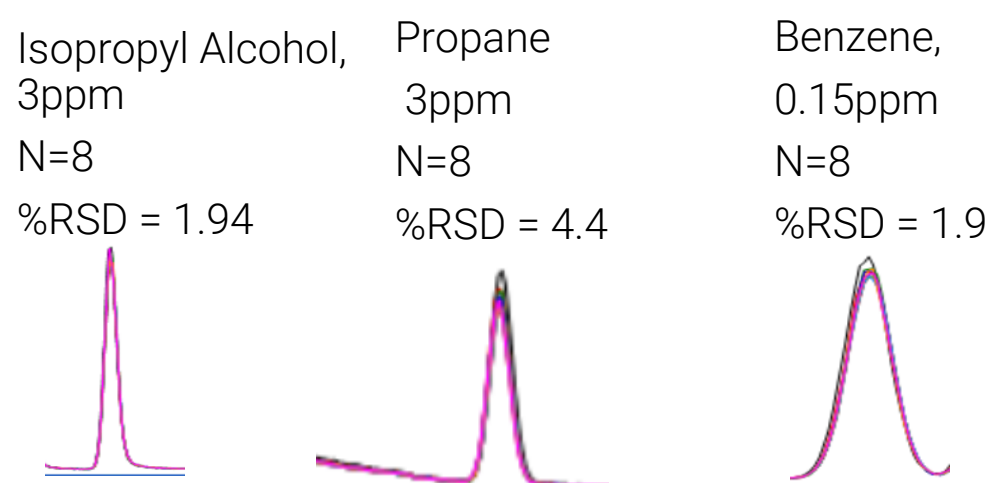


Figure 4: Seven chromatographic overlays for isopropyl alcohol, propane and benzene

Method Precision

Excellent reproducibility was demonstrated by analyzing multiple replicates of the lowest level calibrator. All analytes had %RSD within 10%. Figure 4 shows 7 chromatographic overlays of select analytes, along with the %RSD obtained to demonstrate precision.

Conclusions

Analysis for residual solvents in a variety of hemp consumer products is possible using HS-GC/MS

- Simplified sample extraction and sample preparation makes it easier to evaluate multiple matrices with a single calibration.
- The use of mass spectrometry coupled with headspace gas chromatography allows for identification and quantitation of residual solvents.

References

- ¹ H.R.2-Agriculture Improvement Act of 2018.n.b. SEC. 10111.

Agilent products and solutions are intended to be used for cannabis quality control and safety testing in laboratories where such use is permitted under state/country law.

Poster Reprint

ASMS 2020
WP 175

Quantitative Analysis of Acrylamide in Peanut Butter using LC Triple Quadrupole Mass Spectrometry

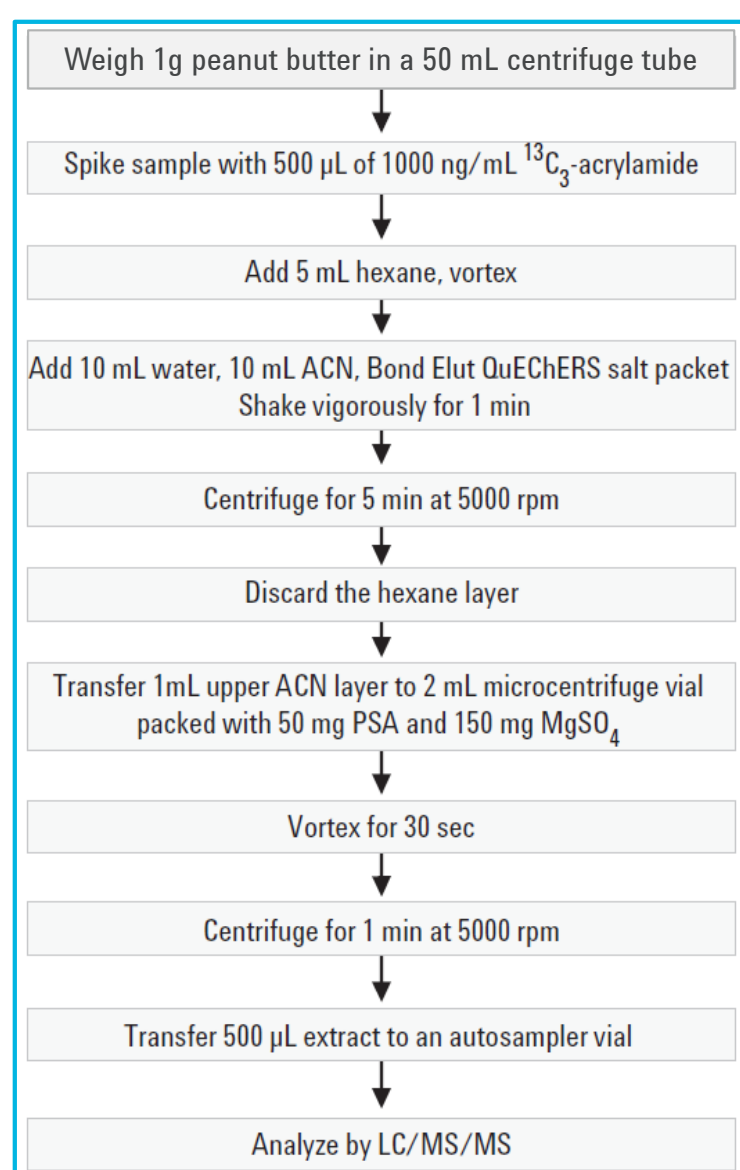
Yanan Yang, Guannan Li and Tina Chambers

Agilent Technologies, Inc., Santa Clara, CA,
USA.

Introduction

Acrylamide forms in carbohydrate-rich foods that are subjected to high temperature such as frying, baking and extrusion. Though epidemiological studies suggest it is unlikely that dietary acrylamide consumption increases people's risk of developing cancer despite it being a probable carcinogen, high levels of acrylamide are found primarily in potato products, bakery products, etc. Due to the low molecular weight and the high solubility in water, the challenges of acrylamide analysis in food arises in both sample preparation and the mass spectrometry method. Herein, this study presents a simple and rapid sample preparation procedure for the analysis of acrylamide in peanut butter that would be directly compatible with a fast and sensitive LC/MS/MS assay.

Experimental



Chemicals and Standard Solutions

Both acrylamide and internal standard acrylamide-d₃ were purchased from Sigma Aldrich. Peanut butter was purchased from local grocery store. Both acrylamide standard and internal standard stock solutions were prepared in acetonitrile.

Sample Preparation

The flow chart of the QuEChERS sample preparation procedure is shown on left¹. One gram of peanut butter was weighed into a 50 mL centrifuge tube from the Agilent Bond Elut QuEChERS Extraction Acrylamide kit (p/n 5982-5850). The internal standard was spiked into the peanut butter sample at 50 ng/g. Hexane (5 mL) was used to defat the extract with water (10 mL) and acetonitrile (10 mL) added². The extraction salt packet was added to the spiked sample and the tube was shaken for 1 min vigorously and centrifuged at 5000 rpm for 5 min. 1 mL of acetonitrile layer was transferred to a 2 mL Bond Elut QuEChERS AOAC Dispersive SPE tube (p/n 5982-5022). The tubes were vortexed for 30 sec and then centrifuged at 5000 rpm for 1 min. The supernatant was then placed in an autosampler vial for LC/MS analysis.

Calibration Curves

Due to the lack of matrix blank, both standard addition ISTD curve and reversed ISTD curve were tested in this study. The standard addition approach started from 5 to 2000 ng/g and the reversed curve was performed from 0.1 to 200 ng/g.

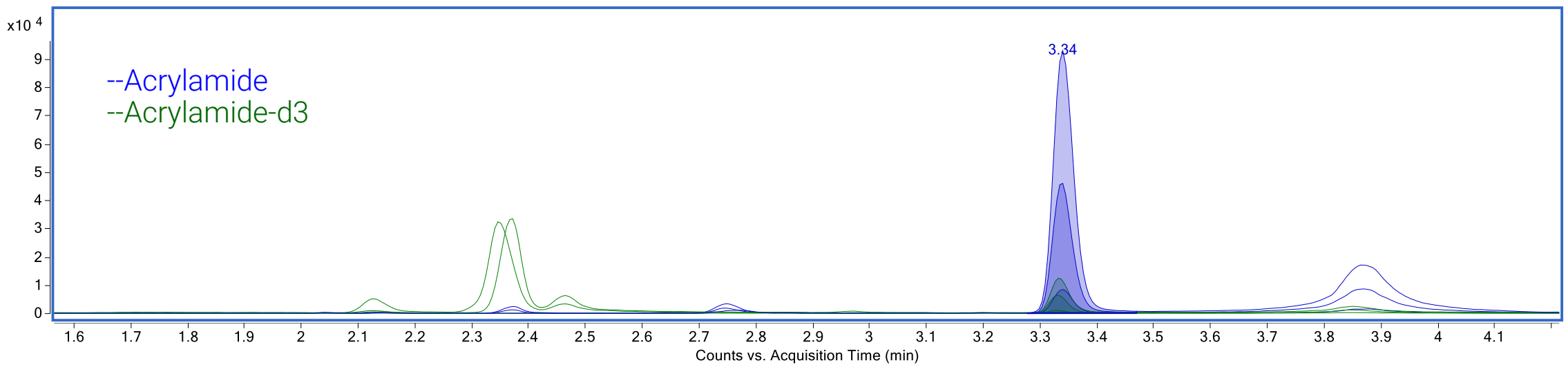
LCMS Method

Agilent 1290 II UHPLC Conditions			
Column	Poroshell 120 EC-C18, 2.7 µm, 3x150mm, p/n 693575-302		
Column temp	40 °C		
Injection volume	1 µL		
Autosampler temp	5 °C		
Needle wash	10 sec, MeOH:water 50:50		
Mobile phase	A = 0.1% formic acid in water B = 0.1% formic acid in acetonitrile		
Gradient program	Time	B (%)	Flow rate (mL/min)
	0.00	2	0.250
	4.00	2	0.250
	4.01	100	0.250
	6.00	100	0.250
	6.01	2	0.250

Agilent 6470 Source Parameters		MRM Parameters	
Ion mode	AJS Positive	Resolution	Q1 / Q2 = unit
Gas temp	150 °C	Cell Accelerator	2 V
Drying gas flow	4 L/min	Total MRMs	6
Nebulizer gas	60 psi	Cycle time	312 ms
Sheath gas temp	400 °C	Dwell time	50 ms
Sheath gas flow	12 L/min	Fragmentor	50 V
Capillary voltage	2000 V		
Nozzle voltage	0 V		
MRM Transitions	Precursor	Product	CE
Acrylamide-d ₃	75.1	58.1/44.2/30.2	12/36/28
Acrylamide	72.1	55.1/44.2/27.2	12/36/28

Extraction, Clean Up and LC Separation

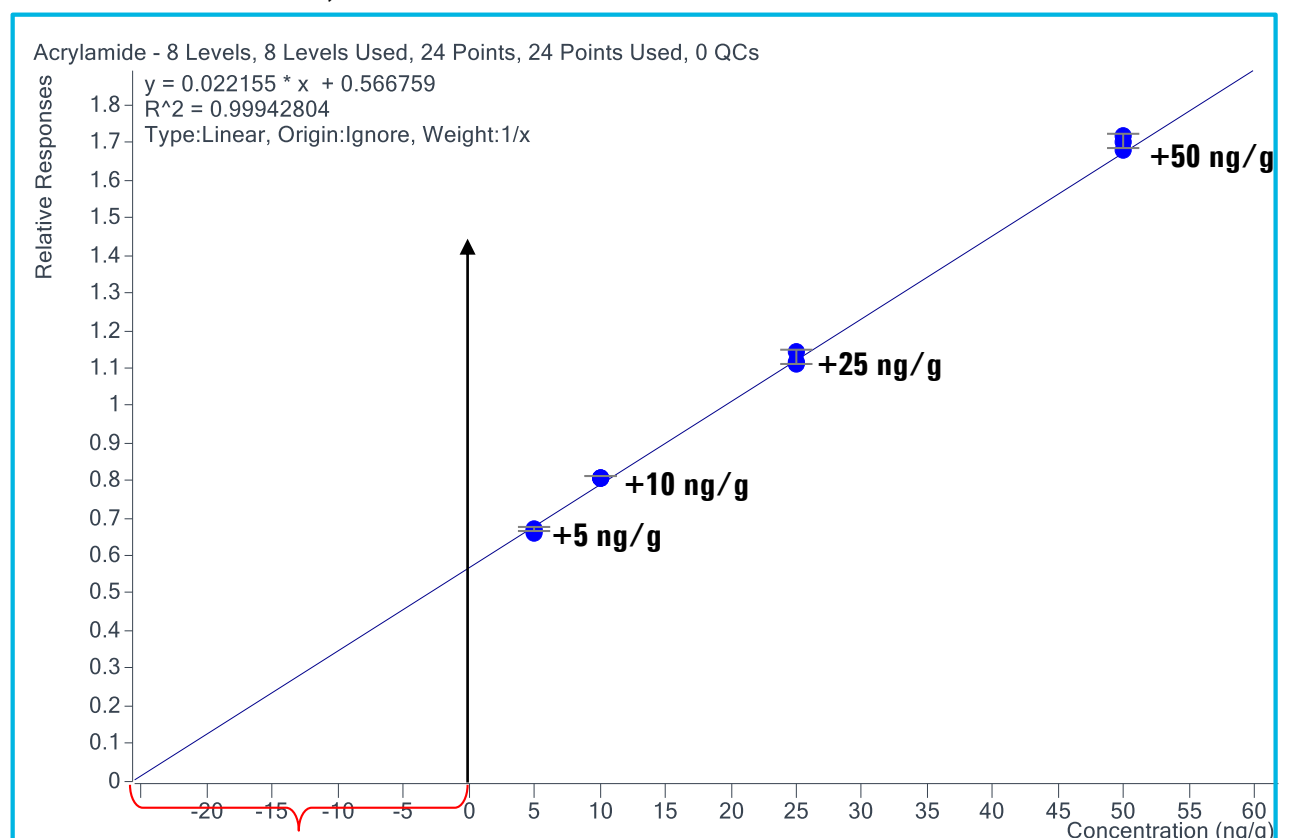
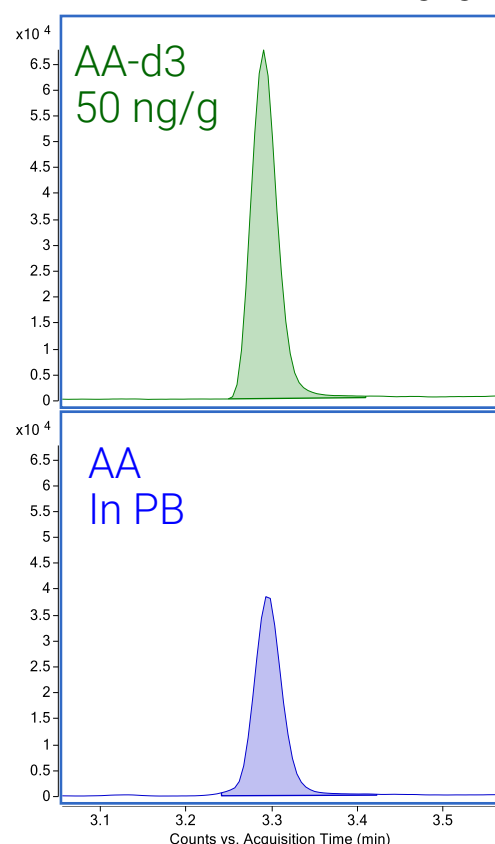
In the extraction, the hexane was used to remove fat from peanut butter. The addition of water was used to facilitate extraction of acrylamide from the matrix. Dispersive SPE was employed for direct sample clean up, without solvent evaporation, to simplify and speed the long and tedious SPE process. The 3 mm ID reversed phase column was compatible with the cleaned-up extract. Only 1 uL of extract, which is mainly in acetonitrile, was injected to avoid possible solvent effects due to acrylamide hydrophilicity. An isocratic gradient with 2% mobile phase B and a low flow rate of 0.25 mL/min was applied to separate acrylamide from the complicated matrix interference. This isocratic gradient retains acrylamide at 3.34 min. A flushing gradient with high organic solvent was applied to clean the column, followed with a longer equilibration time to assure the reproducibility of retention times from injection to injection.



Standard Addition Calibration Curve

Before extraction, standard addition ISTD calibration curves were obtained by constantly spiking the internal standard (acrylamide-d3) at a concentration of 50 ng/g, to the peanut butter sample containing the calibration standard (acrylamide) at levels from 5 to 2000 ng/g. Excellent linearity was observed ($r^2 > 0.9994$). Accuracy across the dynamic range was from 87.3 to 107.9% ($n=3$) with the %RSD lower than 6.30% ($n=3$) (table on left). Abundant response of acrylamide was observed in peanut butter without the spiked internal standard (middle). The acrylamide amount in peanut butter can be calculated by using the linear equation obtained from the standard addition curve (right), $y = 0.022155x + 0.566759$. When the addition amount is zero, i.e. $x=0$, the response on y axis represents the endogenous level of acrylamide in peanut butter as 25.58 ng/g (%RSD of 0.59, $n=3$)

Conc. (ng/g)	Accuracy (% , n=3)	%RSD (n=3)
5	87.3	6.30
10	107.9	0.67
25	100.4	3.39
50	102.3	1.53
100	101.3	2.92
500	99.4	1.13
1000	102.6	2.96
2000	98.7	0.63



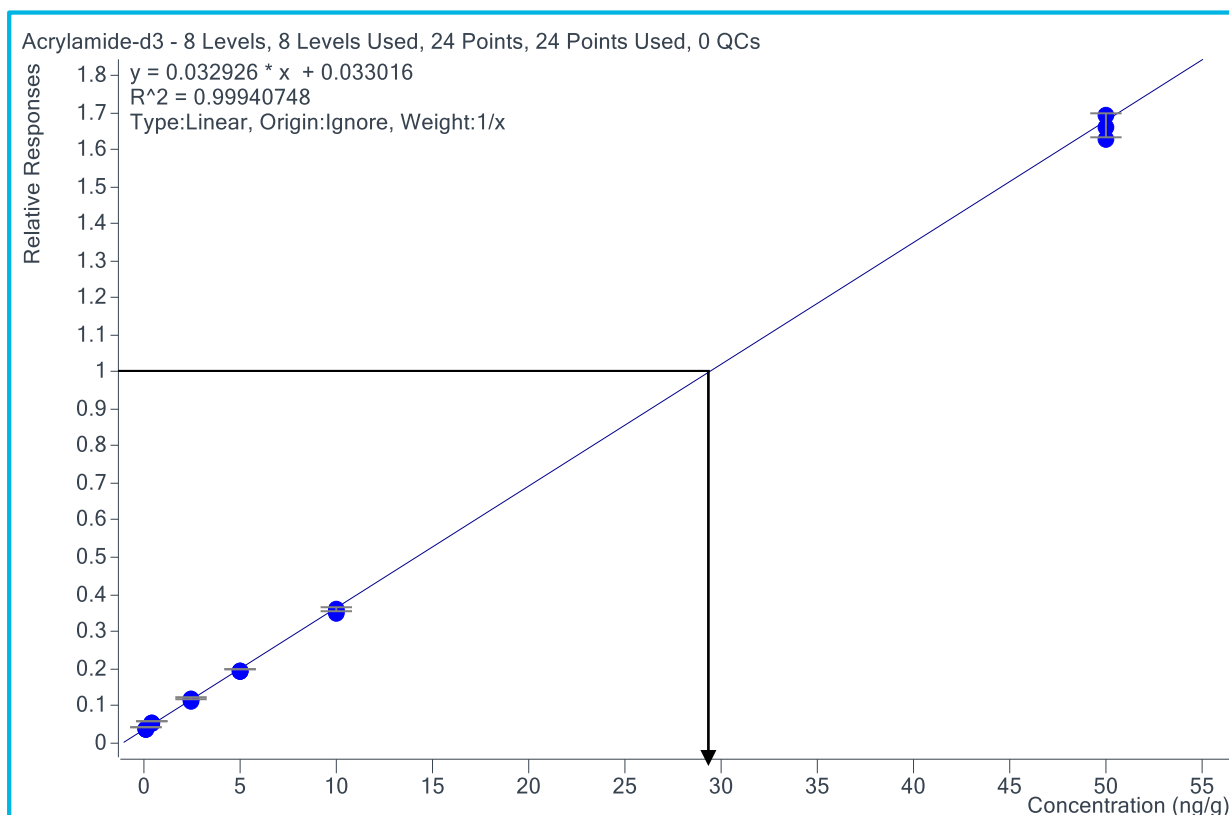
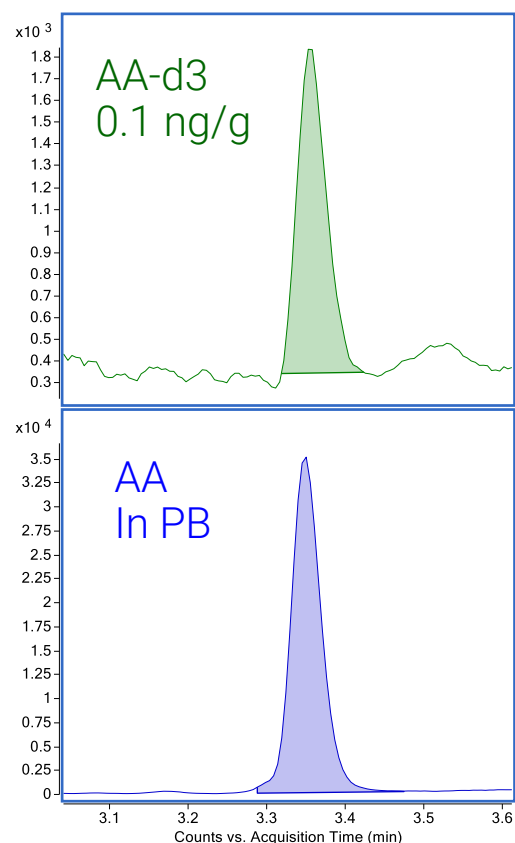
Reversed ISTD Calibration Curve

In the reversed ISTD calibration approach, only the internal standard was spiked into the peanut butter from 0.1 to 200 ng/g before the extraction. The endogenous acrylamide in the peanut butter is assigned as the internal standard while acrylamide-d3 is the targeted AA compound in the quantitative batch.

Results and Discussion

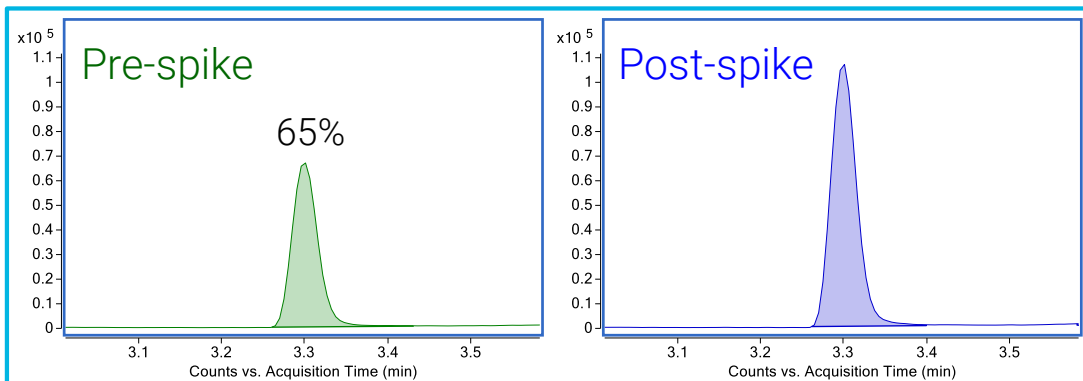
Excellent results were achieved in the reversed calibration approach with linearity ($r^2 > 0.9994$), accuracy from 96.9 to 103.4% ($n=3$) and %RSD lower than 6.15% ($n=3$) (table on left). The LOQ of acrylamide-d3 at 0.1 ng/g was obtained in peanut butter (middle) to demonstrate the whole assay performance, from sample prep to LCMS analysis. The acrylamide amount in peanut butter can be calculated by using the linear equation obtained from the reversed curve (right), $y = 0.032926x + 0.033016$. When the STD/ISTD ratio is 1, i.e. $y=1$, the calculated concentration represents the endogenous level of acrylamide in peanut butter as 29.21 ng/g.

Conc. (ng/g)	Accuracy (% , n=3)	%RSD (n=3)
0.1	103.4	6.15
0.5	102.2	1.38
2.5	100.2	4.47
5	96.9	1.26
10	97.7	1.78
50	98.9	2.05
100	100.4	2.55
200	100.2	3.14



Sample Recovery

Sample recovery was evaluated by spiking 50 ng/g d3-acrylamide into the peanut butter pre- and post-sample preparation. A recovery of 65% was calculated as the response ratio of pre-spiked to post-spiked.



Sample Preparation Reproducibility

The two-step sample preparation was repeated in triplicate and followed with a triplicated LCMS analysis, which had an overall RSD less than 4%. Table below.

AA-d3 50ng/g	LCMS repeats (ng/g)	Average (ng/g)	Stdev (ng/g)	%RSD
Sample Prep 1	42.47	42.46	0.91	2.14
	43.37			
	41.55			
Sample Prep 2	43.07	43.32	0.67	1.54
	44.08			
	42.82			
Sample Prep 3	46.75	45.72	0.98	2.15
	45.60			
	44.79			
Overall %RSD		3.85		

Conclusions

- Acrylamide was detected in peanut butter by using both the standard addition ISTD calibration and the reversed ISTD calibration with similar results.
- The %RSD of this fast and simple preparation, coupled with LCMS analysis, is less than 4%.
- Excellent reproducibility, accuracy, and linearity were achieved on both assays.
- Good LC separation on acrylamide from matrix background was performed by using low flow rate (0.25 mL/min) and larger i.d. column (3 mm).

References

¹Fadwa Al-Taher: Agilent App Note 5990-5940EN: Analysis of Acrylamide in French Fries using Agilent Bond Elut QuEChERS AOAC kit and LC/MS/MS.

²KATERINA MASTOVSKA AND STEVEN J. LEHOTAY: Rapid Sample Preparation Method for LC-MS/MS or GC-MS Analysis of Acrylamide in Various Food Matrices. *Journal of Agricultural and Food Chemistry* 54(19):7001-8. Oct 2006

Poster Reprint

ASMS 2020
WP 555

Determination of Nitrosamine impurities in Losartan Potassium drug substance using Triple Quadrupole Liquid Chromatography Mass Spectrometry

Chander Mani ,Saikat Banerjee and Samir
Vyas

(Agilent Technologies, India.)

Introduction

The announcement for the recall of ARB medicines Valsartan, Losartan and Irbesartan made N-Nitroso impurities a focus for regulatory agencies including the FDA and the European Medicines Agency (EMA). Nitrosamine impurities are byproducts produced in trace amounts during the manufacturing processes of these medicines. These impurities/compounds are classified as probable carcinogens (i.e. potentially genotoxic impurities).

The liquid chromatography mass spectrometry-based method described in this poster was carried out on the 6470 Triple Quadrupole LC/MS (LC/TQ), presenting a comprehensive analysis of 6 nitrosamine impurities in Losartan Potassium drug substance at very low detection limits. All nitrosamine impurities are of very small molecular weight. These nitrosamine impurities include: N-nitrosodimethylamine (NDMA), N-nitrosodiethylamine (NDEA), N-nitroso-4-methyl-4-aminobutyric acid (NMBA), N-nitrosoethylisopropylamine (NEIPA), N-nitrosodiisopropylamine (NDIPA) and N-nitrosodibutylamine (NDBA).

Instrumentation

1290 Infinity II high-speed pump (G7120A)
 1290 Infinity II multisampler (G7167B)
 1290 Infinity II multicolumn thermostat (G7116B)
 1290 Infinity II variable wavelength detector (G7114B)
 6470 triple quadrupole LC/MS (G6470A)

Table 1: Instrumentation detail



Figure 1: 6470 triple quadrupole LC/MS

Experimental

Sample Preparation

The sample preparation procedure was optimized using the following steps.

1. Weigh 100mg(± 2mg) Losartan Potassium drug substance sample in a 15 mL centrifuge tube.
2. Add 5 mL sample diluent and vortex for 2 minutes.
3. Now put the sample in shaker at 450rpm for 40 minutes.
4. Centrifuge the sample at 5000 rpm for 10 minutes.
5. Filter the supernatant using 0.2µm nylon syringe filter into an LCMS vial.
6. Inject the sample into LC/TQ.

LC Conditions

Needle wash	Methanol: Water/ 80:20																											
Sample diluent	Water: Methanol 95:5																											
Multisampler temperature	6 °C																											
Injection volume	20 µL																											
Analytical column	Zorbax Eclipse Plus Phenyl-Hexyl, RRHD 2.1 x 100mm 1.8µm (P/N 959758-912)																											
Column temperature	40 °C																											
Mobile phase A	0.2 % formic acid in water																											
Mobile phase B	Methanol																											
Flow rate	0.25 mL/min																											
Gradient	<table border="1"> <thead> <tr> <th>Time (min)</th> <th>%B</th> <th>Flow(mL/min)</th> </tr> </thead> <tbody> <tr> <td>0.0</td> <td>5</td> <td>0.25</td> </tr> <tr> <td>5.0</td> <td>25</td> <td>0.25</td> </tr> <tr> <td>13.0</td> <td>55</td> <td>0.40</td> </tr> <tr> <td>20.0</td> <td>55</td> <td>0.40</td> </tr> <tr> <td>20.1</td> <td>95</td> <td>0.25</td> </tr> <tr> <td>23.0</td> <td>95</td> <td>0.25</td> </tr> <tr> <td>23.1</td> <td>5</td> <td>0.25</td> </tr> <tr> <td>25.0</td> <td>5</td> <td>0.25</td> </tr> </tbody> </table>	Time (min)	%B	Flow(mL/min)	0.0	5	0.25	5.0	25	0.25	13.0	55	0.40	20.0	55	0.40	20.1	95	0.25	23.0	95	0.25	23.1	5	0.25	25.0	5	0.25
Time (min)	%B	Flow(mL/min)																										
0.0	5	0.25																										
5.0	25	0.25																										
13.0	55	0.40																										
20.0	55	0.40																										
20.1	95	0.25																										
23.0	95	0.25																										
23.1	5	0.25																										
25.0	5	0.25																										
Stop time	25 minutes																											
Post time	2 minutes																											

Table 2: LC conditions

Method Optimization

The 6470 LC/TQ was used for detecting the mass conditions for nitrosamine impurities in positive mode where M+H ion were found to be predominant precursor ions. The method was optimized using atmospheric pressure chemical ionization (APCI) source as most of the nitrosamines give better response and low noise background using APCI source. MRM method was converted into a dynamic MRM method.

MRM Transitions and Conditions

Compound	Prec. Ion (m/z)	Product Ion (m/z)	Frag. (V)	CE (V)	CAV (V)	±
NDEA	103.1	75.1	80	9	3	+
NDEA	103.1	47.1	80	17	3	+
NDMA	75.1	58	60	12	3	+
NDMA	75.1	43.1	60	18	3	+
NMBA	147.1	44.2	60	16	3	+
NMBA	147.1	87.2	60	10	3	+
NEIPA	117.1	75.1	75	8	3	+
NEIPA	117.1	47.1	75	18	8	+
NDIPA	131.1	89.1	75	6	3	+
NDIPA	131.1	43.1	75	12	8	+
NDBA	159.1	57.2	90	12	3	+
NDBA	159.1	41.1	90	22	3	+

Table 3: MRM transitions and conditions

MS Conditions	
Gas Temperature	300 °C
Gas Flow	6 L/min
Capillary Voltage	3000V
Nebulizer Pressure	55 psi
APCI Heater	350 °C
APCI Needle Positive	4 µA

Table 4: MS conditions

The chromatographic separation of Losartan Potassium drug substance and nitrosamine impurities was best achieved using Zorbax Eclipse Plus Phenyl-Hexyl column and diverter valve was programmed such that Losartan Potassium peak was diverted to waste and monitored using variable wavelength detector.

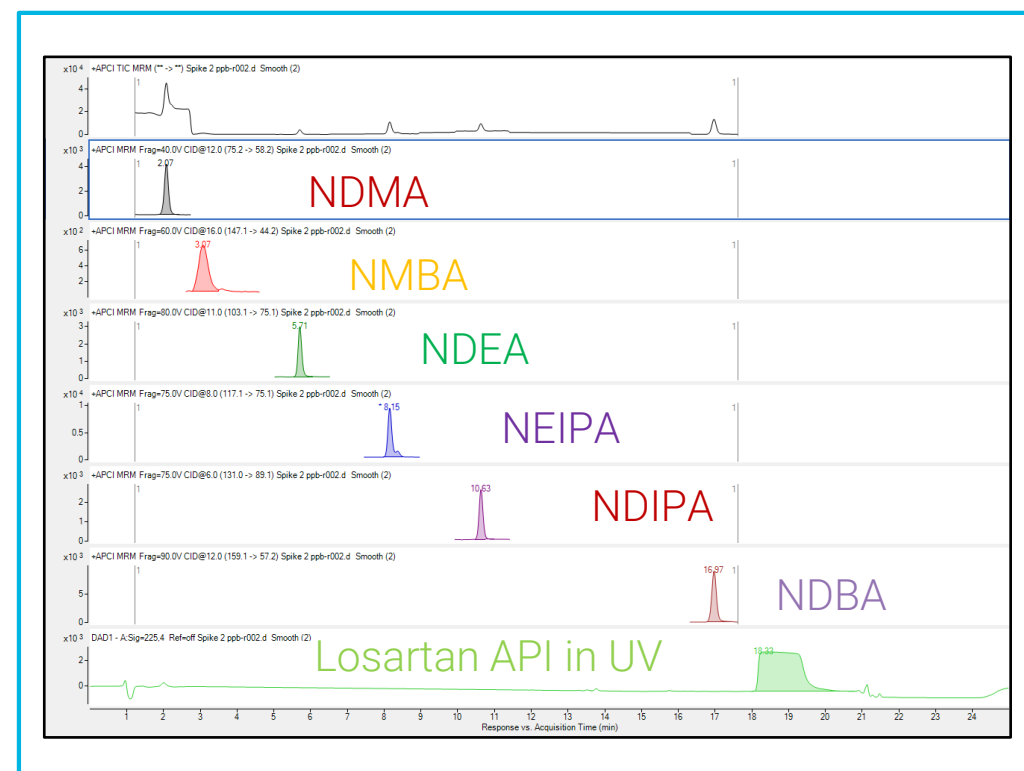


Figure 2: Representative EIC of NDMA, NMBA, NDEA, NEIPA, NDIPA and NDBA at 0.1 ppm conc. using 20mg/mL of Losartan Potassium API.

Below is presented the reproducibility data at 1ng/mL standard concentration for 8 replicates including bracketing standards (# 7 and 8) showing excellent peak area RSD % of < 6 % for each 6 nitrosamine impurities.

Area % RSD at 1ng/mL

#	NDMA	NMBA	NDEA	NEIPA	NDIPA	NDBA
1	2556	5484	10530	36010	14023	18686
2	2409	5609	10727	36593	13478	18853
3	2436	4844	9962	34563	13899	16452
4	2442	4937	10067	32146	13871	16342
5	2435	4827	10066	32805	14375	16942
6	2578	4996	10182	32838	13822	16670
7	2442	4987	10145	33254	14335	16706
8	2434	4966	10193	33108	13868	16691
Avg	2467	5081	10234	33915	13959	17168
SD	63.16	295.66	259.96	1629.64	289.9	1005.5
RSD (%)	2.56	5.82	2.54	4.81	2.08	5.86

Table 5: Peak area % RSD for 8 replicates at 1ng/mL

Method Performance Characterization

Figure 3 shows the calibration curves for the standard calibration of all 6 nitrosamines. The relevant calibration range for NDMA, NMBA and NDEA is from 0.05ng/mL to 25ng/mL and for NEIPA, NDIPA and NDBA is from 0.1 ng/mL to 25ng/mL.

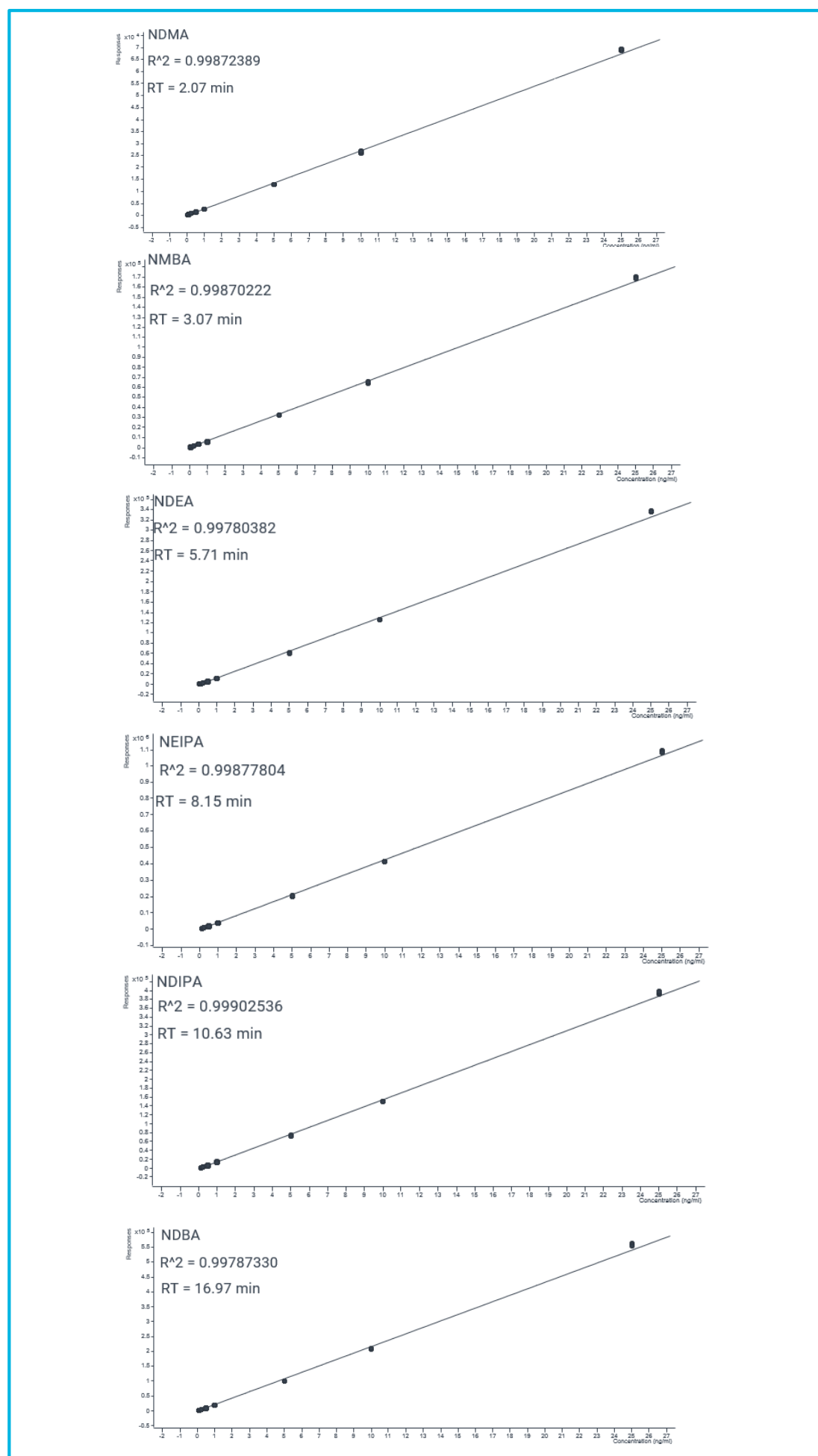


Figure 3: Calibration curves of all 6 nitrosamines with $r^2 > 0.997$

Recovery Study

The recovery experiment shows excellent recovery of $\pm 20\%$ of the spiked concentrations.

Nitrosamine Impurity	Concentration (ng/mL)	Recovery %
NDMA	2	110
NMBA	1	113
NDEA	1	103
NEIPA	1	100
NDIPA	1	98
NDBA	2	91

Table 6: Recovery data in Losartan API

Conclusions

- The method provides excellent reproducibility at USFDA defined LOQ concentrations levels as it shows area RSDs of $< 6\%$ with bracketing standards included in the calculations.
- The method is a ready to use method for analysis of Losartan Potassium drug substance batches as the method shows excellent recovery.
- The Losartan Potassium drug substance peak is chromatographically well separated from nitrosamine peaks so it can easily be diverted from the MS. Therefore, there is no contamination to the mass spectrometer due to a high concentration of API.

References

Poster Reprint

ASMS 2020
WP 567

Development of a cost-effective and highly selective bioanalytical method for the analysis of Montelukast in plasma using LC-MS/MS

Prasanth Joseph¹; Chidella Kartheek Srinivas¹; Arun Kumar P¹; Saikat Banerjee¹; Samir Vyas²

¹Agilent Technologies, BENGALURU, India;

²Agilent Technologies, Mumbai, India

Introduction

Montelukast is a prescription drug that belongs to the class of leukotriene receptor antagonists. This is a combination drug available in tablet form or as granules. Montelukast oral tablets are used to treat symptoms of asthma and is also effective for allergies and exercise-induced bronchoconstriction.

A cost-effective highly selective and reproducible method is developed for the low-level quantification of Montelukast in plasma using Montelukast-D6 as an internal standard. An electrospray ionization (ESI) based multiple reaction monitoring method was developed on a 6470 triple quadrupole LC/MS (LC/TQ) system. A simple liquid-liquid extraction-based sample preparation is adopted for the extraction of drug from plasma.



Figure 1. 1290 Infinity II UHPLC coupled to the 6470 LC/TQ.

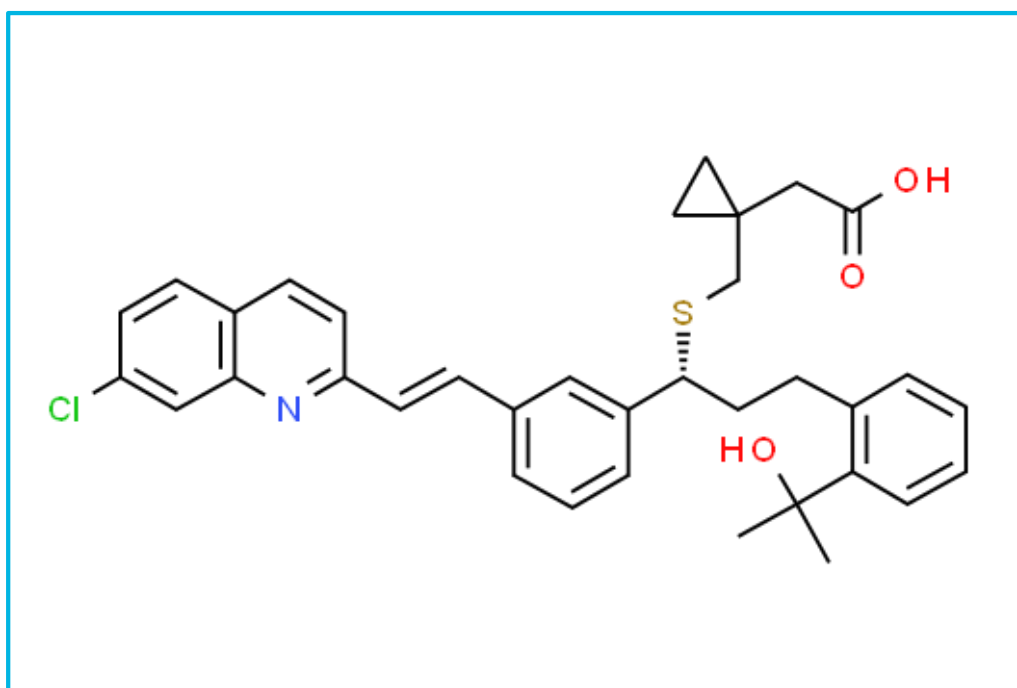


Figure 2. Chemical structure. of Montelukast

Experimental

Sample Preparation

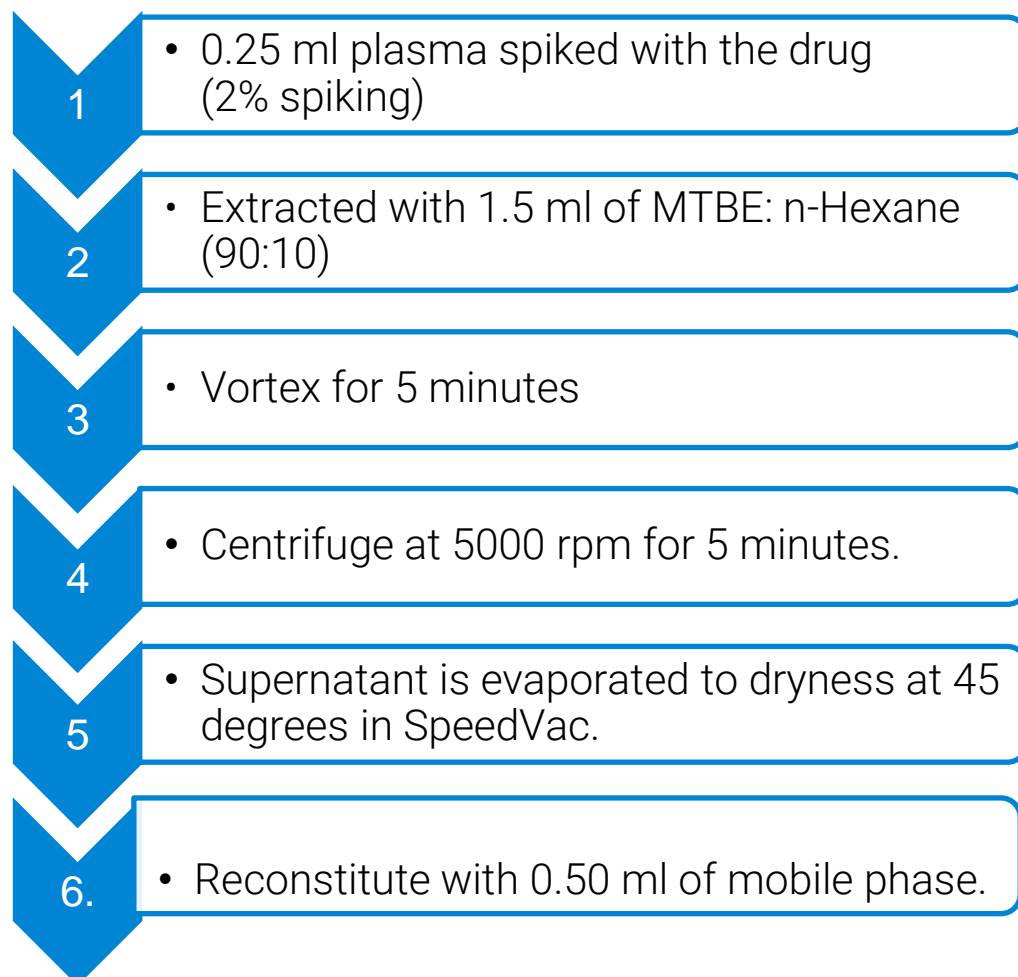


Figure 3. Liquid-liquid extraction protocol for the sample preparation of Montelukast

Chromatographic conditions

Analytical column	XDB C18 (100 X3.0, 3.5um)
Flow rate	0.5 ml/min
Mobile phase A	0.1% Formic acid in water
Mobile phase B	Acetonitrile
Injection volume	1 ul
Elution	Isocratic
Mobile phase ratio	10:90
Needle wash solvent	Acetonitrile: Water (60:40)

Source parameters

Ionization: ESI	Polarity: Positive
Sheath gas temp: 300°C	Sheath gas flow: 10l/min
Drying gas temp: 250°C	Drying gas flow: 8l/min
Cap Voltage: 3500V	Nozzle voltage: 0
Nebulizer pressure: 40 psi	

Method development

Montelukast method was developed using a 6470 LC/TQ installed with an Electrospray ionization source. Both Montelukast and the internal standard Montelukast-D6 were detected in positive ionization mode.

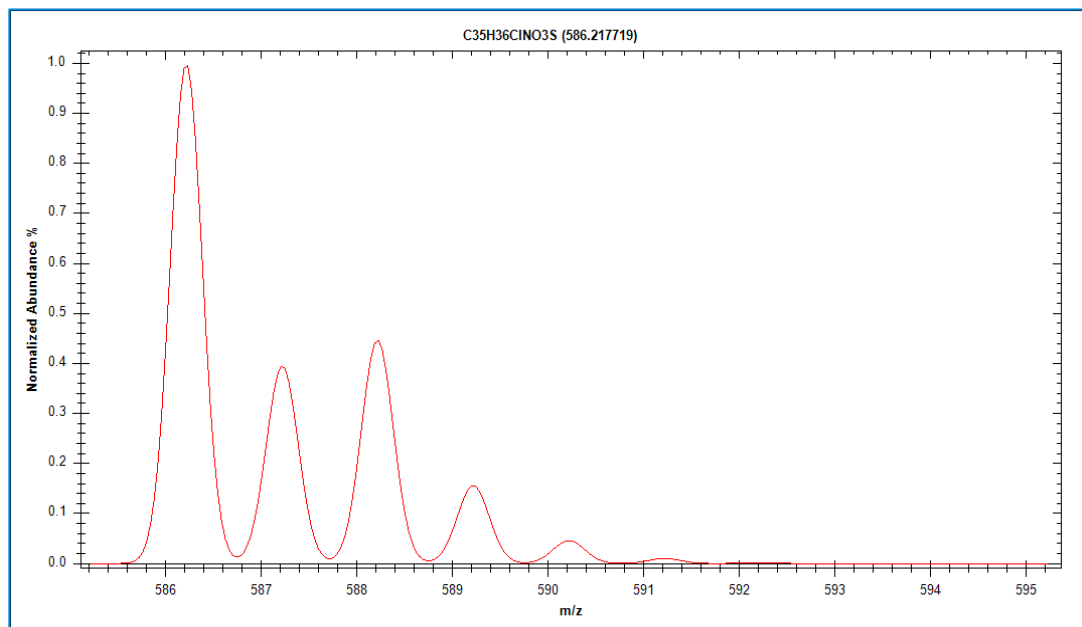


Figure 4. Isotopic pattern of Montelukast

Compound ID	Precursor ion	Product ion	Collision energy
Montelukast	586.2	568.1	16
Montelukast	586.2	422.1	28
Montelukast D6	592.3	574.1	16
Montelukast D6	592.3	427.1	28

Table 1. MRM parameters for Montelukast

Precision and accuracy of the batch was determined to verify the method performance in plasma samples. 3-orders of calibration curve concentrations were generated within the concentration range of 1 ng/ml to 1000 ng/ml and found to be linear. The regression coefficient obtained is 0.9993 when linearity plotted using "area ratio" against "concentration ratio" of analyte to internal standard with a weighing factor of $1/X^2$. The accuracy of each calibration standards measured from the linearity curve was between 96-104%.

Calibration curve

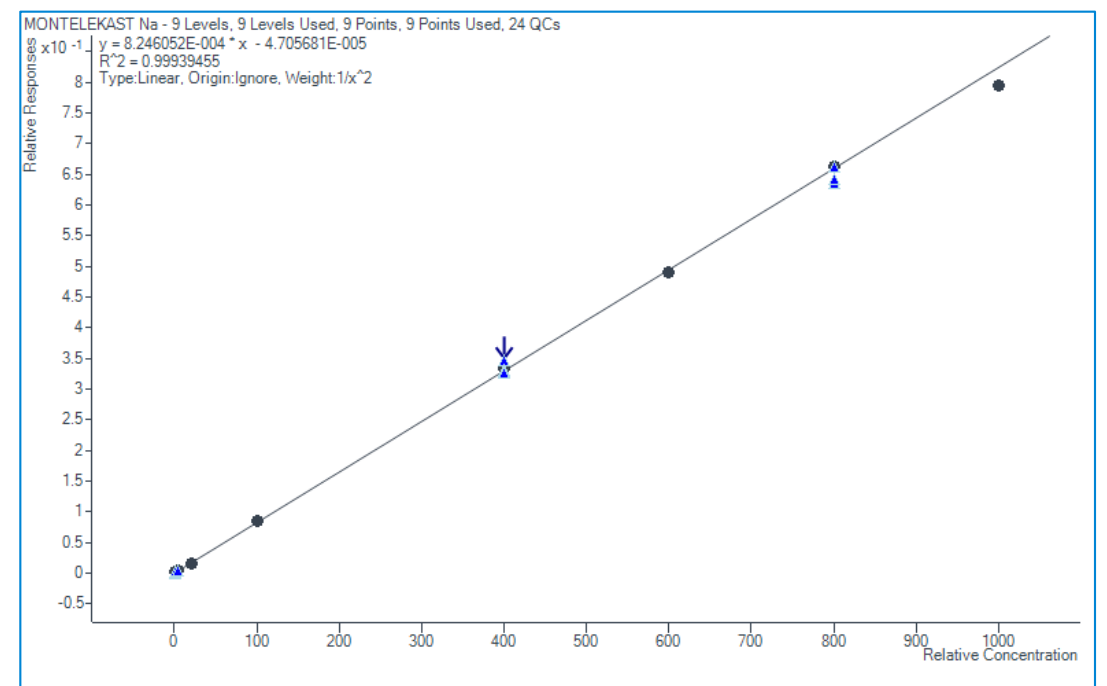


Figure 5. Calibration curve of Montelukast

Following the linearity studies, triplicate injections of LLOQ, LQC, MQC, and HQC were also submitted. Recovery for these QC samples at their respective concentration of 1, 5, 400 and 800 ppb were between 93-110%. The average area response at the LLOQ level was found to be 786 counts.

Batch Table		Sample		MONTELEKAST Na		MONTELEKAST D6		MONTELEKAST Na Results		MONTELEKAST D6 Results		Qualif.		MONTELEKAST Na		Qualif.				
Name	Data File	Type	Level	Acq. Date-Time	Exp. Conc.	RT	Resp.	MI	Calc. Conc.	Accuracy	Final Conc.	ISTD Conc.	Ratio	Height	RR	Ratio	MI	Resp.	Ratio	MI
BLANK	Blank01-r001.d	Blank		01-06-2019 18:26		1.896	11		277.9678		277.9678	278.0	4	0.2292		1.645	48	72.9		
BLANK+IS	Blank+IS.d	Blank		01-06-2019 18:31		1.230	9		0.0680		0.0680	0.0	1	0.0000		1.651	996168	62.1		
MONTE 1 PPB	STD 1.d	Cal	1	01-06-2019 18:36	1.0000	1.665	798		0.9891	98.9	0.9891	1.0	217	0.0008		1.651	1030278	61.8		
MONTE 2 PPB	STD 2.d	Cal	2	01-06-2019 18:39	2.0000	1.665	1645		2.0528	102.6	2.0528	2.1	446	0.0016		1.651	999000	61.8		
MONTE 5 PPB	STD 3.d	Cal	3	01-06-2019 18:43	5.0000	1.665	3927		4.9464	98.9	4.9464	4.9	1065	0.0040		1.651	974008	62.6		
MONTE 20 PPB	STD 4.d	Cal	4	01-06-2019 18:48	20.0000	1.665	15384		19.7857	98.9	19.7857	19.8	4132	0.0163		1.651	945641	62.0		
MONTE 100 PPB	STD 5.d	Cal	5	01-06-2019 18:52	100.0000	1.665	82298		103.9122	103.9	103.9122	103.9	22277	0.0856		1.651	960982	62.5		
MONTE 400 PPB	STD 6.d	Cal	6	01-06-2019 18:56	400.0000	1.659	296078		403.4498	100.9	403.4498	403.4	78382	0.3326		1.651	890086	61.4		
MONTE 600 PPB	STD 7.d	Cal	7	01-06-2019 19:01	600.0000	1.659	439762		593.6190	98.9	593.6190	593.6	116183	0.4896		1.651	898515	62.0		
MONTE 800 PPB	STD 8.d	Cal	8	01-06-2019 19:05	800.0000	1.659	539221		802.9347	100.4	802.9347	802.9	142084	0.6621		1.645	814463	62.1		
MONTE 1000 PPB	STD 9.d	Cal	9	01-06-2019 19:09	1000.0000	1.659	651275		965.1465	96.5	965.1465	965.1	170901	0.7958		1.645	818372	61.4		
MONTE 1 PPB	LLOQ-r001.d	QC	1	01-06-2019 19:13	1.0000	1.659	794		1.0488	104.9	1.0488	1.0	218	0.0008		1.651	970266	61.9		
MONTE 1 PPB	LLOQ-r002.d	QC	1	01-06-2019 19:18	1.0000	1.665	794		1.0967	109.7	1.0967	1.1	211	0.0009		1.651	926178	61.8		
MONTE 1 PPB	LLOQ-r003.d	QC	1	01-06-2019 19:22	1.0000	1.665	769		1.0143	101.4	1.0143	1.0	210	0.0008		1.651	974253	62.6		
MONTE 5 PPB	LQC-r001.d	QC	3	01-06-2019 19:26	5.0000	1.659	3610		4.7084	94.2	4.7084	4.7	989	0.0038		1.651	941206	62.7		
MONTE 5 PPB	LQC-r002.d	QC	3	01-06-2019 19:31	5.0000	1.659	3646		4.6643	93.3	4.6643	4.7	988	0.0038		1.651	959679	61.4		
MONTE 5 PPB	LQC-r003.d	QC	3	01-06-2019 19:35	5.0000	1.659	3637		5.0226	100.5	5.0226	5.0	972	0.0041		1.651	888234	61.8		
MONTE 400PPB	MQC-r001.d	QC	6	01-06-2019 19:39	400.0000	1.659	284913		396.0306	99.0	396.0306	396.0	75465	0.3065		1.651	872569	61.9		
MONTE 400PPB	MQC-r002.d	QC	6	01-06-2019 19:43	400.0000	1.665	296199		402.2789	100.6	402.2789	402.3	78817	0.3317		1.651	893042	61.8		
MONTE 400PPB	MQC-r003.d	QC	6	01-06-2019 19:48	400.0000	1.659	296759		419.8603	105.0	419.8603	419.9	79401	0.3462		1.651	857259	62.6		
MONTE 800PPB	HQC-r001.d	QC	8	01-06-2019 19:52	800.0000	1.659	551106		778.9340	97.4	778.9340	778.9	144700	0.6423		1.645	858065	61.8		
MONTE 800PPB	HQC-r002.d	QC	8	01-06-2019 19:56	800.0000	1.659	554871		771.2006	96.4	771.2006	771.2	145912	0.6359		1.645	872591	61.9		
MONTE 800PPB	HQC-r003.d	QC	8	01-06-2019 20:01	800.0000	1.659	549067		802.2796	100.3	802.2796	802.3	144506	0.6615		1.651	830012	62.6		
MONTE 1 PPB	STD 1-r001.d	QC	1	01-06-2019 20:05	1.0000	1.665	811		1.0929	109.3	1.0929	1.1	221	0.0009		1.651	949495	62.6		
MONTE 1 PPB	STD 1-r002.d	QC	1	01-06-2019 20:09	1.0000	1.665	769		1.0466	104.7	1.0466	1.0	205	0.0008		1.651	930217	62.5		
MONTE 1 PPB	STD 1-r003.d	QC	1	01-06-2019 20:13	1.0000	1.665	802		1.0795	107.0	1.0795	1.1	217	0.0008		1.651	951235	62.4		
MONTE 1 PPB	STD 1-r004.d	QC	1	01-06-2019 20:18	1.0000	1.659	702		0.9570	95.7	0.9570	1.0	193	0.0007		1.651	945969	61.6		
MONTE 1 PPB	STD 1-r005.d	QC	1	01-06-2019 20:22	1.0000	1.659	706		0.9581	95.8	0.9581	1.0	193	0.0007		1.651	950241	62.2		
MONTE 1 PPB	STD 1-r006.d	QC	1	01-06-2019 20:26	1.0000	1.654	811		1.0296	103.0	1.0296	1.0	224	0.0008		1.645	1011321	62.1		
MONTE 400PPB	SST-r001.d	QC	6	01-06-2019 20:30	400.0000	1.665	278497		402.5705	100.6	402.5705	402.6	74352	0.3319		1.651	839062	62.4		
MONTE 400PPB	SST-r002.d	QC	6	01-06-2019 20:35	400.0000	1.659	262763		400.2227	100.1	400.2227	400.2	70068	0.3300		1.645	796303	61.7		
MONTE 400PPB	SST-r003.d	QC	6	01-06-2019 20:39	400.0000	1.659	288142		399.9099	100.0	399.9099	399.9	76726	0.3297		1.645	873897	61.2		
MONTE 400PPB	SST-r004.d	QC	6	01-06-2019 20:43	400.0000	1.659	282297		400.9871	100.2	400.9871	401.0	77792	0.3306		1.645	834161	62.1		
MONTE 400PPB	SST-r005.d	QC	6	01-06-2019 20:48	400.0000	1.659	287539		397.9799	99.5	397.9799	398.0	76496	0.3281		1.651	876298	62.4		
MONTE 400PPB	SST-r006.d	QC	6	01-06-2019 20:52	400.0000	1.659	282105		397.4675	99.4	397.4675	397.5	74809	0.3277		1.651	860846	62.5		

Figure 6. Calibration table of Montelukast

Carryover was also evaluated by injecting the extracted blank sample after injection of the highest concentration standard. Area counts obtained for the blank after the injection of the highest concentration standard was less than 5% of the area of the LLOQ sample. Signal-to-noise ratio was calculated for LLOQ with the peak-to-peak algorithm and found to be more than S/N=30:1.

LLOQ chromatogram

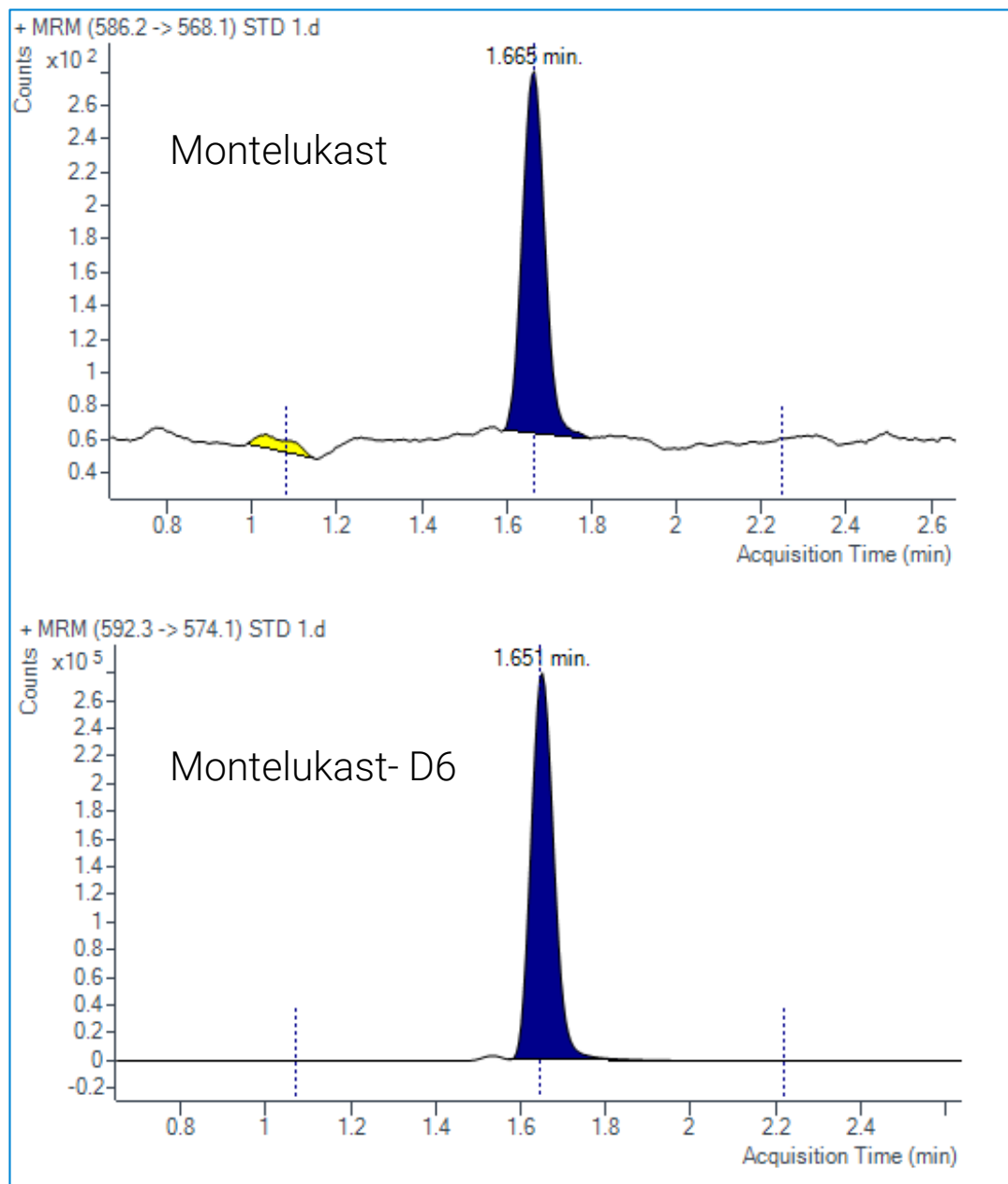


Figure 7. LLOQ chromatogram of Montelukast

The reproducibility of area ratio was measured by performing 300 injections of prepared plasma samples at the LLOQ level. % CV of area ratio for 300 injections was calculated as 6.4%.

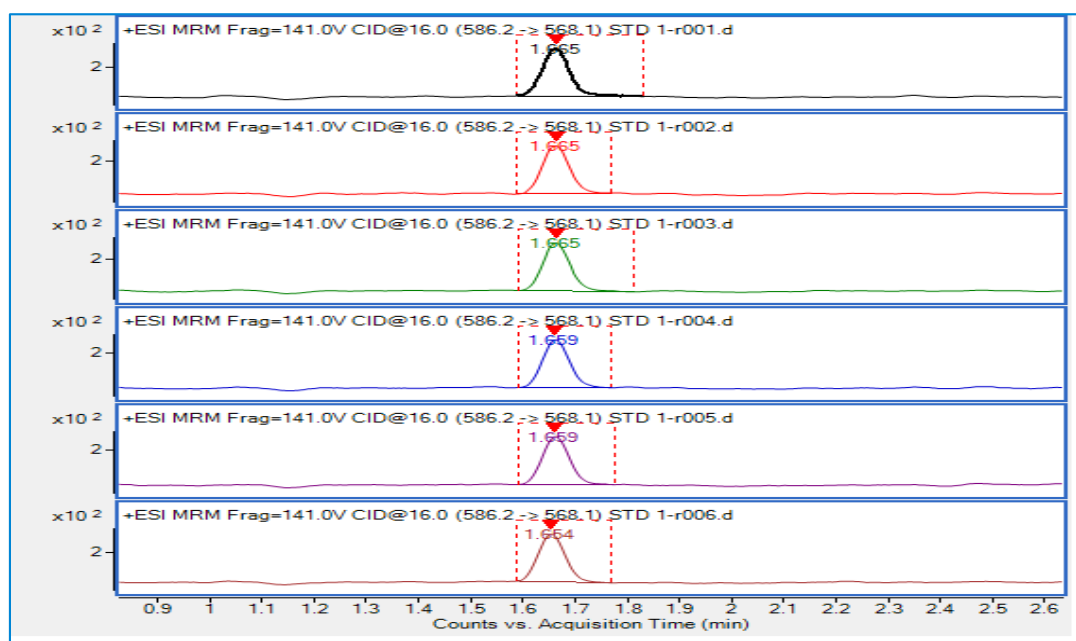


Figure 8. Reproducibility at LLOQ of Montelukast

Recovery of QC samples

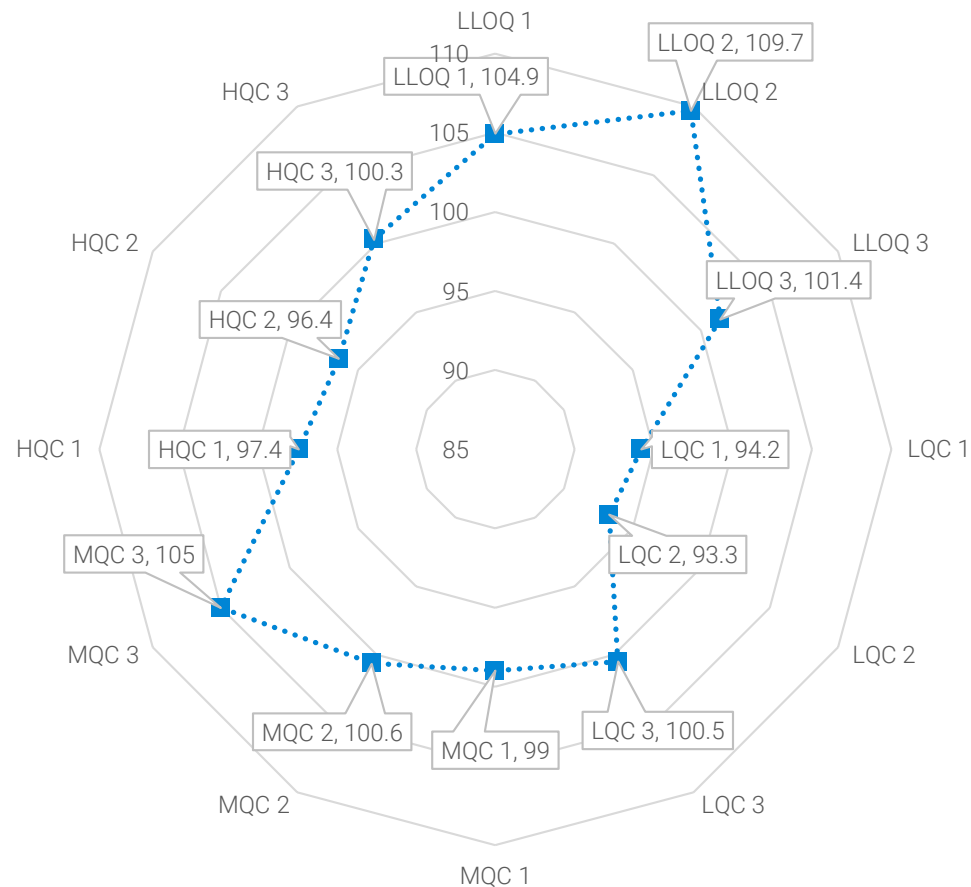


Figure 9. RADAR Plot of recovery of Montelukast in QC samples

Conclusions

- A MRM based Montelukast method was developed showing good sensitivity and linearity from 1 ng/ml to 1000 ng/ml
- The developed method is cost-effective, highly reproducible and shows good recovery from plasma matrix.

References

- Ezzeldin et al. Chemistry Central Journal 2014, 8:17 <http://journal.chemistrycentral.com/content/8/1/17>
- B. R. Challa et al. Sci Pharm. 2010; 78: 411–422; <https://www.ncbi.nlm.nih.gov/pmc/articles/PMC3002811/pdf/scipharm.2010.78.411.pdf>

For Research Use Only. Not for use in diagnostic procedures.